Universidade de Aveiro Departamento de Biologia
2008

Sandra Maria Tavares da Costa Rebelo

A função do domínio funcional NPTY no tráfego subcelular e processamento da PPA

The role of the NPTY functional domain on APP trafficking and processing

Universidade de Aveiro Departamento de Biologia
2008

Sandra Maria Tavares da Costa Rebelo

A função do domínio funcional NPTY no tráfego subcelular e processamento da PPA

The role of the NPTY functional domain on APP trafficking and processing

Tese apresentada à Universidade de Aveiro para cumprimento dos requisitos necessários à obtenção do grau de Doutor em Bioquímica, realizada sob a orientação científica da Doutora Odete Abreu Beirão da Cruz e Silva, Professora Auxiliar da Secção Autónoma de Ciências da Saúde da Universidade de Aveiro.

o júri

presidente

Prof. Doutora Maria Celeste da Silva do Carmo
Professora Catedrática do Departamento de Física da Universidade de Aveiro

Prof. Doutor Samuel Gandy
Full Professor at Mount Sinai School of Medicine
Mount Sinai Alzheimer's Disease Research Center, New York, EUA

Doutor Alexandre Valério de Mendonça
Investigador Principal do Laboratório de Neurociências da Faculdade de Medicina da Universidade de Lisboa

Prof. Doutor Amadeu Mortágua Velho da Maia Soares
Professor Catedrático do Departamento de Biologia da Universidade de Aveiro

Prof. Doutor Edgar Figueiredo da Cruz e Silva
Professor Associado do Departamento de Biologia da Universidade de Aveiro

Prof. Doutor António José Brito Fonseca Mendes Calado
Professor Auxiliar do Departamento de Biologia da Universidade de Aveiro

Prof. Doutora Odete Abreu Beirão da Cruz e Silva
Professora Auxiliar da Secção Autónoma de Ciências da Saúde da Universidade de Aveiro

agradecimentos

Quero expressar um especial agradecimento à minha orientadora, Professora Doutora Odete A. B. da Cruz e Silva, por partilhar comigo as suas vivências científicas e pessoais, pelo incentivo e acompanhamento permanente que permitiram não só a realização do trabalho científico apresentado nesta tese, mas também conduziram ao meu enriquecimento científico e pessoal.

De igual modo, um agradecimento especial ao Professor Doutor Edgar F. da Cruz e Silva, pela sua preciosa colaboração neste trabalho científico e pela disponibilidade e aconselhamento dispensados ao longo destes anos. Para ele uma palavra muito especial de coragem para ultrapassar, aquilo que penso ser, a fase mais complicada da sua vida. Força Professor Edgar.

A ambos um muito obrigada pelas inúmeras oportunidades.

Gostaria exprimir um sincero e profundo agradecimento a todos os meus colegas do Laboratório de Neurociências e do Laboratório de Transdução de Sinais, pelo apoio, incentivo e ajuda facultadas ao longo deste tempo, em particular à Doutora Sandra Isabel Vieira, pois juntas conseguimos trabalhar harmoniosamente o que foi crucial para obtenção dos resultados apresentados nesta tese. Sandra, muito obrigada por teres partilhado comigo sabedoria, companheirismo e amizade que foram essenciais para o meu enriquecimento científico e principalmente pessoal.

Gostaria também de expressar o meu agradecimento aos nossos colaboradores alemães: Prof. Doutor Jens Wiltfang e Doutor Hermann Esselmann pela preciosa ajuda na obtenção dos resultados do Abeta.

Ao Pedro e à Mariana por encherem de alegria os meus dias. Gostaria ainda de expressar o meu reconhecimento e agradecimento à minha família, sem a qual não teria chegado onde cheguei, nomeadamente ao meu pai e à minha mãe e aos meus irmãos.

Ao Centro de Biologia Celular e ao Departamento de Biologia da Universidade de Aveiro agradeço o bom acolhimento que permitiram o desenvolvimento da minha tese de doutoramento.

O desenvolvimento do trabalho experimental e a participação em congressos internacionais foram possíveis graças ao apoio financeiro das seguintes instituições:

- Universidade de Aveiro (Bolsa de Doutoramento);

- FCT (Bolsa de Doutoramento: SFRH/BD/17693/2004);

- Fundação Astrazeneca – Programa de Fundo de Apoio à Investigação 2004 (Área Cientifica: Sistema Nervoso Central);

- Projectos nacionais (34349, 40682 e 58469);

- Projectos internacionais (DIADEM e APOPIS);

palavras-chave

Doença de Alzheimer, proteína precursora de amilóide de Alzheimer, Abeta, fosforilação, endocitose, localização subcellular, proteínas de ligação.

resumo

A Doença de Alzheimer (DA) é uma doença multifactorial e progressiva do sistema nervoso central. Apresenta uma incidência mundial de 2-7% em indivíduos com mais de 65 anos e de cerca de 50% em indivíduos acima dos 85 anos de idade. As principais alterações histopatológicas observadas nos doentes são a presença de tranças neurofibrilhares intracelulares e depósitos extracelulares de um peptídeo de 4 KDa denominado Abeta, que é o principal componente das placas de amilóide. Apesar da sua etiologia multifactorial, há uma correlação bem descrita entre esta patologia e o Abeta (peptídeo neurotóxico). O Abeta deriva fisiológica e proteoliticamente de uma glicoproteína transmembranar com características de receptor: a Proteína Percursora de Amilóide de Alzheimer (PPA). As possíveis funções fisiológicas da proteína PPA, o seu destino e vias de processamento celulares, conjuntamente com possíveis proteínas celulares que com ela interajam, são assim tópicos de interesse e áreas de investigação científica mundial. A PPA possui na sua estrutura primária sequências consenso para fosforilação, quer no seu ectodomínio quer no seu domínio intracelular, já descritas como sofrendo fosforilação “in vitro” e “in vivo”. Mais ainda, em alguns casos esta fosforilação está associada a estados de doença. Assim sendo, 7 dos 8 aminoácidos que hipoteticamente podem ser fosforilados no seu domínio intracelular encontram-se fosforilados em cérebros de doentes de DA, nomeadamente, Tyr^{653}, Ser^{655}, Thr^{668}, Ser^{675}, Try^{682}, Thr^{686}, Tyr^{687}. O último pertence ao domínio funcional NPTY que é um sinal típico de endocitose em receptores associados à membrana e um local consenso para a endocitose. Várias proteínas interagem com este domínio intracelular da PPA, a maioria possui múltiplos domínios de interacção permitindo a formação de multi-complexos de sinalização entre a PPA e proteínas celulares. Existe assim a possibilidade dessas proteínas funcionarem como proteínas adaptadoras direccionando a PPA para vias de sinalização específicas. A interacção da PPA com essas proteínas de ligação parece ser regulada por fosforilação proteica, uma vez que a ligação da PPA à FE65 só ocorre quando a Thr^{668} está desfosforilada.

O uso de proteínas de fusão PPA-GFP permitiu avaliar a função do domínio NPTY, através da mimetização do estado fosforilado (Y687E) e desfosforilado (Y687F) da Tirosina 687. Resultados contrastantes foram observados na localização subcelular destas proteínas. A proteína Y687E-PPA-GFP foi detectada na membrana plasmática mas não foi eficientemente incorporada em vesículas de tranferrina e apresentou uma diminuição significativa na produção de Abeta. Em contraste, a proteína Y687F-PPA-GFP é facilmente endocitada, tal como a proteína selvagem, e produziu mais Abeta, ou seja ocorreu um favorecimento da clivagem pela via da β-secretase. Os resultados obtidos indicam que este resíduo é importante para o direccionamento subcelular da proteína PPA e para o seu processamento nas diferentes vias, nomeadamente secretória e endocítica. A localização subcelular da PPA pode ser mediada por ligação a proteínas específicas. Um desses exemplos é a ligação da PPA à RTN3-B, uma vez que ambas co-localizam no retículo endoplásmico.

Adicionalmente, os resultados apontam no sentido de que as interacções entre a PPA e as suas proteínas parceiras de ligação estejam dependentes do seu estado de fosforilação. Com este propósito o papel da Tirosina 687 no estabelecimento dessas interacções foi avaliado. Os resultados demostram que ambas as proteínas mutantes ligam FE65 e que esta última é a proteína que medeia a conexão entre a PPA e a PP1γ. As implicações destas observações na DA e em novas aplicações terapêuticas para a doença são subsequentemente discutidas.

keywords

Alzheimer's disease, Alzheimer's amyloid precursor protein, Abeta, phosphorylation, endocytosis, subcellular targeting, binding proteins.

abstract

Alzheimer's disease (AD), the most common age-related dementing illness, is a progressive multifactorial neurodegenerative disorder of the central nervous system affecting individuals worldwide with an incidence of 2-7% of post-65 and 50% of post-85 years old. The pathological hallmarks of AD are the presence of intracellular neurofibrillary tangles and extracellular deposits of a 4kDa amyloid beta peptide (Abeta) forming amyloid plaques in the cerebral cortex. This disease is multifactorial in its etiology but central to its pathology is the neurotoxic Abeta peptide. Abeta arises from the proteolytic cleavage of a larger ubiquitous glycophosphoprotein, APP (Alzheimer Amyloid Precursor Protein), whose short cytoplasmic domain contains several phosphorylatable amino acids. The latter can be phosphorylated 'in vitro' and 'in vivo', and in some cases phosphorylation appears to be associated with the disease condition. Furthermore, it was demonstrated that 7 of the 8 potentially phosphorylatable residues in the intracellular domain of APP were phosphorylated in AD patients, namely Tyr^{653}, Ser^{655}, Thr^{668}, Ser^{675}, Tyr^{682}, Thr^{686} and Tyr^{687}. The latter lies within the NPTY domain, a typical internalization signal for membrane-associated receptor proteins, as well as a consensus sequence for coated-pit mediated internalization. Several proteins interact with the above mentioned cytoplasmic domain of APP, most of them possessing multiple protein-protein interacting domains, thus forming large multimolecular APP complexes. It appears therefore that these proteins function as adaptor proteins directing APP to specific molecular pathways. The interaction of APP with these binding proteins appears to be regulated by protein phosphorylation as has been described for FE65 binding, for example. Using APP-GFP fusion proteins to monitor intracellular pathways, the role of the NPTY domain was addressed by mimicking Tyr^{687} constitutive phosphorylation (Y687E) and dephosphorylation (Y687F), respectively. Contrasting effects on subcellular APP distribution were observed. Y687E-APP-GFP was targeted to the membrane but could not be detected in transferrin containing vesicular structures, and exhibited a concomitant and dramatic decrease in Abeta production. In contrast, Y687F-APP-GFP was endocytosed similarly to wild-type APP, but was relatively favoured for beta-secretase cleavage. Overall, Tyr^{687} appears to be a critical residue determining APP targeting and processing via different pathways, including secretory, endocytic and retrograde transport. Significantly, from a disease perspective, mimicking Tyr^{687} phosphorylation resulted in a hitherto undescribed inhibition of Abeta production. Our results provide novel insights into the role of direct APP phosphorylation on APP targeting, processing and Abeta production. Targeting of APP is most likely mediated by binding to specific proteins. One such novel interaction identified was RTN3-B. These two proteins colocalize in the ER. Additionally, our conclusions so far, favour the model that interaction of APP with the binding proteins may also be mediated by the phosphorylation state of APP itself and with this proposal the role of Tyr^{687}on protein-protein interactions was investigated. We demonstrated that FE65 binds to both Tyr^{687} mutants and also that FE65 is the bridging protein between APP and PP1γ.
Our results provide novel insights into the role of direct APP phosphorylation on processing and Abeta production, pointing towards potential intervention strategies for the treatment of Alzheimer's disease.

INDEX

PUBLICATIONS

Nesta dissertação foram utilizados resultados do trabalho publicado abaixo indicado. A autora declara que interveio na concepção e execução do trabalho experimental, na interpretação dos resultados e na sua redacção para publicação.

This thesis contains experimental results included in the publications indicated below. The author of this thesis declares that she participated in the planning and execution of the experimental work, as well as in data interpretation and in the preparation of work for publication.

da Cruz e Silva OAB, Vieira SI, Rebelo S, da Cruz e Silva EF. 2008. A model system to study intracellular trafficking and processing of the Alzheimer's amyloid precursor protein. Neurodegener Dis 1: 196-204.

Rebelo S, Vieira SI, da Cruz e Silva EF, da Cruz e Silva OAB. 2008. Monitoring 'de novo' APP synthesis by taking advantage of the reversible effect of cycloheximide. AJAD (submitted).

Rebelo S, Vieira SI, Esselmann H, Wiltfang J, da Cruz e Silva EF, da Cruz e Silva OAB. 2007a. Tyrosine 687 phosphorylated Alzheimer's amyloid precursor protein is retained intracellularly and exhibits a decreased turnover rate. Neurodegener Dis 4: 78-87.

Rebelo S, Vieira SI, Esselmann H, Wiltfang J, da Cruz e Silva EF, da Cruz e Silva OAB. 2007b. Tyr687 dependent APP endocytosis and Abeta production. J Mol Neurosci 32:1-8.

Rebelo S, Domingues SCTS, Alves, R, da Cruz e Silva EF, da Cruz e Silva, OAB. 2008. Reticulon 3–B, a novel APP binding protein that favours non-amyloidogenic processing (in preparation).

Rebelo S, Domingues SCTS, Vintém APB, Vieira SI, Fardilha M, Esteves LC, Wu W, da Cruz e Silva EF, da Cruz e Silva OAB. 2008. FE65 is the bridging protein between APP and PP1 in a trimeric complex. Mol and Cell Neurosci. (submitted).

ABBREVIATIONS

aa	Amino acid
Aβ	Abeta
AD	Alzheimer's disease
ADAM	A desintegrin and metalloproteinase
AICD/AID	APP intracellular domain
ANOVA	One way analysis of variance
AP	Amyloid plaque (same as senile plaque)
APH-1	Anterior pharynx defective 1
APLP1/2	APP-Like Protein 1/2
APP	Alzheimer's Amyloid Precursor Protein
APPL	Drosophila APP homolog
APL-1	*C. elegans* APP homolog
APP-GFP	APP695-GFP fusion constructs or proteins
ApoE	Apolipoprotein E
ARH	Autossomal recessive hypercholesterolemia
ATP	Adenosine triphosphate
BACE	β-site APP cleaving enzyme
BCA	Bicinchoninic acid
BCIP	5-Bromo-4-Chloro-3-Indolyl phosphate
BSA	Bovine serum albumin
CAM	Cell adhesion molecule
Cdk5	Cyclin-dependent protein kinase 5
Cdk2	Cyclin-dependent protein kinase 2
cDNA	Complementary DNA
CDK	Cyclin-dependent kinase
CID	CASK interacting domain
CSF	Cerebral spinal fluid
CHX	Cicloheximide
CNS	Central nervous system
(α/β) CTF	APP Carboxy-terminal Fragment of α/β-secretase processing
DMEM	Dulbecco's Modified Eagle's Medium
DNA	Deoxyribonucleic acid
E. coli	Escherichia coli
ECL	Enhanced chemiluminescence

EDTA	Ethylenodiaminoetetraacaetic acid
EGF	Epidermal growth factor
EGFP	Enhanced green fluorescent protein
ERK	Extracellular signal-regulated kinase
ER	Endoplasmic reticulum
FAD	Familial Alzheimer's Disease
FBS	Fetal bovine serum
g	Gravitational acceleration
G	Glicine amino acid residue
G_0	Heterotrimeric (α, β, and γ subunits) G_0 protein
GFLD	Growth factor like domain
GFP	Green fluorescent protein
GSK	Glycogen synthase kinase
GTP	Guanosine triphosphate
HEPES	4-(2-HydroxyEthyl)-1-PiperazineEthane sulfonic acid
h	Hour
IgGs	Immunoglobulins G
JIP	JNK interacting protein
Kai1	"Kang ai" (Chinese for anticancer) protein 1
KLC	Kinesin light chain
KPI	Kunitz-type serine proteinase inhibitor
LB	Luria broth media
LTD	Long-term depression
LTP	Long-term potentiation
LRP	LDL receptor-related protein
MAPK	Mitogen-activated protein kinase
MDCK	Madine-Darby Canine Kidney cell line
MENA	Mammalian enabled
MID	Munc18- interacting domain
min	Minute
mm	Milimeters
mRNA	Messenger ribonucleic acid
NBT	Nitro blue tetrazolium
NFTs	Neurofibrillary tangles
NICD	Notch intracellular domain
NMR	Nuclear magnetic resonance spectroscopy
PAGE	PolyAcrylamide gel electrophoresis

PBS	Phosphate buffer saline (modified Dulbecco's)
PCR	Polymerase chain reaction
PDBu	Phorbol dibutyrate
pEGFP	EGFP-encoding mammalian expression plasmid vector
PEN-2	Presenilin enhancer
PHFs	Paired helical filaments
PKC	Protein kinase C
PM	Plasma membrane
PMA	Phorbol 12-myristate 13-acetate
PSEN1/2	Presenilin 1 and 2
PP1/2	Protein phosphatase type 1/2
PTB	Phospho tyrosine binding
Q/Gln	Glutamine amino acid residue
RER	Rough endoplasmic reticulum
RIP	Regulated intramembranar proteolysis
rpm	Rotations per minute
RT-PCR	Reverse transcriptase-polymerase chain reaction
RT	Room temperature
S/SerXXX	Serine amino acid residue at position XXX
(α/β)sAPP	Secreted APP of α/β-secretase processing origin
SAM	Substrate adhesion molecule
SDS	Sodium dodecyl sulfate
sec	Second
SEM	Standard error of the mean
SH2	Src homology 2
T/ThrXXX	Threonine amino acid residue at position XXX
TACE	Tumor necrosis factor-α converting enzyme
TBS	Tris buffered saline
TBS-T	TBS supplemented with Tween detergent
TEMED	N,N,N',N'-tetramethylethylenediamine
TGN	Trans-golgi network
Tip60	Tat interactive protein, 60 kDa
TMD	Transmembrane domain
TR	Transferrin receptor
Tris-HCl	Tris (hydroxymethyl)-aminoethane chloride
UV	Ultraviolet light
UV-DDB	UV-damaged DNA-binding

WR	Working reagent
Wt	Wild-type
Y/Tyr	Tyrosine amino acid residue
Y687E	APP Tyrosine 687 mutated to glutamate
Y687F	APP Tyrosine 687mutated to phenylalanine
Y2H	Yeast two-hybrid
Y3H	Yeast tri-hybrid

CHAPTER I

CHAPTER I

GENERAL INTRODUCTION

1.1 ALZHEIMER'S DISEASE

Alzheimer's disease (AD), the most common age-related dementia, is characterized by progressive and insidious neurodegeneration of the central nervous system leading to gradual decline in cognitive function that ultimately leads to dementia. AD represents more than 50% of all dementia cases and is the most frequent human disorder featuring accumulation of abnormal proteins in the brain. It was first described by Alois Alzheimer in 1906 after characterization of a patient named Auguste D., who suffered from strong jealousy towards her husband, increased memory impairment, disorientation, hallucinations and aggressive behaviour. After four and half years of rapid deteriorating mental illness, August D. died in a completely demoted state. This disease, bearing his name, largely remained an enigma until the end of the 20th century.

United Nations population projections estimate that the number of people older than 80 years will be 370 million by the year 2050. Currently, it is estimated that 50% of people over the age 85 are afflicted with AD. Therefore, if these predictions hold true, in 50 years, more than 100 million people worldwide will suffer from this dementia. The vast number of individuals requiring constant care and other services will severely strain medical, monetary and human resources (Chang and Suh 2005). Nowadays AD affects 20 million people worldwide (Selkoe and Schenk 2003), and it is estimated that approximately 55 000 people are affected in Portugal.

1.2 NEUROPATHOLOGICAL HALLMARKS OF AD

Brains of AD patients are characterized by cortical atrophy in the form of gyral shrinkage, widening of the sulci and enlargement of the ventricles. The first regions to be affected are the hippocampus and the entorhinal cortex (Figure 1; Braak and Braak 1994).

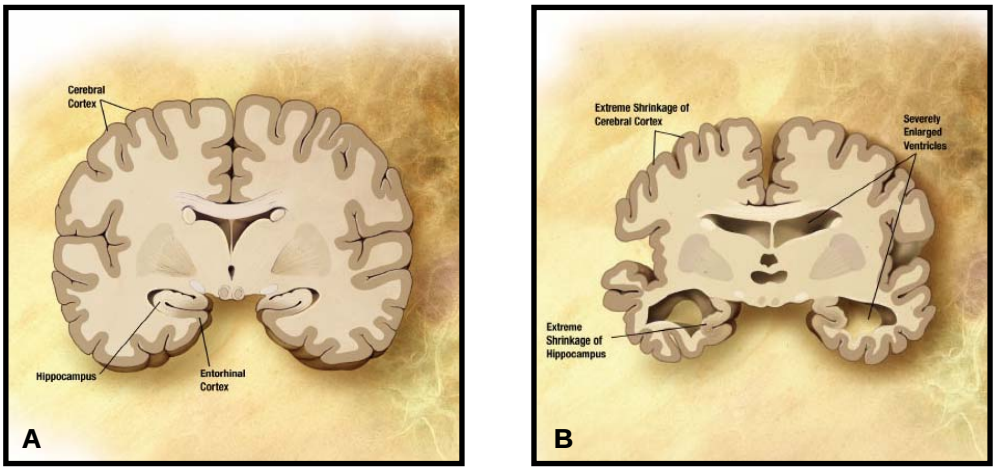

Figure 1. Normal brain (A) and Alzheimer's brain (B) (taken from http://images.google.pt).

Moreover, with disease progression, a pronounced neurodegeneration occurs in the temporal and parietal lobes. The frontal and occipital lobes may also be affected in some patients. The key neuropathological features of AD detected by microscopy are: the presence of intracellular neurofibrillary tangles (NFTs), extracellular amyloid plaques, neuronal cell death and synaptic degeneration. The origin and the role of the neurofibrillary tangles and amyloid plaques are quite different, although both lead to degeneration.

The NFTs are composed of paired helical filaments (PHFs), aggregates of abnormally phosphorylated tau protein which accumulate in the cytoplasmic compartment of neurons and are primarily found in the pyramidal regions of amygdala, hippocampus and neocortex (Figure 2). Tau is a microtubule-associated protein that regulates cytoskeleton structure. When highly phosphorylated, tau is sequestered into paired helical filaments and causes disruption of microtubules, that ultimately leads to cell death.

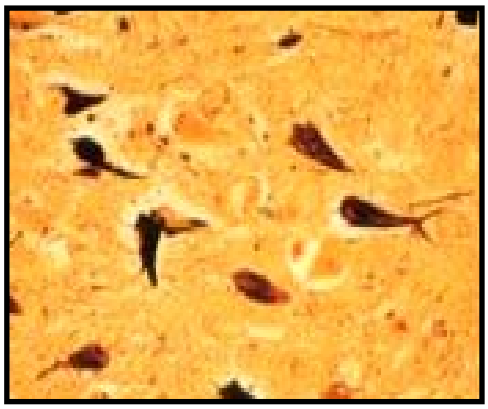

Figure 2.Neurofibrillary tangles (NFTs). The NFTs are composed of paired helical filaments (PHFs) (taken from http://images.google.pt).

In brains of AD patients, neurofibrillary tangles can also appear as ghost cells, having the shape of dead neurons. The density of NFTs correlates well with the loss of cells and synapses and also with the neuropathological disease stage. Tau, belonging to the family of microtubule-associated proteins is required for initiation and stabilization of neuronal microtubules through tubulin binding. More than 40 different phosphorylation sites on tau have been identified, mainly on serine and threonine residues followed by proline (Grundke-Iqbal et al. 1986).These sites are phosphorylated by several kinases (e.g. glycogen synthase kinase 3β, GSK-3β) and seem to confer different functional properties to tau. Furthermore, phosphorylation of tau by protein kinases such as the neuron-specific cyclin dependent kinase 5 (cdk5) precedes the formation of PHFs that causes neurodegeneration (Noble et al. 2003). In AD, tau is hyperphosphorylated, causing impaired microtubule function and leading to a fatal breakdown of the neuronal cytoskeleton.

The classical amyloid plaques (APs; Figure 3), can also be called as senile plaques. They consist of a central amorphous core that can be identified by histopathological stains such as Congo red and Thioflavin T. The core is surrounded by neuronal and glial processes. Moreover, amyloid plaques are found diffusely throughout the brain, but notably in the central cortex and hippocampus of AD patients (El Khoury 1996; Noble et al. 2003)

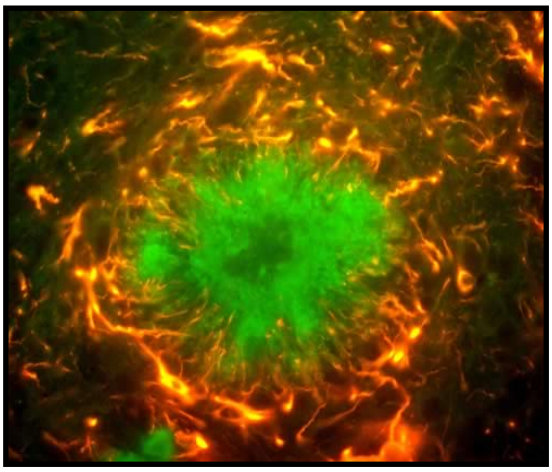

Figure 3. Amyloid plaque (AP). The major component of the AP is the Abeta peptide (taken from http://images.google.pt).

The major proteinaceous component of these deposits is a 40-42 amino acid aggregated polypeptides termed Abeta (Abeta$_{1-40}$ and Abeta$_{1-42}$), derived by proteolytic cleavage from the larger Alzheimer's Amyloid precursor protein (APP) (Glenner and Wong 1984; Masters et al. 1985). The majority of Abeta peptides are 40 amino acids long (Abeta$_{1-40}$), soluble and apparently less neurotoxic, whereas the more hydrophobic peptides (less soluble) are 42 amino acids long (Abeta$_{1-42}$) and although they are less prevalent, overall they predominate in the protein core of plaques (Jarrett et al. 1993; Jarrett and Lansbury 1992). Diffuse plaques, which are focal diffuse deposits of amyloid without accompanying dystrophic neurites, and that may represent an early stage of AD plaques, contain predominantly Abeta$_{1-42}$ and low levels of Abeta$_{1-43}$ rather than Abeta$_{1-40}$ (Gowing et al. 1994; Iizuka et al. 1995; Iwatsubo et al. 1995; Iwatsubo et al. 1994; Lemere et al. 1996).

The term "soluble Abeta" generally is applied either to the newly generated, cell-secreted Abeta or to the fraction of tissue or synthetic Abeta that is taken into aqueous phase of a non-detergent-containing extraction buffer. "Misfolded" and aggregated" Abeta are terms used to describe very early, nonspecific changes in Abeta

folding states or solubiltity sates, respectively. "Oligomeric" Abeta refers to peptide assemblies with limited stoichiometric (e.g. dimmers, trimers, etc.), while protofibrils (PFs) are structures of intermediate orther between aggregates and fibrils. The term "Abeta-derived diffusible ligands" (ADDLs) is also applied to pre-protofibrillar intermediates (Figure 4). Indded, oligomers, PFs and ADDLs are believed to be the assembly states of Abeta with the most potent toxicity and also that are the proximate mediatotors of Abeta induced neurotoxicity, specially in neuronal cultures models (Kayed et al. 2004; Klein et al. 2001). The final assemblies, called fibrils, are the basic building blocks of the amyloid plaque (Figure 3) and are so named because of their characteristic ultrastructural appearance.

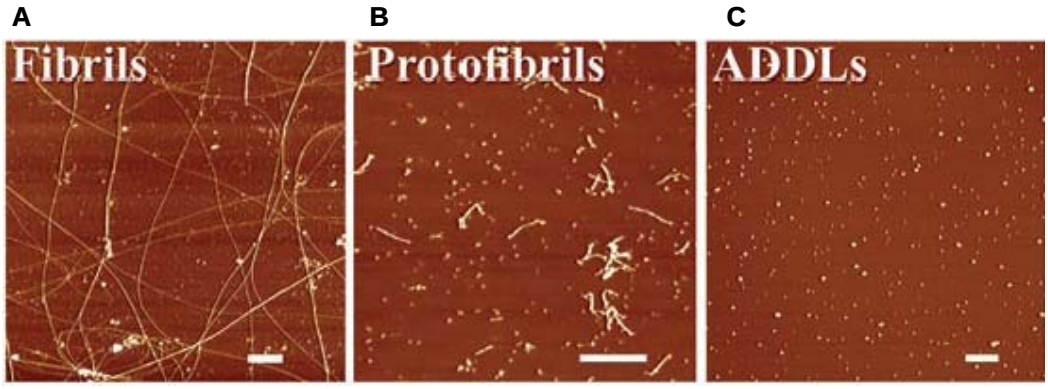

Figure 4. Different assembly (biophysical) states of Aβ. The assembled forms obtained from incubation of synthetic Aβ are highly sensitive to preparation and incubation. Widely differing proportions of insoluble fibrils (A), soluble PFs (B), and oligomers (C), also known as ADDLs are revealed by atomic force microscopy. Scale bars: 200 nm. (Adapted from Gandy 2005).

Several other components, such as proteoglycans, inflammatory molecules and apolipoprotein E have also been identified in plaques.

Amyloid vs NFTs. Evidence points to amyloid deposition preceding and leading to the formation of NFTs in some patients, with Abeta preceding Tau aggregation. In agreement with this, Tau deposition in transgenic mice is influenced by Abeta (Lewis et al. 2001; Stalder et al. 1999). In young Down's syndrome patients, Abeta deposits exist in the absence of NFTs, notably in areas of the brain most affected by AD (Gouras et al. 2000b; Iwatsubo et al. 1995; Leverenz and Raskind 1998). Typically, these two aggregates (APs and NFTs) constitute the neuropathologic criteria confirming AD. Post-mortem brain autopsy is still the most accurate and

definitive means of diagnosing AD (Crimson and Eggert 1999) but the patient's death often occurs long after the onset of the dementia. Consequently, the relationship between the pathology and the actual mechanism of the disease remains unclear.

1.3 GENETICS OF ALZHEIMER'S DISEASE

It is now widely accepted that genes play an essential role in predisposing to AD onset and in modifying the progression of the disease. Thus, AD can be classified into several subgroups. Familial (FAD) versus sporadic AD are grouped according to the occurrence or absence of other demented persons in the family. AD has also been divided into early versus late-onset AD, depending on whether the patient presented the first symptoms before or after the age of 65 years. However, the pathological hallmarks of different forms of AD seem to be the same, inspite the the difference in the genetic background. Approximately 10% of all familial Alzheimer's disease cases are inherited in an autossomal dominant Mendelian pattern (Selkoe and Podlisny 2002). Other familial cases and sporadic AD have more complex modes of inheritance. Besides age as the main risk factor, a number of susceptibility genes were found which contribute to the occurrence of sporadic AD.

A. Early-onset AD:

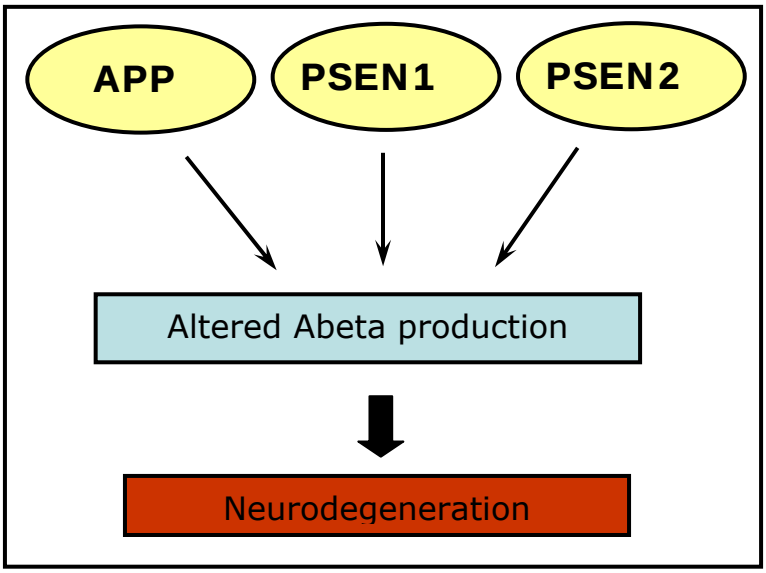

B. Late-onset AD:

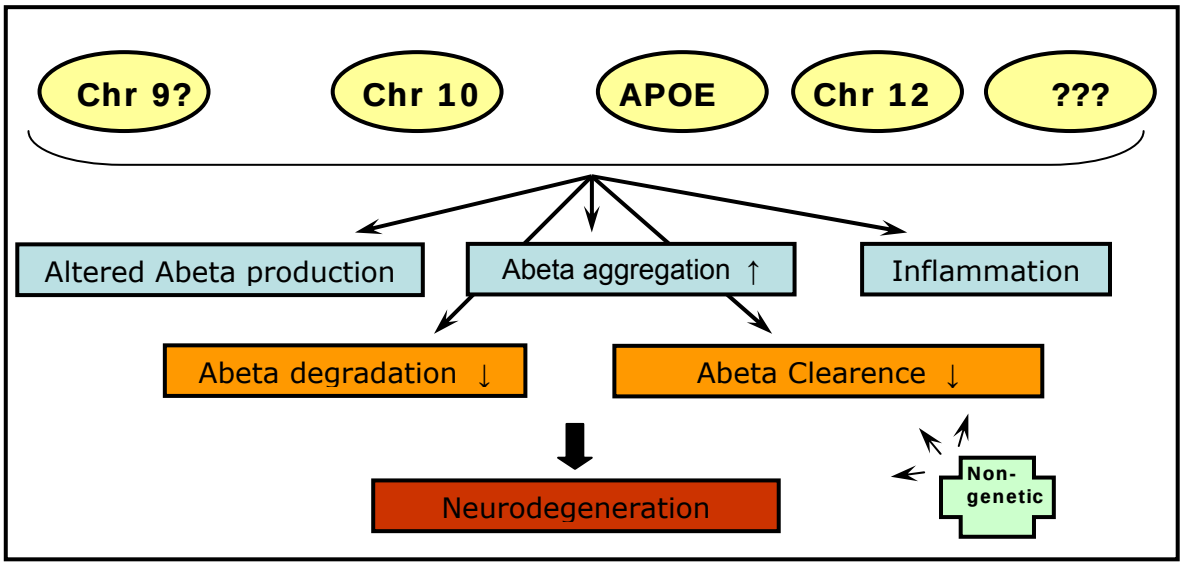

Figure 5. Scheme of contribution and interaction of the known and putative AD related genes. A. Mutations in the early-onset AD genes: APP, PSEN1 and PSEN2 all lead to an increase in Abeta production. **B.** Representation of the interaction of known and proposed late-onset AD genes. These risk-factor genes are each likely to affect one or more of the known pathogenic mechanisms resulting in neurodegeneration. Their effects are further influenced by gene-gene interactions and the contribution from non-genetic risk-factors (Adapted from Bertram and Tanzi 2004).

To date, three genes responsible for familial AD have been identified: APP gene, Presenilin 1 gene (PSEN1) and Presenilin 2 gene (PSEN2) (Table 1 and Figure 5A). Pathogenic mutations in these genes account for up to 50% of familial cases of early-onset AD. If one of the genes is mutated, the gene product leads to the development of AD with almost always 100% penetrance. Together, these mutations are estimated as less than 1% of the total number of AD cases (Delacourte et al. 2002).

Table 1. Overview of Alzheimer's disease genes, their incidence and functional relevance to AD pathogenesis. Chromo., Chromosome location

Gene	Chrom. location	Mode of inheritance	Number of pathogenic mutations	Mean Familial onset age	Revelance to AD pathogenesis
APP	21q21.3	Autossomal-dominant	18	51.5 years	Increase in Aβ: ($A\beta_{42}/A\beta_{40}$ ratio)
PSEN1	14q24.3	Autossomal-dominant	142	44.1 years	Increase in Aβ: ($A\beta_{42}/A\beta_{40}$ ratio)
PSEN2	1q31-42	Autossomal-dominant	10	57.1 years	Increase in Aβ: ($A\beta_{42}/A\beta_{40}$ ratio)
APOE (ε4-allele)	19q13.32	Complex (risk increased)	n.a.	Onset-age modifier	Increase in Aβ Aggregation

1.3.1 APP hereditary mutations

So far, 18 mutations of the APP gene (Table 1; chromosome 21) have been described in AD families with early onset and autosomal dominant inheritance from different parts of world (Alzheimer Disease and Frontotemporal Dementia Mutation Database, available at http://www.molgen.ua.ac.be/AD). The first mutation discovered in the APP gene was Glu^{22} to Gln within the Abeta sequence and was termed the "Dutch mutation" (Figure 6) (Hardy and Allsop 1991). Synthetic peptides containing this mutation were shown to have an increased propensity to aggregate (Clements et al. 1993; Wisniewski et al. 1991). Furthermore, some British families with early-onset AD were found to have pathogenic mutations at positions 642 of APP (APP_{695} numbering) resulting in a change from Val^{642} to Ile, Gly or Phe (Figure 6; (Chartier-Harlin et al. 1991; Goate et al. 1991; Murrell et al. 1991). This mutation was named the "London mutation". These APP mutations were all shown to result in an increase in the relative amounts of long $Abeta_{1-42}$ compared with $Abeta_{1-40}$ (increased $Abeta_{1-42}$/$Abeta_{1-40}$ ratio). Being that synthetic $Abeta_{1-42}$ aggregates more readily in vitro than $Abeta_{1-40}$ (Burdick et al. 1992), suggests that these mutations directly affect amyloid deposition, in this case by diverting the proteolytic processing of APP towards the production of the longer, more amyloidogenic forms of Abeta. The Swedish double mutation (Lys^{595} and Met^{596} are mutated to Asn and Leu; Figure 6) resulting in increased secretion of Abeta, presumably through enhanced cleavage at the β-secretase site (Cai et al. 1993; Citron et al. 1992).Thus, familial pedigrees have been identified worldwide, and the geographical origin of the initial discovery is often used to name the mutant molecule. A recently discovered pathogenic mutation, found in AD patients from northern Sweden, near the Arctic circle, was named of Artic mutation and effectivelly decreases the levels of total Abeta production and the molecules that are generated have increased propensity to oligomerize (Nilsberth et al. 2001; Paivio et al. 2004). The number of carriers of the various mutations may differ across clinical populations. In the general population, not more than 0.5% of early-onset AD patients carry a mutation in the APP gene (Sleegers and Van Duijn 2001). Amoung all AD patients, not more than 0.005% carry a mutation in APP.

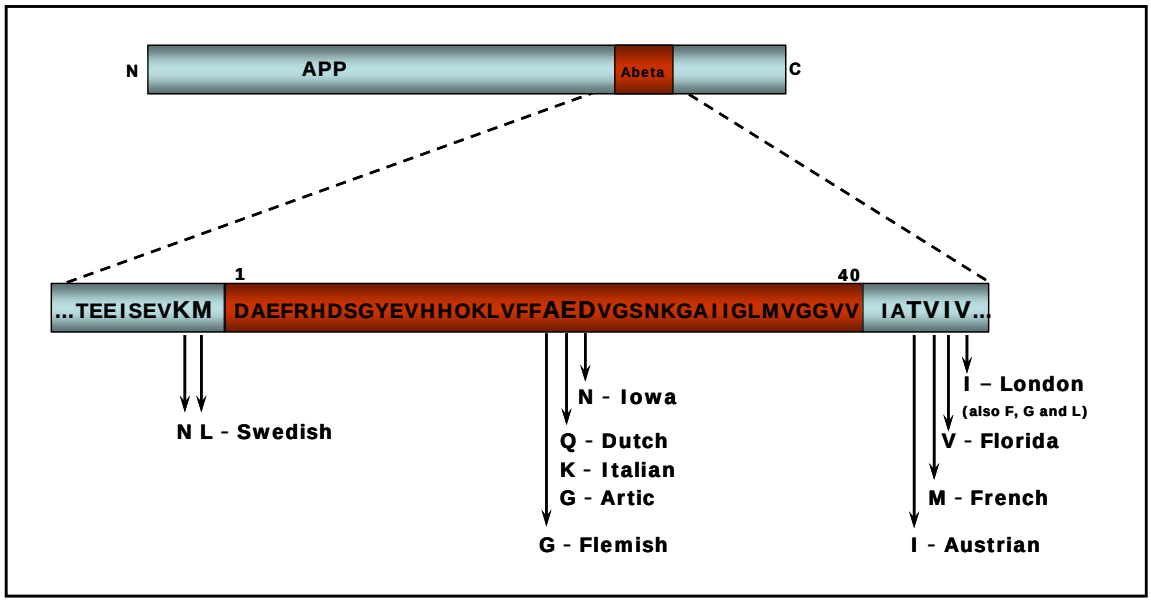

Figure 6. APP mutations. Abeta region showing the pathogenic APP mutations (residues are numbered according to APP_{695} or the Abeta position).

1.3.2 PSEN hereditary mutations

Mutations in two other genes have been found to lead to early-onset autosomal dominant forms of AD (Table 1). The *presenilin-1* (*PSEN1*) and *presenilin-2* (*PSEN2*) genes were localized using linkage analysis (Levy-Lahad et al. 1995; Sherrington et al. 1995). These genes encode proteins that are involved in the normal cleavage of the APP protein, increasing the production of $Abeta_{1-42}$ (Citron et al. 1997; Xia et al. 1997).However, the PSEN1 sequence does not point to a specific enzymatic activity for this protein, it may play a role as chaperone in the γ-secretase complex that includes other proteins like nicastrin. This molecule was identified in association with PSEN1 and influences APP metabolism (Yu et al. 2000). A total of 142 mutations have been found in PSEN1 in 281 families (Table 1; http://molgen-www.uia.ac.be/ADMutations/). This is the gene with highest number of pathogenic mutations in AD. For PSEN2, 10 mutations have been found in 16 families (Table 1). In the general population, mutations in the presenilin genes explain about 7.5% of early-onset AD (6.5% for *PSEN1* and 1% for *PSEN2*). When considering all patients, both early and late onset, sporadic and familial cases, the presenilin genes explain less than 0.075% of the cases (Sleegers and Van Duijn 2001). PSEN mutations may disturb protein

interactions in the complex through subtle conformational alterations (Cruts et al. 1998). The effects of PSEN1 and PSEN2 mutations on Abeta levels have been analysed in cellular models and in biological samples from patients. Overproduction of $Abeta_{1-42}$ was found in the media of several cell types co-transfected with PSEN1 and APP cDNA in wild-type or mutated form. The expression of mutated PSEN1 or PSEN2 leads to a 1.5-5 fold increase in the concentration of $Abeta_{1-42}$ in the media compared to cells expressing wild-type PSEN1 and 2.

1.3.3 APOE

Apolipoprotein E (APOE) was identified as a risk factor or a susceptibility gene for AD in 1993 (Table 1; Strittmatter et al. 1993). APOE plays a major role in lipoprotein metabolism and cholesterol homeostasis in the brain (Mahley 1988). The relationship between APOE and AD has been confirmed in more than 100 studies conducted in diverse ethnic backgrounds (Farrer et al. 1997). There are three isoforms of the protein: E2, E3 and E4, which are encoded by three different alleles ε2, ε3 and ε4 (Kowalska et al. 1998). Carriers of the APOE ε4 allele are at higher risk of developing AD in a dose dependent manner (Kowalska et al. 2003). Thus, homozygotes for the APOE ε4 allele usually develop AD at an earlier age than heterozygotes (Corder et al. 1993). However, the presence of the APOE ε4 allele is neither necessary nor sufficient to develop AD. Moreover, there is a strong evidence of the role of APOE in AD. This gene has been implicated in different pathophysiological pathways leading to neurodegeneration, including $Abeta_{1-42}$ deposition and antioxidative stress (Lahiri and Greig 2004). Neuropathological studies using brain tissues in AD patients have shown a higher density of neuritic plaques and neurofibrillary tangles in APOE ε4 carriers (Tiraboschi et al. 2004). Biochemical studies have demonstrated that the APOE protein can bind both the $Abeta_{1-42}$ and tau protein. Furthermore, transgenic knock-out mice expressing human APOE ε4 have an imparment in cognitive function and also show neuropathological changes. Finally, higher levels of APOE expression have been associated with AD in several studies (Strittmatter et al. 1993). However, the exact mechanism by which the APOE gene increases the risk of AD remains to be determined. On the population level, the APOE ε4 allele plays an important role, explaining up to 17% of all patients.

It has been suggested that as much as 50-60% of all AD cases might be genetically influenced by different susceptibility genes, such as IL-1, tumor necrosis factor and α2-macroglobulin (Daw et al. 2000). Recently new susceptibility loci for late AD have been identified on chromosomes 1, 9, 10, 12 and 13 (Figure 5B; Bertram and Tanzi 2004; Blacker et al. 2003).

1.4 THE "AMYLOID CASCADE" OF AD ETIOLOGY

The "amyloid cascade hypothesis" of AD (Figure 7), which is now widely accepted, describes the pathogenesis of this disease as a cascade of several steps, from the initial generation of the Abeta peptide to cognitive impairment and neuronal loss. Thus, several lines of evidence suggest that the small pepide Abeta is central to the progression of the disease. Firstly, genetic studies in cases of familial AD have demonstrated that over 150 mutations in three autosomal dominant genes: *APP*, *PSEN1* and *PSEN2* are associated with increased production of Abeta peptides by altering the proteolytic processing of APP (Robakis and Pangalos 1994). Secondly, Down's syndrome (trisomy 21) patients with three copies of APP, deposit increased levels of Abeta peptide resulting in amyloid plaque deposition and dementia (Holtzman et al. 2000). Thirdly, the APOE ε4 genotype is a significant risk factor for developing late-onset AD, and has been shown to modulate both levels of Abeta peptide and the aggregation state and clearance of the peptide (Walsh et al. 2002). Finally, multiple reports have demonstrated the neurotoxic effects of fibrillar and soluble oligomeric species of Abeta peptides both *in vitro* and *in vivo* (Lammich et al. 1999). Irrespective of the cause (or toxic Abeta species), it is likely that during the disease process the balance between Abeta production and Abeta catabolism is altered, resulting in the slow accumulation of toxic Abeta species, amyloid deposition in the brain, and ultimately neuronal dysfunction and degeneration.

At the molecular level, diffuse neurocentric amyloid deposits would progress over time and eventually become neuritic amyloid plaques. One hypothesis is that deposition of $Abeta_{1-42}$ may form a "precipitation core" to which soluble $Abeta_{1-40}$ could aggregate, in an AD-specific process. The "in vivo" aggregation of Abeta may precipitate a chronic and destructive inflammatory process in the brain, occurring in the immediate vicinity of amyloid plaques in AD patient brains (Eikelenboom et al. 1994). Some of the proinflammatory molecules thereby produced may be locally toxic to neuronal processes in the vicinity of the amyloid plaque, such as complement, cytokines, reactive oxygen and nitrogen intermediates. They also produce factors, such as Interleukin-1 (IL-1), which stimulate APP synthesis, leading to a vicious cycle of reciprocal activation and growth, which potentiates a local inflammatory cascade. These would culminate in the neurodegenerative process possibly via free radical production by microglia cells and/or complement lysis of neuronal membranes (Allsopp 2000). Although it is not clear if Abeta accumulation is a cause or effect in AD, its production nonetheless plays a central role.

AMYLOID CASCADE HYPOTHESIS:

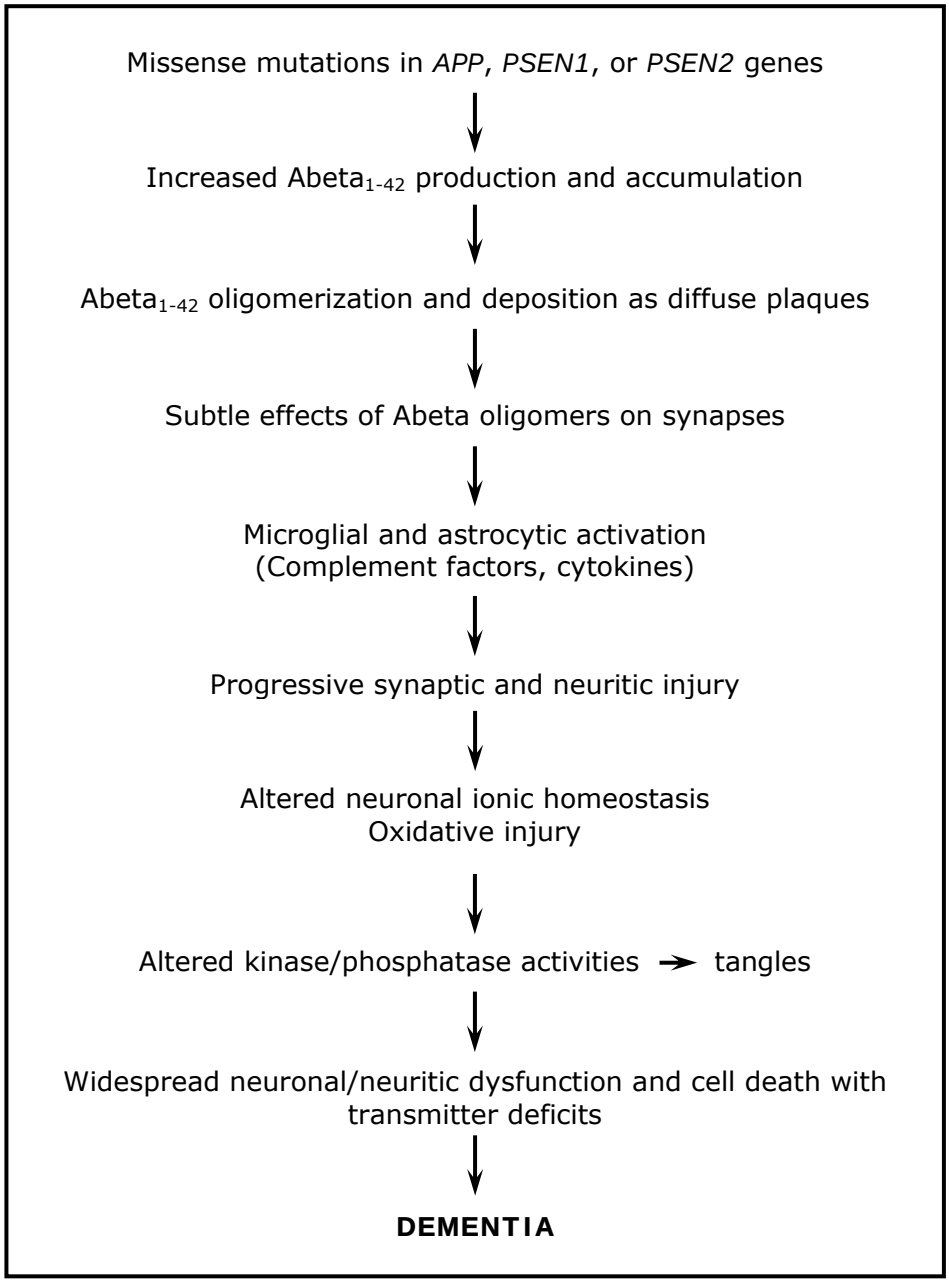

Figure 7. The sequence of pathogenic events leading to AD was proposed as amyloid the cascade hypothesis. The cascade is initiated when the Abeta$_{1-42}$ is generated. In familial early onset AD, the Abeta$_{1-42}$ is overproduced as a result of pathogenic mutations. In sporadic AD, various factors can contribute to an increased load of Abeta$_{1-42}$ oligomers and their aggregation (Adapted from Citron 2004; Hardy and Selkoe 2002).

1.5 THE ALZHEIMER'S AMYLOID PRECURSOR PROTEIN

1.5.1 Gene family

APP and related family members, amyloid precursor like protein-1 and -2 (APLP-1 and APLP-2), are homologous type-I transmembrane proteins (Selkoe 2001) that are similarly post-translationally modified and processed, as well as having overlapping expression in brain (Bayer et al. 1999). The nearest relative to APP is APLP-2, sharing 50% homology. Thus, these three proteins are well-conserved in evolution, functionally and structurally related, and probably share similar functions (Bayer et al. 1999; Coulson et al. 2000). Moreover, knockout mice studies reveal a functional redundancy among APP family members but knockout of all three genes simultaneously, or of APLP-2 and APP, is lethal in utero (Heber et al. 2000). Structurally, the mammalian APP family members possess a single transmembrane domain, as well as a large extracellular domain and short intracellular domain. Of note is that APLP-1 and APLP-2 share homology at the amino acid sequence, domain structure and protein organization with APP, but lack the Abeta domain. Moreover, because of the high degree of homology in the N-terminal region between APLP's and the amyloidogenic APP isoforms, some N-terminal antibodies recognizes both APP and APLP's (Slunt et al. 1994; Webster et al. 1995).

Other members of the APP superfamily have been identified in non-mammalian species and include APPL in *Drosophila* (Luo et al. 1992; Rosen et al. 1989), APL-1 in *C. elegans* (Daigle and Li 1993) and an APP homologue protein in *Xenopus* (Okado and Okamoto 1992).

1.5.2 Isoforms

The APP gene is located on human chromosome 21 (21q21.2-3) and contains 18 exons (GenBank A.N. D87675), with the Abeta sequence divided between exons 16 and 17 (Figure 8). The sequence of the Abeta peptide starts at residue 597 (except when otherwise indicated, numbering is according to the APP_{695} isoform) and spans the extracellular and membrane domains. At least eight APP isoforms have been described, numbered according to their length in amino acids: L-677, 695, L-696,

714, L-733, 751, L-752, 770 (Kitaguchi et al. 1988; Ponte et al. 1988). These isoforms arise from alternative splicing of exons 7, 8 and 15 of the APP mRNA (Kosik 1993) and differ only in size of the extracellular domain. Analysis of APP mRNA expression levels revealed that APP can be detected in almost all tissues examined, as well as in cultured cells. It is ubiquitously expressed in mammalian cells (Golde et al. 1990; Neve et al. 1988; Sisodia and Price 1995; Tanzi et al. 1987; Tanzi et al. 1988) with a broad tissue distribution. The tissue-specific pattern of APP mRNA splicing was studied by RT-PCR analysis (Sandbrink et al. 1994a). The less abundant L-APP isoforms, lacking exon 15, are mainly expressed in leukocyte cells, such as T-lymphocytes, macrophages and microglial cells. They are also ubiquitously expressed in rat tissues, including brain, but not in neurons (Ohgami et al. 1993; Sandbrink et al. 1994a).

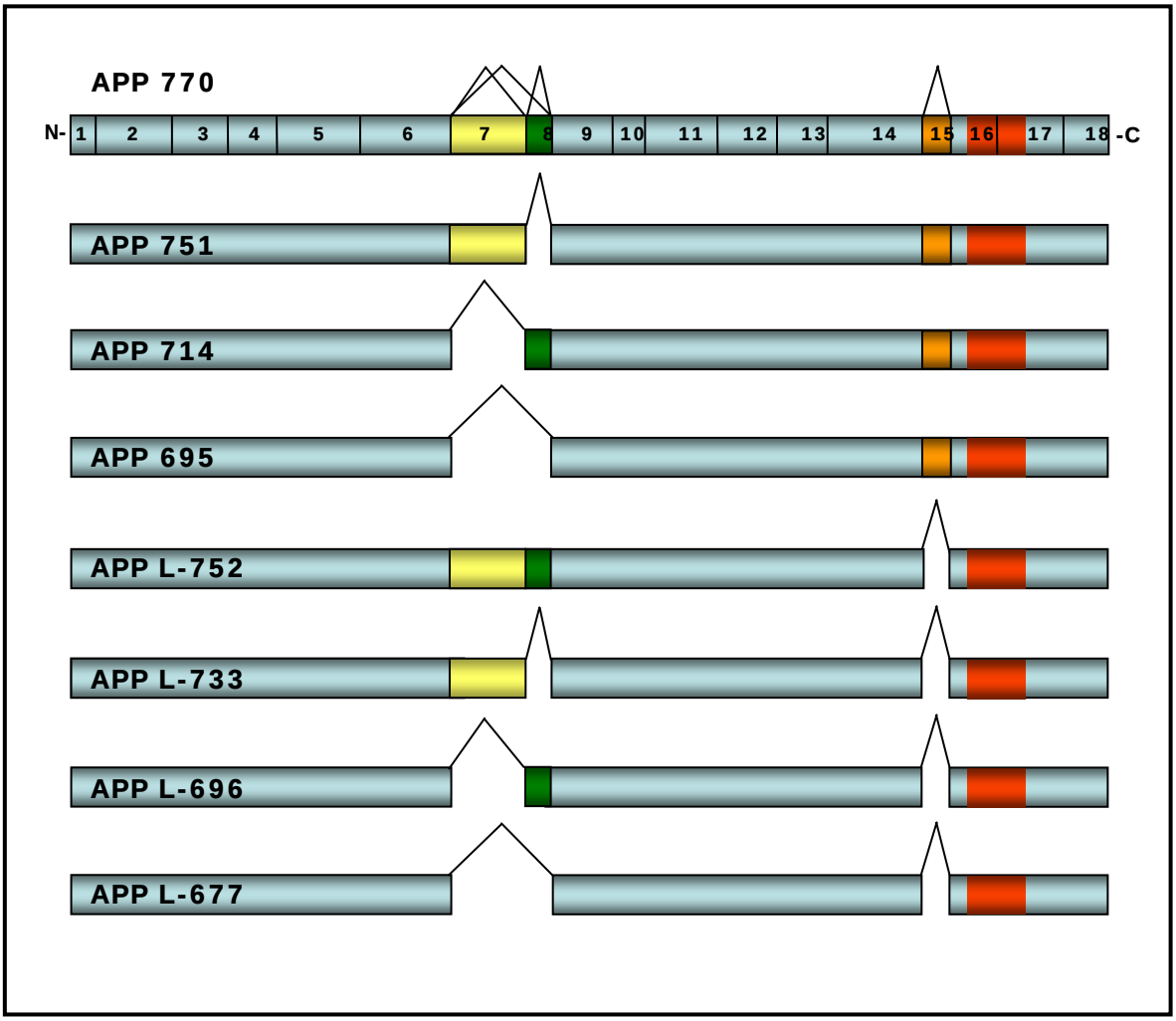

Figure 8. Exon structure of the full length APP transcript and the final eight isoforms. The alternatively spliced exons are indicated in colour: yellow, exon 7; green, exon 8; orange, exon 15. The Abeta sequence is indicated in red.

The three major APP isoforms were found to be the 695, 751 and 770 (Figure 8). Of these, APP_{695} is the only one lacking exon 7. The exon 7-containing APP mRNA isoforms (751 and 770) are predominantly expressed in peripheral tissues. Brain tissue expresses little APP_{770} and, depending on the animal species and brain region analysed, low, intermediate or high levels of APP_{751} (Kang and Muller-Hill 1990; Konig et al. 1989; Neve et al. 1988; Tanaka et al. 1989). However, the exon 7-containing isoforms predominate in cultured astrocytes (Gray and Patel 1993a; Gray and Patel 1993b; Rohan de Silva et al. 1997), with the 695:751:770 ratio being 1:4:2 (Gray and Patel 1993a; Gray and Patel 1993b). A number of studies have indicated that alternative splicing of exons 7 and 8 changes in brain with aging and in AD, but results obtained are still inconsistent and controversial to consider altered alternative splicing as an AD risk factor (Moir et al. 1998; Panegyres et al. 2000; Rockenstein et al. 1995; Sandbrink et al. 1994b). Conversely to the 751 and 770 isoforms, the 695 is the APP isoform predominantly produced in the mammalian brain, with the 695:751:770 mRNA ratios being approximately 20:10:1 (Tanaka et al. 1989). Furthermore, APP_{695} is most highly expressed in neurons, representing 95% of total neuronal APP (LeBlanc et al. 1991; Tanzi et al. 1987; Weidemann et al. 1989), and is therefore often referred to as the "cerebral" or "neuronal" isoform. In conclusion, as APP_{695} is the isoform predominantly produced in the brain, and predominates within the CNS (Neve et al. 1988; Tanzi et al. 1993), this isoform has received the most attention in AD research.

1.5.3 Functional domains

APP exon 7 encodes a 56-amino acid (aa) stretch with homologies to the Kunitz-type protease inhibitors (KPI) that inhibits proteases, such as trypsin or plasmin, and blood coagulation factors (Kitaguchi et al. 1988; Ponte et al. 1988; Van Nostrand and Cunningham 1987; Wagner et al. 1992). Exon 8 encodes a 19-aa domain with homologies to the MRC OX-2 antigen found on the surface of neurons and certain immune cells such as thymocytes (Clark et al. 1985; Kitaguchi et al. 1988; Tanzi et al. 1988). In adition to KPI and OX-2, several other structural features have been identified within the APP ectodomain (Figure 9).

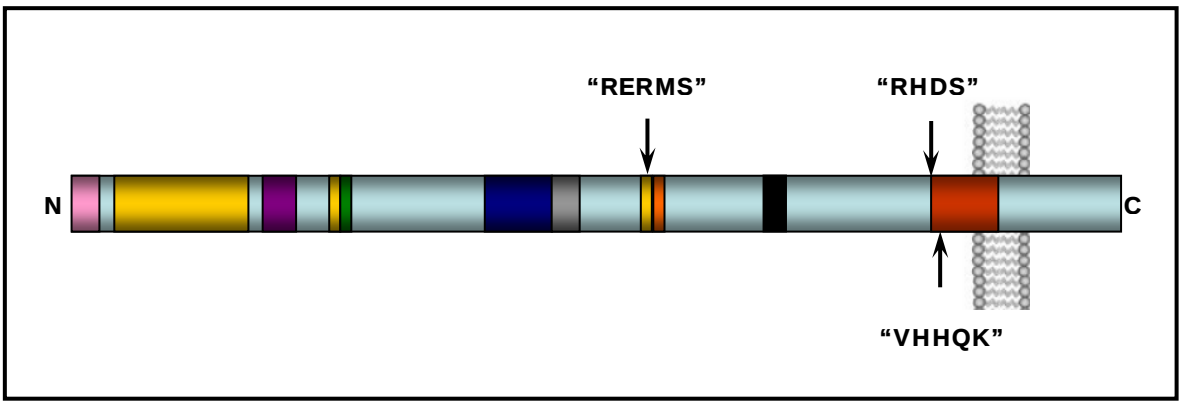

Figure 9. APP functional subdomains (APP_{770} numbering). Pink, signal peptide (1-17); yellow, heparin-binding domains (28-123; 174-185; 391-412); violet, copper-binding domain (135-155); green, zinc-binding domain (181-188); dark blue, KPI domain; grey, OX-2 domain; "RERMS", putative growth-promoting motif (403-407); orange, gelateinase A (matrix metalloproteinase) inhibitor (407-417); black, collagen-binding site (523-540); red, Abeta; "RHDS", integrin-binding motif (aa 5-8 of Abeta); "VHHQK", heparin-binding motif (aa 12-16 of Abeta).

Two subdomains (328-332 and 444-612) were deduced to have a neuroprotective function. The "RERMS" sequence with putative growth-promoting properties (Ninomiya et al. 1993). Several heparin-binding domains (Small et al. 1994), a collagen-binding site (Beher et al. 1993), an integrin-binding motif (amino acid sequence RHDS at residues 5-8 of Abeta) (Ghiso et al. 1992) and N-linked carbohydrate attachment sites (Weidemann et al. 1989) were also found in this region. Indeed, APP has been shown to bind laminin, collagen, and heparin sulphate proteoglycans (Breen et al. 1991; Kibbey et al. 1993). The ectodomain also contains two binding-sites for metals such as zinc (Bush et al. 1993; Bush et al. 1994) and copper (Hesse et al. 1994; Multhaup et al. 1996).

1.5.4 Proteolytic processing

APP is processed by three different proteases named α-, β-, and γ-secretase (Esler and Wolfe 2001) (Figure 10). Their cleavage sites were therefore named α-, β- and γ-sites. In its simplest form, APP proteolytic processing was described as occurring via two distinct pathways, one being non-amyloidogenic and the other amyloidogenic.

This classification arose as α- and β-cleavages appear to be mutually exclusive events, with one precluding and the other leading to Abeta production (Nunan and Small 2000; Small and McLean 1999).

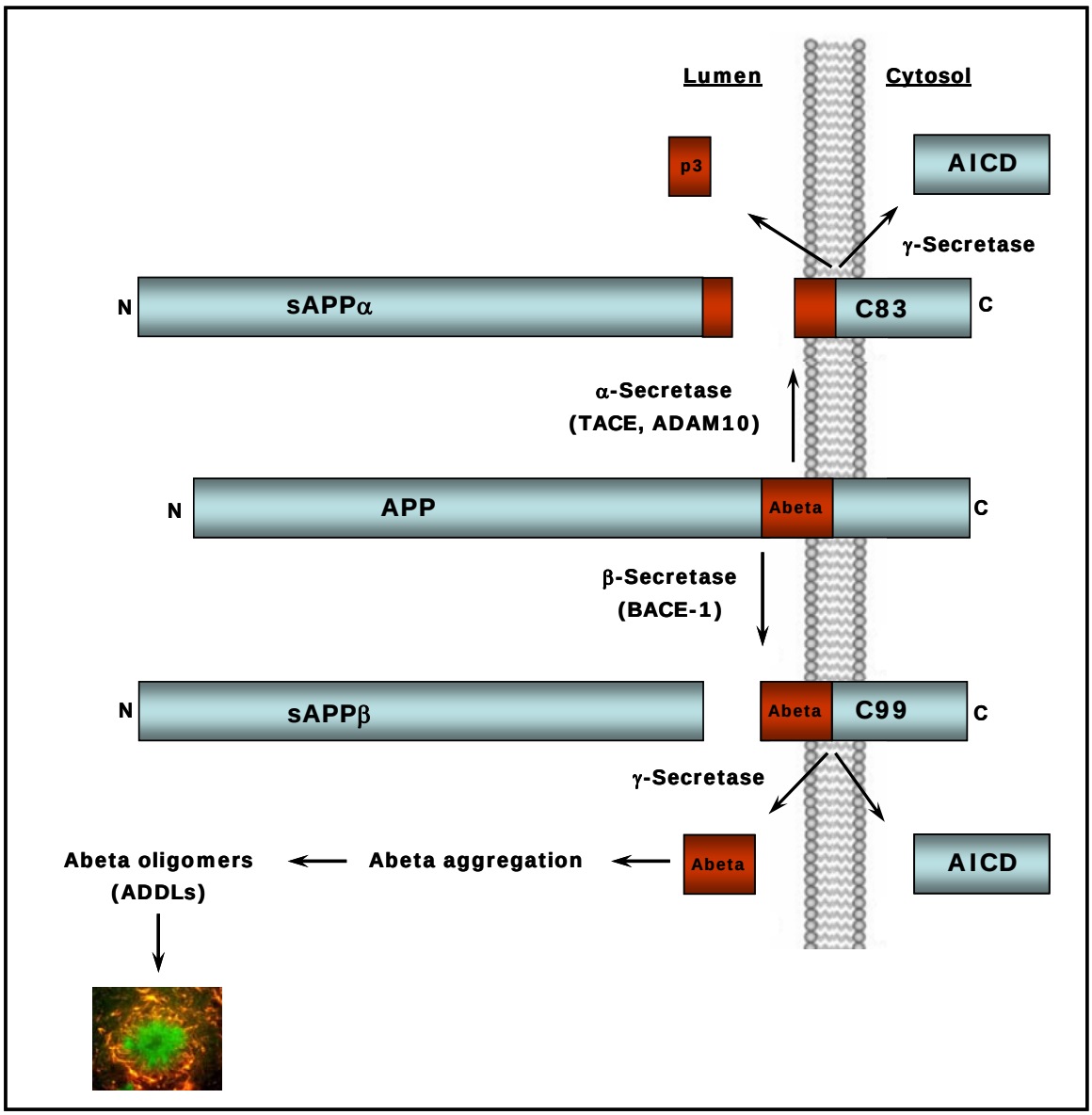

Figure 10. APP is processed by either α-secretase or β-secretase, which cleave at two different sites in the extracellular domain. Cleavage of APP by α-secretase (TACE and ADAM10) results in formation of C83, which precludes Abeta formation. After α-secretase cleavage of C83, a small peptide fragment called p3 is produced. Alternatively, by the sequential action of β-secretase (BACE1) and γ-secretase, the Abeta peptide is produced. AICD, APP intracellular domain (Adapted from Kerr and Small 2005).

α-secretase

The predominant pathway by which APP is processed does not give rise to Abeta fragments and involves the cleavage of APP by the α-secretase, and it is referred to as the non-amyloidogenic pathway (Figure 10). Moreover, once cleaved by α-secretase, APP can no longer be processed to form Abeta by other enzymatic pathways. This suggests that the processing of APP by this pathway not only does not lead to AD, but may also be neuroprotective. The α-secretase cleaves APP within the Abeta sequence, between lysine 16 and leucine 17 and produces a secreted form of APP (sAPPα) of 105-125 KDa and an 83-residue fragment called C83, an approximately 10 KDa C-terminal fragment, which remains membrane associated. Further processing of C83 by γ-secretase yields a p3 fragment (approximately 3 KDa) and a γ-cleaved C-terminal fragment (γCTF), also known as the APP intracellular domain (AICD). The p3 peptides are not generally found in the amyloid cores of classical plaques or in amyloid deposits in cerebral vasculature. Both sAPPα and p3 are secreted by a variety of cultured cells and are found in human brain as well as in CSF (Oltersdorf et al. 1990; Palmert et al. 1989a; Palmert et al. 1989b; Schubert et al. 1989a; Schubert et al. 1989b; Selkoe et al. 1988; Weidemann et al. 1989). The trafficking of APP mainly follows the constitutive secretory route which involves α-secretase in the trans-Golgi network (Kuentzel et al. 1993; Sambamurti et al. 1992) and at the cell surface (Sisodia 1992).

In order to explore the upregulation of α-secretase activity as a therapeutical target for AD, it is essencial to identify the protease responsible for the α-secretase activity. In 1999 it was indicated that a disintegrin and metalloproteinase-10 (ADAM10) has α-secretase activity *in vitro* and in cultured cells (Lammich et al. 1999). Purified ADAM10 cleaved APP derived peptides at the α-secretase cleavage site and overexpression of ADAM10 in several cell lines resulted in increased α-secretase activity. Consistently, expression of mutated ADAM10 significantly decreased endogenous α-secretase activity. Finally, it was possible to stimulate the α-secretase activity of ADAM10 with phorbol esters, and to inhibit it by hydroxamic acid-based inhibitors for metalloproteinases. *In vivo* studies using transgenic mice which overexpress either ADAM10 or the catalytic inactive ADAM10 mutant have shown that a moderate overexpression of ADAM10 in mice transgenic human APP [V717I] increased the release of the neurotrophic N-terminal APP domain (sAPPα), reduced the formation of $Abeta_{1-40}$ and $Abeta_{1-42}$, and prevented their deposition in plaques. Functionally, impaired long-term potentiation and cognitive deficits were alleviated. Thus, ADAM10 has been found to possess both a constitutive and a regulated

secretase activity and so has been proposed as the major APP-processing enzyme in the brain (Postina et al. 2004).

A transmembrane glycoprotein, tumor necrosis factor α-converting enzyme (TACE) or ADAM17 is another member of the ADAM family that shows α-secretase activity in cellular systems.

β-secretase

A second pathway for the proteolysis of APP, referred to as the amyloidogenic pathway, involves a first cleavage by β-secretase (Figure 10). β-secretase cleaves APP at the N-terminal side of Asp_1 of the Abeta sequence. This is the major cleavage site for β-secretase, although some cleavage adjacent to Glu_{11} can also occur. Cleavage at Asp_1 results in the production of a N-terminal fragment of APP (sAPPβ) that is released from the membrane (Schubert et al. 1993) and a C-terminal membrane associated fragment called C99 (Figure 10). The C99 is processed by γ-secretase to generate predominantly $Abeta_{1-40}$ (90%) and $Abeta_{1-42}$ (10%) fragments (Haass et al. 1992; Seubert et al. 1992). Abeta species from 1-39 to 1-43 amino acids long can also be produced, with fragments appearing to be more amyloidogenic with increasing length. Moreover, using C99 as a substrate, the additional product of γ-secretase processing is a short 59/57 amino acid long C-terminal peptide, named the APP intracellular domain (AICD) or γCTF. However, gamma CTF is very unstable "in vivo" and difficult to be detected both in brain or cell lysates (Kimberly et al. 2005; Pinnix et al. 2001; Zheng et al. 2003). In fact, the CTF gamma/C59 AICD is rapidly degraded (half-life of approximately 5 min) by a mechanism that is not inhibited by endosomal/lysosomal or proteasome inhibitors (Cupers et al. 2001). By sequence analysis of the AICD fragment, researchers have found that γ-secretase cleaves APP at an additional site (ε-site) (Sastre et al. 2001), a few amino acids downstream of the γ-site (Figure 11). Although both cleavages are independent of one another, they may occur nearly simultaneously (for review see Selkoe and Kopan 2003). This ε-site cleavage is thought to occur for better AICD membranar release, and as both cleavages render an AICD peptide of 50 aa long, it was unknown which AICD peptide (C59/57 or C50) was physiologically functional (Selkoe and Kopan 2003). Nonetheless, evidence points to the C50 AICD as the physiologically functional peptide (von Rotz et al. 2004).

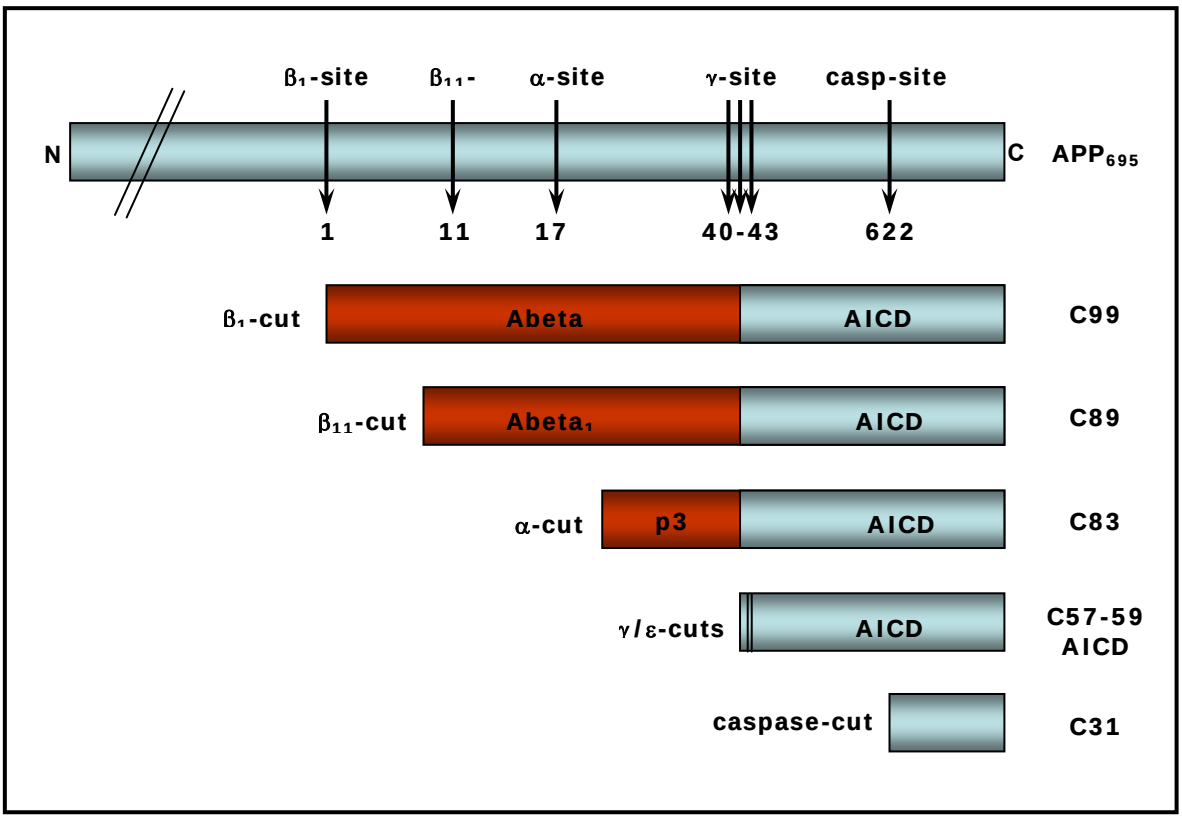

Figure 11. Schematic representation of the progressive cleavage of APP by α, β, γ-secretases. The fragments generated by proteolytic activity of the different secretases are represented (adapted from Russo et al. 2005).

Additional reports have revealed that APP can also be proteolytic processed at its C-terminus by caspases, like caspase-3 (Gervais et al. 1999), caspase-6 and -8 (Pellegrini et al. 1999), or caspase-9 (Lu et al. 2000). The target residue for the caspase-directed APP cleavage is Asp^{622} (Gervais et al. 1999; Weidemann et al. 1999; Zambrano et al. 2004). The resulting C-terminus C31 peptide is a potent inducer of apoptosis, and this cleavage was shown to reduce APP internalization and to have varying effects on the secreted levels of Abeta (Lu et al. 2000; Pellegrini et al. 1999; Soriano et al. 2001).

The generation of Abeta is initiated by β-secretase cleavage of APP (Golde et al. 1992; Seubert et al. 1993). The endoprotease catalyzing this cleavage at the N-terminus of Abeta peptide has been identified as β-site APP cleaving enzyme (BACE-1) (Hussain et al. 1999; Sinha et al. 1999; Sinha and Lieberburg 1999; Vassar et al. 1999; Yan et al. 1999). The enzimatically active BACE-1 protein derives from cleavage of a pro-peptide within the endoplasmic reticulum (Bennett et al. 2000) and

undergoes complex N-glycosilation during the maturation process (Capell et al. 2000; Haniu et al. 2000; Huse et al. 2000). Since the enzymatic activity of BACE1 is a prerequisite for the generation of Abeta peptides, BACE-1 appears to be a promising pharmacological target to reduce the formation of amyloid plaques in AD brains. In brain, BACE-1 is primarily expressed by neurons (Bigl et al. 2000) and has been localized in known subcellular structures of Abeta generation, i.e. to the Golgi complex and to endossomes (Vassar et al. 1999). BACE-1 mRNA and protein levels are rather stable during aging of mice and humans (Bigl et al. 2000; Irizarry et al. 2001), whereas increased BACE-1 enzimatic activity was detected in several species during aging (Fukumoto et al. 2004). In AD, however, increases in both BACE-1 protein concentrations and enzymatic activities have been reported (Fukumoto et al. 2002; Holsinger et al. 2002).

In humans, another β-secretase gene has been identified, referred to as BACE-2, however only BACE-1 is significantly expressed in brain. The therapeutic potential of BACE-1 inhibition was demonstrated by findings that BACE-1 knockout mice develop normally, but the production of Abeta was completely abolished, suggesting that BACE-1 is the principal β-secretase in neurons (Luo et al. 2001; Roberds et al. 2001; Westmeyer et al. 2004). Developing specific BACE inhibitors has been difficult, in part, because there appears to be a non-linear relationship between decreased BACE activity *in vivo*, and reduced Abeta in brain. Studies using heterozygous BACE-1 knockout animals have shown that a 50% decrease in BACE activity leads to a much smaller decrease (~15%) in brain Abeta levels. A further difficulty is the low brain penetration of most inhibitors, probably due to the fact that many are substrates for glycoproteins, plasma membrane proteins that actively extrude a wide range of amphiphilic and hydrophobic drugs from cells, and this is an important mechanism in preventing the accumulation of several drugs in the brain. Finally, crystallography of BACE-1 has revealed a large catalytic domain making it more difficult to identify small molecule transition-state analogues. This problem is further exacerbated if active BACE is a dimmer, with a potentially even larger substrate-binding pocket (Paganetti et al. 2005). Nevertheless, a number of small molecule inhibitors are close to entering clinical trials and should provide much needed efficacy and reliability information.

γ-secretase

The C-terminal fragments of APP, C83 and C99, which result from cleavage by the α- and β-secretases, remain associated with the membrane and can be further processed by a third enzyme, γ-secretase, to produce p3 and Abeta, respectively (Figures 10 and 11). The site of γ-secretase cleavage is variable, creating several Abeta peptides of different lengths. Although γ-secretase cleavage and the production of Abeta are involved in AD pathogenesis, they are also associated with the normal processing of APP (Estus et al. 1992; Haass et al. 1992). It is generally accepted that a complex of proteins is responsible for γ-secretase cleavage, but the active site of the enzyme has not yet been determined unequivocally. Proteins known as PSEN1 and PSEN2 are essential for γ-secretase activity (Zhang et al. 2000) and, therefore, could possess the active site. A complex containing PSEN1 and PSEN2, the transmembrane glycoprotein nicastrin, APH-1, and PEN-2 has been proposed as forming the complete γ-secretase complex (Esler et al. 2002; Francis et al. 2002; Lee et al. 2002; Li et al. 2000a; Li et al. 2000b; Steiner et al. 2002; Wolfe et al. 1999). Their simultaneous expression in yeast, an organism that lacks any endogenous γ-secretase activity, results in reconstitution of γ-secretase complex formation and activity, demonstrating that these four (PSEN1/PSEN2, Nicastrin, APH-1 and PEN-2) membrane proteins are the core components of the complex (Edbauer et al. 2003). γ-secretase activity depends on the presence of two conserved aspartate residues in either the PSEN1 or PSEN2, two polytopic membrane proteins with a partially redundant function (Haass 2004). Presenilins constitutively undergo endoproteolysis, leading to the generation of N- and C-terminal fragments which remain bound to each other and apparently constitute the catalytic site of the γ-secretase. The active site aspartate residues of the presenilins reside within their TMDs 6 and 7, in agreement with an intramembrane cleavage mechanism. The TMD 7 aspartate is located within a highly conserved sequence motif GxGD (Steiner et al. 2002), which is also found in other intramembrane cleaving proteases, the bacterial type 4 prepilin peptidases and signal peptide peptidases. These data strongly suggest that the presenilins are the proteolytically active components of the γ-secretase complex. In contrast, the role of the other three subunits is less well understood. The type I glycoprotein nicastrin and the polytopic membrane protein APH-1 might form a precomplex to which first presenilin holoprotein is added (Takasugi et al. 2003).

Moreover, studies aimed at understanding the functional activity of nicastrin led to the evidence that PSEN1 and nicastrin require each other to become fully mature (reviewed in Selkoe and Kopan 2003), and the two can be released from the endoplasmic reticulum and be sorted to the plasma membrane where the complex PSEN1-nicastrin is biologically active (Kaether et al. 2004; Kaether and Haass 2004; Kaether et al. 2002).

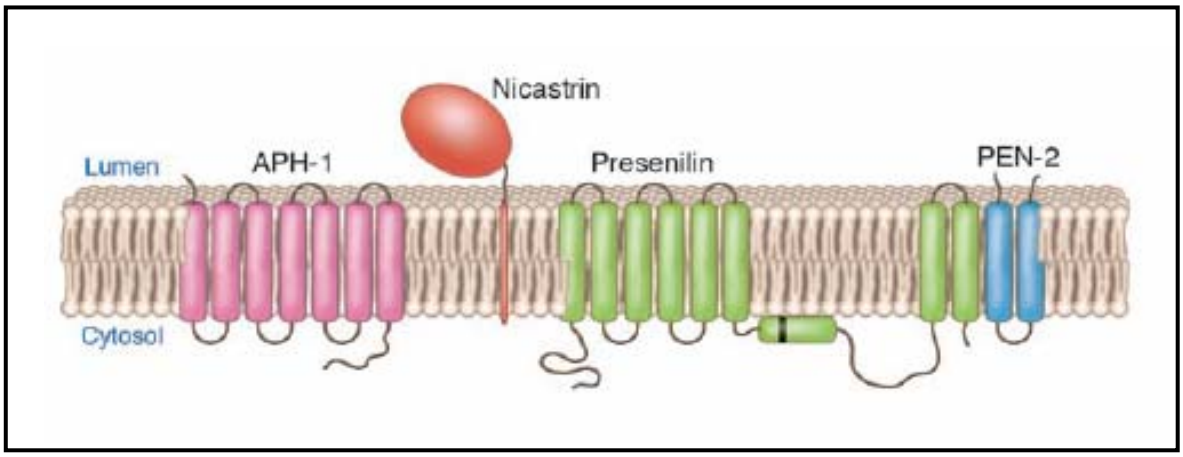

Figure 12. Topology of the 4 components that comprise the high molecular weight γ-secretase complex. Black bar represents the cleavage site for processing of the zymogen form of PS1 into the amino and carboxyterminal fragments that self associate and form the active enzyme (adapted from Gandy 2005).

Because of its large extracellular domain, it was speculated that the role of nicastrin within the γ-secretase complex would be to recognize the substrate by measuring the length of the membrane-inserted stub (Struhl and Adachi 2000). It has been recently demonstrated that nicastrin functions as a γ-secretase substrate receptor (Shah et al. 2005), since it binds specifically to the N-terminal side of the APP and Notch C-terminal stubs, but not the full length proteins generated upon proteolysis at the extracellular domains, and recruits these substrates within the γ-secretase complex for further cleavage.

APH-1 and PEN-2 were isolated as part of the γ-secretase complex in two genetic screens in *C. elegans* (Francis et al. 2002; Goutte et al. 2000). These studies showed that APH-1 and PEN-2 are required for Notch signalling and Abeta formation (Francis et al. 2002). In turn, APH-1 is required together with presenilin for the correct localization of the mature form of nicastrin at the cell surface (Goutte et al. 2000). Interestingly, these studies also reported that APH-1 exists in more than one isoform,

that can be variably involved in the formation of the γ-secretase complex, with the form APH-1a being the one mostly involved in Notch signalling and the processing of APP (Serneels et al. 2005; Shirotani et al. 2004). Furthermore, it was proposed that the physiological significance of PEN-2 together with APH-1 within the γ-secretase complex is to stabilize mature presenilin and nicastrin (Steiner et al. 2002), and to regulate the endoproteolysis of presenilin leading to the formation of the active heterodimer (Hu and Fortini 2003; Luo et al. 2003). Moreover, Prokov et al. (2004) showed that the C-terminal domain of PEN-2 is involved in the maturation of nicastrin and the formation of presenilin heterodimer. From these observations it could be speculated that PEN-2 associates with the complex nicastrin/ PSEN1 in the ER, regulating its maturation and sorting to the plasma membrane.

So far, it is not clear how these four elements (PSEN1, Nicastrin, APH-1 and PEN-2) orchestrate γ-secretase activity and so these aspects are under intense investigation. Although the catalytic activity of the γ-secretase complex resides in the two aspartate residues of PSEN1, these four proteins indeed participate in the regulation of one another's activation and/or maturation, associated with the active γ-secretase complex and are required to reconstitute γ-secretase in mammalian cells (Kimberly and Wolfe 2003) and in yeast (Edbauer et al. 2003).

The β- and γ-secretases are obvious targets for drug development for prevention and treatment of AD, but these proteases have a widespread tissue distribution and multiple substrates including Notch1 for presenlin/γ-secretase (Selkoe and Kopan 2003). Thus, protease inhibitors may engender toxic side effects.

1.5.5 Cellular functions of APP and APP fragments

Several functions have been attributed to APP, including a role in brain development and signal transduction. As discussed previously, APP is processed to produce distinct proteolytic fragments, which in turn have been associated with specific functions, different from the holo protein. Some of these putative functions are discussed below.

Memory

AD is associated with dementia, so it is perhaps not surprising to find evidence for a specific role of APP in long term memory (Doyle et al. 1990; Flood et al. 1991; Huber et al. 1993). Specifically, APP knockout mice show impaired behavioral performance (Muller et al. 1994; Zheng et al. 1996). Additionally, blocking the extracellular domain of APP by intracerebral and intracerebroventricular administration of anti-APP antibodies targeted against various isoforms of APP, differentially impairs behaviour and memory in rats (Chan et al. 2002; Doyle et al. 1990; Huber et al. 1993; Turner et al. 2003). Conversely, exposure of hippocampal slices to sAPPα results in altered frequency of LTD and an increase in LTP (Ishida et al. 1994), strengthening a role for APP in learning and memory processes. Indeed, infusion of sAPPα and the RERMS sequence enhances memory formation (Meziane et al. 1998) and prevent APP anti-sense induced memory loss (Mileusnic et al. 2000).

Brain development

It has been suggested that the APP protein family has a role in the reelin signalling pathway, and may participate in neuronal migration and positioning during brain development (Bothwell and Giniger 2000; Ishida et al. 1994). Supporting the hypothesis for APP involvement in cell differentiation and synaptogenesis, APP isoform levels were found to reach their maximum peak during the second postnatal week of the rat, the time which coinsides with brain maturation and completion of synaptic connections (Loffler and Huber 1992). Also of note is the finding that APP can be regulated by cholinergic mechanisms (Bayer et al. 2001).

Cell surface receptor

The analogy of the secondary structures and proteolytic processing profiles between Notch and APP predicts that APP could function as a cell surface receptor similar to Notch (reviewed in Selkoe and Kopan 2003). Supporting this hypothesis, Bruce Yankner's group reported that the Abeta peptide could bind APP and thus be a candidate ligand for APP (Lorenzo et al. 2000). Evidence from Ho and Sudhof (2004) showed that the APP extracellular domain binds to F-spondin, a neuronally secreted glycoprotein, and this interaction regulates Abeta production and downstream signalling (Ho and Sudhof 2004). Similarly, Nogo-66 receptor was recently shown to interact with the APP ectodomain and this interaction affects Abeta production (Park et al. 2006).

Cell adhesion

Data linking cell surface APP with cell-substratum and cell-cell adhesion are perhaps particularly convincing. The exon 1 and 2 regions have been shown to interact with extracellular matrix proteins and heparin sulphate proteoglycans (reviewed in Small and McLean 1999), supporting a role in cell-substratum adhesion. The same sequences have also been implicated in cell-cell interactions. Specifically, X-ray analysis revealed that the exon 2 domain of APP could form antiparallel dimers (Wang and Ha 2004). Such structure has the potential to function in trans-cellular adhesion. Cell culture studies addressing the homo- or hetero-dimer formation of the APP family members, and the trans-dimerizations have shown that this level of organization promotes cell-cell adhesion (Soba et al. 2005). However, this activity appears to be mediated by the exon 1 domain. Downstream of the exon 1 and exon 2 regions, a "RHDS" motif (Figure 9) in the extracellular domain of APP within the Abeta sequence also appears to promote cell adhesion. It is believed that this region acts in an integrin-like manner by homology to the "RGD" sequence (Ghiso et al. 1992). In this regard, it is interesting that APP colocalizes with integrins on the surface of axons and at sites of adhesion (Storey et al. 1996; Yamazaki et al. 1997).

Neurite outgrowth and synaptogenesis

A neurotrophic and synaptogenic role for APP is perhaps the most consistently documented and arguably the best established, further this function may be linked to

its adhesive properties described above. A number of publications have supported such a role for the APP extracellular domain in this context, both as holo protein and as sAPP following ectodomain shedding. Consistently, APP may exert these activities both in an autocrine and paracrine fashion. Thus, APP expression is upregulated during neuronal maturation and differentiation (Bibel et al. 2004; Hung et al. 1992). The latter is also induced after traumatic injury both in mammals and in *Drosophila* (Leyssen et al. 2005; Murakami et al. 1998; Van den Heuvel et al. 1999). Moreover, APP undergoes rapid anterograde transport and is targeted to synaptic sites (Koo et al. 1990; Lyckman et al. 1998; Sisodia et al. 1993; Yamazaki et al. 1995), where the levels of secreted APP coincide with synaptogenesis (Moya et al. 1994). The crystal structure of the exon 1 domain shows similarities to known cysteine-rich growth factors, known as the growth factor like domain (GFLD, Rossjohn et al. 1999). Previous indications of this APP function came from the observation that assessing fibroblasts treated with an antisense APP construct grew slower and the growth retardation could be restored by treatment with sAPP (Saitoh et al. 1989). The active domain was subsequently mapped to a pentapetide motif "RERMS" in the E2 domain (Ninomiya et al. 1993). The activity is not restricted to fibroblasts because the infusion of this pentapeptide or sAPP in brain resulted in increased synaptic density and improved memory retention in animals (Meziane et al. 1998; Roch et al. 1994), while the injection of APP antibodies directly into the brain led to impairment in behavioural tasks in the adult rat (Meziane et al. 1998). This result is in agreement with reports showing that reduction of APP is associated with impairment of neurite outgrowth and neuronal viability *in vitro* and synaptic activity *in vivo* (Allinquant et al. 1995; Herard et al. 2006; Perez et al. 1997). A recent report demonstrated that the growth promoting property is mediated by the ability of the sAPPα to down regulate Cdk5 and inhibit tau hyperphosphorylation (Han et al. 2005). Finally, Caille et al. (2004) has identified the binding sites for sAPP in epidermal growth factor (EGF)-responsive neural stem cells, in the subventricular zone of the adult rodent brain. Furthermore, sAPPα acts as a cofactor with EGF to stimulate the proliferation of these cells both in neurospheres in culture and *in vivo*. Because the levels of sAPP have been reported to be reduced in individuals with AD (Palmert et al. 1990), this result raises the possibility that the loss of the trophic activity of sAPP, and the reduction of other growth factors in the brain, may contribute to the neurodegeneration in AD.

Axonal transport

The neuron is unique in cellular morphology with a long axon and a rich dendritic arbour. Elaborated protein trafficking exists in neurons for selected proteins to reach their designed compartments and to be transported back to the cell soma. Protein processing and modifications are known to take place during the transit along axons. APP is transported in axons via fast anterograde transport machinery, a process that requires kinesin molecular motors, and at least one documented source of amyloid deposits originates from the synaptically released Abeta pool (Lazarov et al. 2002; Sheng et al. 2002). The anterograde transport of APP is proposed to be mediated by binding of APP to the Kinesin light chain (KLC) subunit, a component of the kinesin-1 transport machinery (Kamal et al. 2000). However, recent evidence is more consistent with the view that the interaction is mediated indirectly through adaptor proteins, of which JIP-1, a member of the JNK-interacting protein family (JIP), is a likely candidate as it is known to interact with both KLC and APP (Sisodia 2002).

Unresolved by this model is how APP is initially sorted into a particular class of vesicles. The potential importance of the initial sorting of APP is underscored by the report that BACE-1 and Presenelins are contained within the same Kinesin-1 dependent APP transport vesicles (Kamal et al. 2001). This finding suggests that not only is APP required for the delivery of the enzymatic machinery necessary for Abeta production, but Abeta generation also occurs from the cell body to the nerve terminals within the transport cargo that is required by APP. However, the report that APP is a kinesin-1 receptor and a common vesicular compartment carrying all the processing machinery necessary for Abeta generation has not been confirmed by others (Lazarov et al. 2005). Nevertheless, KLC deficient animals when crossed with APP transgenic mice, showed axonal pathology manifested by axonal swellings and increased amyloid levels and deposits in brain (Stokin et al. 2005). The latter argue that perturbations of the axonal transport during aging may predispose to the development of AD pathology.

Cell signalling

In addition to the γ-secretase that yields $Abeta_{1-40}$ and $Abeta_{1-42}$, PSEN-dependent proteolysis also occurs at other positions including the ε-site ($Abeta_{1-49}$) downstream of the γ-site proximal to the membrane-intracellular boundary (Figure 11; Sabo et al. 2003; Sastre et al. 2001; Weidemann et al. 2002; Zhao et al. 2004). Recent data provide support for a sequential cleavage model in which ε-cleavage

serves as the initial cutting site, followed by δ- and γ-processing within the membrane (Kakuda et al. 2006; Qi-Takahara et al. 2005; Zhao et al. 2004). Thus, ε-cleavage of APP may represent the primary PSEN-dependent processing event. The importance of the latter event is significant being that it releases an APP intracellular domain (AICD) that is highly reminiscent of the release of the Notch intracellular domain (NICD) after γ-secretase processing, the latter being an obligatory step in Notch mediated signalling (reviewed in Selkoe and Kopan 2003). Moreover, PSEN-dependent AICD has been shown to translocate to nucleus and could function as a transcriptional regulator (Cupers et al. 2001; Gao and Pimplikar 2001; Kimberly et al. 2001). AICD is very labile but can be stabilized by FE65 (Cupers et al. 2001). Using a heterogenous reporter system, AICD is shown to form a transcriptionally active complex, presumably in the nucleus with FE65 and Tip60 (Cao and Sudhof 2001; Gao and Pimplikar 2001). However, further studies have revealed that the previous model may be too simplistic and incomplete. Firstly, follow up studies showed that nuclear translocation of AICD is not required but signalling may be indirect through FE65 (Cao and Sudhof 2004). Secondly, PSEN-dependent AICD production is not required for APP signalling activity because it happens normally in either PSEN null cells or using a PSEN inhibitor (Haass and Yankner 2005). Furthermore, the authors provide an alternative pathway for this activity that involves the Tip60 phosphorylation. Finally, a recent report has shown that the proposed signalling activity is executed by FE65 and that APP is not required (Yang et al. 2006). Overall, a potential nuclear signalling activity remains to be clearly established.

In spite of the unclear nature of how AICD may activate signalling pathways, a trans-activating role of APP/FE65/Tip60 complex has been consistently documented, at least in overexpression systems. Accordingly, downstream targets have been identified. Two genes have been proposed, KAI1, a tumor suppressor gene, and neprilysin, a neural endopeptidase with Abeta degrading activity. The latter pathway is particularly interesting because it suggests that γ-secretase release of AICD can regulate the degradation of Abeta in the extracellular space.

The proposed AICD signalling has also been implicated in phosphoinositide-mediated calcium signalling and cell cycle regulation (Leissring et al. 2002) and reviewed in (Neve and McPhie 2006). Specifically, fibroblast cells lacking APP exhibit calcium signalling defects which can be rescued by expressing AICD.

Cell migration and synapse remodeling

In addition to stabilizing AICD and modulating nuclear signalling, the binding of APP to FE65 has been implicated in the regulation of cell motility and growth cone dynamics. In H4 neuroglioma and MDCK cells, APP is found to be associated with FE65 and a mammalian homolog of Enabled (Sabo et al. 2001; Sabo et al. 2003), a cytoskeletal protein expressed in actin remodelling areas, such as lamellipodia and growth cones (reviewed in Bearer 2001). The functional role of this complex was demonstrated using a wound healing assay in MDCK cells where the authors showed increased rate of cell migration and wound closure by overexpressing APP and FE65. This process appears to be partially dependent on the Mena/actin complex (Sabo et al. 2001). Further studies by the same group showed that in primary neurons, APP and FE65 are concentrated in actin-rich area of the growth cones, supporting the idea for an active role of the APP/FE65 complex in growth cone dynamics and synapse remodelling (Sabo et al. 2003).

Apoptosis

Interestingly, there is a lengthy history regarding the cytotoxic properties of APP, especially when APP or the β-cleaved C-terminal fragment of APP (C99 or C100) are overexpressed (Yankner et al. 1989; Yoshikawa et al. 1992). Indeed, overexpression of C100 is associated with neuronal degeneration in brain (Oster-Granite et al. 1996), perhaps by perturbing APP signal transduction. Another pathway by which APP CTF is cytotoxic may be through AICD. Specifically, the cytotoxicity of APP CTF appears to require an intact caspase site within the cytoplasmic tail (Lu et al. 2003). In this culture model, loss of this caspase site by mutating the aspartate residue at position 622 to alanine (D622A) resulted in a loss of C100 associated cytotoxicity. It has been proposed that release of smaller fragments (C31 and jcasp) from AICD after cleavage at position 622 results in the generation of new cytotoxic APP related peptides (Figure 11). Indeed, in an APP transgenic mouse line in which the caspase site is mutated to render APP noncleavable, the predicted Abeta-related phenotypes in brain, including synaptic, behaviour, and electrophysiological abnormalities, were absent in spite of abundant amyloid deposits in the brain. Therefore, release of C99 may result in the activation of genes that contribute to cell death in a γ-secretase dependent manner. In essence, there are at present several potential mechanisms whereby APP may contribute to neurotoxicity: via γ-secretase

cleavage to release AICD or via alternative cleavage of the APP C-teminus to release other cytotoxic peptides.

1.5.6 APP C-terminus domains and APP-binding proteins

Whereas the APP ectodomain contains many potential functional domains, previously described, the short cytoplasmic tail possesses few regions capable of interacting with intracellular proteins. Most of these interacting proteins possess multiple protein-protein interacting domains, which in turn form complexes with other proteins, suggesting that the latter function as adaptor proteins bridging APP to specific molecular pathways. The number of APP binding proteins thus far identified is quite vast and can be loosely divided into two overlapping categories: signal transduction and subcellular localization (da Cruz e Silva et al. 2004b). For both there is an emerging consensus that the APP C-terminus is critical in these interactions. Examples of APP binding proteins involved in signal transduction are: c-Abl, Disabled-1 protein (mDab-1), Fe65 and Fe65-like proteins, SET protein, X11 family proteins, Numb, and G_0. Fewer APP binding proteins involved in APP targeting have been described and include APPBP2 (or PAT1) and the X11 family proteins, important in microtubule association. Moreover, X11 was also found to potentially function as an APP vesicle coat-protein (Hill et al. 2003). Recent contributions have brought to light two other proteins putatively involved in APP traffic: the neuronal sorting receptor sorLA/LR11 (Andersen et al. 2005), and a novel sorting nexin (SNX30) (Lichtenthaler et al. (2005)). The APP-G_0 binding (Nishimoto et al. 1993) may also have a role in APP targeting, as G_0 was found to be located at subcellular membrane domains specialized in the sorting of trafficking proteins (Qian et al. 2003). Other known APP binding proteins involved in trafficking are the Kinesin Light Chain (KLC) and JIP-1 [Jun N-terminal kinase (JNK) interacting protein 1]. Further, examples exist where the binding to APP has not been clarified, as in the case of caveolin (Ikezu et al. 1998; Nishiyama et al. 1999).

The function of all the APP binding proteins has yet to be completely elucidated, but considerable contributions have already been made. For review on APP binding proteins involved in APP signal transduction see da Cruz e Silva et al. (2004b). Several other APP binding proteins have been described that appear to have very diverse roles such as in Abeta clearance and/or aggregation, as for example APOE.

Proteins which bind the N-terminus of APP have not been extensively documented, but examples include fibulin-1, whose binding blocks neural stem cells

sAPP-mediated proliferation (Ohsawa et al. 2001), and F-spondin, which may mediate APP CAM (cellular adhesion molecule) and neurite outgrowth functions (Ho and Sudhof 2004). In fact, almost all known APP binding proteins bind to its C-terminus, and specifically at one of two APP domains: ^{653}YTSI^{656} and ^{682}YENPTY^{687} (Table 2 and Table 3). Recently, it was reprted that Pin1 binds to Thr^{668} located in the third domain (^{667}VTPEER^{672}). These domains can be classified according to their attributed functions and are thought to be involved in regulating APP rate of secretion, endocytosis, and Abeta production (Ando et al. 2001; Ando et al. 1999; da Cruz e Silva et al. 2004b; Iijima et al. 2000; Mueller et al. 2000; Roncarati et al. 2002; Sabo et al. 2001).

Of particular interest is the YENPTY motif at the C-terminus of APP, because it is the only region in the cytoplasmic domain that is completely conserved from C. elegans to humans (King et al. 2003). The NPTY motif was first identified in the low-density lipoprotein (LDL) receptor as a requirement for the transmembrane receptor internalization and was subsequently identified in APP (Chen et al. 1990). The ^{682}YENPTY^{687} motif binds phosphotyrosine-binding (PTB) domains of adaptor proteins (Wolf et al. 1995). However, the binding of PTB domais to the NPTY sequence has been reported to be largely independent of phosphorylation (Borg et al. 1996).

Internalization of APP and trafficking through the endocytic pathway are an important step in APP proteolysis. Several studies have demonstrated that disruption of this process substantially reduces the secretion of Abeta (Koo and Squazzo 1994; LeBlanc and Gambetti 1994; Perez et al. 1999). The internalization of transmembrane proteins in clathrin-coated vesicles is a multistep process requiring the initial binding of adaptor proteins to the cytoplasmic domain and subsequent assembly of clathrin-coats and vesicle formation (Schmid 1997). Thus, this motif is thought to function through interaction with various known APP binding protein that are described below and summarized in Table 2.

Table 2. YENPTY domain interacting proteins. YENPTY dependent APP interacting proteins are indicated as well as their putative role and subcellular localization. ND, not determined.

APP BINDING PROTEIN	PUTATIVE ROLE	SUBCELLULAR LOCALIZATION	REFERENCE
FE65 **FE65L1** **FE65L2**	– Regulation of APP secretion – Regulation of cell movement – Promotion of gene transactivation	– Cytoplasm and Nucleus – In AD colocalizes with tau protein in NFTs – Synaptic sites and in neuronal growth cones, specially in actin-rich lamellopodia	– Fiore et al., 1995 – Breesler et al., 1996 – Guenette et al., 1999 – Kimberly et al., 2001 – Sabo et al., 2001 –Kinoshita et al., 2002
X11α **X11 family**	– APP trafficking – APP coat vesicle protein – APP synaptic localization – Regulation of APP processing and metabolism	–Cytosolic/Golgi adaptor protein –APP/Mint/Cask complexes are localized in neuronal processes and in the Golgi	– Borg et al., 1996 – McLoughlin and Miller, 1996 – Sastre et al., 1998 – Mueller et al., 2000 – Hill et al., 2003 – King et al., 2003, 2004
Dab1 **Dab2**	– Neuron migration (cell movement) – Links APP to signal transduction processes – Neuronal development	– Co-localizes with APLP1 in membrane ruffles and vesicular structures	– Trommsdorf et al., 1998 – Homayouni et al., 1999 – Mishra et al., 2002 – Yun et al., 2003
c-Abl	– Abl active form phosphorylates APP at Y682 – Forms a trimeric complex with APP and Fe65 – APP internalization	– Cytoplasm and nucleus	– Russo et al., 2001 – Zambrano et al., 2001 – Tarr et al., 2002
Numb	– Link between APP and Notch signalling pathways – Endocytosis	– Neurons cytoplasm, dendritic and axonal processes; excluded from nuclei	– Roncarati et al., 2002 – Berdnick et al., 2002 – Santolini et al., 2000
JIP-1b	– Scaffolds APP with c-Jun Kinase (JNK) – Links APP to stress kinase signalling pathways – Involved in APP axonal trafficking	– APP and JIP-1b exhibit similar subcellular location: cytoplasmic significantly overlapped staining	– Matsuda et al., 2001 – Scheinfeld et al., 2002 – Sisodia, 2002

Shc	– Tyrosine kinase-mediated signal transduction – ShcA upregulated in AD brains	– Cytoplasm	– Russo et al., 2001 – Zambrano et al., 2001 – Tarr et al., 2002 – Russo et al., 2002
Grb2	– Mediated signal transduction – Grb2 upregulated in AD brains	– ND	– Zhou et al., 2004 – Venezia et al., 2004
ARH	– APP internalization	– Plasma membrane	– Noviello et al., 2003
UV-DDB	– ND	– cytosolic fraction (PC12 cells)	– Watanabe et al., 1999

FE65

Y2H screens have revealed that the FE65 family of adaptor proteins, including FE65, FE65L1 and FE65L2, can bind to the YENPTY sequence of APP (Borg et al. 1996; Duilio et al. 1998; Fiore et al. 1995; Guenette et al. 1996). Both FE65 and APP colocalized in human neuroglioma cells (Sabo et al. 1999) and they are expressed during neuronal development (Kesavapany et al. 2002). Members of FE65 proteins contain several protein interacting domains, including two PTB domains and a WW region. Furthermore, the WW domain binds to MENA (mammalian enabled) which binds actin and thus links FE65 and APP to cytoskeletal dynamics and cellular motility and morphology (Ermekova et al. 1997). The PTB_1 domain of FE65 binds either the transcription factor complex CP2-LSF-LBP-1c, or the low density lipoprotein receptor-related protein (LRP). The PTB_2 domain of FE65 binds the APP C-terminus, providing a potential scaffold between APP and LRP (Kinoshita et al. 2001). The interaction between APP and FE65 involves binding of YENPTY sequence and dephosphorylated Thr^{668} residue in APP to the PTB domain closest to the C-terminus of FE65 (Ando et al. 2001; Borg et al. 1996)

The C-terminal product of γ-secretase cleavage, AICD, has been shown to also bind to FE65 and translocate to the nucleus to form a transcriptionally active complex with Tip60 (Cao and Sudhof 2001; Kimberly et al. 2001). The initial binding of FE65 to AICD occurs before the APP fragment dissociates from the membrane, and the three functional domains of FE65 have to be intact (Cao and Sudhof 2001; Cao and Sudhof 2004). Furthermore, it was reported that FE65-mediated transcriptional activation by

APP, upregulates the expression of many genes including APP and BACE (von Rotz et al. 2004). This suggests that γ-secretase proteolysis of APP, which regulates AICD, may result in the up-regulation of the amyloidogenic processing.

The effect of FE65 expression on APP processing is unclear and may be dependent on both the cell type in which expression occurs and the FE65 family member. FE65 can increase secretion of Abeta and sAPP from cells expressing APP (Sabo et al. 1999), and overexpression of FE65L1 leads to a decrease in cellular C83 and increased secretion of $Abeta_{1-40}$ resulting from increased processing through the γ-secretase pathway (Chang et al. 2003). FE65L1 has also been shown to enhance the maturation and secretion of APP (Duilio et al. 1998; Guenette et al. 1999). The remaining family member, FE65L2, has been demonstrated to increase secretion of Abeta without affecting the production of other proteolytic products of APP (Tanahashi and Tabira 2002).

The binding of FE65 to APP has also been reported to promote formation of receptor complexes. It was demonstrated by Pietrzik et al. (2004) a complex similar to that proposed by Trommsdorff et al. (1998), consisting of APP and LDL receptor-related protein (LRP) linked through their binding to separate PTB domains of FE65. This finding is of particular interest for AD, because one allelic form of the LRP ligand, apolipoprotein E (APOE ε4), is a risk factor to develop late-onset AD. Thus, the APP-FE65-LRP complex formation is responsible for the alteration of APP processing (Pietrzik et al. 2004), suggesting that APOE may influence Abeta production, and therefore AD pathology, via the APP-LRP receptor complex.

X11α and X11 family (Mint family)

Members of the X11 family of adaptor proteins also interact with the YENPTY motif of APP (Borg et al. 1996; Tanahashi and Tabira 1999a; Tomita et al. 1999). This family consists of three proteins, X11α, -β and -γ (or Mint1, -2, -3, respectively), all of which possess both PTB and PDZ domains. The N-terminal domains of X11α and X11β contain a munc18-interacting domain (MID), and the PDZ domain may interact with several different proteins, including PSEN1 (Lau et al. 2000). X11α contains an additional mLin-2/CASK interacting domain (CID; Borg et al. 1998). Whereas X11γ expression is ubiquitous, X11α and X11β are considered neuron specific and are expressed only in the brain (Okamoto and Sudhof 1998). The binding between the X11 PTB domain and an APP C-terminal peptide containing the YENPTY motif was shown to be of high affinity (Zhang et al. 1997), and deletion of this sequence completely abolished the interaction (Tomita et al. 1999).

X11α coexpression with APP has been shown to delay the maturation, trafficking and processing of APP, thus increasing cellular levels of APP and reducing the secretion of amyloidogenic peptides (Borg et al. 1998; King et al. 2003; Sastre et al. 1998). Although an overall slowing of APP processing was demonstrated in these studies, the interaction between X11α and APP is also reported to block the action of the γ-secretase processing of APP selectively (King and Scott Turner 2004). These results suggest that the X11 family, and X11α in particular, may function as regulators of cellular processing and metabolism of APP.

Dab1 and Dab2

Another protein that is potentially involved in APP internalization is Dab2, a member of the Disabled family. The PTB domain of Dab2 binds to the NPTY motif in APP (Yun et al. 2003). Evidence supports the involvement of the latter protein in endocytosis, firstly given its localization at the plasma membrane and secondly its capacity to bind both clathrin and AP-2 (Mishra et al. 2002). Furthermore, both co-immunoprecipitation and yeast two-hybrid (Y2H) screens have revealed that the PTB domain of an additional Disabled family member, Dab1, can bind the YENPTY motif (Homayouni et al. 1999; Trommsdorff et al. 1998). However, Dab1 binds stronger to APLP1 than APP_{695} (Homayouni et al. 1999). Dab1 is involved in neuronal migration to cortical layers during development and has been implicated in neuronal development.

c-Abl

The Src homology 2 (SH2) domain of Abl (Zambrano et al. 2001) may interact with APP when the tyrosine in the YENP sequence is phosphorylated, also suggesting a role for APP in tyrosine kinase-mediated signal transduction.

Numb

The APP cytoplasmic domain also interacts with Numb, an adaptor protein that was originally identified for its role in Notch signalling (Roncarati et al. 2002). The binding of Numb to Notch promotes its internalization, inhibiting its signal transduction from the cell surface and consequently influencing Notch-mediated cell-fate decisions during differentiation (Berdnik et al. 2002). Numb may be involved in endocytosis because it binds to endocytic vesicles (Table 2; Santolini et al. 2000).

JIP1b

APP can bind to the JNK interacting protein 1b (JIP1b) (Matsuda et al. 2001; Taru et al. 2002). However, the affinity of the Jip1b PTB domain for APP is lower than for the X11, Dab1 and FE65 PTB domains (Matsuda et al. 2001). The Jip1b-APP interaction may enhance *in vitro* phosphorylation of APP at Thr^{668} by JNK (Inomata et al. 2003). The role of this interaction is unclear, although coexpression of APP and Jip1b has been shown to reduce the secretion of Abeta (Taru et al. 2002). The binding of Jip1b to APP may be involved in the cellular sorting of APP. Jip1b reportedly enhances the association of APP to KCL1 (Inomata et al. 2003), which is a component of the axonal transport machinery.

SHC

Shc A and Shc C are members of a family of cytoplasmic adaptor proteins, that also includes ShcB, whose PTB domain binds to the YENPTY APP motif (Russo et al. 2002; Tarr et al. 2002). However, unlike the other PTB-containing proteins that interact with APP, ShcA and ShcC seem to associate with APP only when the tyrosine is phosphorylated, suggesting a role of APP in tyrosine kinase-mediated signal transduction. Interestingly, the expression level of ShcA is increased in AD brains as compared to normal, non-demented brains (Russo et al. 2002).

Grb2

Grb2 directly interacts with APP reqiring the phosphorylation of APP Tyr^{682} (Venezia et al. 2004). Un like other interacting proteins that bind the YENPTY motif via their PTB domain, Grb2 binds to YENPTY via its SH2 domain (Zhou et al. 2004). Moreover, the Grb2-APP complex is detectable in human brains and its amount apparently increases in AD brains.

ARH

The functional significance of adaptor protein interactions is suggested for the autosomal recessive hypercholesterolemia (ARH). A disorder of defective internalization of the LDL receptor caused by mutations in the *SRH* gene (Garcia et al. 2001). The ARH protein directs the internalization of the LDL receptor through the binding of its PTB domain to the NPTY sequence. The ARH protein has also been shown to bind to APP YENPTY motif (Noviello et al. 2003). Moreover, inhibition of this interaction resulted in an increased level of APP at the cell surface supporting a role for ARH in internalization (Table 2; Noviello et al. 2003).

UV-DDB

The UV-damaged DNA-binding (UV-DDB) protein was demonstrated to bind the APP cytoplasmic tail, and this binding is dependent on an intact YENPTY sequence (Watanabe et al. 1999).

The previously mentioned amino acid sequence ^{653}YTSI^{656} forms a 4-residue tyrosine-based characteristic internalization and/or basolateral sorting signal (YXXI) (Haass et al. 1995; Lai et al. 1995; Zheng et al. 1998b). When transplanted to the cytoplasmic domain of the transferrin receptor (TR), this sequence promoted the internalization of a TR-YTSI chimera in COS-1 cells and seemed to be partially responsible for its post-Golgi degradation (Lai et al. 1995). This domain has received less attention and until now only one protein (APPBP2) was shown to specifically bind to it. As the exact site of APP binding to the KLC protein is still unknown, the binding of KLC to the ^{653}YTSI^{656} domain is speculative and supported only by KLC homology to APPBP2. Nonetheless, this is a domain that could contribute to the targeting of APP to correct plasma membrane subdomains and be involved in APP signalling functions. The characteristics of both the putative and known ^{653}YTSI^{656} domain binding proteins are described below (Table 3).

Table 3. Putative and known YTSI domain binding proteins. The YTSI dependent APP interacting proteins are indicated as well as their putative role and subcellular localization.

APP BINDING PROTEIN	PUTATIVE ROLE	SUBCELLULAR LOCALIZATION	REFERENCE
APPBP2 (or PAT1)	– Translocation of APP along microtubules toward the cell surface – Involved in nuclear gene transactivation/repression	– Nucleus, cytoplasm and membrane – Golgi and in filamentous cytoplasmic structures emanating from the Golgi, where it co-localizes with APP	– Zheng et al., 1998 – Gao and Pimplikar, 2001 – Richards et al., 2003 – Zhang et al., 2004
KLC (?)	– Axonal transport of APP containing vesicles (anterograde and retrograde)	– Cellular cytoskeleton/ Microtubules	– Kaether et al., 2000 – Kamal et al., 2000; 2001
SET (?)	– Transactivation of the KAI1 gene (AICD/SET/Fe65/ Tip60 complex) – Mediation of APP C-terminal-induced apoptosis	– Co-localizes with AICD at the nucleus (on the *kai1* gene promoter)	– Madeira et al., 2005; – Telese et al., 2005

Several other cytoplasmic proteins (Table 4) have been identified that bind the intracellular domain of APP. A putative G-protein (G_0) interacting domain has been identified in the cytoplasmic domain (Nishimoto et al. 1993), indicating a possible role for APP in signal transduction from the plasma membrane. Another APP binding protein, named APP-binding protein (APPBP1) was described and has a putative role in apoptotic signalling pathways (Chen et al. 2003; Chow et al. 1996). Also of note is the recent report that the Pin1 protein binds to the phosphorylated Thr^{668} APP (Pastorino et al. 2006) and this binding regulates isomerization between the *cis*- and *trans*-conformations, affecting APP processing. Pin1 is a prolyl-isomerase that binds to and isomerizes specific phosphorylated S/T-P motifs (for review see Lu et al. 1999) been proposed that Pin1 catalyses the APP conformational change helping the prevention of its amyloidogenic processing, thus preventing the pathogenic mechanisms that lead to AD pathology (Pastorino et al. 2006). It was also shown both *in vivo* and *in vitro* that the ablation of *Pin1* gene resulted in increased Abeta secretion, as well as increased sAPPβ and decreased sAPPα secretion in an age-dependent fashion. Furthermore, Pin1 promotes the accumulation of intracellular $Abeta_{1-42}$ at a neuronal level, suggesting that Pin1 favors the amyloidogenic over the non-amyloidogenic processing of APP.

Table 4. Other APP binding proteins. Other C-terminus dependent APP interacting proteins are indicated, as well as their putative role and subcellular localization. ND, not determined.

APP BINDING PROTEIN	PUTATIVE ROLE	SUBCELLULAR LOCALIZATION	REFERENCE
G_0	– APP cellular signalling – APP targeting	– Co-localizes with APP at neuronal growth cones – Co-localizes with APP at neuronal membrane microdomains	–Strittmatter and Fishman, 1991 –Nishimoto et al., 1993 –Okamoto et al., 1995 –Qian et al., 2003
APPBP1	– Apoptotic signalling pathways	– ND	– Chow et al., 1996 – Chen et al., 2003
Hsc73	– APP/AICD traffic – APP/AICD proteasomal or lysosomal degradation	– Mainly cytosol, lysosomal membrane, also in nucleus	– Kouchi et al., 1999
AIDA-1a	– Modulator of APP processing	– Diffuse localization with some nuclear accumulation	– Ghersi et al., 2004
hARD1	– ND	– ND	– Asaumi et al., 2005
Pin1	– Regulation of Thr^{668} APP isomerization between the *cis*- and *trans*-conformations – Regulate tau function, dephosphorylates phosphorylated tau	– ND	– Lu et al., 1999 – Liou et al., 2003 – Pastorino et al., 2006

1.5.7 APP subcellular trafficking

APP trafficking and maturation

In neuronal and non-neuronal cells, APP is known to be transported via the secretory pathway, a continoum of separate membrane-enclosed organelles leading to the cell surface. Newly synthesized proteins that are destined for secretion or cell-surface expression enter this pathway at the rough endoplasmic reticulum (RER). APP is known to undergo post-translational modifications that include N- and O-linked glycosylation and tyrosine sulfation (Oltersdorf et al. 1990; Weidemann et al. 1989). APP N-glycosylation starts at the ER and the carbohydrate chains are further processed in the cis-Golgi, with immature N-glycated APP being found at both locations (Tomita et al. 1998). Two residues in the APP ectodomain (Asn^{467} and Asn^{496}) have consensus sequences for N-glycosylation, although only one appears to be N-glycosylated "in vivo" (Pahlsson and Spitalnik 1996). APP maturation by O-glycosylation and tyrosyl-sulfation occurs while moving through the trans-Golgi network (TGN) (Weidemann et al. 1989). Maturation of all metabolic labelled APP cell-associated proteins reached maximum intensity after 30 min of chase (Peraus et al. 1997).

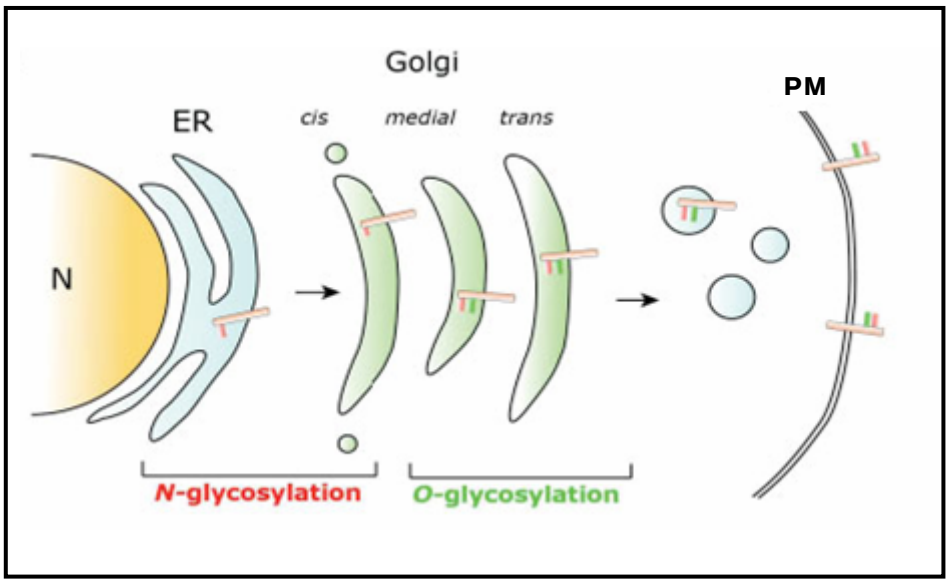

Figure 13. APP secretory pathway. APP in the classical secretory pathway. APP is subjected to N-glycosylation in the ER, O-glycosylation in the Golgi apparatus, and then reaches the plasma membrane. **N**, Nucleus, **ER**, Endoplasmic reticulum; **PM**, Plasma Membrane (adapted from Suzuki et al. 2006).

O-glycosylation does not depend on correct APP N-glycosylation to precede it but, as it is performed at the TGN, is a subsequent process (Pahlsson and Spitalnik 1996). Inhibition of APP O-glycosylation does not appear to affect APP biosynthesis or secretion (Pahlsson and Spitalnik 1996). Nonetheless, the majority of APP cleavage by secretases occurs after O-glycosylation, as shown by using HEK293 cells expressing mutant APP defective in O-glycosylation (Tomita et al. 1998). This mutant accumulated in subcellular reticular compartments and exhibited decreased cleavage to αCTFs or to Abeta$_{1\text{-}40}$/$_{1\text{-}42}$.

Mature APP (N-,O-glycated and sulfated) is therefore located in compartments from the trans-Golgi to the plasma membrane (Tomita et al. 1998). Most APP resides in the Golgi complex (Caporaso et al. 1994), but a small pool is carried into post-TGN secretory vesicles that carry it to the plasma membrane (Koo et al. 1996; Peraus et al. 1997; Yamazaki et al. 1996). In SH-SY5Y cells, the pool of TGN mature APP that is targeted to the plasma membrane takes 30 to 45 min to reach this cellular destination following APP translation (Cai et al. 2003). At the cell surface, APP can be cleaved or undergo re-internalization as a holoprotein via endocytosis, to be recycled back to the membrane, retrogradely delivered to the TGN or incorporated into secondary endosomes. Secondary endosomes target APP for complete degradation at the lysosomes or to be recycled back to the TGN/Golgi (Koo et al. 1996; Tagawa et al. 1993; Yamazaki et al. 1996). In central and peripheral neurons a pool of APP molecules is also transported from the cell body down axons by fast axonal transport (Ferreira et al. 1993; Kaether et al. 2000; Koo et al. 1990). Presynaptically targeted full-length APP (and APLP2) occurs in its mature form (syalated and N- and O-glycosylated) (Lyckman et al. 1998). APP was also detected in both pre- and post-synaptic sites, in the axoplasm of myelinated and unmyelinated nerve fibres, within vesicular structures in axonal, dendritic and synaptic compartments, as well as on the surface of axons and dendrites (Allinquant et al. 1994; Caporaso et al. 1994; Ferreira et al. 1993; Schubert et al. 1991; Simons et al. 1995). Of note is that APP was suggested to be up-regulated in synapses with increased membrane activity, such as in synapses subject to high transmission rates or during synaptogenesis (Schubert et al. 1991).

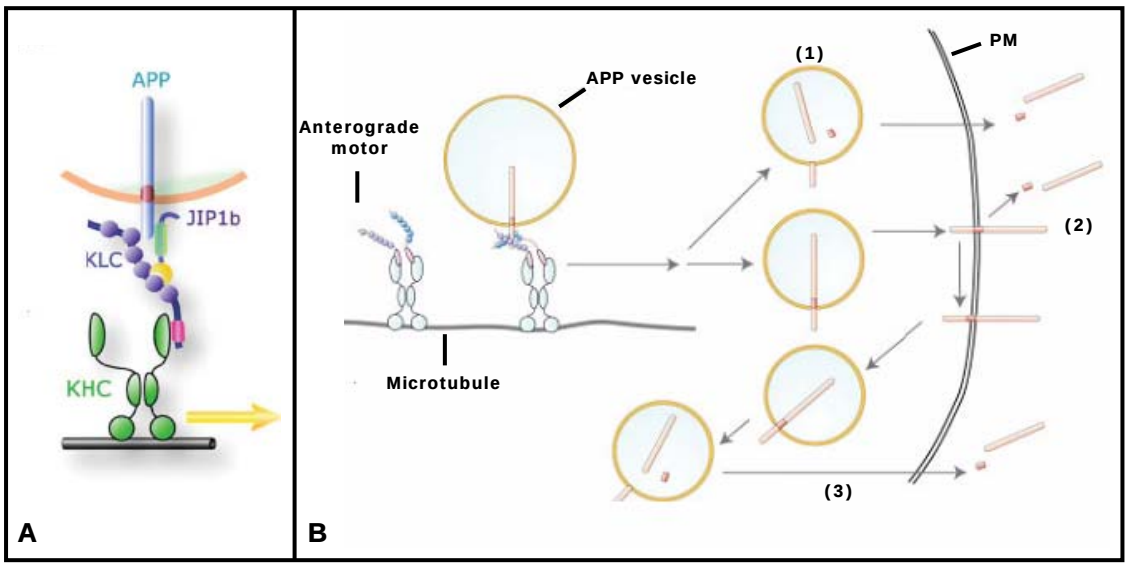

Figure 14. A. Association of APP with the kinesin-I motor. APP binds to KLC through an association with JIP1b, but does not bind to KLC directly. Thus, APP serves as a cargo-receptor via JIP1b **B. APP trafficking.** Anterograde transport of APP vesicles and metabolism of APP. APP can be cleaved during axonal transport **(1)**, at the plasma membrane **(2)**, or during the endocytic cycle **(3)**, generating neurotoxic Abeta (adapted from Suzuki et al. 2006).

In addition, pools of unprocessed synaptic APP are also transported retrogradely (transcytotic movement) from axonal synaptic compartments to neuronal cell bodies and dendrites (Simons et al. 1995; Yamazaki et al. 1995). In rat forebrain and PC12 cells, APP was observed in Rab5-containing endocytic organelles that derive from an endocytic pathway distinct from the one involved in synaptic vesicle recycling (Ikin et al. 1996; Marquez-Sterling et al. 1997). Further, cell-surface APP was initially internalized with membrane proteins of recycling synaptic vesicles, but subsequently sorted away from these vesicles and retrogradely transported to the soma (Marquez-Sterling et al. 1997).

APP processing and its intracellular trafficking

Through the use of radioactivity-based techniques, the half-life of total cellular APP was estimated to be of approximately 1 h (Koo et al. 1996; Weidemann et al. 1989). Nascent and immature (only N-glycosylated) APP can be degraded to a high degree by the proteasome, probably via the smooth ER (Kouchi et al. 1999; Yang et al. 1998). Additionally, immature APP may be cleaved by secretases at a low rate in the ER or the cis-Golgi but, as explained above, the majority of these cleavages occur after APP maturation complete. Mature APP is processed rapidly (turnover of 45 min) as it is transported to or from the cell surface via the secretory or endocytic pathways (Cook et al. 1997; De Strooper et al. 1993; Haass et al. 1992; Hartmann et al. 1997; Kuentzel et al. 1993; Marambaud et al. 1997b; Sambamurti et al. 1992; Shoji et al. 1992). In several types of cultured cells, part of the TGN/Golgi APP pool was observed to be locally cleaved by α-secretase. β-secretases can also cleave a fraction of Golgi APP but to a lesser extent. Approximately 30% of surface APP is cleaved to sAPP (Koo et al. 1996), with 20% being cleaved within 10 min (Lai et al. 1995). The remaining full-length APP and the cleavage products (CTFs) are re-internalized via coated pits and vesicles by receptor-mediated endocytosis (Yamazaki et al. 1996). The net result of cell surface APP proteolytic cleavage and endocytosis is the rapid removal of cell surface APP. Indeed, the estimated half-life for surface-expressed APP is less than 10 min (Koo et al. 1996). Consequently, only minor amounts of APP (as compared to the total cellular pool) are detected at the cell surface (Kuentzel et al. 1993). The half-life of internalized APP was calculated to be ~30 min (Koo et al. 1996), with a pool of endosomal APP being delivered to lysosomes. The remaining cell surface CTFs may be subsequentially cleaved by γ-secretase to AICD, at the cell surface or upon endocytosis in endosomes, or further degraded in lysosomes (Chen et al. 2000; Kaether et al. 2006b; Mathews et al. 2002). CTFs produced at the TGN/Golgi are thought to be cleaved locally or to be delivered to lysosomes for degradation (Chen et al. 2000). In neurons, sAPP may also be generated and released at the synaptic terminals via α-secretase cleavage (McLaughlin and Breen 1999).

During the APP secretory pathway, the majority of Abeta fragments are thought to be generated in the late Golgi, from where these peptides are packaged into post-TGN vesicles destined for extracellular secretion (Gouras et al. 2000a; Xia 2001). This Abeta production seems to occur at the TGN and does not need post-TGN vesicle formation (Xu et al. 2001). At the TGN, the absolute levels of both $Abeta_{1-40}$ and $Abeta_{1-42}$ are high and the ratio $Abeta_{1-42}$ to total Abeta is 0.05-0.16 (Greenfield et al. 1999). A minority of Abeta peptides (1-40, 1-42 and x-42) is thought to be generated in the ER (Greenfield et al. 1999; Xia 2001; Xia et al. 1998), but some authors

arguethat the γ-secretase complex is still not formed or active in the ER (Kaether et al. 2006a). A major portion of Abeta peptides are also generated in the endocytic pathway, following internalization of APP from the plasma membrane. In fact, mutations of the APP ^{682}YENPTY^{687} domain that significantly impair APP endocytosis simultaneously inhibit Abeta levels (Perez et al. 1999). Recent findings locate β- and γ-secretases within the cholesterol-enriched plasma membrane lipid rafts, but Abeta production at the cellular membrane was reported to occur at a lower level. APP was thus suggested to be potentially segregated from its proteases by the rafts lipid boundary (Kaether and Haass 2004). Finally, Abeta production was also reported in axonal vesicular compartments (Kamal et al. 2001). The putative subcellular localization of APP proteolytic processing is shown in Figure 16.

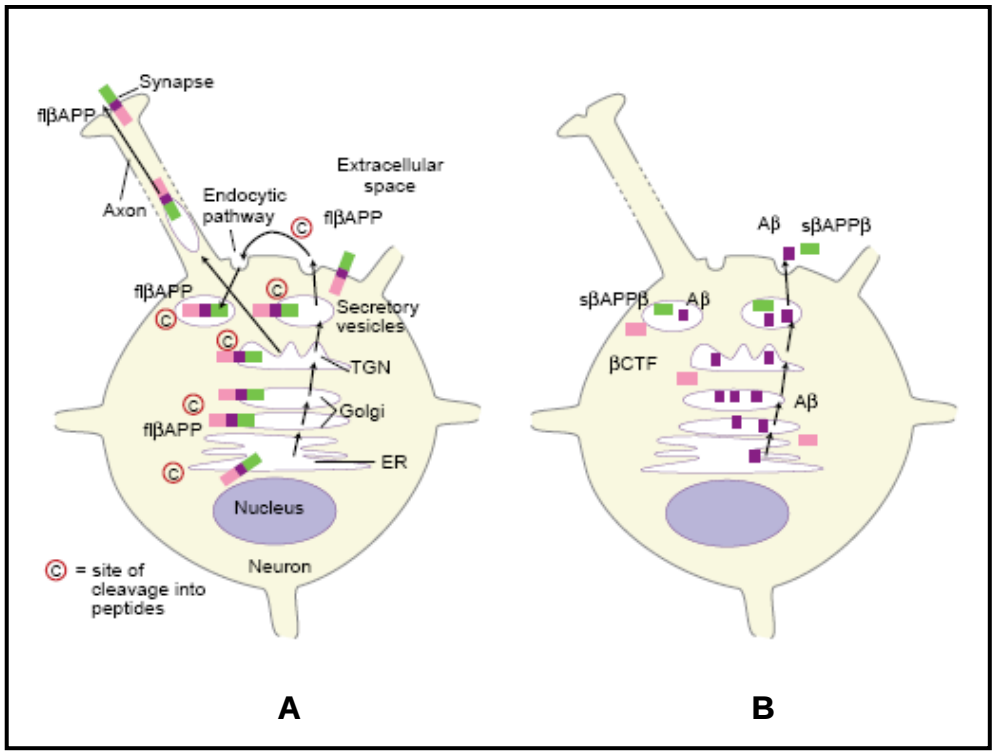

Figure 3. Possible cellular trafficking of β-amyloid (Aβ). (A) In the cell body of a neuron, full-length β-amyloid precursor protein holoprotein (flβAPP) is generated in the endoplasmic reticulum (ER), transported through the Golgi complex, and carried in post-trans Golgi network (post-TGN) secretory vesicles to the plasma membrane. Most flβAPP resides in the Golgi complex, but some is also transported from the cell body down axons by fast axonal transport and reportedly is contained in multivesicular bodies of synaptic preparations. **(B)** A subset of flβAPP molecules are cleaved during export. A minority of Aβ peptides are generated in the ER, butthe majority are generated in the Golgi complex, from where most Aβ peptides are packaged into post-TGN vesicles destined for secretion into the extracellular space. Soluble α-

cleaved βAPP (sβAPPα) is also generatedin post-TGN vesicles and/or at the plasma membrane, from where it is secreted into the extracellular space. Aβ is also thought to be generated in the endocytic pathway following internalisation of βAPP from the plasmamembrane (taken from Gouras 2001).

1.6 PHOSPHORYLATION-DEPENDENT APP REGULATION

1.6.1 Protein phosphorylation in AD

Several neurodegenerative disorders are the result of altered signal transduction pathways. One of these disorders is AD where the abnormal protein kinase (Jin and Saitoh 1995), as well as protein phosphatase (Gong et al. 1993), activities in brains were reported when compared with their normal aged controls. Moreover, it has been suggested that altered/abnormal signalling may lead to an increased neuronal Abeta load (Nitsch et al. 1992; Selkoe 1993). The overall result of such dysfunction is the association of neurodegenerative conditions with abnormal phosphorylation of key proteins, as has been reported for tau (Grundke-Iqbal et al. 1986). Thus, this key event in cell regulation, reversible protein phosphorylation, consists in the transfer of a phosphate group from ATP to the substrate protein, altering its conformation and function. A protein kinase facilitates the transfer and a protein phosphatase removes the phosphate, and returns the protein to its original state.

Interestingly, the brain is the mammalian tissue with the highest levels of protein kinases and phosphatases, indicating that protein phosphorylation is particularly important to brain function. Impaired balance of cellular phosphorylation systems has been reported to occur in AD. These abnormalities include both expression and activity levels of kinases and phosphatases, which result in alterations in the processing of APP and consequently Abeta production (da Cruz e Silva et al. 1995; Gandy and Greengard 1994; Tian and Wang 2002). Furthermore, altered protein kinase C (PKC) levels and activity, decreased activity of protein phosphatases PP1 and PP2A, overexpression of calcineurin mRNA levels, protein tau and β-Tubulin hyperphosphorylation states (Bennecib et al. 2000; Gong et al. 1993; Hata et al. 2001; Matsushima et al. 1996; Vijayan et al. 2001) have all been reported in AD. Several proteins associated with AD, including APP, tau, PSEN1, PSEN2 and BACE are phosphorylated *in vivo* and can be regulated by protein phosphorylation. Alterations in the phosphorylation state of APP C-terminal fragments were demonstrated in AD

patients (Lee et al. 2003b). In hippocampal pyramidal neurons phospho-APP was observed to accumulate inside large vesicular structures where it colocalizes with endossome markers and BACE-1 (Lee et al. 2003b).

PKC levels and activity have been reported to be altered in AD brain (Cole et al. 1988), as well as in fibroblasts derived from patients with sporadic AD, familial AD and Down's syndrome (Koo 1997; Maasch et al. 2000). A significant decrease in PKC levels and activity was observed in the membranous fraction of AD human cortex (Cole et al. 1988; Shimohama et al. 1993) and altered immunohistochemical distribution of some PKC isozymes in AD brain has also been reported (Masliah et al. 1990). Comparative studies on phosphatase activities in AD versus control brains (Gong et al. 1993) led to the findings that the activity of the Ser/Thr protein phosphatase PP1 and phosphotyrosyl-protein phosphatases in grey matter and of the Ser/Thr phosphatase PP2A in both grey and white matters were significantly lower in AD brains. In contrast, the mRNA of a PP2B catalytic subunit was found to be up-regulated in AD brain (Hata et al. 2001). The authors used cDNA microarray technology to study altered gene expression in an AD patient afflicted hippocampus. The most up-regulated gene in AD proved to be the β isoform of the catalytic subunit of calcineurin (PP2B Aβ). Indeed, *in situ* hybridization, histochemistry and RT-PCR analysis revealed that PP2B-Abeta was significantly up-regulated in the pyramidal neurons of AD hippocampus (Hata et al. 2001). Interestingly, work from Ermak et al. (2001) revealed that the mRNA levels of a calcineurin inhibitor (DSCR1) were also overexpressed in AD and Down's syndrome patients.

1.6.2 Phosphorylation and APP processing

Although the factors regulating APP processing and Abeta production have not been fully elucidated, it is now widely accepted that protein phosphorylation is involved. Processing of APP and Abeta production were shown to be regulated by phosphorylation and phosphorylation-dependent events (Ando et al. 2001; da Cruz e Silva and da Cruz e Silva 2003; da Cruz e Silva et al. 1995; Gillespie et al. 1992). As APP proteolytic processing is a necessary step in APP RIP cellular signalling and phosphorylation is involved in signal transduction pathways, further elucidation of the molecular mechanisms underlying phosphorylation-dependent regulation of APP processing is required.

Protein kinase C

Previous studies revealed that APP levels and APP processing are regulated by PKC. Long-term exposure of a human glial cell line to PKC stimulating agents, such as the phorbol ester PMA (phorbol 12-myristate 13-acetate), increased APP mRNA levels and protein-binding activity to the APP promoter (Lahiri and Nall 1995; Trejo et al. 1994). Short-term exposures to phorbol esters invariably results in a higher non-amyloidogenic APP processing rate. Phorbol esters such as PMA or phorbol 12,13-dibutyrate (PDBu) enhance α-secretase cleavage of APP and αsAPP production in several cultured cell lines (Buxbaum et al. 1990; Caporaso et al. 1992; da Cruz e Silva et al. 1993; Demaerschalck et al. 1993; Dyrks et al. 1994; Gabuzda et al. 1993; Gillespie et al. 1992; Marambaud et al. 1997a; Marambaud et al. 1997b; Mills et al. 1997; Slack et al. 1993). The phorbol ester-induced APP processing is also evident in primary cultures of rat cortical neurons (Mills and Reiner 1996), and specifically in rat cortical synaptosomes (McLaughlin and Breen 1999). Furthermore, *in vivo* studies using rats expressing hyperactivated PKC demonstrated enhanced synaptosomal sAPP production and decreased levels of synaptosomal membrane-bound APP in selected brain regions (cortex and hippocampus) (Caputi et al. 1997). PKC-mediated stimulation of sAPP has been shown to be specific insofar as down-regulation of PKC blocked the phorbol ester-stimulated sAPP release (Buxbaum et al. 1994). Nonetheless, there is controversy in the effects of this α-secretase pathway induction and the consequential decrease in Abeta production, raising the question of competition between α- and β- secretases for substrate. In fact, PKC-activators or carbachol, which are known α-secretase pathway inducers, were reported to decrease Abeta secretion in cultured cells transfected with APP FAD mutant forms (Felsenstein et al. 1994; Gabuzda et al. 1993; Hung et al. 1993). Constitutive overactivation of PKC in guinea pig brain also enhanced cortical α-secretory APP processing but without decreasing Abeta generation (Rossner et al. 2001). The mechanisms of PKC-dependent induction of APP α-secretase cleavage are complex and still being unravelled. PKC is known to be involved in the process of post-TGN vesicle formation, through binding and activating the phospholipase involved in vesicles scission (Sabatini et al. 1996; Simon et al. 1996). Activation of endogenous PKC by phorbol esters or addition of purified PKC increases formation of APP-containing secretory vesicles from the trans-Golgi network (Xu et al. 1995), and drastically reduces the amount of APP at the cell surface (Koo 1997). This can be explained by accelerated APP trafficking through the exocytotic pathway and accelerated α-secretase APP cleavage intracellularly and at the plasma membrane. The hypothesis that PKC phosphorylation at sites within the APP intracellular carboxy terminus may change the

conformation of its extracellular domain and make it a better substrate for the cleaving enzyme was recently advanced (Turner et al. 2003). Nonetheless, da Cruz e Silva et al. (1993) showed that cleavage of APP tailless constructs (with a stop codon at the KKK sequence) to yield sAPP was still stimulated by phorbol esters. Hence, PKC-dependent sAPP-induction may occur as a sum of direct and indirect actions.

Ser/Thr Protein Phosphatase 1

Okadaic acid (OA), a Ser/Thr protein phosphatases type 1 (PP1) and type 2A (PP2A) inhibitor, was found to stimulate APP processing increasing sAPP secretory from COS-1 cells (da Cruz e Silva et al. 1995). APP processing and secretion modulation by OA was also observed in primary guinea pig neurons (Holzer et al. 2000). da Cruz e Silva et al. (1995) were able to specifically implicate PP1 in this APP regulation through the use of OA and other phosphatase inhibitors with different inhibitory potencies against PP1/PP2A. Interestingly, PP1 is known to be involved in long-term potentiation (LTP) and in long-term depression (LTD), thereby influencing learning and memory (Genoux et al. 2002; Mulkey et al. 1994; Waddell 2003). Furthermore, PP1 and PP2B activities are interconnected, because PP2B is able to inhibit (dephosphorylate) DARPP-32 and I2, a potent PP1 inhibitor (Mulkey et al. 1994; Yan and Mumby 1999), providing a further mechanism for PP2B modulation in APP processing. The mechanism by which PP1 down-regulates APP processing and/or sAPP secretion are not yet defined, but direct APP dephosphorylation remains a possibility (Oishi et al. 1997).

APP secretase phosphorylation

Another potential stage for phosphorylation-dependent regulation of APP proteolytic processing is through modulation of APP secretases. All three members of the ADAM family are synthesized as preproteins, so that their proteolytic function is regulated to prevent damage to other proteins, or the premature cleavage of their substrates, including APP (Turner et al. 2003). The TACE cytoplasmic domain contains potential phosphorylation sites, and the enzyme was reported to be phosphorylated at Ser^{819} after growth factor stimulation of the Erk/MAPK pathway or after PMA-induced PKC-activation (Black et al. 1997; Diaz-Rodriguez et al. 2002). PMA exposure did not alter TACE maturation or cellular distribution (Hooper and Turner 2002), suggesting unknown roles for this phosphorylation that may involve its enzymatic kinetics of APP

proteolysis (Fan et al. 2003). ADAM 10 is also stimulated after PKC activation (Etcheberrigaray et al. 2004). MDC9 was likewise phosphorylated after PMA activation of the PKC isozyme δ (Izumi et al. 1998; Roghani et al. 1999). The role of BACE-1 phosphorylation on a cytoplasmic serine residue is better known and involves regulation of BACE-1 subcellular traffic. When phosphorylated on Ser^{498}, this enzyme enters the recycling pathway of Golgi-retrieval after endocytosis (Walter et al. 2001). Phosphorylation at this serine, which is immediately upstream of the BACE-1 binding sequence for its vesicle coating protein GGA, was recently reported to enhance by three-fold the affinity of this binding (Shiba et al. 2004).

Phosphorylation may also affect γ-secretase activity. The PSEN2 protein can be highly phosphorylated, whereas little phosphorylation is observed for PSEN1 (Walter et al. 1996; Walter et al. 1998). Casein kinases 1 and 2 (CK1, CK2) phosphorylate PSEN2 at three serine residues in its N-terminus before PSEN2 maturational cleavage by caspases, and after this cleavage its C-terminus is also phosphorylated at three serine residues, putatively by the same casein kinases (Walter et al. 1999).

1.6.3 APP as a phosphoprotein

APP can be phosphorylated by different kinases, which are involved in diverse signal transduction pathways, such that APP phosphorylation potentially represents an important target for therapeutical intervention. Moreover, drugs aimed at sustaining PKC activity could help in the prevention of AD, since APP phosphorylation by PKC favors the non-amyloidogenic processing of the protein. Indeed, direct APP phosphorylation is an essential mechanism for regulating APP binding, traffic and processing, and therefore worthwhile pursuing. APP is a phosphoprotein with putative phosphorylation sites on its extracellular and intracellular domains. Of particular note is the finding that AD patients exhibit altered APP phosphorylation (Lee et al. 2003b). APP has ten potentially phosphorylatable residues, which have been shown to be phosphorylated "in vitro" and/or "in vivo" (Iijima et al. 2000; Koo 1997; Minopoli et al. 2001; Oishi et al. 1997; Standen et al. 2001; Walter et al. 2000). Two of these are located in the APP ectodomain and the other eight in the APP cytoplasmic domain (Figure 17).

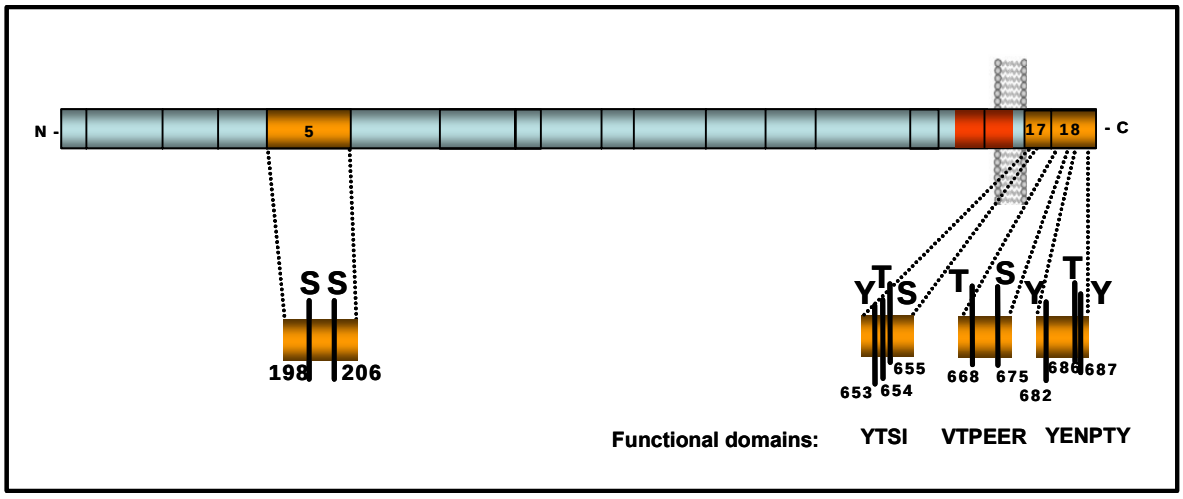

Figure 17. Exon localization of APP phosphorylatable residues. The extracellular (NH2-terminal) APP domain has two phosphorylatable residues (Ser^{198} and Ser^{206}) and the intracellular (COOH-terminal) APP domain contains eight residues (Ser^{653}, Thr^{654}, Ser^{655}, Thr^{668},Ser^{675}, Tyr^{682}, Thr^{686} and Tyr^{687}). (adapted from da Cruz e Silva et al. 2004b).

In its ectodomain APP was reported to be phosphorylated on serine residues (Ser^{198} and Ser^{206}). Phosphorylation of the two serine residues occurs in two distinct cellular locations: in a post-Golgi secretory compartment (most likely within secretory vesicles) and at the cell surface by ectoprotein kinases (Walter et al. 1997). The authors also found that "in vivo" sAPP was detected exclusively in the double phosphorylated form. Subsequently, it was shown that ectocasein kinases 1 and 2 were the kinases involved in the "in vivo" cell surface APP phosphorylation at residues Ser^{198} and Ser^{206}, respectively, in a process strongly inhibited by heparin (Walter et al. 2000). A possible role of these phosphorylations is an involvement in LTP, in neurons, as well as synaptogenesis.

The Ser/Thr and Tyr cytoplasmic phosphorylatable residues are located within three APP functional motifs, previously mentioned and shown in Figure 17: ^{653}YTSI^{656}, ^{667}VTPEER^{672} and ^{682}YENPTY^{687}. Additionally, other potentially phosphorylatable residues (Tyr^{653}, Ser^{675} and Thr^{686}) were reported by (Lee et al. 2003b) but have received little attention.Table 5 summarises APP phosphorylatable residues located in the cytoplasmic domain, with their putative kinases.

Table 5. APP C-terminal phosphorylatable residues. APP residues that can be phosphorylated are indicated, as well as the phosphorylation state in AD brains. The kinases responsible for these phosphorylations are indicated. **Phospho.**, Phosphorylation.

RESIDUE	PHOSPHO. AD BRAINS	PHOSPHO. CAD CELLS	KINASE	REFERENCE
Y^{653}	– Present	– Present	– Not determined	– Lee et al., 2003
T^{654}	– Absent	– Present	– CaMKII	– Gandy et al., 1988 – Oishi et al., 1997 – Ramelot and Nichlson, 2001 – Lee et al., 2003
S^{655}	– Present	– Present	– PKC – CaMKII – APP Kinase I	– Gandy et al., 1988 – Suzuki et al., 1992 – Oishi et al., 1997 – Ramelot and Nichlson, 2001 – Lee et al., 2003
T^{668}	– Present	– Present	– Cdk5 – Cdc2 – GSK-3 – JNK-3	– Suzuki et al., 1994 – Aplin et al., 1996 – Oishi et al., 1997 – Ando et al., 2001 – Ramelot and Nichlson, 2001 – Standen et al., 2001 – Sisodia et al., 2002 – Lee et al., 2003
S^{675}	– Present	– Absent	– Not determined	– Lee et al., 2003
Y^{682}	– Present	– Absent	– TrKA, – c-Abl	– Lee et al., 2003
T^{686}	– Present	– Absent	– Not determined	– Lee et al., 2003
Y^{687}	– Present	– Absent	– Not determined	– Lee et al., 2003

The amino acid sequence ^{653}YTSI^{656} functions as an APP sorting signal. Central to the domain are two consensus residues for phosphorylation, Thr^{654} and Ser^{655}, found to be phosphorylated *in vitro* and *in vivo* (see Table 5). The occurrence of full length APP phosphorylated at Thr^{654} or Ser^{655} has been reported in cultured cell lines and rat cortex (Gandy et al. 1988; Oishi et al. 1997). However, in human hippocampus of AD patients only phospho Ser^{655} CTFs, and not phospho Thr^{654}, was observed (Lee et al. 2003b). It is also believed that these phosphorylations may have a regulatory role for the ^{653}YTSI^{656} APP binding proteins.

The Thr^{668} residue of the ^{667}VTPEER^{672} domain is found phosphorylated in rat brain and in several cell lines (Oishi et al. 1997). In PC12 cells immature APP is preferentially phosphorylated at this residue during the G2/M phase of the cell cycle (Oishi et al. 1997; Suzuki et al. 1994). At this phase total levels of holo APP do not change but the levels of secreted sAPP decrease and the levels of the CTFs increase (Suzuki et al. 1994). Additionally, the Thr^{668} precedes a proline, and can be phosphorylated by several proline-directed kinases, such as the cyclin dependent kinase cdc2, the neuronal analogue cdk5, GSK-3 and JNK. Such phosphorylation has a dual role regulating both neuronal development and neurodegeneration (for review Pastorino and Lu 2006), depending on the kinase involved phosphorylation. For example, cdk5 phosphorylation of Thr^{668} was reported to regulate either the neuronal differentiation (Ando et al., 1999; Iijima et al., 2000) or the amyloidogenic processing of APP (Lee et al. 2003b). Moreover, the GSK-3 dependent phosphorylation of APP was linked to neurodegeneration (Lee et al. 2004; Leroy et al. 2002) and Abeta production (Phiel et al. 2003).

Additionally, it could be speculated that, in the cell, the role of APP phosphorylation at Thr^{668} could determine the exact subcellular localization of the protein. It has been reported that JNK dependent Thr^{668} phosphorylation relocates phosphorylated APP within the neurites, promoting their extension (Muresan and Muresan 2005b) probably through the formation of complexes with the JIP1 and kinesin1 (Muresan and Muresan 2005a) that are specifically located in vesicles at the neuritis and not in the cell bodies. Interestingly, it has been shown that JNK3 dependent phosphorylation of Thr^{668} negatively regulates neuronal differentiation, which is mediated by AICD (Kimberly et al. 2005). In particular, they showed that when phosphorylated at Thr^{668}, AICD is no longer stabilized by FE65, and associates less with FE65. Since the AICD is known to form a complex with FE65 and Tip60 that is directed to the nucleus and regulates transcription, it could be hypothesized that phosphorylation at Thr^{668} affects the AICD-mediated transcriptional activity due to the interference with association of AICD with FE65.

Recent experimental evidence link the phosphorylation at Thr^{668} to increased amyloidogenic processing of APP by γ-secretase (Vingtdeux et al. 2005), and to down-regulation of FE65-mediated transcriptional activity regulated by the factor 14-3-3g, which was shown to bind to the ^{667}VTPEER^{672} domain of AICD and facilitate FE65-dependent gene transactivation forming a complex containing AICD and FE65 (Sumioka et al., 2005).

Indeed, the phosphorylation of APP at Thr^{668} had already been shown to affect the interaction between APP and FE65, probably because the phosphorylation of this residue induces structural changes from *trans*- to *cis*-conformations in the C-terminal domain of the protein (Ramelot and Nicholson 2001). Recently, it was reported that the Pin1 protein binds to the phosphorylated Thr^{668} in APP and regulates its isomerization between the *cis*-and *trans*-conformations, affecting the processing of APP (Pastorino et al. 2006).

Another important domain is the internalization signal domain ^{682}YENPTY^{687}, that is the object of study in this thesis. Of the two tyrosine residues present in the domain Tyr^{682} phosphorylation has been demonstrated to be of functional significance while Tyr^{687} which was initially reported not to undergo phosphorylation (Haass and Selkoe 1993; Koo and Squazzo 1994; Minopoli et al. 2001). APP is tyrosine-phosphorylated in cells expressing a constitutively active form of the Abl proto-oncogene, a non-receptor tyrosine kinase similar to c-Src, which can form a stable complex with APP and Fe65 (Zambrano et al. 2001). Abl-dependent Tyr^{682} phosphorylation appears to involve the nerve growth factor receptor TrkA, to mediate APP membrane internalization and to result in reduced γ-secretase APP processing (Koo and Squazzo 1994; Lai et al. 1995; Tarr et al. 2002). Recently, however and in contrast to previous findings *in vivo* phosphorylation of Tyr^{687} was reported (Lee et al. 2003b). This renews interest on this residue and refocus the functional significance of Tyr^{687} phosphorylation.

The key players controlling signal transduction cascades, the protein kinases and phosphatases, as well as their corresponding regulatory proteins, take on added importance and they can be key targets for therapeutic intervention. Accordingly, several studies have demonstrated that APP subcellular localization, proteolytic processing and protein-protein interaction can be regulated by protein phosphorylation or by phosphorylation-dependent events. APP direct phosphorylation studies that emerge focus on the phosphorylatable residues from the ^{653}YTSI^{656}, ^{667}VTPEER^{672} and ^{682}YENPTY^{687} motifs, previously described. The domain ^{682}YENPTY^{687} comprises a NPTY motif which is a typical internalization signal for membrane-associated receptor proteins, two tyrosine's: Tyr^{682} and Tyr^{687} that can be phosphorylated. This domain is

also responsible for APP interaction with several PTB-containing adaptor proteins. So far, data strongly suggests an involvement of ^{682}YENPTY^{687} domain and Tyr^{682} and Tyr^{687} in particular, on APP traffic, processing and correspondent Abeta production. Of particular note is the importance of both phosphorylatable residues on protein-protein interaction. Nonetheless, little is known about the physiological relevance of APP Tyr^{687} phosphorylation including a role in signal transduction, and this will be addressed in the work presented here.

1.7. AIM OF THIS THESIS

APP processing has been the subject of many studies, and our knowledge in this area has increased considerably with several pathways and the proteolytic fragments formed being unravelled. The regulatory mechanism underlying APP processing have been more elusive. Further, although APP is a phosphoprotein functional links have not been made to all its phosphorylatable residues.

Thus, the aim of this thesis is to study the putative role of direct APP phosphorylation at the Tyr^{687} residue and the consequent protein's cellular fate, both in terms of APP intracellular targeting and proteolytic processing. Understanding molecular mechanisms controlling these APP trafficking and processing events and their relevance in terms of APP function will provide us novel insights in terms the molecular and cellular of AD pathology.

The central hypothesis to this thesis is that direct APP phosphorylation of the NPTY domain is of consequence to APP metabolism. As such, the specific aims were as follows:

1. To develop a model system to study APP trafficking and processing;

2. To analyze the effect of the Tyr^{687} phosphorylation on APP trafficking and processing by using phosphorylation/dephosphorylation mimicking mutants (Y687E and Y687F, respectively);

3. To identify novel APP interacting proteins and to determine how the phosphorylation state of APP regulates multiprotein complex formation.

1.8. REFERENCES

Allinquant B, Hantraye P, Mailleux P, Moya K, Bouillot C, Prochiantz A. 1995. Downregulation of amyloid precursor protein inhibits neurite outgrowth in vitro. J Cell Biol 128(5):919-927.

Allinquant B, Moya KL, Bouillot C, Prochiantz A. 1994. Amyloid precursor protein in cortical neurons: coexistence of two pools differentially distributed in axons and dendrites and association with cytoskeleton. J Neurosci 14(11 Pt 2):6842-6854.

Allsopp TE. 2000. Transduction of survival signals in neurons - take your PIK? Trends Neurosci 23(12):593.

Andersen OM, Reiche J, Schmidt V, Gotthardt M, Spoelgen R, Behlke J, von Arnim CA, Breiderhoff T, Jansen P, Wu X, Bales KR, Cappai R, Masters CL, Gliemann J, Mufson EJ, Hyman BT, Paul SM, Nykjaer A, Willnow TE. 2005. Neuronal sorting protein-related receptor sorLA/LR11 regulates processing of the amyloid precursor protein. Proc Natl Acad Sci U S A 102(38):13461-13466.

Ando K, Iijima KI, Elliott JI, Kirino Y, Suzuki T. 2001. Phosphorylation-dependent regulation of the interaction of amyloid precursor protein with Fe65 affects the production of beta-amyloid. J Biol Chem 276(43):40353-40361.

Ando K, Oishi M, Takeda S, Iijima K, Isohara T, Nairn AC, Kirino Y, Greengard P, Suzuki T. 1999. Role of phosphorylation of Alzheimer's amyloid precursor protein during neuronal differentiation. J Neurosci 19(11):4421-4427.

Bayer TA, Cappai R, Masters CL, Beyreuther K, Multhaup G. 1999. It all sticks together--the APP-related family of proteins and Alzheimer's disease. Mol Psychiatry 4(6):524-528.

Bayer TA, Wirths O, Majtenyi K, Hartmann T, Multhaup G, Beyreuther K, Czech C. 2001. Key factors in Alzheimer's disease: beta-amyloid precursor protein processing, metabolism and intraneuronal transport. Brain Pathol 11(1):1-11.

Bearer CF. 2001. L1 cell adhesion molecule signal cascades: targets for ethanol developmental neurotoxicity. Neurotoxicology 22(5):625-633.

Beher D, Hesse L, Masters CL, Multhaup G. 1993 Regulation of amyloid protein precursor (APP) binding to collagen and mapping of the binding sites on APP and collagen type I. J Biol Chem 271 1613-1620.

Bennecib M, Gong CX, Grundke-Iqbal I, Iqbal K. 2000. Role of protein phosphatase-2A and -1 in the regulation of GSK-3, cdk5 and cdc2 and the phosphorylation of tau in rat forebrain. FEBS Lett 485(1):87-93.

Bennett BD, Denis P, Haniu M, Teplow DB, Kahn S, Louis JC, Citron M, Vassar R. 2000. A furin-like convertase mediates propeptide cleavage of BACE, the Alzheimer's beta -secretase. J Biol Chem 275(48):37712-37717.

Berdnik D, Torok T, Gonzalez-Gaitan M, Knoblich JA. 2002. The endocytic protein alpha-Adaptin is required for numb-mediated asymmetric cell division in Drosophila. Dev Cell 3(2):221-231.

Bertram L, Tanzi RE. 2004. The current status of Alzheimer's disease genetics: what do we tell the patients? Pharmacol Res 50(4):385-396.

Bibel M, Richter J, Schrenk K, Tucker K, Staiger V, Korte M, Goetz M, Barde Y. 2004. Differentiation of mouse embryonic stem cells into a defined neuronal lineage. Nat Neurosci 7:1003-1009.

Bigl M, Apelt J, Luschekina EA, Lange-Dohna C, Rossner S, Schliebs R. 2000. Expression of beta-secretase mRNA in transgenic Tg2576 mouse brain with Alzheimer plaque pathology. Neurosci Lett 292(2):107-110.

Black RA, Rauch CT, Kozlosky CJ, Peschon JJ, Slack JL, Wolfson MF, Castner BJ, Stocking KL, Reddy P, Srinivasan S, Nelson N, Boiani N, Schooley KA, Gerhart M, Davis R, Fitzner JN, Johnson RS, Paxton RJ, March CJ, Cerretti DP. 1997. A metalloproteinase disintegrin that releases tumour-necrosis factor-alpha from cells. Nature 385(6618):729-733.

Blacker D, Bertram L, Saunders AJ, Moscarillo TJ, Albert MS, Wiener H, Perry RT, Collins JS, Harrell LE, Go RC, Mahoney A, Beaty T, Fallin MD, Avramopoulos D,

Chase GA, Folstein MF, McInnis MG, Bassett SS, Doheny KJ, Pugh EW, Tanzi RE. 2003. Results of a high-resolution genome screen of 437 Alzheimer's disease families. Hum Mol Genet 12(1):23-32.

Borg JP, Ooi J, Levy E, Margolis B. 1996. The phosphotyrosine interaction domains of X11 and FE65 bind to distinct sites on the YENPTY motif of amyloid precursor protein. Mol Cell Biol 16(11):6229-6241.

Borg JP, Yang Y, De Taddeo-Borg M, Margolis B, Turner RS. 1998. The X11alpha protein slows cellular amyloid precursor protein processing and reduces Abeta40 and Abeta42 secretion. J Biol Chem 273(24):14761-14766.

Bothwell M, Giniger E. 2000. Alzheimer's disease: neurodevelopment converges with neurodegeneration. Cell 102(3):271-273.

Braak H, Braak E. 1994. Morphological criteria for the recognition of Alzheimer's disease and the distribution pattern of cortical changes related to this disorder. Neurobiol Aging 15(3):355-356; discussion 379-380.

Breen KC, Bruce M, Anderton BH. 1991. Beta amyloid precursor protein mediates neuronal cell-cell and cell-surface adhesion. J Neurosci Res 28(1):90-100.

Burdick D, Soreghan B, Kwon M, Kosmoski J, Knauer M, Henschen A, Yates J, Cotman C, Glabe C. 1992. Assembly and aggregation properties of synthetic Alzheimer's A4/beta amyloid peptide analogs. J Biol Chem 267(1):546-554.

Bush AI, Multhaup G, Moir RD, Williamson TG, Small DH, Rumble B, Pollwein P, Beyreuther K, Masters CL. 1993. A novel zinc(II) binding site modulates the function of the beta A4 amyloid protein precursor of Alzheimer's disease. J Biol Chem 268(22):16109-16112.

Bush AI, Pettingell WH, Jr., de Paradis M, Tanzi RE, Wasco W. 1994. The amyloid beta-protein precursor and its mammalian homologues. Evidence for a zinc-modulated heparin-binding superfamily. J Biol Chem 269(43):26618-26621.

Buxbaum JD, Gandy SE, Cicchetti P, Ehrlich ME, Czernik AJ, Fracasso RP, Ramabhadran TV, Unterbeck AJ, Greengard P. 1990. Processing of Alzheimer beta/A4 amyloid precursor protein: modulation by agents that regulate protein phosphorylation. Proc Natl Acad Sci U S A 87(15):6003-6006.

Buxbaum JD, Koo EH, Greengard P. 1993. Protein phosphorylation inhibits production of Alzheimer amyloid beta/A4 peptide. Proc Natl Acad Sci U S A 90(19):9195-9198.

Buxbaum JD, Ruefli AA, Parker CA, Cypess AM, Greengard P. 1994. Calcium regulates processing of the Alzheimer amyloid protein precursor in a protein kinase C-independent manner. Proc Natl Acad Sci U S A 91(10):4489-4493.

Cai D, Leem JY, Greenfield JP, Wang P, Kim BS, Wang R, Lopes KO, Kim SH, Zheng H, Greengard P, Sisodia SS, Thinakaran G, Xu H. 2003. Presenilin-1 regulates intracellular trafficking and cell surface delivery of beta-amyloid precursor protein. J Biol Chem 278(5):3446-3454.

Cai XD, Golde TE, Younkin SG. 1993. Release of excess amyloid beta protein from a mutant amyloid beta protein precursor. Science 259(5094):514-516.

Caille I, Allinquant B, Dupont E, Bouillot C, Langer A, Muller U, Prochiantz A. 2004. Soluble form of amyloid precursor protein regulates proliferation of progenitors in the adult subventricular zone. Development 131(9):2173-2181.

Cao X, Sudhof TC. 2001. A transcriptionally [correction of transcriptively] active complex of APP with Fe65 and histone acetyltransferase Tip60. Science 293(5527):115-120.

Cao X, Sudhof TC. 2004. Dissection of amyloid-beta precursor protein-dependent transcriptional transactivation. J Biol Chem 279(23):24601-24611.

Capell A, Steiner H, Willem M, Kaiser H, Meyer C, Walter J, Lammich S, Multhaup G, Haass C. 2000. Maturation and pro-peptide cleavage of beta-secretase. J Biol Chem 275(40):30849-30854.

Caporaso GL, Gandy SE, Buxbaum JD, Ramabhadran TV, Greengard P. 1992. Protein phosphorylation regulates secretion of Alzheimer beta/A4 amyloid precursor protein. Proc Natl Acad Sci U S A 89(7):3055-3059.

Caporaso GL, Takei K, Gandy SE, Matteoli M, Mundigl O, Greengard P, De Camilli P. 1994. Morphologic and biochemical analysis of the intracellular trafficking of the Alzheimer beta/A4 amyloid precursor protein. J Neurosci 14(5 Pt 2):3122-3138.

Caputi A, Barindelli S, Pastorino L, Cimino M, Buxbaum JD, Cattabeni F, Di Luca M. 1997. Increased secretion of the amino-terminal fragment of amyloid precursor protein in brains of rats with a constitutive up-regulation of protein kinase C. J Neurochem 68(6):2523-2529.

Chan SL, Furukawa K, Mattson MP. 2002. Presenilins and APP in neuritic and synaptic plasticity: implications for the pathogenesis of Alzheimer's disease. Neuromolecular Med 2(2):167-196.

Chang KA, Suh YH. 2005. Pathophysiological roles of amyloidogenic carboxy-terminal fragments of the beta-amyloid precursor protein in Alzheimer's disease. J Pharmacol Sci 97(4):461-471.

Chang L, Bakhos L, Wang Z, Venton DL, Klein WL. 2003. Femtomole immunodetection of synthetic and endogenous amyloid-beta oligomers and its application to Alzheimer's disease drug candidate screening. J Mol Neurosci 20(3):305-313.

Chartier-Harlin MC, Crawford F, Hamandi K, Mullan M, Goate A, Hardy J, Backhovens H, Martin JJ, Broeckhoven CV. 1991. Screening for the beta-amyloid precursor protein mutation (APP717: Val----Ile) in extended pedigrees with early onset Alzheimer's disease. Neurosci Lett 129(1):134-135.

Chen F, Yang DS, Petanceska S, Yang A, Tandon A, Yu G, Rozmahel R, Ghiso J, Nishimura M, Zhang DM, Kawarai T, Levesque G, Mills J, Levesque L, Song YQ, Rogaeva E, Westaway D, Mount H, Gandy S, St George-Hyslop P, Fraser PE. 2000. Carboxyl-terminal fragments of Alzheimer beta-amyloid precursor protein accumulate in restricted and unpredicted intracellular compartments in presenilin 1-deficient cells. J Biol Chem 275(47):36794-36802.

Chen WJ, Goldstein JL, Brown MS. 1990. NPXY, a sequence often found in cytoplasmic tails, is required for coated pit-mediated internalization of the low density lipoprotein receptor. J Biol Chem 265(6):3116-3123.

Chen Y, Liu W, McPhie DL, Hassinger L, Neve RL. 2003. APP-BP1 mediates APP-induced apoptosis and DNA synthesis and is increased in Alzheimer's disease brain. J Cell Biol 163(1):27-33.

Chow N, Korenberg JR, Chen XN, Neve RL. 1996. APP-BP1, a novel protein that binds to the carboxyl-terminal region of the amyloid precursor protein. J Biol Chem 271(19):11339-11346.

Citron M. 2004. Beta-secretase inhibition for the treatment of Alzheimer's disease--promise and challenge. Trends Pharmacol Sci 25(2):92-97.

Citron M, Oltersdorf T, Haass C, McConlogue L, Hung AY, Seubert P, Vigo-Pelfrey C, Lieberburg I, Selkoe DJ. 1992. Mutation of the beta-amyloid precursor protein in familial Alzheimer's disease increases beta-protein production. Nature 360(6405):672-674.

Citron M, Westaway D, Xia W, Carlson G, Diehl T, Levesque G, Johnson-Wood K, Lee M, Seubert P, Davis A, Kholodenko D, Motter R, Sherrington R, Perry B, Yao H, Strome R, Lieberburg I, Rommens J, Kim S, Schenk D, Fraser P, St George Hyslop P, Selkoe DJ. 1997. Mutant presenilins of Alzheimer's disease increase production of 42-residue amyloid beta-protein in both transfected cells and transgenic mice. Nat Med 3(1):67-72.

Clark MJ, Gagnon J, Williams AF, Barclay AN. 1985. MRC OX-2 antigen: a lymphoid/neuronal membrane glycoprotein with a structure like a single immunoglobulin light chain. EMBO J 4:113-118.

Clements A, Walsh DM, Williams CH, Allsop D. 1993. Effects of the mutations Glu22 to Gln and Ala21 to Gly on the aggregation of a synthetic fragment of the Alzheimer's amyloid beta/A4 peptide. Neurosci Lett 161(1):17-20.

Cole G, Dobkins KR, Hansen LA, Terry RD, Saitoh T. 1988. Decreased levels of protein kinase C in Alzheimer brain. Brain Res 452(1-2):165-174.

Cook DG, Forman MS, Sung JC, Leight S, Kolson DL, Iwatsubo T, Lee VM, Doms RW. 1997. Alzheimer's A beta(1-42) is generated in the endoplasmic reticulum/intermediate compartment of NT2N cells. Nat Med 3(9):1021-1023.

Corder EH, Saunders AM, Strittmatter WJ, Schmechel DE, Gaskell PC, Small GW, Roses AD, Haines JL, Pericak-Vance MA. 1993. Gene dose of apolipoprotein E type 4 allele and the risk of Alzheimer's disease in late onset families. Science 261(5123):921-923.

Coulson EJ, Paliga K, Beyreuther K, Masters CL. 2000. What the evolution of the amyloid protein precursor supergene family tells us about its function. Neurochem Int 36(3):175-184.

Crimson M, Eggert A. 1999. Alheimer's disease. DiPiro JT TR, Yee GC, Matzke GR, Well BG, Posey LM, editor. New York: Appleton and Lange.

Cruts M, van Duijn CM, Backhovens H, Van den Broeck M, Wehnert A, Serneels S, Sherrington R, Hutton M, Hardy J, St George-Hyslop PH, Hofman A, Van Broeckhoven C. 1998. Estimation of the genetic contribution of presenilin-1 and -2 mutations in a population-based study of presenile Alzheimer disease. Hum Mol Genet 7(1):43-51.

Cupers P, Orlans I, Craessaerts K, Annaert W, De Strooper B. 2001. The amyloid precursor protein (APP)-cytoplasmic fragment generated by gamma-secretase is rapidly degraded but distributes partially in a nuclear fraction of neurones in culture. J Neurochem 78(5):1168-1178.

da Cruz e Silva EF, da Cruz e Silva OA. 2003. Protein phosphorylation and APP metabolism. Neurochem Res 28(10):1553-1561.

da Cruz e Silva EF, da Cruz e Silva OA, Zaia CT, Greengard P. 1995. Inhibition of protein phosphatase 1 stimulates secretion of Alzheimer amyloid precursor protein. Mol Med 1(5):535-541.

da Cruz e Silva OA, Fardilha M, Henriques AG, Rebelo S, Vieira S, da Cruz e Silva EF. 2004a. Signal transduction therapeutics: relevance for Alzheimer's disease. J Mol Neurosci 23(1-2):123-142.

da Cruz e Silva OA, Iverfeldt K, Oltersdorf T, Sinha S, Lieberburg I, Ramabhadran TV, Suzuki T, Sisodia SS, Gandy S, Greengard P. 1993. Regulated cleavage of Alzheimer beta-amyloid precursor protein in the absence of the cytoplasmic tail. Neuroscience 57(4):873-877.

da Cruz e Silva OA, Vieira SI, Rebelo S, da Cruz e Silva EF. 2004b. A model system to study intracellular trafficking and processing of the Alzheimer's amyloid precursor protein. Neurodegener Dis 1(4-5):196-204.

Daigle I, Li C. 1993. apl-1, a Caenorhabditis elegans gene encoding a protein related to the human beta-amyloid protein precursor. Proc Natl Acad Sci U S A 90(24):12045-12049.

Daw EW, Payami H, Nemens EJ, Nochlin D, Bird TD, Schellenberg GD, Wijsman EM. 2000. The number of trait loci in late-onset Alzheimer disease. Am J Hum Genet 66(1):196-204.

De Strooper B, Umans L, Van Leuven F, Van Den Berghe H. 1993. Study of the synthesis and secretion of normal and artificial mutants of murine amyloid precursor protein (APP): cleavage of APP occurs in a late compartment of the default secretion pathway. J Cell Biol 121(2):295-304.

Delacourte A, Sergeant N, Champain D, Wattez A, Maurage CA, Lebert F, Pasquier F, David JP. 2002. Nonoverlapping but synergetic tau and APP pathologies in sporadic Alzheimer's disease. Neurology 59(3):398-407.

Demaerschalck I, Delvaux A, Octave JN. 1993. Activation of protein kinase C increases the extracellular release of the transmembrane amyloid protein precursor of Alzheimer's disease. Biochim Biophys Acta 1181(3):214-218.

Diaz-Rodriguez E, Montero JC, Esparis-Ogando A, Yuste L, Pandiella A. 2002. Extracellular signal-regulated kinase phosphorylates tumor necrosis factor alpha-converting enzyme at threonine 735: a potential role in regulated shedding. Mol Biol Cell 13(6):2031-2044.

Doyle E, Bruce MT, Breen KC, Smith DC, Anderton B, Regan CM. 1990. Intraventricular infusions of antibodies to amyloid-beta-protein precursor impair the acquisition of a passive avoidance response in the rat. Neurosci Lett 115(1):97-102.

Duilio A, Faraonio R, Minopoli G, Zambrano N, Russo T. 1998. Fe65L2: a new member of the Fe65 protein family interacting with the intracellular domain of the Alzheimer's beta-amyloid precursor protein. Biochem J 330 (Pt 1):513-519.

Dyrks T, Monning U, Beyreuther K, Turner J. 1994. Amyloid precursor protein secretion and beta A4 amyloid generation are not mutually exclusive. FEBS Lett 349(2):210-214.

Edbauer D, Winkler E, Regula JT, Pesold B, Steiner H, Haass C. 2003. Reconstitution of gamma-secretase activity. Nat Cell Biol 5(5):486-488.

Eikelenboom P, Zhan SS, van Gool WA, Allsop D. 1994. Inflammatory mechanisms in Alzheimer's disease. Trends Pharmacol Sci 15(12):447-450.

El Khoury HS, Thomas CA, Cao L, Silverstein SC, Loike JD. 1996. Scavenger receptor-mediated adhesion of microglia to beta-amyloid fibrils. nature 382:716-719.

Ermak G, Morgan TE, Davies KJ. 2001. Chronic overexpression of the calcineurin inhibitory gene DSCR1 (Adapt78) is associated with Alzheimer's disease. J Biol Chem 276(42):38787-38794.

Ermekova KS, Zambrano N, Linn H, Minopoli G, Gertler F, Russo T, Sudol M. 1997. The WW domain of neural protein FE65 interacts with proline-rich motifs in Mena, the mammalian homolog of Drosophila enabled. J Biol Chem 272(52):32869-32877.

Esler WP, Kimberly WT, Ostaszewski BL, Ye W, Diehl TS, Selkoe DJ, Wolfe MS. 2002. Activity-dependent isolation of the presenilin- gamma -secretase complex reveals nicastrin and a gamma substrate. Proc Natl Acad Sci U S A 99(5):2720-2725.

Esler WP, Wolfe MS. 2001. A portrait of Alzheimer secretases--new features and familiar faces. Science 293(5534):1449-1454.

Estus S, Golde TE, Younkin SG. 1992. Normal processing of the Alzheimer's disease amyloid beta protein precursor generates potentially amyloidogenic carboxyl-terminal derivatives. Ann N Y Acad Sci 674:138-148.

Etcheberrigaray R, Tan M, Dewachter I, Kuiperi C, Van der Auwera I, Wera S, Qiao L, Bank B, Nelson TJ, Kozikowski AP, Van Leuven F, Alkon DL. 2004. Therapeutic effects of PKC activators in Alzheimer's disease transgenic mice. Proc Natl Acad Sci U S A 101(30):11141-11146.

Fan H, Turck CW, Derynck R. 2003. Characterization of growth factor-induced serine phosphorylation of tumor necrosis factor-alpha converting enzyme and of an alternatively translated polypeptide. J Biol Chem 278(20):18617-18627.

Farrer LA, Cupples LA, Haines JL, Hyman B, Kukull WA, Mayeux R, Myers RH, Pericak-Vance MA, Risch N, van Duijn CM. 1997. Effects of age, sex, and ethnicity on the association between apolipoprotein E genotype and Alzheimer disease. A meta-analysis. APOE and Alzheimer Disease Meta Analysis Consortium. Jama 278(16):1349-1356.

Felsenstein KM, Ingalls KM, Hunihan LW, Roberts SB. 1994. Reversal of the Swedish familial Alzheimer's disease mutant phenotype in cultured cells treated with phorbol 12,13-dibutyrate. Neurosci Lett 174(2):173-176.

Ferreira A, Caceres A, Kosik KS. 1993. Intraneuronal compartments of the amyloid precursor protein. J Neurosci 13(7):3112-3123.

Fiore F, Zambrano N, Minopoli G, Donini V, Duilio A, Russo T. 1995. The regions of the Fe65 protein homologous to the phosphotyrosine interaction/phosphotyrosine binding domain of Shc bind the intracellular domain of the Alzheimer's amyloid precursor protein. J Biol Chem 270(52):30853-30856.

Flood JF, Morley JE, Roberts E. 1991. Amnestic effects in mice of four synthetic peptides homologous to amyloid beta protein from patients with Alzheimer disease. Proc Natl Acad Sci U S A 88(8):3363-3366.

Francis R, McGrath G, Zhang J, Ruddy DA, Sym M, Apfeld J, Nicoll M, Maxwell M, Hai B, Ellis MC, Parks AL, Xu W, Li J, Gurney M, Myers RL, Himes CS, Hiebsch R, Ruble C, Nye JS, Curtis D. 2002. aph-1 and pen-2 are required for Notch pathway signaling, gamma-secretase cleavage of betaAPP, and presenilin protein accumulation. Dev Cell 3(1):85-97.

Fukumoto H, Cheung BS, Hyman BT, Irizarry MC. 2002. Beta-secretase protein and activity are increased in the neocortex in Alzheimer disease. Arch Neurol 59(9):1381-1389.

Fukumoto H, Rosene DL, Moss MB, Raju S, Hyman BT, Irizarry MC. 2004. Beta-secretase activity increases with aging in human, monkey, and mouse brain. Am J Pathol 164(2):719-725.

Gabuzda D, Busciglio J, Yankner BA. 1993. Inhibition of beta-amyloid production by activation of protein kinase C. J Neurochem 61(6):2326-2329.

Gandy S. 2005. The role of cerebral amyloid beta accumulation in common forms of Alzheimer disease. J Clin Invest 115(5):1121-1129.

Gandy S, Czernik AJ, Greengard P. 1988. Phosphorylation of Alzheimer disease amyloid precursor peptide by protein kinase C and Ca2+/calmodulin-dependent protein kinase II. Proc Natl Acad Sci U S A 85(16):6218-6221.

Gandy S, Greengard P. 1994. Regulated cleavage of the Alzheimer amyloid precursor protein: molecular and cellular basis. Biochimie 76(3-4):300-303.

Gao Y, Pimplikar SW. 2001. The gamma -secretase-cleaved C-terminal fragment of amyloid precursor protein mediates signaling to the nucleus. Proc Natl Acad Sci U S A 98(26):14979-14984.

Garcia CK, Wilund K, Arca M, Zuliani G, Fellin R, Maioli M, Calandra S, Bertolini S, Cossu F, Grishin N, Barnes R, Cohen JC, Hobbs HH. 2001. Autosomal recessive hypercholesterolemia caused by mutations in a putative LDL receptor adaptor protein. Science 292(5520):1394-1398.

Genoux D, Haditsch U, Knobloch M, Michalon A, Storm D, Mansuy IM. 2002. Protein phosphatase 1 is a molecular constraint on learning and memory. Nature 418(6901):970-975.

Gervais FG, Xu D, Robertson GS, Vaillancourt JP, Zhu Y, Huang J, LeBlanc A, Smith D, Rigby M, Shearman MS, Clarke EE, Zheng H, Van Der Ploeg LH, Ruffolo SC, Thornberry NA, Xanthoudakis S, Zamboni RJ, Roy S, Nicholson DW. 1999. Involvement of caspases in proteolytic cleavage of Alzheimer's amyloid-beta precursor protein and amyloidogenic A beta peptide formation. Cell 97(3):395-406.

Ghiso J, Rostagno A, Gardella JE, Liem L, Gorevic PD, Frangione B. 1992. A 109-amino-acid C-terminal fragment of Alzheimer's-disease amyloid precursor protein contains a sequence, -RHDS-, that promotes cell adhesion. Biochem J 288 (Pt 3):1053-1059.

Gillespie SL, Golde TE, Younkin SG. 1992. Secretory processing of the Alzheimer amyloid beta/A4 protein precursor is increased by protein phosphorylation. Biochem Biophys Res Commun 187(3):1285-1290.

Glenner GG, Wong CW. 1984. Alzheimer's disease: initial report of the purification and characterization of a novel cerebrovascular amyloid protein. Biochem Biophys Res Commun 120(3):885-890.

Goate A, Chartier-Harlin MC, Mullan M, Brown J, Crawford F, Fidani L, Giuffra L, Haynes A, Irving N, James L, et al. 1991. Segregation of a missense mutation in the amyloid precursor protein gene with familial Alzheimer's disease. Nature 349(6311):704-706.

Golde TE, Estus S, Usiak M, Younkin LH, Younkin SG. 1990. Expression of beta amyloid protein precursor mRNAs: recognition of a novel alternatively spliced form and quantitation in Alzheimer's disease using PCR. Neuron 4(2):253-267.

Golde TE, Estus S, Younkin LH, Selkoe DJ, Younkin SG. 1992. Processing of the amyloid protein precursor to potentially amyloidogenic derivatives. Science 255(5045):728-730.

Gong CX, Singh TJ, Grundke-Iqbal I, Iqbal K. 1993. Phosphoprotein phosphatase activities in Alzheimer disease brain. J Neurochem 61(3):921-927.
Gouras GK, Tsai J, Naslund J, Vincent B, Edgar M, Checler F, Greenfield JP, Haroutunian V, Buxbaum JD, Xu H, Greengard P, Relkin NR. 2000a. Intraneuronal Ab 42 accumulation in human brain. American Journal of Pathology 156:15-20.
Gouras GK, Xu H, Gross RS, Greenfield JP, Hai B, Wang R, Greengard P. 2000b. Testosterone reduces neuronal secretion of Alzheimer's beta-amyloid peptides. Proc Natl Acad Sci U S A 97(3):1202-1205.
Goutte C, Hepler W, Mickey KM, Priess JR. 2000. aph-2 encodes a novel extracellular protein required for GLP-1-mediated signaling. Development 127(11):2481-2492.
Gowing E, Roher AE, Woods AS, Cotter RJ, Chaney M, Little SP, Ball MJ. 1994. Chemical characterization of A beta 17-42 peptide, a component of diffuse amyloid deposits of Alzheimer disease. J Biol Chem 269(15):10987-10990.
Gray CW, Patel AJ. 1993a. Induction of beta-amyloid precursor protein isoform mRNAs by bFGF in astrocytes. Neuroreport 4(6):811-814.
Gray CW, Patel AJ. 1993b. Regulation of beta-amyloid precursor protein isoform mRNAs by transforming growth factor-beta 1 and interleukin-1 beta in astrocytes. Brain Res Mol Brain Res 19(3):251-256.
Greenfield JP, Tsai J, Gouras GK, Hai B, Thinakaran G, Checler F, Sisodia SS, Greengard P, Xu H. 1999. Endoplasmic reticulum and trans-Golgi network generate distinct populations of Alzheimer beta-amyloid peptides. Proc Natl Acad Sci U S A 96(2):742-747.
Grundke-Iqbal I, Iqbal K, Tung YC, Quinlan M, Wisniewski HM, Binder LI. 1986. Abnormal phosphorylation of the microtubule-associated protein tau (tau) in Alzheimer cytoskeletal pathology. Proc Natl Acad Sci U S A 83(13):4913-4917.
Guenette SY, Chen J, Ferland A, Haass C, Capell A, Tanzi RE. 1999. hFE65L influences amyloid precursor protein maturation and secretion. J Neurochem 73(3):985-993.
Guenette SY, Chen J, Jondro PD, Tanzi RE. 1996. Association of a novel human FE65-like protein with the cytoplasmic domain of the beta-amyloid precursor protein. Proc Natl Acad Sci U S A 93(20):10832-10837.
Haass C. 2004. Take five--BACE and the gamma-secretase quartet conduct Alzheimer's amyloid beta-peptide generation. Embo J 23(3):483-488.
Haass C, Koo EH, Capell A, Teplow DB, Selkoe DJ. 1995. Polarized sorting of beta-amyloid precursor protein and its proteolytic products in MDCK cells is regulated by two independent signals. J Cell Biol 128(4):537-547.
Haass C, Koo EH, Mellon A, Hung AY, Selkoe DJ. 1992. Targeting of cell-surface beta-amyloid precursor protein to lysosomes: alternative processing into amyloid-bearing fragments. Nature 357(6378):500-503.
Haass C, Selkoe DJ. 1993. Cellular processing of beta-amyloid precursor protein and the genesis of amyloid beta-peptide. Cell 75(6):1039-1042.
Haass C, Yankner BA. 2005. A gamma-secretase-independent mechanism of signal transduction by the amyloid precursor protein. J Biol Chem 280:36895-36904.
Han P, Dou F, Li F, Zhang X, Zhang YW, Zheng H, Lipton SA, Xu H, Liao FF. 2005. Suppression of cyclin-dependent kinase 5 activation by amyloid precursor protein: a novel excitoprotective mechanism involving modulation of tau phosphorylation. J Neurosci 25(50):11542-11552.
Haniu M, Denis P, Young Y, Mendiaz EA, Fuller J, Hui JO, Bennett BD, Kahn S, Ross S, Burgess T, Katta V, Rogers G, Vassar R, Citron M. 2000. Characterization of Alzheimer's beta -secretase protein BACE. A pepsin family member with unusual properties. J Biol Chem 275(28):21099-21106.
Hardy J, Allsop D. 1991. Amyloid deposition as the central event in the aetiology of Alzheimer's disease. Trends Pharmacol Sci 12(10):383-388.

Hardy J, Selkoe DJ. 2002. The amyloid hypothesis of Alzheimer's disease: progress and problems on the road to therapeutics. Science 297(5580):353-356.

Hartmann T, Bieger SC, Bruhl B, Tienari PJ, Ida N, Allsop D, Roberts GW, Masters CL, Dotti CG, Unsicker K, Beyreuther K. 1997. Distinct sites of intracellular production for Alzheimer's disease A beta40/42 amyloid peptides. Nat Med 3(9):1016-1020.

Hata R, Masumura M, Akatsu H, Li F, Fujita H, Nagai Y, Yamamoto T, Okada H, Kosaka K, Sakanaka M, Sawada T. 2001. Up-regulation of calcineurin Abeta mRNA in the Alzheimer's disease brain: assessment by cDNA microarray. Biochem Biophys Res Commun 284(2):310-316.

Heber S, Herms J, Gajic V, Hainfellner J, Aguzzi A, Rulicke T, von Kretzschmar H, von Koch C, Sisodia S, Tremml P, Lipp HP, Wolfer DP, Muller U. 2000. Mice with combined gene knock-outs reveal essential and partially redundant functions of amyloid precursor protein family members. J Neurosci 20(21):7951-7963.

Herard AS, Besret L, Dubois A, Dauguet J, Delzescaux T, Hantraye P, Bonvento G, Moya KL. 2006. siRNA targeted against amyloid precursor protein impairs synaptic activity in vivo. Neurobiol Aging 27(12):1740-1750.

Hesse L, Beher D, Masters CL, Multhaup G. 1994. The beta A4 amyloid precursor protein binding to copper. FEBS Lett 349(1):109-116.

Hill K, Li Y, Bennett M, McKay M, Zhu X, Shern J, Torre E, Lah JJ, Levey AI, Kahn RA. 2003. Munc18 interacting proteins: ADP-ribosylation factor-dependent coat proteins that regulate the traffic of beta-Alzheimer's precursor protein. J Biol Chem 278: :36032-36040.

Ho A, Sudhof TC. 2004. Binding of F-spondin to amyloid-beta precursor protein: a candidate amyloid-beta precursor protein ligand that modulates amyloid-beta precursor protein cleavage. Proc Natl Acad Sci U S A 101(8):2548-2553.

Holsinger RM, McLean CA, Beyreuther K, Masters CL, Evin G. 2002. Increased expression of the amyloid precursor beta-secretase in Alzheimer's disease. Ann Neurol 51(6):783-786.

Holtzman DM, Fagan AM, Mackey B, Tenkova T, Sartorius L, Paul SM, Bales K, Ashe KH, Irizarry MC, Hyman BT. 2000. Apolipoprotein E facilitates neuritic and cerebrovascular plaque formation in an Alzheimer's disease model. Ann Neurol 47(6):739-747.

Holzer M, Bruckner MK, Beck M, Bigl V, Arendt T. 2000. Modulation of APP processing and secretion by okadaic acid in primary guinea pig neurons. J Neural Transm 107(4):451-461.

Homayouni R, Rice DS, Sheldon M, Curran T. 1999. Disabled-1 binds to the cytoplasmic domain of amyloid precursor-like protein 1. J Neurosci 19(17):7507-7515.

Hooper NM, Turner AJ. 2002. The search for alpha-secretase and its potential as a therapeutic approach to Alzheimer s disease. Curr Med Chem 9(11):1107-1119.

Hu Y, Fortini ME. 2003. Different cofactor activities in gamma-secretase assembly: evidence for a nicastrin-Aph-1 subcomplex. J Cell Biol 161(4):685-690.

Huber G, Martin JR, Loffler J, Moreau JL. 1993. Involvement of amyloid precursor protein in memory formation in the rat: an indirect antibody approach. Brain Res 603(2):348-352.

Hung AY, Haass C, Nitsch RM, Qiu WQ, Citron M, Wurtman RJ, Growdon JH, Selkoe DJ. 1993. Activation of protein kinase C inhibits cellular production of the amyloid beta-protein. J Biol Chem 268(31):22959-22962.

Hung AY, Koo EH, Haass C, Selkoe DJ. 1992. Increased expression of beta-amyloid precursor protein during neuronal differentiation is not accompanied by secretory cleavage. Proc Natl Acad Sci U S A 89(20):9439-9443.

Huse JT, Pijak DS, Leslie GJ, Lee VM, Doms RW. 2000. Maturation and endosomal targeting of beta-site amyloid precursor protein-cleaving enzyme. The Alzheimer's disease beta-secretase. J Biol Chem 275(43):33729-33737.

Hussain I, Powell D, Howlett DR, Tew DG, Meek TD, Chapman C, Gloger IS, Murphy KE, Southan CD, Ryan DM, Smith TS, Simmons DL, Walsh FS, Dingwall C, Christie G. 1999. Identification of a novel aspartic protease (Asp 2) as beta-secretase. Mol Cell Neurosci 14(6):419-427.

Iijima K, Ando K, Takeda S, Satoh Y, Seki T, Itohara S, Greengard P, Kirino Y, Nairn AC, Suzuki T. 2000. Neuron-specific phosphorylation of Alzheimer's beta-amyloid precursor protein by cyclin-dependent kinase 5. J Neurochem 75(3):1085-1091.

Iizuka T, Shoji M, Harigaya Y, Kawarabayashi T, Watanabe M, Kanai M, Hirai S. 1995. Amyloid beta-protein ending at Thr43 is a minor component of some diffuse plaques in the Alzheimer's disease brain, but is not found in cerebrovascular amyloid. Brain Res 702(1-2):275-278.

Ikezu T, Trapp BD, Song KS, Schlegel A, Lisanti MP, Okamoto T. 1998. Caveolae, plasma membrane microdomains for alpha-secretase-mediated processing of the amyloid precursor protein. J Biol Chem 273(17):10485-10495.

Ikin AF, Annaert WG, Takei K, De Camilli P, Jahn R, Greengard P, Buxbaum JD. 1996. Alzheimer amyloid protein precursor is localized in nerve terminal preparations to Rab5-containing vesicular organelles distinct from those implicated in the synaptic vesicle pathway. J Biol Chem 271(50):31783-31786.

Inomata H, Nakamura Y, Hayakawa A, Takata H, Suzuki T, Miyazawa K, Kitamura N. 2003. A scaffold protein JIP-1b enhances amyloid precursor protein phosphorylation by JNK and its association with kinesin light chain 1. J Biol Chem 278(25):22946-22955.

Irizarry MC, Locascio JJ, Hyman BT. 2001. beta-site APP cleaving enzyme mRNA expression in APP transgenic mice: anatomical overlap with transgene expression and static levels with aging. Am J Pathol 158(1):173-177.

Ishida A, Shimazaki K, Terashima T, Kawai N. 1994. An electrophysiological and immunohistochemical study of the hippocampus of the reeler mutant mouse. Brain Res 662(1-2):60-68.

Iwatsubo T, Mann DM, Odaka A, Suzuki N, Ihara Y. 1995. Amyloid beta protein (A beta) deposition: A beta 42(43) precedes A beta 40 in Down syndrome. Ann Neurol 37(3):294-299.

Iwatsubo T, Odaka A, Suzuki N, Mizusawa H, Nukina N, Ihara Y. 1994. Visualization of A beta 42(43) and A beta 40 in senile plaques with end-specific A beta monoclonals: evidence that an initially deposited species is A beta 42(43). Neuron 13(1):45-53.

Izumi Y, Hirata M, Hasuwa H, Iwamoto R, Umata T, Miyado K, Tamai Y, Kurisaki T, Sehara-Fujisawa A, Ohno S, Mekada E. 1998. A metalloprotease-disintegrin, MDC9/meltrin-gamma/ADAM9 and PKCdelta are involved in TPA-induced ectodomain shedding of membrane-anchored heparin-binding EGF-like growth factor. Embo J 17(24):7260-7272.

Jarrett JT, Berger EP, Lansbury PT, Jr. 1993. The carboxy terminus of the beta amyloid protein is critical for the seeding of amyloid formation: implications for the pathogenesis of Alzheimer's disease. Biochemistry 32(18):4693-4697.

Jarrett JT, Lansbury PT, Jr. 1992. Amyloid fibril formation requires a chemically discriminating nucleation event: studies of an amyloidogenic sequence from the bacterial protein OsmB. Biochemistry 31(49):12345-12352.

Jin LW, Saitoh T. 1995. Changes in protein kinases in brain aging and Alzheimer's disease. Implications for drug therapy. Drugs Aging 6(2):136-149.

Kaether C, Capell A, Edbauer D, Winkler E, Novak B, Steiner H, Haass C. 2004. The presenilin C-terminus is required for ER-retention, nicastrin-binding and gamma-secretase activity. Embo J 23(24):4738-4748.

Kaether C, Haass C. 2004. A lipid boundary separates APP and secretases and limits amyloid beta-peptide generation. J Cell Biol 167(5):809-812.

Kaether C, Haass C, Steiner H. 2006a. Assembly, trafficking and function of gamma-secretase. Neurodegener Dis 3(4-5):275-283.

Kaether C, Lammich S, Edbauer D, Ertl M, Rietdorf J, Capell A, Steiner H, Haass C. 2002. Presenilin-1 affects trafficking and processing of betaAPP and is targeted in a complex with nicastrin to the plasma membrane. J Cell Biol 158(3):551-561.

Kaether C, Schmitt S, Willem M, Haass C. 2006b. Amyloid precursor protein and Notch intracellular domains are generated after transport of their precursors to the cell surface. Traffic 7(4):408-415.

Kaether C, Skehel P, Dotti CG. 2000. Axonal membrane proteins are transported in distinct carriers: a two-color video microscopy study in cultured hippocampal neurons. Mol Biol Cell 11(4):1213-1224.

Kakuda N, Funamoto S, Yagishita S, Takami M, Osawa S, Dohmae N, Ihara Y. 2006. Equimolar production of amyloid beta-protein and amyloid precursor protein intracellular domain from beta-carboxyl-terminal fragment by gamma-secretase. J Biol Chem 281(21):14776-14786.

Kamal A, Almenar-Queralt A, LeBlanc JF, Roberts EA, Goldstein LS. 2001. Kinesin-mediated axonal transport of a membrane compartment containing beta-secretase and presenilin-1 requires APP. Nature 414(6864):643-648.

Kamal A, Stokin GB, Yang Z, Xia CH, Goldstein LS. 2000. Axonal transport of amyloid precursor protein is mediated by direct binding to the kinesin light chain subunit of kinesin-I. Neuron 28(2):449-459.

Kang J, Muller-Hill B. 1990. Differential splicing of Alzheimer's disease amyloid A4 precursor RNA in rat tissues: PreA4(695) mRNA is predominantly produced in rat and human brain. Biochem Biophys Res Commun 166(3):1192-1200.

Kerr ML, Small DH. 2005. Cytoplasmic domain of the beta-amyloid protein precursor of Alzheimer's disease: function, regulation of proteolysis, and implications for drug development. J Neurosci Res 80(2):151-159.

Kesavapany S, Banner SJ, Lau KF, Shaw CE, Miller CC, Cooper JD, McLoughlin DM. 2002. Expression of the Fe65 adapter protein in adult and developing mouse brain. Neuroscience 115(3):951-960.

Kibbey MC, Jucker M, Weeks BS, Neve RL, Van Nostrand WE, Kleinman HK. 1993. beta-Amyloid precursor protein binds to the neurite-promoting IKVAV site of laminin. Proc Natl Acad Sci U S A 90(21):10150-10153.

Kimberly WT, Wolfe MS. 2003. Identity and function of gamma-secretase. J Neurosci Res 74(3):353-360.

Kimberly WT, Zheng JB, Guenette SY, Selkoe DJ. 2001. The intracellular domain of the beta-amyloid precursor protein is stabilized by Fe65 and translocates to the nucleus in a notch-like manner. J Biol Chem 276(43):40288-40292.

Kimberly WT, Zheng JB, Town T, Flavell RA, Selkoe DJ. 2005. Physiological regulation of the beta-amyloid precursor protein signaling domain by c-Jun N-terminal kinase JNK3 during neuronal differentiation. J Neurosci 25(23):5533-5543.

King GD, Perez RG, Steinhilb ML, Gaut JR, Turner RS. 2003. X11alpha modulates secretory and endocytic trafficking and metabolism of amyloid precursor protein: mutational analysis of the YENPTY sequence. Neuroscience 120(1):143-154.

King GD, Scott Turner R. 2004. Adaptor protein interactions: modulators of amyloid precursor protein metabolism and Alzheimer's disease risk? Exp Neurol 185(2):208-219.

Kinoshita A, Whelan CM, Smith CJ, Mikhailenko I, Rebeck GW, Strickland DK, Hyman BT. 2001. Demonstration by fluorescence resonance energy transfer of two sites of interaction between the low-density lipoprotein receptor-related protein and the amyloid precursor protein: role of the intracellular adapter protein Fe65. J Neurosci 21(21):8354-8361.

Kitaguchi N, Takahashi Y, Tokushima Y, Shiojiri S, Ito H. 1988. Novel precursor of Alzheimer's disease amyloid protein shows protease inhibitory activity. Nature 331(6156):530-532.

Konig G, Beyreuther K, Masters CL, Schmitt HP, Salbaum JM. 1989. PreA4 mRNA distribution in brain areas. Prog Clin Biol Res 317:1027-1036.
Koo EH. 1997. Phorbol esters affect multiple steps in beta-amyloid precursor protein trafficking and amyloid beta-protein production. Mol Med 3(3):204-211.
Koo EH, Sisodia SS, Archer DR, Martin LJ, Weidemann A, Beyreuther K, Fischer P, Masters CL, Price DL. 1990. Precursor of amyloid protein in Alzheimer disease undergoes fast anterograde axonal transport. Proc Natl Acad Sci U S A 87(4):1561-1565.
Koo EH, Squazzo SL. 1994. Evidence that production and release of amyloid beta-protein involves the endocytic pathway. J Biol Chem 269(26):17386-17389.
Koo EH, Squazzo SL, Selkoe DJ, Koo CH. 1996. Trafficking of cell-surface amyloid beta-protein precursor. I. Secretion, endocytosis and recycling as detected by labeled monoclonal antibody. J Cell Sci 109 (Pt 5):991-998.
Kosik KS. 1993. Alzheimer's disease: a cell biological perspective. Science 256:780-783.
Kouchi Z, Sorimachi H, Suzuki K, Ishiura S. 1999. Proteasome inhibitors induce the association of Alzheimer's amyloid precursor protein with Hsc73. Biochem Biophys Res Commun 254(3):804-810.
Kowalska A, Wender M, Florczak J, Pruchnik-Wolinska D, Modestowicz R, Szczech J, Rossa G, Kozubski W. 2003. Molecular genetics of Alzheimer's disease: presenilin 1 gene analysis in a cohort of patients from the Poznan region. J Appl Genet 44(2):231-234.
Kowalska A, Wiechmann I, Walter H. 1998. Genetic variability of apolipoprotein E in a Polish population. Hum Biol 70(6):1093-1099.
Kuentzel SL, Ali SM, Altman RA, Greenberg BD, Raub TJ. 1993. The Alzheimer beta-amyloid protein precursor/protease nexin-II is cleaved by secretase in a trans-Golgi secretory compartment in human neuroglioma cells. Biochem J 295 (Pt 2):367-378.
Lahiri DK, Greig NH. 2004. Lethal weapon: amyloid beta-peptide, role in the oxidative stress and neurodegeneration of Alzheimer's disease. Neurobiol Aging 25(5):581-587.
Lahiri DK, Nall C. 1995. Promoter activity of the gene encoding the beta-amyloid precursor protein is up-regulated by growth factors, phorbol ester, retinoic acid and interleukin-1. Brain Res Mol Brain Res 32(2):233-240.
Lai A, Sisodia SS, Trowbridge IS. 1995. Characterization of sorting signals in the beta-amyloid precursor protein cytoplasmic domain. J Biol Chem 270(8):3565-3573.
Lammich S, Kojro E, Postina R, Gilbert S, Pfeiffer R, Jasionowski M, Haass C, Fahrenholz F. 1999. Constitutive and regulated alpha-secretase cleavage of Alzheimer's amyloid precursor protein by a disintegrin metalloprotease. Proc Natl Acad Sci U S A 96(7):3922-3927.
Lau KF, McLoughlin DM, Standen C, Miller CC. 2000. X11 alpha and x11 beta interact with presenilin-1 via their PDZ domains. Mol Cell Neurosci 16(5):557-565.
Lazarov O, Lee M, Peterson DA, Sisodia SS. 2002. Evidence that synaptically released beta-amyloid accumulates as extracellular deposits in the hippocampus of transgenic mice. J Neurosci 22(22):9785-9793.
Lazarov O, Robinson J, Tang YP, Hairston IS, Korade-Mirnics Z, Lee VM, Hersh LB, Sapolsky RM, Mirnics K, Sisodia SS. 2005. Environmental enrichment reduces Abeta levels and amyloid deposition in transgenic mice. Cell 120(5):701-713.
LeBlanc AC, Chen HY, Autilio-Gambetti L, Gambetti P. 1991. Differential APP gene expression in rat cerebral cortex, meninges, and primary astroglial, microglial and neuronal cultures. FEBS Lett 292(1-2):171-178.
LeBlanc AC, Gambetti P. 1994. Production of Alzheimer 4kDa beta-amyloid peptide requires the C-terminal cytosolic domain of the amyloid precursor protein. Biochem Biophys Res Commun 204(3):1371-1380.

Lee MS, Kao SC, Lemere CA, Xia W, Tseng HC, Zhou Y, Neve R, Ahlijanian MK, Tsai LH. 2003. APP processing is regulated by cytoplasmic phosphorylation. J Cell Biol 163(1):83-95.

Lee SF, Shah S, Li H, Yu C, Han W, Yu G. 2002. Mammalian APH-1 interacts with presenilin and nicastrin and is required for intramembrane proteolysis of amyloid-beta precursor protein and Notch. J Biol Chem 277(47):45013-45019.

Lee W, Boo JH, Jung MW, Park SD, Kim YH, Kim SU, Mook-Jung I. 2004. Amyloid beta peptide directly inhibits PKC activation. Mol Cell Neurosci 26(2):222-231.

Leissring MA, Murphy MP, Mead TR, Akbari Y, Sugarman MC, Jannatipour M, Anliker B, Muller U, Saftig P, De Strooper B, Wolfe MS, Golde TE, LaFerla FM. 2002. A physiologic signaling role for the gamma -secretase-derived intracellular fragment of APP. Proc Natl Acad Sci U S A 99(7):4697-4702.

Lemere CA, Blusztajn JK, Yamaguchi H, Wisniewski T, Saido TC, Selkoe DJ. 1996. Sequence of deposition of heterogeneous amyloid beta-peptides and APO E in Down syndrome: implications for initial events in amyloid plaque formation. Neurobiol Dis 3(1):16-32.

Leroy K, Boutajangout A, Authelet M, Woodgett JR, Anderton BH, Brion JP. 2002. The active form of glycogen synthase kinase-3beta is associated with granulovacuolar degeneration in neurons in Alzheimer's disease. Acta Neuropathol (Berl) 103(2):91-99.

Leverenz JB, Raskind MA. 1998. Early amyloid deposition in the medial temporal lobe of young Down syndrome patients: a regional quantitative analysis. Exp Neurol 150(2):296-304.

Levy-Lahad E, Wasco W, Poorlkaj P, Romano D, Oshima J, Pettingell W, Yu C, Jondro PD, Schmit S, Wang K. 1995. Candidate gene for the chromossome 1 familial Alzheimer's disease locus. science 269:973-977.

Lewis J, Dickson DW, Lin WL, Chisholm L, Corral A, Jones G, Yen SH, Sahara N, Skipper L, Yager D, Eckman C, Hardy J, Hutton M, McGowan E. 2001. Enhanced neurofibrillary degeneration in transgenic mice expressing mutant tau and APP. Science 293(5534):1487-1491.

Leyssen M, Ayaz D, Hebert SS, Reeve S, De Strooper B, Hassan BA. 2005. Amyloid precursor protein promotes post-developmental neurite arborization in the Drosophila brain. Embo J 24(16):2944-2955.

Li YM, Lai MT, Xu M, Huang Q, DiMuzio-Mower J, Sardana MK, Shi XP, Yin KC, Shafer JA, Gardell SJ. 2000a. Presenilin 1 is linked with gamma-secretase activity in the detergent solubilized state. Proc Natl Acad Sci U S A 97(11):6138-6143.

Li YM, Xu M, Lai MT, Huang Q, Castro JL, DiMuzio-Mower J, Harrison T, Lellis C, Nadin A, Neduvelil JG, Register RB, Sardana MK, Shearman MS, Smith AL, Shi XP, Yin KC, Shafer JA, Gardell SJ. 2000b. Photoactivated gamma-secretase inhibitors directed to the active site covalently label presenilin 1. Nature 405(6787):689-694.

Lichtenthaler SF, Schobel S, Neumann S, Haass C. A novel sorting nexin modifies the alpha- and beta-secretase cleavage of APP. In: AD/PD tIC, editor; (2005); Sorrento, Italy.

Liou YC, Sun A, Ryo A, Zhou XZ, Yu ZX, Huang HK, Uchida T, Bronson R, Bing G, Li X, Hunter T, Lu KP. 2003. Role of the prolyl isomerase Pin1 in protecting against age-dependent neurodegeneration. Nature 424(6948):556-561.

Loffler J, Huber G. 1992. Beta-amyloid precursor protein isoforms in various rat brain regions and during brain development. J Neurochem 59:1316-1324.

Lorenzo A, Yuan M, Zhang Z, Paganetti PA, Sturchler-Pierrat C, Staufenbiel M, Mautino J, Vigo FS, Sommer B, Yankner BA. 2000. Amyloid beta interacts with the amyloid precursor protein: a potential toxic mechanism in Alzheimer's disease. Nat Neurosci 3(5):460-464.

Lu DC, Rabizadeh S, Chandra S, Shayya RF, Ellerby LM, Ye X, Salvesen GS, Koo EH, Bredesen DE. 2000. A second cytotoxic proteolytic peptide derived from amyloid beta-protein precursor. Nat Med 6(4):397-404.

Lu DC, Soriano S, Bredesen DE, Koo EH. 2003. Caspase cleavage of the amyloid precursor protein modulates amyloid beta-protein toxicity. J Neurochem 87(3):733-741.
Lu PJ, Zhou XZ, Shen M, Lu KP. 1999. Function of WW domains as phosphoserine- or phosphothreonine-binding modules. Science 283(5406):1325-1328.
Luo L, Tully T, White K. 1992. Human amyloid precursor protein ameliorates behavioral deficit of flies deleted for Appl gene. Neuron 9(4):595-605.
Luo WJ, Wang H, Li H, Kim BS, Shah S, Lee HJ, Thinakaran G, Kim TW, Yu G, Xu H. 2003. PEN-2 and APH-1 coordinately regulate proteolytic processing of presenilin 1. J Biol Chem 278(10):7850-7854.
Luo Y, Bolon B, Kahn S, Bennett BD, Babu-Khan S, Denis P, Fan W, Kha H, Zhang J, Gong Y, Martin L, Louis JC, Yan Q, Richards WG, Citron M, Vassar R. 2001. Mice deficient in BACE1, the Alzheimer's beta-secretase, have normal phenotype and abolished beta-amyloid generation. Nat Neurosci 4(3):231-232.
Lyckman AW, Confaloni AM, Thinakaran G, Sisodia SS, Moya KL. 1998. Post-translational processing and turnover kinetics of presynaptically targeted amyloid precursor superfamily proteins in the central nervous system. J Biol Chem 273(18):11100-11106.
Maasch C, Wagner S, Lindschau C, Alexander G, Buchner K, Gollasch M, Luft FC, Haller H. 2000. Protein kinase calpha targeting is regulated by temporal and spatial changes in intracellular free calcium concentration [Ca(2+)](i). Faseb J 14(11):1653-1663.
Mahley RW. 1988. Apolipoprotein E: cholesterol transport protein with expanding role in cell biology. Science 240(4852):622-630.
Marambaud P, Lopez-Perez E, Wilk S, Checler F. 1997a. Constitutive and protein kinase C-regulated secretory cleavage of Alzheimer's beta-amyloid precursor protein: different control of early and late events by the proteasome. J Neurochem 69(6):2500-2505.
Marambaud P, Rieunier F, Wilk S, Martinez J, Checler F. 1997b. Contribution of the proteasome to the alpha-secretase pathway in Alzheimer's disease. Adv Exp Med Biol 421:267-272.
Marquez-Sterling NR, Lo AC, Sisodia SS, Koo EH. 1997. Trafficking of cell-surface beta-amyloid precursor protein: evidence that a sorting intermediate participates in synaptic vesicle recycling. J Neurosci 17(1):140-151.
Masliah E, Cole G, Shimohama S, Hansen L, DeTeresa R, Terry RD, Saitoh T. 1990. Differential involvement of protein kinase C isozymes in Alzheimer's disease. J Neurosci 10(7):2113-2124.
Masters CL, Simms G, Weinman NA, Multhaup G, McDonald BL, Beyreuther K. 1985. Amyloid plaque core protein in Alzheimer disease and Down syndrome. Proc Natl Acad Sci U S A 82(12):4245-4249.
Mathews PM, Guerra CB, Jiang Y, Grbovic OM, Kao BH, Schmidt SD, Dinakar R, Mercken M, Hille-Rehfeld A, Rohrer J, Mehta P, Cataldo AM, Nixon RA. 2002. Alzheimer's disease-related overexpression of the cation-dependent mannose 6-phosphate receptor increases Abeta secretion: role for altered lysosomal hydrolase distribution in beta-amyloidogenesis. J Biol Chem 277(7):5299-5307.
Matsuda S, Yasukawa T, Homma Y, Ito Y, Niikura T, Hiraki T, Hirai S, Ohno S, Kita Y, Kawasumi M, Kouyama K, Yamamoto T, Kyriakis JM, Nishimoto I. 2001. c-Jun N-terminal kinase (JNK)-interacting protein-1b/islet-brain-1 scaffolds Alzheimer's amyloid precursor protein with JNK. J Neurosci 21(17):6597-6607.
Matsushima H, Shimohama S, Chachin M, Taniguchi T, Kimura J. 1996. Ca2+-dependent and Ca2+-independent protein kinase C changes in the brain of patients with Alzheimer's disease. J Neurochem 67(1):317-323.
McLaughlin M, Breen KC. 1999. Protein kinase C activation potentiates the rapid secretion of the amyloid precursor protein from rat cortical synaptosomes. J Neurochem 72(1):273-281.

Meziane H, Dodart JC, Mathis C, Little S, Clemens J, Paul SM, Ungerer A. 1998. Memory-enhancing effects of secreted forms of the beta-amyloid precursor protein in normal and amnestic mice. Proc Natl Acad Sci U S A 95(21):12683-12688.

Mileusnic R, Lancashire CL, Johnston AN, Rose SP. 2000. APP is required during an early phase of memory formation. Eur J Neurosci 12(12):4487-4495.

Mills J, Laurent Charest D, Lam F, Beyreuther K, Ida N, Pelech SL, Reiner PB. 1997. Regulation of amyloid precursor protein catabolism involves the mitogen-activated protein kinase signal transduction pathway. J Neurosci 17(24):9415-9422.

Mills J, Reiner PB. 1996. Phorbol esters but not the cholinergic agonists oxotremorine-M and carbachol increase release of the amyloid precursor protein in cultured rat cortical neurons. J Neurochem 67(4):1511-1518.

Minopoli G, de Candia P, Bonetti A, Faraonio R, Zambrano N, Russo T. 2001. The beta-amyloid precursor protein functions as a cytosolic anchoring site that prevents Fe65 nuclear translocation. J Biol Chem 276(9):6545-6550.

Mishra SK, Keyel PA, Hawryluk MJ, Agostinelli NR, Watkins SC, Traub LM. 2002. Disabled-2 exhibits the properties of a cargo-selective endocytic clathrin adaptor. Embo J 21(18):4915-4926.

Moir RD, Lynch T, Bush AI, Whyte S, Henry A, Portbury S, Multhaup G, Small DH, Tanzi RE, Beyreuther K, Masters CL. 1998. Relative increase in Alzheimer's disease of soluble forms of cerebral Abeta amyloid protein precursor containing the Kunitz protease inhibitory domain. J Biol Chem 273(9):5013-5019.

Moya KL, Benowitz LI, Schneider GE, Allinquant B. 1994. The amyloid precursor protein is developmentally regulated and correlated with synaptogenesis. Dev Biol 161(2):597-603.

Mueller HT, Borg JP, Margolis B, Turner RS. 2000. Modulation of amyloid precursor protein metabolism by X11alpha /Mint-1. A deletion analysis of protein-protein interaction domains. J Biol Chem 275(50):39302-39306.

Mulkey RM, Endo S, Shenolikar S, Malenka RC. 1994. Involvement of a calcineurin/inhibitor-1 phosphatase cascade in hippocampal long-term depression. Nature 369(6480):486-488.

Muller U, Cristina N, Li ZW, Wolfer DP, Lipp HP, Rulicke T, Brandner S, Aguzzi A, Weissmann C. 1994. Behavioral and anatomical deficits in mice homozygous for a modified beta-amyloid precursor protein gene. Cell 79(5):755-765.

Multhaup G, Schlicksupp A, Hesse L, Beher D, Ruppert T, Masters CL, Beyreuther K. 1996. The amyloid precursor protein of Alzheimer's disease in the reduction of copper(II) to copper(I). Science 271(5254):1406-1409.

Murakami N, Yamaki T, Iwamoto Y, Sakakibara T, Kobori N, Fushiki S, Ueda S. 1998. Experimental brain injury induces expression of amyloid precursor protein, which may be related to neuronal loss in the hippocampus. J Neurotrauma 15(11):993-1003.

Muresan Z, Muresan V. 2005a. c-Jun NH2-terminal kinase-interacting protein-3 facilitates phosphorylation and controls localization of amyloid-beta precursor protein. J Neurosci 25(15):3741-3751.

Muresan Z, Muresan V. 2005b. Coordinated transport of phosphorylated amyloid-beta precursor protein and c-Jun NH2-terminal kinase-interacting protein-1. J Cell Biol 171(4):615-625.

Murrell J, Farlow M, Ghetti B, Benson MD. 1991. A mutation in the amyloid precursor protein associated with hereditary Alzheimer's disease. Science 254(5028):97-99.

Neve RL, Finch EA, Dawes LR. 1988. Expression of the Alzheimer amyloid precursor gene transcripts in the human brain. Neuron 1(8):669-677.

Neve RL, McPhie DL. 2006. The cell cycle as a therapeutic target for Alzheimer's disease. Pharmacol Ther 111(1):99-113.

Nilsberth C, Westlind-Danielsson A, Eckman CB, Condron MM, Axelman K, Forsell C, Stenh C, Luthman J, Teplow DB, Younkin SG, Naslund J, Lannfelt L. 2001. The 'Arctic' APP mutation (E693G) causes Alzheimer's disease by enhanced Abeta protofibril formation. Nat Neurosci 4(9):887-893.

Ninomiya H, Roch JM, Sundsmo MP, Otero DA, Saitoh T. 1993. Amino acid sequence RERMS represents the active domain of amyloid beta/A4 protein precursor that promotes fibroblast growth. J Cell Biol 121(4):879-886.

Nishimoto I, Okamoto T, Matsuura Y, Takahashi S, Okamoto T, Murayama Y, Ogata E. 1993. Alzheimer amyloid protein precursor complexes with brain GTP-binding protein G(o). Nature 362(6415):75-79.

Nishiyama K, Trapp BD, Ikezu T, Ransohoff RM, Tomita T, Iwatsubo T, Kanazawa I, Hsiao KK, Lisanti MP, Okamoto T. 1999. Caveolin-3 upregulation activates beta-secretase-mediated cleavage of the amyloid precursor protein in Alzheimer's disease. J Neurosci 19(15):6538-6548.

Nitsch RM, Slack BE, Wurtman RJ, Growdon JH. 1992. Release of Alzheimer amyloid precursor derivatives stimulated by activation of muscarinic acetylcholine receptors. Science 258(5080):304-307.

Noble W, Olm V, Takata K, Casey E, Mary O, Meyerson J, Gaynor K, LaFrancois J, Wang L, Kondo T, Davies P, Burns M, Veeranna, Nixon R, Dickson D, Matsuoka Y, Ahlijanian M, Lau LF, Duff K. 2003. Cdk5 is a key factor in tau aggregation and tangle formation in vivo. Neuron 38(4):555-565.

Noviello C, Vito P, Lopez P, Abdallah M, D'Adamio L. 2003. Autosomal recessive hypercholesterolemia protein interacts with and regulates the cell surface level of Alzheimer's amyloid beta precursor protein. J Biol Chem 278(34):31843-31847.

Nunan J, Small DH. 2000. Regulation of APP cleavage by alpha-, beta- and gamma-secretases. FEBS Lett 483(1):6-10.

Ohgami T, Kitamoto T, Tateishi J. 1993. The rat central nervous system expresses Alzheimer's amyloid precursor protein APP695, but not APP677 (L-APP form). J Neurochem 61(4):1553-1556.

Ohsawa I, Takamura C, Kohsaka S. 2001. Fibulin-1 binds the amino-terminal head of beta-amyloid precursor protein and modulates its physiological function. J Neurochem 76(5):1411-1420.

Oishi M, Nairn AC, Czernik AJ, Lim GS, Isohara T, Gandy SE, Greengard P, Suzuki T. 1997. The cytoplasmic domain of Alzheimer's amyloid precursor protein is phosphorylated at Thr654, Ser655, and Thr668 in adult rat brain and cultured cells. Mol Med 3(2):111-123.

Okado H, Okamoto H. 1992. A Xenopus homologue of the human beta-amyloid precursor protein: developmental regulation of its gene expression. Biochem Biophys Res Commun 189(3):1561-1568.

Oltersdorf T, Ward PJ, Henriksson T, Beattie EC, Neve R, Lieberburg I, Fritz LC. 1990. The Alzheimer amyloid precursor protein. Identification of a stable intermediate in the biosynthetic/degradative pathway. J Biol Chem 265(8):4492-4497.

Oster-Granite ML, McPhie DL, Greenan J, Neve RL. 1996. Age-dependent neuronal and synaptic degeneration in mice transgenic for the C terminus of the amyloid precursor protein. J Neurosci 16(21):6732-6741.

Paganetti P, Calanca V, Galli C, Stefani M, Molinari M. 2005. beta-site specific intrabodies to decrease and prevent generation of Alzheimer's Abeta peptide. J Cell Biol 168(6):863-868.

Pahlsson P, Spitalnik SL. 1996. The role of glycosylation in synthesis and secretion of beta-amyloid precursor protein by Chinese hamster ovary cells. Arch Biochem Biophys 331(2):177-186.

Paivio A, Jarvet J, Graslund A, Lannfelt L, Westlind-Danielsson A. 2004. Unique physicochemical profile of beta-amyloid peptide variant Abeta1-40E22G protofibrils: conceivable neuropathogen in arctic mutant carriers. J Mol Biol 339(1):145-159.

Palmert M, Usiak M, Mayeux R, Raskind M, Tourtellotte WW, Younkin S. 1990. Soluble derivates of the beta amyloid protein precursor in cerebrospinal fluid: alterations in normal aging and in Alzheimer's disease. Neurology 40:1038-1034.

Palmert MR, Podlisny MB, Witker DS, Oltersdorf T, Younkin LH, Selkoe DJ, Younkin SG. 1989a. The beta-amyloid protein precursor of Alzheimer disease has soluble derivatives found in human brain and cerebrospinal fluid. Proc Natl Acad Sci U S A 86(16):6338-6342.

Palmert MR, Siedlak SL, Podlisny MB, Greenberg B, Shelton ER, Chan HW, Usiak M, Selkoe DJ, Perry G, Younkin SG. 1989b. Soluble derivatives of the beta amyloid protein precursor of Alzheimer's disease are labeled by antisera to the beta amyloid protein. Biochem Biophys Res Commun 165(1):182-188.

Panegyres PK, Zafiris-Toufexis K, Kakulas BA. 2000. Amyloid precursor protein gene isoforms in Alzheimer's disease and other neurodegenerative disorders. J Neurol Sci 173(2):81-92.

Park JH, Gimbel DA, GrandPre T, Lee JK, Kim JE, Li W, Lee DH, Strittmatter SM. 2006. Alzheimer precursor protein interaction with the Nogo-66 receptor reduces amyloid-beta plaque deposition. J Neurosci 26(5):1386-1395.

Pastorino L, Sun A, Lu PJ, Zhou XZ, Balastik M, Finn G, Wulf G, Lim J, Li SH, Li X, Xia W, Nicholson LK, Lu KP. 2006. The prolyl isomerase Pin1 regulates amyloid precursor protein processing and amyloid-beta production. Nature 440(7083):528-534.

Pellegrini L, Passer BJ, Tabaton M, Ganjei JK, D'Adamio L. 1999. Alternative, non-secretase processing of Alzheimer's beta-amyloid precursor protein during apoptosis by caspase-6 and -8. J Biol Chem 274(30):21011-21016.

Peraus GC, Masters CL, Beyreuther K. 1997. Late compartments of amyloid precursor protein transport in SY5Y cells are involved in beta-amyloid secretion. J Neurosci 17(20):7714-7724.

Perez RG, Soriano S, Hayes JD, Ostaszewski B, Xia W, Selkoe DJ, Chen X, Stokin GB, Koo EH. 1999. Mutagenesis identifies new signals for beta-amyloid precursor protein endocytosis, turnover, and the generation of secreted fragments, including Abeta42. J Biol Chem 274(27):18851-18856.

Perez RG, Zheng H, Van der Ploeg LH, Koo EH. 1997. The beta-amyloid precursor protein of Alzheimer's disease enhances neuron viability and modulates neuronal polarity. J Neurosci 17(24):9407-9414.

Phiel CJ, Wilson CA, Lee VM, Klein PS. 2003. GSK-3alpha regulates production of Alzheimer's disease amyloid-beta peptides. Nature 423(6938):435-439.

Pietrzik CU, Yoon IS, Jaeger S, Busse T, Weggen S, Koo EH. 2004. FE65 constitutes the functional link between the low-density lipoprotein receptor-related protein and the amyloid precursor protein. J Neurosci 24(17):4259-4265.

Pinnix I, Musunuru U, Tun H, Sridharan A, Golde T, Eckman C, Ziani-Cherif C, Onstead L, Sambamurti K. 2001. A novel gamma -secretase assay based on detection of the putative C-terminal fragment-gamma of amyloid beta protein precursor. J Biol Chem 276(1):481-487.

Ponte P, Gonzalez-DeWhitt P, Schilling J, Miller J, Hsu D, Greenberg B, Davis K, Wallace W, Lieberburg I, Fuller F. 1988. A new A4 amyloid mRNA contains a domain homologous to serine proteinase inhibitors. Nature 331(6156):525-527.

Postina R, Schroeder A, Dewachter I, Bohl J, Schmitt U, Kojro E, Prinzen C, Endres K, Hiemke C, Blessing M, Flamez P, Dequenne A, Godaux E, van Leuven F, Fahrenholz F. 2004. A disintegrin-metalloproteinase prevents amyloid plaque formation and hippocampal defects in an Alzheimer disease mouse model. J Clin Invest 113(10):1456-1464.

Prokop S, Shirotani K, Edbauer D, Haass C, Steiner H. 2004. Requirement of PEN-2 for stabilization of the presenilin N-/C-terminal fragment heterodimer within the gamma-secretase complex. J Biol Chem 279(22):23255-23261.

Qi-Takahara Y, Morishima-Kawashima M, Tanimura Y, Dolios G, Hirotani N, Horikoshi Y, Kametani F, Maeda M, Saido TC, Wang R, Ihara Y. 2005. Longer forms of amyloid beta protein: implications for the mechanism of intramembrane cleavage by gamma-secretase. J Neurosci 25(2):436-445.

Qian L, Yang T, Chen H, Xie J, Zeng H, Warren DW, MacVeigh M, Meneray MA, Hamm-Alvarez SF, Mircheff AK. 2003. Heterotrimeric GTP-binding proteins in the lacrimal acinar cell endomembrane system. Exp Eye Res 74:7-22.

Ramelot TA, Nicholson LK. 2001. Phosphorylation-induced structural changes in the amyloid precursor protein cytoplasmic tail detected by NMR. J Mol Biol 307(3):871-884.

Robakis NK, Pangalos MN. 1994. Involvement of amyloid as a central step in the development of Alzheimer's disease. Neurobiol Aging 15 Suppl 2:S127-129.

Roberds SL, Anderson J, Basi G, Bienkowski MJ, Branstetter DG, Chen KS, Freedman SB, Frigon NL, Games D, Hu K, Johnson-Wood K, Kappenman KE, Kawabe TT, Kola I, Kuehn R, Lee M, Liu W, Motter R, Nichols NF, Power M, Robertson DW, Schenk D, Schoor M, Shopp GM, Shuck ME, Sinha S, Svensson KA, Tatsuno G, Tintrup H, Wijsman J, Wright S, McConlogue L. 2001. BACE knockout mice are healthy despite lacking the primary beta-secretase activity in brain: implications for Alzheimer's disease therapeutics. Hum Mol Genet 10(12):1317-1324.

Roch JM, Masliah E, Roch-Levecq AC, Sundsmo MP, Otero DA, Veinbergs I, Saitoh T. 1994. Increase of synaptic density and memory retention by a peptide representing the trophic domain of the amyloid beta/A4 protein precursor. Proc Natl Acad Sci U S A 91(16):7450-7454.

Rockenstein EM, McConlogue L, Tan H, Power M, Masliah E, Mucke L. 1995. Levels and alternative splicing of amyloid beta protein precursor (APP) transcripts in brains of APP transgenic mice and humans with Alzheimer's disease. J Biol Chem 270(47):28257-28267.

Roghani M, Becherer JD, Moss ML, Atherton RE, Erdjument-Bromage H, Arribas J, Blackburn RK, Weskamp G, Tempst P, Blobel CP. 1999. Metalloprotease-disintegrin MDC9: intracellular maturation and catalytic activity. J Biol Chem 274(6):3531-3540.

Rohan de Silva HA, Jen A, Wickenden C, Jen LS, Wilkinson SL, Patel AJ. 1997. Cell-specific expression of beta-amyloid precursor protein isoform mRNAs and proteins in neurons and astrocytes. Brain Res Mol Brain Res 47:147-156.

Roncarati R, Sestan N, Scheinfeld MH, Berechid BE, Lopez PA, Meucci O, McGlade JC, Rakic P, D'Adamio L. 2002. The gamma-secretase-generated intracellular domain of beta-amyloid precursor protein binds Numb and inhibits Notch signaling. Proc Natl Acad Sci U S A 99(10):7102-7107.

Rosen DR, Martin-Morris L, Luo LQ, White K. 1989. A Drosophila gene encoding a protein resembling the human beta-amyloid protein precursor. Proc Natl Acad Sci U S A 86(7):2478-2482.

Rossjohn J, Cappai R, Feil SC, Henry A, McKinstry WJ, Galatis D, Hesse L, Multhaup G, Beyreuther K, Masters CL, Parker MW. 1999. Crystal structure of the N-terminal, growth factor-like domain of Alzheimer amyloid precursor protein. Nat Struct Biol 6(4):327-331.

Rossner S, Mehlhorn G, Schliebs R, Bigl V. 2001. Increased neuronal and glial expression of protein kinase C isoforms in neocortex of transgenic Tg2576 mice with amyloid pathology. Eur J Neurosci 13(2):269-278.

Russo C, Dolcini V, Salis S, Venezia V, Zambrano N, Russo T, Schettini G. 2002. Signal transduction through tyrosine-phosphorylated C-terminal fragments of amyloid precursor protein via an enhanced interaction with Shc/Grb2 adaptor proteins in reactive astrocytes of Alzheimer's disease brain. J Biol Chem 277(38):35282-35288.

Russo C, Venezia V, Repetto E, Nizzari M, Violani E, Carlo P, Schettini G. 2005. The amyloid precursor protein and its network of interacting proteins: physiological and pathological implications. Brain Res Brain Res Rev 48(2):257-264.

Sabatini DD, Adesnik M, Ivanov IE, Simon JP. 1996. Mechanism of formation of post Golgi vesicles from TGN membranes: Arf-dependent coat assembly and PKC-regulated vesicle scission. Biocell 20(3):287-300.

Sabo SL, Ikin AF, Buxbaum JD, Greengard P. 2001. The Alzheimer amyloid precursor protein (APP) and FE65, an APP-binding protein, regulate cell movement. J Cell Biol 153(7):1403-1414.

Sabo SL, Ikin AF, Buxbaum JD, Greengard P. 2003. The amyloid precursor protein and its regulatory protein, FE65, in growth cones and synapses in vitro and in vivo. J Neurosci 23(13):5407-5415.

Sabo SL, Lanier LM, Ikin AF, Khorkova O, Sahasrabudhe S, Greengard P, Buxbaum JD. 1999. Regulation of beta-amyloid secretion by FE65, an amyloid protein precursor-binding protein. J Biol Chem 274(12):7952-7957.

Saitoh T, Sundsmo M, Roch JM, Kimura N, Cole G, Schubert D, Oltersdorf T, Schenk DB. 1989. Secreted form of amyloid beta protein precursor is involved in the growth regulation of fibroblasts. Cell 58(4):615-622.

Sambamurti K, Refolo LM, Shioi J, Pappolla MA, Robakis NK. 1992. The Alzheimer's amyloid precursor is cleaved intracellularly in the trans-Golgi network or in a post-Golgi compartment. Ann N Y Acad Sci 674:118-128.

Sandbrink R, Masters CL, Beyreuther K. 1994a. Beta A4-amyloid protein precursor mRNA isoforms without exon 15 are ubiquitously expressed in rat tissues including brain, but not in neurons. J Biol Chem 269(2):1510-1517.

Sandbrink R, Masters CL, Beyreuther K. 1994b. Similar alternative splicing of a non-homologous domain in beta A4-amyloid protein precursor-like proteins. J Biol Chem 269(19):14227-14234.

Santolini E, Puri C, Salcini AE, Gagliani MC, Pelicci PG, Tacchetti C, Di Fiore PP. 2000. Numb is an endocytic protein. J Cell Biol 151(6):1345-1352.

Sastre M, Steiner H, Fuchs K, Capell A, Multhaup G, Condron MM, Teplow DB, Haass C. 2001. Presenilin-dependent gamma-secretase processing of beta-amyloid precursor protein at a site corresponding to the S3 cleavage of Notch. EMBO Rep 2(9):835-841.

Sastre M, Turner RS, Levy E. 1998. X11 interaction with beta-amyloid precursor protein modulates its cellular stabilization and reduces amyloid beta-protein secretion. J Biol Chem 273(35):22351-22357.

Schmid SL. 1997. Clathrin-coated vesicle formation and protein sorting: an integrated process. Annu Rev Biochem 66:511-548.

Schubert D, Cole G, Saitoh T, Oltersdorf T. 1989a. Amyloid beta protein precursor is a mitogen. Biochem Biophys Res Commun 162(1):83-88.

Schubert D, LaCorbiere M, Saitoh T, Cole G. 1989b. Characterization of an amyloid beta precursor protein that binds heparin and contains tyrosine sulfate. Proc Natl Acad Sci U S A 86(6):2066-2069.

Schubert W, Masters CL, Beyreuther K. 1993. APP+ T lymphocytes selectively sorted to endomysial tubes in polymyositis displace NCAM-expressing muscle fibers. Eur J Cell Biol 62(2):333-342.

Schubert W, Prior R, Weidemann A, Dircksen H, Multhaup G, Masters CL, Beyreuther K. 1991. Localization of Alzheimer beta A4 amyloid precursor protein at central and peripheral synaptic sites. Brain Res 563(1-2):184-194.

Selkoe D, Kopan R. 2003. Notch and Presenilin: regulated intramembrane proteolysis links development and degeneration. Annu Rev Neurosci 26:565-597.

Selkoe DJ. 1993. Physiological production of the beta-amyloid protein and the mechanism of Alzheimer's disease. Trends Neurosci 16(10):403-409.

Selkoe DJ. 2001. Alzheimer's disease: genes, proteins, and therapy. Physiol Rev 81(2):741-766.

Selkoe DJ, Podlisny MB. 2002. Deciphering the genetic basis of Alzheimer's disease. Annu Rev Genomics Hum Genet 3:67-99.
Selkoe DJ, Podlisny MB, Joachim CL, Vickers EA, Lee G, Fritz LC, Oltersdorf T. 1988. Beta-amyloid precursor protein of Alzheimer disease occurs as 110- to 135-kilodalton membrane-associated proteins in neural and nonneural tissues. Proc Natl Acad Sci U S A 85(19):7341-7345.
Selkoe DJ, Schenk D. 2003. Alzheimer's disease: molecular understanding predicts amyloid-based therapeutics. Annu Rev Pharmacol Toxicol 43:545-584.
Serneels L, Dejaegere T, Craessaerts K, Horre K, Jorissen E, Tousseyn T, Hebert S, Coolen M, Martens G, Zwijsen A, Annaert W, Hartmann D, De Strooper B. 2005. Differential contribution of the three Aph1 genes to gamma-secretase activity in vivo. Proc Natl Acad Sci U S A 102(5):1719-1724.
Seubert P, Oltersdorf T, Lee MG, Barbour R, Blomquist C, Davis DL, Bryant K, Fritz LC, Galasko D, Thal LJ, et al. 1993. Secretion of beta-amyloid precursor protein cleaved at the amino terminus of the beta-amyloid peptide. Nature 361(6409):260-263.
Seubert P, Vigo-Pelfrey C, Esch F, Lee M, Dovey H, Davis D, Sinha S, Schlossmacher M, Whaley J, Swindlehurst C, et al. 1992. Isolation and quantification of soluble Alzheimer's beta-peptide from biological fluids. Nature 359(6393):325-327.
Shah S, Lee SF, Tabuchi K, Hao YH, Yu C, LaPlant Q, Ball H, Dann CE, 3rd, Sudhof T, Yu G. 2005. Nicastrin functions as a gamma-secretase-substrate receptor. Cell 122(3):435-447.
Sheng JG, Price DL, Koliatsos VE. 2002. Disruption of corticocortical connections ameliorates amyloid burden in terminal fields in a transgenic model of Abeta amyloidosis. J Neurosci 22(22):9794-9799.
Sherrington R, Rogaev EI, Liang Y, Rogaeva EA, Levesque G, Ikeda M, Chi H, Lin C, Li G, Holman K, et al. 1995. Cloning of a gene bearing missense mutations in early-onset familial Alzheimer's disease. Nature 375(6534):754-760.
Shiba T, Kametaka S, Kawasaki M, Shibata M, Waguri S, Uchiyama Y, Wakatsuki S. 2004. Insights into the phosphoregulation of beta-secretase sorting signal by the VHS domain of GGA1. Traffic 5(6):437-448.
Shimohama S, Narita M, Matsushima H, Kimura J, Kameyama M, Hagiwara M, Hidaka H, Taniguchi T. 1993. Assessment of protein kinase C isozymes by two-site enzyme immunoassay in human brains and changes in Alzheimer's disease. Neurology 43(7):1407-1413.
Shirotani K, Edbauer D, Kostka M, Steiner H, Haass C. 2004. Immature nicastrin stabilizes APH-1 independent of PEN-2 and presenilin: identification of nicastrin mutants that selectively interact with APH-1. J Neurochem 89(6):1520-1527.
Shoji M, Golde TE, Ghiso J, Cheung TT, Estus S, Shaffer LM, Cai XD, McKay DM, Tintner R, Frangione B, et al. 1992. Production of the Alzheimer amyloid beta protein by normal proteolytic processing. Science 258(5079):126-129.
Simon JP, Ivanov IE, Adesnik M, Sabatini DD. 1996. The production of post-Golgi vesicles requires a protein kinase C-like molecule, but not its phosphorylating activity. J Cell Biol 135(2):355-370.
Simons M, Tienari PJ, Dotti CG, Beyreuther K. 1995. Two-dimensional gel mapping of the processing of the human amyloid precursor protein in rat hippocampal neurons. FEBS Lett 368(2):363-366.
Sinha S, Anderson JP, Barbour R, Basi GS, Caccavello R, Davis D, Doan M, Dovey HF, Frigon N, Hong J, Jacobson-Croak K, Jewett N, Keim P, Knops J, Lieberburg I, Power M, Tan H, Tatsuno G, Tung J, Schenk D, Seubert P, Suomensaari SM, Wang S, Walker D, Zhao J, McConlogue L, John V. 1999. Purification and cloning of amyloid precursor protein beta-secretase from human brain. Nature 402(6761):537-540.
Sinha S, Lieberburg I. 1999. Cellular mechanisms of beta-amyloid production and secretion. Proc Natl Acad Sci U S A 96(20):11049-11053.

Sisodia SS. 1992. Beta-amyloid precursor protein cleavage by a membrane-bound protease. Proc Natl Acad Sci U S A 89(13):6075-6079.
Sisodia SS. 2002. Biomedicine. A cargo receptor mystery APParently solved? Science 295(5556):805-807.
Sisodia SS, Koo EH, Hoffman PN, Perry G, Price DL. 1993. Identification and transport of full-length amyloid precursor proteins in rat peripheral nervous system. J Neurosci 13(7):3136-3142.
Sisodia SS, Price DL. 1995. Role of the beta-amyloid protein in Alzheimer's disease. Faseb J 9(5):366-370.
Slack BE, Nitsch RM, Livneh E, Kunz GM, Jr., Eldar H, Wurtman RJ. 1993. Regulation of amyloid precursor protein release by protein kinase C in Swiss 3T3 fibroblasts. Ann N Y Acad Sci 695:128-131.
Sleegers K, Van Duijn CM. 2001. Alzheimer's Disease: Genes, Pathogenesis and Risk Prediction. Community Genet 4(4):197-203.
Slunt HH, Thinakaran G, Von Koch C, Lo AC, Tanzi RE, Sisodia SS. 1994. Expression of a ubiquitous, cross-reactive homologue of the mouse beta-amyloid precursor protein (APP). J Biol Chem 269(4):2637-2644.
Small DH, McLean CA. 1999. Alzheimer's disease and the amyloid beta protein: What is the role of amyloid? J Neurochem 73(2):443-449.
Small DH, Nurcombe V, Reed G, Clarris H, Moir R, Beyreuther K, Masters CL. 1994. A heparin-binding domain in the amyloid protein precursor of Alzheimer's disease is involved in the regulation of neurite outgrowth. J Neurosci 14(4):2117-2127.
Soba P, Eggert S, Wagner K, Zentgraf H, Siehl K, Kreger S, Lower A, Langer A, Merdes G, Paro R, Masters CL, Muller U, Kins S, Beyreuther K. 2005. Homo- and heterodimerization of APP family members promotes intercellular adhesion. Embo J 24(20):3624-3634.
Soriano S, Lu DC, Chandra S, Pietrzik CU, Koo EH. 2001. The amyloidogenic pathway of amyloid precursor protein (APP) is independent of its cleavage by caspases. J Biol Chem 276(31):29045-29050.
Stalder M, Phinney A, Probst A, Sommer B, Staufenbiel M, Jucker M. 1999. Association of microglia with amyloid plaques in brains of APP23 transgenic mice. Am J Pathol 154(6):1673-1684.
Standen CL, Brownlees J, Grierson AJ, Kesavapany S, Lau KF, McLoughlin DM, Miller CC. 2001. Phosphorylation of thr(668) in the cytoplasmic domain of the Alzheimer's disease amyloid precursor protein by stress-activated protein kinase 1b (Jun N-terminal kinase-3). J Neurochem 76(1):316-320.
Steiner H, Winkler E, Edbauer D, Prokop S, Basset G, Yamasaki A, Kostka M, Haass C. 2002. PEN-2 is an integral component of the gamma-secretase complex required for coordinated expression of presenilin and nicastrin. J Biol Chem 277(42):39062-39065.
Stokin GB, Lillo C, Falzone TL, Brusch RG, Rockenstein E, Mount SL, Raman R, Davies P, Masliah E, Williams DS, Goldstein LS. 2005. Axonopathy and transport deficits early in the pathogenesis of Alzheimer's disease. Science 307(5713):1282-1288.
Storey E, Beyreuther K, Masters CL. 1996. Alzheimer's disease amyloid precursor protein on the surface of cortical neurons in primary culture co-localizes with adhesion patch components. Brain Res 735(2):217-231.
Strittmatter WJ, Saunders AM, Schmechel D, Pericak-Vance M, Enghild J, Salvesen GS, Roses AD. 1993. Apolipoprotein E: high-avidity binding to beta-amyloid and increased frequency of type 4 allele in late-onset familial Alzheimer disease. Proc Natl Acad Sci U S A 90(5):1977-1981.
Struhl G, Adachi A. 2000. Requirements for presenilin-dependent cleavage of notch and other transmembrane proteins. Mol Cell 6(3):625-636.
Suzuki T, Araki Y, Yamamoto T, Nakaya T. 2006. Trafficking of Alzheimer's disease-related membrane proteins and its participation in disease pathogenesis. J Biochem (Tokyo) 139(6):949-955.

Suzuki T, Oishi M, Marshak DR, Czernik AJ, Nairn AC, Greengard P. 1994. Cell cycle-dependent regulation of the phosphorylation and metabolism of the Alzheimer amyloid precursor protein. Embo J 13(5):1114-1122.

Tagawa K, Yazaki M, Kinouchi T, Maruyama K, Sorimachi H, Tsuchiya T, Suzuki K, Ishiura S. 1993. Amyloid precursor protein is found in lysosomes. Gerontology 39 Suppl 1:24-29.

Takasugi N, Tomita T, Hayashi I, Tsuruoka M, Niimura M, Takahashi Y, Thinakaran G, Iwatsubo T. 2003. The role of presenilin cofactors in the gamma-secretase complex. Nature 422(6930):438-441.

Tanahashi H, Tabira T. 1999. Genome structure and chromosomal mapping of the gene for Fe65L2 interacting with Alzheimer's beta-amyloid precursor protein. Biochem Biophys Res Commun 258(2):385-389.

Tanahashi H, Tabira T. 2002. Characterization of an amyloid precursor protein-binding protein Fe65L2 and its novel isoforms lacking phosphotyrosine-interaction domains. Biochem J 367(Pt 3):687-695.

Tanaka S, Shiojiri S, Takahashi Y, Kitaguchi N, Ito H, Kameyama M, Kimura J, Nakamura S, Ueda K. 1989. Tissue-specific expression of three types of beta-protein precursor mRNA: enhancement of protease inhibitor-harboring types in Alzheimer's disease brain. Biochem Biophys Res Commun 165(3):1406-1414.

Tanzi RE, Gusella JF, Watkins PC, Bruns GA, St George-Hyslop P, Van Keuren ML, Patterson D, Pagan S, Kurnit DM, Neve RL. 1987. Amyloid beta protein gene: cDNA, mRNA distribution, and genetic linkage near the Alzheimer locus. Science 235(4791):880-884.

Tanzi RE, McClatchey AI, Lamperti ED, Villa-Komaroff L, Gusella JF, Neve RL. 1988. Protease inhibitor domain encoded by an amyloid protein precursor mRNA associated with Alzheimer's disease. Nature 331(6156):528-530.

Tanzi RE, Wenniger JJ, Hyman BT. 1993. Cellular specificity and regional distribution of amyloid beta protein precursor alternative transcripts are unaltered in Alzheimer hippocampal formation. Brain Res Mol Brain Res 18(3):246-252.

Tarr PE, Roncarati R, Pelicci G, Pelicci PG, D'Adamio L. 2002. Tyrosine phosphorylation of the beta-amyloid precursor protein cytoplasmic tail promotes interaction with Shc. J Biol Chem 277(19):16798-16804.

Taru H, Iijima K, Hase M, Kirino Y, Yagi Y, Suzuki T. 2002. Interaction of Alzheimer's beta -amyloid precursor family proteins with scaffold proteins of the JNK signaling cascade. J Biol Chem 277(22):20070-20078.

Tian Q, Wang J. 2002. Role of serine/threonine protein phosphatase in Alzheimer's disease. Neurosignals 11(5):262-269.

Tiraboschi P, Hansen LA, Masliah E, Alford M, Thal LJ, Corey-Bloom J. 2004. Impact of APOE genotype on neuropathologic and neurochemical markers of Alzheimer disease. Neurology 62(11):1977-1983.

Tomita S, Kirino Y, Suzuki T. 1998. Cleavage of Alzheimer's amyloid precursor protein (APP) by secretases occurs after O-glycosylation of APP in the protein secretory pathway. Identification of intracellular compartments in which APP cleavage occurs without using toxic agents that interfere with protein metabolism. J Biol Chem 273(11):6277-6284.

Tomita S, Ozaki T, Taru H, Oguchi S, Takeda S, Yagi Y, Sakiyama S, Kirino Y, Suzuki T. 1999. Interaction of a neuron-specific protein containing PDZ domains with Alzheimer's amyloid precursor protein. J Biol Chem 274(4):2243-2254.

Trejo J, Massamiri T, Deng T, Dewji NN, Bayney RM, Brown JH. 1994. A direct role for protein kinase C and the transcription factor Jun/AP-1 in the regulation of the Alzheimer's beta-amyloid precursor protein gene. J Biol Chem 269(34):21682-21690.

Trommsdorff M, Borg JP, Margolis B, Herz J. 1998. Interaction of cytosolic adaptor proteins with neuronal apolipoprotein E receptors and the amyloid precursor protein. J Biol Chem 273(50):33556-33560.

Turner PR, O'Connor K, Tate WP, Abraham WC. 2003. Roles of amyloid precursor protein and its fragments in regulating neural activity, plasticity and memory. Prog Neurobiol 70(1):1-32.

Van den Heuvel C, Blumbergs PC, Finnie JW, Manavis J, Jones NR, Reilly PL, Pereira RA. 1999. Upregulation of amyloid precursor protein messenger RNA in response to traumatic brain injury: an ovine head impact model. Exp Neurol 159(2):441-450.

Van Nostrand WE, Cunningham DD. 1987. Purification of protease nexin II from human fibroblasts. J Biol Chem 262:8508-8514.

Vassar R, Bennett BD, Babu-Khan S, Kahn S, Mendiaz EA, Denis P, Teplow DB, Ross S, Amarante P, Loeloff R, Luo Y, Fisher S, Fuller J, Edenson S, Lile J, Jarosinski MA, Biere AL, Curran E, Burgess T, Louis JC, Collins F, Treanor J, Rogers G, Citron M. 1999. Beta-secretase cleavage of Alzheimer's amyloid precursor protein by the transmembrane aspartic protease BACE. Science 286(5440):735-741.

Vijayan S, El-Akkad E, Grundke-Iqbal I, Iqbal K. 2001. A pool of beta-tubulin is hyperphosphorylated at serine residues in Alzheimer disease brain. FEBS Lett 509(3):375-381.

Vingtdeux V, Hamdane M, Gompel M, Begard S, Drobecq H, Ghestem A, Grosjean ME, Kostanjevecki V, Grognet P, Vanmechelen E, Buee L, Delacourte A, Sergeant N. 2005. Phosphorylation of amyloid precursor carboxy-terminal fragments enhances their processing by a gamma-secretase-dependent mechanism. Neurobiol Dis 20(2):625-637.

von Rotz RC, Kohli BM, Bosset J, Meier M, Suzuki T, Nitsch RM, Konietzko U. 2004. The APP intracellular domain forms nuclear multiprotein complexes and regulates the transcription of its own precursor. J Cell Sci 117:4435-4448.

Waddell S. 2003. Protein phosphatase 1 and memory: practice makes PP1 imperfect? Trends Neurosci 26(3):117-119.

Wagner SL, Siegel RS, Vedvick TS, Raschke WC, van Nostrand WE. 1992. High level expression, purification, and characterization of the Kunitz-type protease inhibitor domain of protease nexin-2/amyloid beta-protein precursor. Biochem Biophys Res 186: 1138-1145.

Walsh DM, Klyubin I, Fadeeva JV, Cullen WK, Anwyl R, Wolfe MS, Rowan MJ, Selkoe DJ. 2002. Naturally secreted oligomers of amyloid beta protein potently inhibit hippocampal long-term potentiation in vivo. Nature 416(6880):535-539.

Walter J, Capell A, Grunberg J, Pesold B, Schindzielorz A, Prior R, Podlisny MB, Fraser P, Hyslop PS, Selkoe DJ, Haass C. 1996. The Alzheimer's disease-associated presenilins are differentially phosphorylated proteins located predominantly within the endoplasmic reticulum. Mol Med 2(6):673-691.

Walter J, Capell A, Hung AY, Langen H, Schnolzer M, Thinakaran G, Sisodia SS, Selkoe DJ, Haass C. 1997. Ectodomain phosphorylation of beta-amyloid precursor protein at two distinct cellular locations. J Biol Chem 272(3):1896-1903.

Walter J, Grunberg J, Schindzielorz A, Haass C. 1998. Proteolytic fragments of the Alzheimer's disease associated presenilins-1 and -2 are phosphorylated in vivo by distinct cellular mechanisms. Biochemistry 37(17):5961-5967.

Walter J, Kaether C, Steiner H, Haass C. 2001. The cell biology of Alzheimer's disease: uncovering the secrets of secretases. Curr Opin Neurobiol 11(5):585-590.

Walter J, Schindzielorz A, Grunberg J, Haass C. 1999. Phosphorylation of presenilin-2 regulates its cleavage by caspases and retards progression of apoptosis. Proc Natl Acad Sci U S A 96(4):1391-1396.

Walter J, Schindzielorz A, Hartung B, Haass C. 2000. Phosphorylation of the beta-amyloid precursor protein at the cell surface by ectocasein kinases 1 and 2. J Biol Chem 275(31):23523-23529.

Wang y, Ha y. 2004. The X-ray structure of an antiparallel dimer of the human amyloid precursor protein E2 domain. Mol Cell 15:343-353.

Watanabe T, Sukegawa J, Sukegawa I, Tomita S, Iijima K, Oguchi S, Suzuki T, Nairn AC, Greengard P. 1999. A 127-kDa protein (UV-DDB) binds to the cytoplasmic domain of the Alzheimer's amyloid precursor protein. J Neurochem 72(2):549-556.

Webster S, Glabe C, Rogers J. 1995. Multivalent binding of complement protein C1Q to the amyloid beta-peptide (A beta) promotes the nucleation phase of A beta aggregation. Biochem Biophys Res Commun 217(3):869-875.

Weidemann A, Eggert S, Reinhard FB, Vogel M, Paliga K, Baier G, Masters CL, Beyreuther K, Evin G. 2002. A novel epsilon-cleavage within the transmembrane domain of the Alzheimer amyloid precursor protein demonstrates homology with Notch processing. Biochemistry 41(8):2825-2835.

Weidemann A, Konig G, Bunke D, Fischer P, Salbaum JM, Masters CL, Beyreuther K. 1989. Identification, biogenesis, and localization of precursors of Alzheimer's disease A4 amyloid protein. Cell 57(1):115-126.

Weidemann A, Paliga K, Durrwang U, Reinhard FB, Schuckert O, Evin G, Masters CL. 1999. Proteolytic processing of the Alzheimer's disease amyloid precursor protein within its cytoplasmic domain by caspase-like proteases. J Biol Chem 274(9):5823-5829.

Westmeyer GG, Willem M, Lichtenthaler SF, Lurman G, Multhaup G, Assfalg-Machleidt I, Reiss K, Saftig P, Haass C. 2004. Dimerization of beta-site beta-amyloid precursor protein-cleaving enzyme. J Biol Chem 279(51):53205-53212.

Wisniewski T, Ghiso J, Frangione B. 1991. Peptides homologous to the amyloid protein of Alzheimer's disease containing a glutamine for glutamic acid substitution have accelerated amyloid fibril formation. Biochem Biophys Res Commun 179(3):1247-1254.

Wolf BA, Wertkin AM, Jolly YC, Yasuda RP, Wolfe BB, Konrad RJ, Manning D, Ravi S, Williamson JR, Lee VM. 1995. Muscarinic regulation of Alzheimer's disease amyloid precursor protein secretion and amyloid beta-protein production in human neuronal NT2N cells. J Biol Chem 270(9):4916-4922.

Wolfe MS, De Los Angeles J, Miller DD, Xia W, Selkoe DJ. 1999. Are presenilins intramembrane-cleaving proteases? Implications for the molecular mechanism of Alzheimer's disease. Biochemistry 38(35):11223-11230.

Xia W. 2001. Amyloid metabolism and secretases in Alzheimer's disease. Curr Neurol Neurosci Rep 1(5):422-427.

Xia W, Zhang J, Ostaszewski BL, Kimberly WT, Seubert P, Koo EH, Shen J, Selkoe DJ. 1998. Presenilin 1 regulates the processing of beta-amyloid precursor protein C-terminal fragments and the generation of amyloid beta-protein in endoplasmic reticulum and Golgi. Biochemistry 37(47):16465-16471.

Xia W, Zhang J, Perez R, Koo EH, Selkoe DJ. 1997. Interaction between amyloid precursor protein and presenilins in mammalian cells: implications for the pathogenesis of Alzheimer disease. Proc Natl Acad Sci U S A 94(15):8208-8213.

Xu H, Greengard P, Gandy S. 1995. Regulated formation of Golgi secretory vesicles containing Alzheimer beta-amyloid precursor protein. J Biol Chem 270(40):23243-23245.

Xu J, Chen S, Ahmed SH, Chen H, Ku G, Goldberg MP, Hsu CY. 2001. Amyloid-beta peptides are cytotoxic to oligodendrocytes. J Neurosci 21(1):RC118.

Yamazaki T, Koo EH, Selkoe DJ. 1996. Trafficking of cell-surface amyloid beta-protein precursor. II. Endocytosis, recycling and lysosomal targeting detected by immunolocalization. J Cell Sci 109 (Pt 5):999-1008.

Yamazaki T, Koo EH, Selkoe DJ. 1997. Cell surface amyloid beta-protein precursor colocalizes with beta 1 integrins at substrate contact sites in neural cells. J Neurosci 17(3):1004-1010.

Yamazaki T, Selkoe DJ, Koo EH. 1995. Trafficking of cell surface beta-amyloid precursor protein: retrograde and transcytotic transport in cultured neurons. J Cell Biol 129(2):431-442.

Yan R, Bienkowski MJ, Shuck ME, Miao H, Tory MC, Pauley AM, Brashier JR, Stratman NC, Mathews WR, Buhl AE, Carter DB, Tomasselli AG, Parodi LA, Heinrikson RL, Gurney ME. 1999. Membrane-anchored aspartyl protease with Alzheimer's disease beta-secretase activity. Nature 402(6761):533-537.

Yan Y, Mumby MC. 1999. Distinct roles for PP1 and PP2A in phosphorylation of the retinoblastoma protein. PP2a regulates the activities of G(1) cyclin-dependent kinases. J Biol Chem 274(45):31917-31924.

Yang Y, Turner RS, Gaut JR. 1998. The chaperone BiP/GRP78 binds to amyloid precursor protein and decreases Abeta40 and Abeta42 secretion. J Biol Chem 273(40):25552-25555.

Yang Z, Cool BH, Martin GM, Hu Q. 2006. A dominant role for FE65 (APBB1) in nuclear signaling. J Biol Chem 281(7):4207-4214.

Yankner BA, Dawes LR, Fisher S, Villa-Komaroff L, Oster-Granite ML, Neve RL. 1989. Neurotoxicity of a fragment of the amyloid precursor associated with Alzheimer's disease. Science 245(4916):417-420.

Yoshikawa K, Aizawa T, Hayashi Y. 1992. Degeneration in vitro of post-mitotic neurons overexpressing the Alzheimer amyloid protein precursor. Nature 359(6390):64-67.

Yu G, Chen F, Nishimura M, Steiner H, Tandon A, Kawarai T, Arawaka S, Supala A, Song YQ, Rogaeva E, Holmes E, Zhang DM, Milman P, Fraser P, Haass C, St George-Hyslop P. 2000. Mutation of conserved aspartates affect maturation of presenilin 1 and presenilin 2 complexes. Acta Neurol Scand Suppl 176:6-11.

Yun M, Keshvara L, Park CG, Zhang YM, Dickerson JB, Zheng J, Rock CO, Curran T, Park HW. 2003. Crystal structures of the Dab homology domains of mouse disabled 1 and 2. J Biol Chem 278(38):36572-36581.

Zambrano N, Bruni P, Minopoli G, Mosca R, Molino D, Russo C, Schettini G, Sudol M, Russo T. 2001. The beta-amyloid precursor protein APP is tyrosine-phosphorylated in cells expressing a constitutively active form of the Abl protoncogene. J Biol Chem 276(23):19787-19792.

Zambrano N, Gianni D, Bruni P, Passaro F, Telese F, Russo T. 2004. Fe65 is not involved in the platelet-derived growth factor-induced processing of Alzheimer's amyloid precursor protein, which activates its caspase-directed cleavage. J Biol Chem 279(16):16161-16169.

Zhang Z, Lee CH, Mandiyan V, Borg JP, Margolis B, Schlessinger J, Kuriyan J. 1997. Sequence-specific recognition of the internalization motif of the Alzheimer's amyloid precursor protein by the X11 PTB domain. Embo J 16(20):6141-6150.

Zhang Z, Nadeau P, Song W, Donoviel D, Yuan M, Bernstein A, Yankner BA. 2000. Presenilins are required for gamma-secretase cleavage of beta-APP and transmembrane cleavage of Notch-1. Nat Cell Biol 2(7):463-465.

Zhao G, Mao G, Tan J, Dong Y, Cui MZ, Kim SH, Xu X. 2004. Identification of a new presenilin-dependent zeta-cleavage site within the transmembrane domain of amyloid precursor protein. J Biol Chem 279(49):50647-50650.

Zheng B, Kimberly WT, Selkoe DJ. Temporal Regulation of the endogenous APP intracellular domain (AICD) in primary neurons. ; 2003. SFN.

Zheng H, Jiang M, Trumbauer ME, Hopkins R, Sirinathsinghji DJ, Stevens KA, Conner MW, Slunt HH, Sisodia SS, Chen HY, Van der Ploeg LH. 1996. Mice deficient for the amyloid precursor protein gene. Ann N Y Acad Sci 777:421-426.

Zheng P, Eastman J, Vande Pol S, Pimplikar SW. 1998. PAT1, a microtubule-interacting protein, recognizes the basolateral sorting signal of amyloid precursor protein. Proc Natl Acad Sci U S A 95(25):14745-14750.

CHAPTER II

CHAPTER II

DEVELOPMENT OF MODEL SYSTEMS TO STUDY APP TRAFFICKING AND PROCESSING

During the last decade various studies have addressed APP expression, processing and subcellular localization, in order to identify factors that affect APP cellular metabolic pathways and subsequently modulate Abeta production. Among these studies, we can refer RT-PCR (Sandbrink et al. 1994), phosphorylation site mutants (Haass et al. 1995, da Cruz e Silva et al 1993), *in situ* hybridization (Rockeinstein et al. 1995), immunocytochemistry (Caporaso et al., 1994) and subcellular fractionation (Xia et al., 1998). Although extremely informative, these methods are mostly nondynamic analytical methods that may be insufficient to address alternative APP-processing pathways. Clearly, new approaches are needed to further refine our understanding of APP processing and trafficking. With this purpose, we developed a novel approach with the following considerations: (1) site-directed mutagenesis of target amino acids to mimic a constitutive phosphorylation/dephosphorylation state, (2) expression of Wild type and mutant APP-GFP (green fluorescent protein) fusion proteins to facilitate visualization, (3) controlled low level expression to avoid 'flooding' cellular pathways, and (4) the use of cycloheximide to inhibit "de novo" protein synthesis.

Using this methodology, we were able to detect specific differences in APP processing that correlated with the mimicked phosphorylation state. This approach is extensively described in the first manuscript (da Cruz e Silva et al. 2004) presented in this section. The use of this powerful methodology allows the detailed analysis of key control points in the cellular metabolism of specific proteins that are central to neurodegenerative diseases.

Additionally, we were able to monitor a specific APP population using a different approach called the modified model system. The major difference between the two systems is that in the first cycloheximide (CHX) was added and 'de novo' protein synthesis was inhibited, whereas in the latter the CHX was removed thus allowing 'de novo' protein synthesis. APP trafficking was monitored in both cases. Consequently, we were able to show that CHX inhibition was reversible and well suited to monitor

specific stages of APP intracellular targeting. The second approach will be described in detail in the second manuscript (Rebelo et al. 2008, submitted).

Caporaso GL, Takei K, Gandy SE, Matteoli M, Mundigl O, Greengard P, De Camilli P. 1994. Morphologic and biochemical analysis of the intracellular trafficking of the Alzheimer beta/A4 amyloid precursor protein. J Neurosci 14(5 Pt 2):3122-3138.

da Cruz e Silva OA, Vieira SI, Rebelo S, da Cruz e Silva EF. 2004. A model system to study intracellular trafficking and processing of the Alzheimer's amyloid precursor protein. Neurodegener Dis 1: 196-204.

da Cruz e Silva AO, Iverfeldt K, Oltersdorf T,.Sinha S, Lieberburg I, Ramabhadran TV, Suzuki T, Sisodia SS, Gandy S, Greengard P. 1993. Regulated cleavage of Alzheimer beta-amyloid precursor protein in the absence of the cytoplasmic tail. Neurosci. 54: 873-7.

Haass C, Koo EH, Capell A, Teplow DB, Selkoe DJ. 1995. Polarized sorting of beta-amyloid precursor protein and its proteolytic products in MDCK cells is regulated by two independent signals. J Cell Biol 128(4):537-547.

Rebelo S, Vieira SI, da Cruz e Silva EF, da Cruz e Silva, OA 2004.A reversible effect of cycloheximide on intracellullar APP tracking. AJAD (sumitted).

Rockenstein EM, McConlogue L, Tan H, Power M, Masliah E, Mucke L. 1995. Levels and alternative splicing of amyloid beta protein precursor (APP) transcripts in brains of APP transgenic mice and humans with Alzheimer's disease. J Biol Chem 270(47):28257-28267.

Sandbrink R, Masters CL, Beyreuther K. 1994a. APP gene family: unique age-associated changes in splicing of Alzheimer's betaA4-amyloid protein precursor. Neurobiol Dis 1(1-2):13-24.

Xia W, Zhang J, Ostaszewski BL, Kimberly WT, Seubert P, Koo EH, Shen J, Selkoe DJ. 1998. Presenilin 1 regulates the processing of beta-amyloid precursor protein C-terminal fragments and the generation of amyloid beta-protein in endoplasmic reticulum and Golgi. Biochemistry 37(47):16465-16471.

Neuro–degenerative Diseases

Neurodegenerative Dis 2004;1:196–204
DOI: 10.1159/000080986

A Model System to Study Intracellular Trafficking and Processing of the Alzheimer's Amyloid Precursor Protein

Odete A.B. da Cruz e Silva[a] Sandra Isabel Vieira[a] Sandra Rebelo[a]
Edgar F. da Cruz e Silva[b]

[a]Laboratório de Neurociências and [b]Laboratório de Transdução de Sinais, Centro de Biologia Celular, Universidade de Aveiro, Aveiro, Portugal

Key Words
Alzheimer's disease · Amyloid precursor protein · Green fluorescent protein fusion · Protein phosphorylation · Phosphorylation site mutants · Transfection

Abstract
The occurrence of consensus phosphorylation sites in the intracellular domain of the Alzheimer's amyloid precursor protein (APP), coupled with observations of their in vivo phosphorylation, prompted several workers to investigate the effects that phosphorylation of such sites could have on APP metabolism and subsequent Aβ production. However, hitherto all attempts to dissect the role played by such phosphorylation events failed to reveal substantial effects. Having decided to revisit this problem, our new approach was based on the following vectors: (1) site-directed mutagenesis of the target amino acids to mimic a specific phosphorylation state, (2) expression of wild-type and mutant APP-GFP (green fluorescent protein) fusion proteins for ease of visualization, (3) controlled low level expression to avoid 'flooding' cellular pathways, and (4) the use of cycloheximide to inhibit de novo protein synthesis. Using this method we were able to detect specific differences in APP processing that were correlated with the mimicked phosphorylation state of several phosphorylation sites. New combined methodologies, like the one described here, allow for the detailed analysis of key control points in the cellular metabolism of specific proteins that are central to neurodegenerative diseases and may be under the control of specific posttranslational modifications, such as reversible phosphorylation.

Introduction

The amyloid cascade of Alzheimer's disease is widely accepted as a hypothesis of the molecular basis of this complex multifactorial neurodegenerative disorder [1]. In essence, the theory defends that one of the most important steps in the disease onset and/or development involves the formation and deposition of characteristic cerebral amyloid plaques, whose main constituent is a 4-kD toxic peptide termed Aβ [2, 3]. In fact, Aβ appears to comprise a heterogeneous mixture of peptides ranging in size from 38 to 44 amino acids. These peptides arise from sequential proteolytic cleavages of the Alzheimer's amyloid precursor protein (APP). This large and ubiquitous protein can exist in various alternatively spliced isoforms [4, 5]. Although the specific functions of each isoform have not been fully elucidated, of the various known splice variants, APP_{695} (comprising 695 amino acids) is typically referred to as the neuronal isoform, being relatively abundant in the brain [4, 5]. APP can be processed via the secretory pathway, travel-

KARGER
Fax + 41 61 306 12 34
E-Mail karger@karger.ch
www.karger.com

1660–2854/04/0015–0196$21.00/0

Accessible online at:
www.karger.com/ndd

Odete A.B. da Cruz e Silva
Centro de Biologia Celular
Universidade de Aveiro
PT–3810-193 Aveiro (Portugal)
Tel. +351 234 370 778, Fax +351 234 426 408, E-Mail odetecs@bio.ua.pt

ing sequentially from the endoplasmic reticulum (ER), through the Golgi network, to the cell surface. It is N-glycosylated [6] and subsequently matures through O-glycosylation upon being transported through the Golgi complex [7]. Once inserted into post-trans Golgi network (post-TGN) secretory vesicles, APP travels to the plasma membrane where it can be cleaved and secreted, or undergoes endocytosis to be recycled or degraded [for review see 8]. Subcellular localization studies indicate that most APP resides in the Golgi complex [9], and in neuronal cells it can also be transported from the cell body down axons by fast axonal transport [10, 11].

APP molecules are cleaved during intracellular trafficking, producing various cleavage products, including secreted APP (sAPP), which is released into the medium of cells in culture, and Aβ [12–14]. A small proportion of Aβ peptides are generated in the ER [15], but the majority is thought to be generated in the Golgi complex [16], packaged into post-TGN vesicles and then secreted extracellularly. Adding to the complexity of Aβ production, this toxic peptide can also be produced following APP endocytosis from the cell membrane [17].

During the last decade various studies have addressed APP expression, processing and subcellular localization in an attempt to identify factors affecting APP cellular metabolic pathways and to subsequently modulate the rate of Aβ production. Studies have included RT-PCR [18], phosphorylation site mutants [19], in situ hybridization [4], immunocytochemistry [9] and subcellular fractionation [20]. Although extremely informative, such approaches are mostly nondynamic analytical methods that may be insufficient to address alternative APP-processing pathways. Clearly, new approaches are needed to further refine our understanding of APP trafficking, particularly with regard to signal transduction. Recently, Pimpl and Denecke [21] underlined the importance of recent developments in the field of vital fluorescence imaging enabling quantitative protein transport assays and allowing the implementation of in vivo approaches. Indeed, the combination of several methods can be used to unravel protein traffic kinetics and protein interactions. The use of fluorescently tagged proteins, like GFP (green fluorescent protein) translational fusions, provides an extremely powerful tool to address specific protein-trafficking questions. Since protein processing via the secretory pathway involves protein-protein interactions, the introduction of specific alterations in the functional domains of APP may allow us to address the role of the mutated residues in the protein's traffic. Furthermore, protein-protein interactions are highly regulated by protein phosphorylation systems, e.g. binding of APP to the adaptor protein Fe65 [22]. Protein phosphorylation-dependent processing of APP has been demonstrated by several groups [22–25]. The production of APP fragments (among them sAPP and Aβ) appears to be regulated by direct or indirect protein phosphorylation, given that both phorbol esters and protein phosphatase inhibitors significantly increase sAPP secretion and decrease Aβ production [24, 26–29]. Nonetheless, the precise role of protein phosphorylation in APP processing remains to be elucidated. In this paper we describe the development of a dynamic system using a combination of molecular biology, fluorescence imaging, cell culture and biochemical techniques to monitor APP trafficking and to evaluate the effects of mutating potential phosphorylation sites and the modulation of specific signaling pathways.

Methods

APP-GFP Fusion Constructs

Point mutations were introduced in specific serine, threonine or tyrosine residues on the APP cytoplasmic domain using site-directed mutagenesis, as previously described [26]. Mutations were introduced into all three signaling domains known to be phosphorylated on the cytoplasmic domain of APP [30]. Serine and threonine residues were mutated to mimic a constitutively phosphorylated site (Glu) or a constitutively dephosphorylated site (Ala), whereas tyrosine residues were mutated to Glu or Phe, respectively [31]. Both wild-type and mutated APP cDNAs were fused in frame with GFP in the pEGFP mammalian expression vector (Clontech, USA) using standard molecular biology techniques. Briefly, APP cDNAs were amplified by polymerase chain reaction using specifically designed primers that removed the stop codon and introduced appropriate restriction sites for ligation into the pEGFP expression vector. All constructs were verified by DNA sequencing to ensure that GFP was fused C-terminally to the APP-coding region and that the required mutations were present.

Cell Culture and Recombinant APP Expression

Monkey kidney COS-7 cells were grown in Dulbecco's modified Eagle's medium (DMEM) supplemented with 10% fetal bovine serum at 37 °C and in an atmosphere of 5% CO_2/95% air. Cells were normally grown in 100-mm plates at subconfluent conditions before transfection. Cell transfections with both wild-type and mutant APPGFP expression constructs were performed using the LipofectAMINE 2000 (Invitrogen Life Technologies) cationic lipidic transporter. After 8 h, cells were divided into six-well plates with (trafficking studies) or without (processing studies) coverslips pretreated with 100 mg/ml poly-ornithine, and allowed to recover for a 4-hour period. For our experimental model, cells were incubated in serum-free DMEM supplemented with 50 mg/ml cycloheximide (Sigma) to inhibit de novo protein synthesis. At the indicated times, cultures were either fixed in 4% paraformaldehyde (trafficking studies) or collected as described below (processing studies). The concentration of cycloheximide to be used in the experimental model was assessed in a pilot experiment. Cycloheximide at different concentrations (15–100 mg/ml) was added to cul-

tured cells and after 1 h the levels of intracellular APP were determined by immunoblot analysis, as described below.

Monitoring Intracellular APP-GFP Trafficking by Fluorescence Microscopy

After fixation, coverslips were observed using an Olympus IX-81 inverted epifluorescence microscope. Transfected cells were easily identified by the expression of GFP-tagged APP. Cell populations (120 cells/coverslip) were monitored for the presence or absence of fluorescence in specific subcellular compartments, such as the ER, Golgi apparatus, cytoplasmic vesicles, plasma membrane or nucleus. In order to verify the correct identification of the subcellular structures, antibodies against specific marker proteins were used for colocalization studies. For example, anti-calnexin antibodies (Stressgen) were used to mark the ER and anti-syntaxin 6 antibodies (BD Transduction Laboratories) to mark the Golgi network. Subsequent immunodetection was carried out using Texas Red-linked secondary antibodies (Molecular Probes).

Immunoblot Analysis of APP and APP-GFP Processing

In parallel with the protein trafficking assays, the processing of APP-GFP fusion proteins (both wild-type and phosphomutants) was also analyzed by immunobloting. At the specified time points, both cells and conditioned medium were harvested into 1% SDS and processed as previously reported [32]. Holo-APP was detected by immunoblotting with the anti-APP N-terminal 22C11 antibody (Roche), followed by incubation with a horseradish peroxidase-linked secondary antibody and detection by enhanced chemiluminescence (Amersham Pharmacia). Quantitative analysis of specific immunoreactive proteins was carried out [33] by densitometric analysis of the autoradiograms using Quantity One software (BioRad).

In order to analyze the expression of the different APP isoforms several peripheral tissues and brain regions were dissected, homogenized in 1% SDS and APP expression was assessed by immunoblotting using the 22C11 antibody. Various cell lines were also tested for APP expression.

Results

Constitutive phosphorylation of serine, threonine and tyrosine residues can be simulated by mutating those amino acids to glutamate, whereas their constitutive dephosphorylated state can be mimicked by alanine (for serine and threonine) or phenylalanine (for tyrosine). Serine, threonine and tyrosine are amino acids with hydroxyl groups that can be phosphorylated by protein kinases, yielding negatively charged phosphoryl groups (fig. 1). Glutamate and aspartate are nonphosphorylatable amino acids with a carboxylic group whose negative charge and size mimic the presence of the phosphate-negative charge in a phosphorylated amino acid. Alanine and phenylalanine are nonphosphorylatable (lacking the phosphorylatable hydroxyl group) and nonpolar residues that are similar in size to serine/threonine and tyrosine amino acid residues, respectively.

The power of designing specific single or multiple amino acid substitutions in the cytoplasmic domain of APP by site-directed mutagenesis was further extended and refined, by subsequently tagging wild-type and mutant APP with GFP, in order to allow their intracellular localization to be easily tracked. Besides wild-type APP-GFP, several mutant constructs were prepared in the expression vector pEGFP (fig. 2, table 1). Constitutive phosphorylation of Ser655, Thr668, Tyr682 and Tyr687 was mimicked by mutating each to glutamic acid. All expression constructs used the APP_{695} isoform, which is commonly referred to as the neuronal isoform owing to its relative abundance in brain. In fact, immunoblot analysis of both peripheral tissues and brain regions, and a comparison of nonneuronal cell lines to cells with neuronal characteristics confirmed this assertion (fig. 3). COS-7 cells were chosen for subsequent use since they expressed low levels of the APP_{695} isoform, can be easily and efficiently transfected and have already been used previously for APP-processing studies.

Another aspect essential to the success of our model involved optimizing the transfection in order to maintain relatively low levels of recombinant APP expression. The model relies on expressing recombinant APP and endogenous APP at similar levels, thus avoiding overexpression of transfected APP that could result in the saturation of normal cellular pathways. Preliminary studies indicated that since not all constructs exhibited similar transfection efficiencies, the amounts of recombinant APPGFP produced needed to be assessed for each by immunoblot analysis. Since they are relatively easy to transfect and usually exhibit robust expression of recombinant proteins, COS-7 cells were transfected to produce low levels of protein expression. Using the manufacturer's recommended conditions excessively high transfection levels were achieved. Therefore, the amount of recombinant plasmid DNA used in the transfection mixture was reduced to tightly control the production of recombinant protein. Hence, APP-GFP expression levels similar to endogenous APP levels were obtained (fig. 3). In this respect, the B103 cell line may also represent a potentially interesting model. Although previously described as not expressing detectable APP [34, 35], our results clearly indicate that this cell line expresses basal amounts of APP that, although lower than for COS-7 cells, can nonetheless be easily detected (fig. 3d). Quantitative analysis indicated that basal APP levels in B103 are approximately 25% that of COS-7 cells.

Also critical to the methodology developed was that de novo protein synthesis was inhibited by the addition of

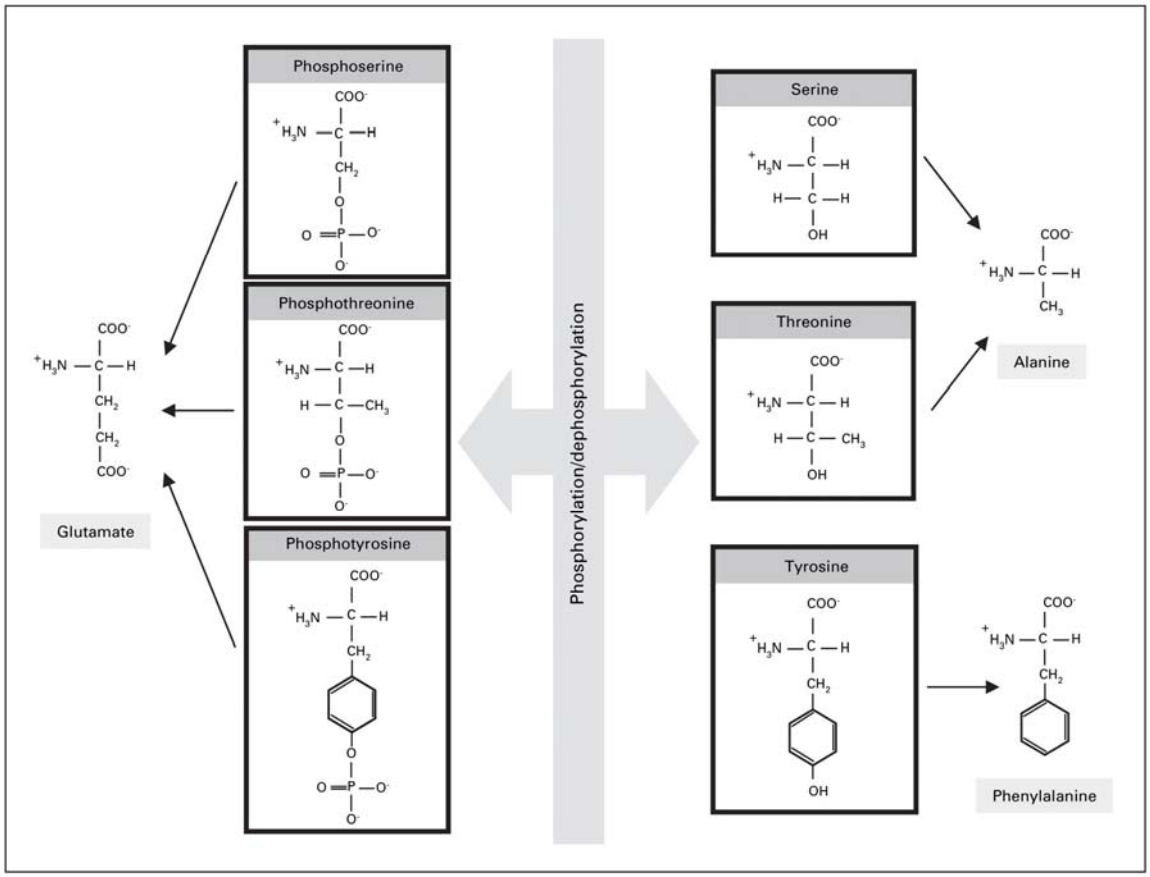

Fig. 1. Comparison of phospho- and dephosphoamino acid structures with their corresponding mutants. Phosphorylated and dephosphorylated serine, threonine and tyrosine residues are shown in boxes. Phosphorylation is catalyzed by protein kinases, whereas dephosphorylation is catalyzed by protein phosphatases. The thin arrows indicate how each amino acid compares with its structural mimic. All mutations were performed by site-directed mutagenesis and confirmed by DNA sequence analysis.

cycloheximide to the culture medium and APP trafficking/degradation was monitored and compared over time. Cycloheximide reversibly inhibits protein synthesis by blocking mRNA translation at the level of polypeptide translocation, without affecting the cellular constitutive secretory pathway, at the concentration and incubation times used [36]. The concentration of cycloheximide chosen for the experimental model was 50 mg/ml, since this concentration produced 60 and 80% decreases in immunodetectable intracellular APP at 1 and 3 h (fig. 4, 5a, c), respectively.

Wild-type APP_{695}-GFP fusion protein appears to be processed and degraded in approximately 4 h (data not shown) and to follow the expected cellular secretory pathway [9]. Thus, APP-GFP fluorescence was first detected in the ER with a typical perinuclear distribution (fig. 5a, 1 h), traveled to and through the Golgi complex as it matured (fig. 5a, 1:00–3:00 h), and was subsequently found in cytoplasmic vesicles (e.g. Golgi secretory vesicles) and the plasma membrane (fig. 5a, 3:00 h). Subcellular localizations were confirmed by colocalization studies with several markers, in particular calnexin and syntaxin 6 which label

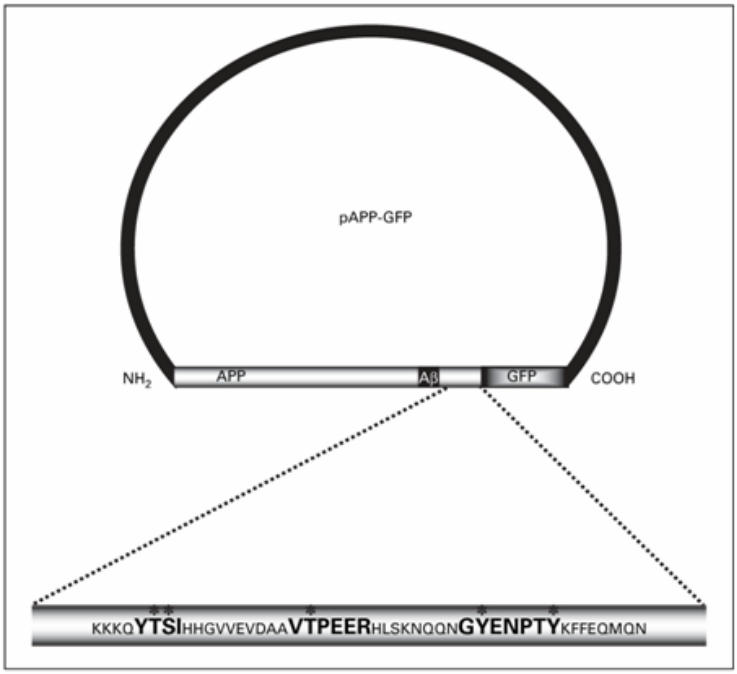

Fig. 2. APP-GFP expression vectors. APP_{695} wild-type and mutant cDNAs were subcloned into pEGFP to produce the corresponding pAPP-GFP expression vectors. APP and GFP are expressed as in-frame fusion proteins, as shown. The amino acid sequence of the cytoplasmic domain of APP is enlarged below, with the putative phosphorylation sites indicated by asterisks within the three signal transduction domains (larger font in bold). The approximate location of the Aβ sequence is indicated by a black box.

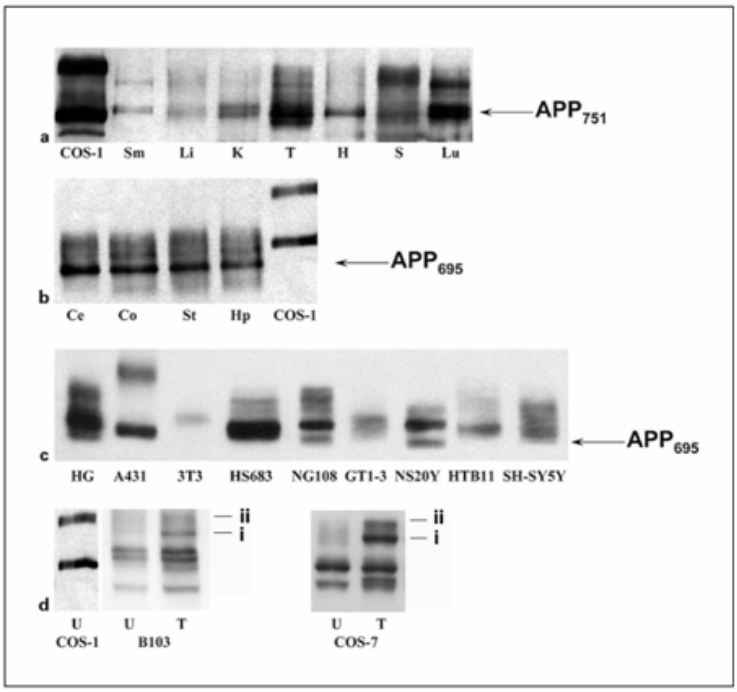

Fig. 3. Comparison of APP expression in different cell lines and tissues. The expression and relative abundance of the different APP isoforms in different tissues and cell lines was assessed by immunoblot analysis (**a**–**d**). **a** Peripheral tissues. Sm = Skeletal muscle; Li = liver; K = kidney; T = testis; H = heart; S = spleen; Lu = lung. **b** Brain regions. Ce = Cerebellum; Co = cortex; St = striatum; Hp = hippocampus. **a**, **b** COS-1 cells are included for comparative purposes. **c** Untransfected cells, including both nonneuronal cell lines (A431, 3T3) and cell lines with neuronal characteristics (HS683, NG108, GT1–3, NS20Y, HTB11, SH-SY5Y). Human grey matter (HG) was included for comparison. **d** Comparison of APP expression in untransfected (U) and wild-type pAPP-GFP-transfected (T) nonneuronal COS-1 and COS-7 cells, and neuronal B103 cells. For immunoblot analysis 30 µg of total protein was used for the different tissues or cell lysates (**a**–**c**), whereas 20 µg of total protein were used for COS-1 and COS-7 cells, and 50 µg of total protein were loaded for B103 cells (**d**). Arrows indicate the migration of the indicated APP isoforms and i and ii indicate transfected APP_{695}-GFP in its immature and mature forms, respectively.

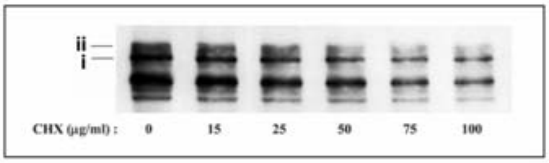

Fig. 4. Effect of increasing cycloheximide concentration on basal APP expression. COS-7 cells were transfected with wild-type pAPP-GFP and treated with increasing concentrations of cycloheximide (CHX). Cells were collected for immunoblot analysis after 1 h and APP expression was analyzed with the 22C11 antibody. Intact remaining APP was assessed by quantitative densitometric analysis of the blot. i and ii transfected APP-GFP in its immature and mature forms, respectively.

Table 1. List of APP phosphorylation site mutants under study

Target amino acid	Constitutive phosphomutant	Constitutive dephosphomutant
Serine 655	S655E	S655A
Threonine 668	T668E	T668A
Tyrosine 682	Y682E	Y682F
Tyrosine 687	Y687E	Y687F

Amino acid numbering according to APP_{695} isoform.

the ER and TGN, respectively (fig. 5b). Corresponding studies monitoring intracellular and sAPP revealed that wild-type APP-GFP matured and was secreted in a similar manner to endogenous APP (fig. 5c).

Interesting differences between the intracellular trafficking kinetics of wild-type and phosphomutant APP proteins could be observed (fig. 6). Data thus far obtained has elucidated that specific mutations have a direct effect on intracellular APP targeting and its subsequent processing. For example, mimicking constitutive phosphorylation of residues Ser655, Tyr682 and Tyr687 resulted in clear differences in the efficiency of APP incorporation into cytoplasmic vesicles. Whereas the incorporation of the S655E mutant into vesicles was similar to wild-type APP, the Y682E and Y687E mutants were largely absent from cytoplasmic vesicles. Interestingly, constitutive dephosphorylation of the Tyr682 site (Y682F) appears to result in retention of APP in the Golgi (fig. 6). Further experiments are under way to allow a detailed comparison of the processing not only of the mutants described above (table 1), but also of specific double mutants and deletion mutants.

Discussion

Recent work from our laboratory has been successful in developing a model system directed at unraveling phosphorylation-dependent APP processing. Prerequisites for studies aimed at clarifying the functional impact of the phosphorylation of specific amino acids necessitate quantitative and stable modification of the target residues. Thus, mimicking constitutive phosphorylation/dephosphorylation allows the in vivo and in vitro evaluation of the functional impact of phosphorylating specific amino acids, without the potential interference of cellular phosphatase and/or kinase activities that may act upon those sites [31]. The inclusion of cycloheximide was particularly useful since it dramatically reduced the background of fluorescent fusion proteins being continuously synthesized. In its presence, since de novo protein synthesis was considerably inhibited, the previously synthesized APP-GFP population was preferentially detected and followed. This drug has been used previously to study the importance of specific posttranslational protein modifications, such as prenylation [37], and the role of protein synthesis in apoptosis [38], gene expression [39] and steroidogenesis [40]. The data presented here were obtained using COS-7 cells, as justified in the Results section. However, for subsequent experimentation, neuronal B103 cells are also being used, given that they express low levels of APP and provide an attractive model for studying neuronal systems.

The methodology established consisted of the combined usage of site-directed mutagenesis, in-frame fusion with a reporter gene (GFP) in a mammalian expression vector, mammalian cell culture techniques coupled with controlled transfection and expression levels, and inhibition of 'de novo' protein synthesis, thus allowing the monitoring of an APP protein pool in a time-dependent manner by means of fluorescence microscopy and immunoblot analysis (fig. 5). The results obtained (fig. 6) indicate that this new methodology represents an attractive model to study APP metabolism, including not only the tracking of its subcellular localization, traffic and rates of processing and degradation, but also to test the subcellular effects of direct APP phosphorylation.

The usefulness of our model system was entirely validated by the results obtained, since the wild type and the different mutants of the same residue were processed differently with time (fig. 6). Our results lend support to the notion that the phosphorylation state of specific amino acids in the intracellular domain of APP are of paramount importance in deciding its processing and metabolic fate. That is, the exact processing of APP is dependent on the

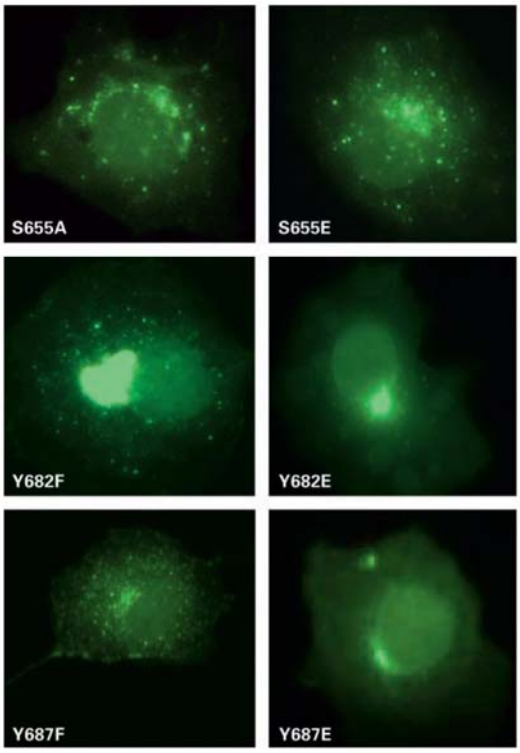

Fig. 6. Comparison of the subcellular localization of different APP-GFP mutants. Representative APP-GFP cell fluorescence distribution patterns for different phosphorylation site mutants after a 3-hour incubation period with cycloheximide. The putative effects of both constitutive phosphorylation (S655E, Y682E and Y687E) and dephosphorylation (S655A, Y682F and Y687F) are clearly observed.

phosphorylation and dephosphorylation of APP itself. The model thus developed not only represents a powerful tool in the study of intracellular protein trafficking, but also provides a useful method for studying the role that some amino acid residues and/or specific posttranslational modifications may have in a protein's intracellular fate. A significantly novel aspect to the method described is provided by the fact that we can mimic a constitutively phosphorylated or dephosphorylated residue and thus dramatically affect APP trafficking. For example, the Y682F mutant is clearly retained in the Golgi, whereas the Y682E mutant is not. This then points to the importance of Y682 phosphorylation for the exit of APP from the Golgi. Additionally, preliminary analysis of the results obtained with the different APP phosphomutants indicates that direct APP phosphorylation may also be important for e.g. incorporation of APP into vesicles. Thus, the overriding aspect is not whether or not a residue is mutated, but rather whether the mutation is mimicking a constitutively phosphorylated or dephosphorylated state. More detailed studies are currently under way to unravel the exact physiological importance of the phosphorylation of the target amino acids in the signaling domains identified within the cytoplasmic tail of APP (fig. 2, table 1), including the production of Aβ itself.

By comparative analysis of the characteristics and relative kinetics of wild-type and mutant proteins, it is possible to unravel the absolute and relative importance of specific amino acid residues, protein domains, or protein interactions, in its targeting and/or in the mechanism itself of protein translocation over the different subcellular compartments towards its final destination within the cell. Of particular note are the recent findings that APP binds to several other proteins which effectively affect its fate. In fact, complex formation is a critical step in signal transduction systems and is highly regulated by protein phosphorylation [30]. Several binding proteins are common in the processing and metabolism of target proteins. The model described here is potentially useful to study different proteins, among them proteins involved in other neurodegenerative disorders. Both Alzheimer's disease and other neurodegenerative disorders are associated with dysfunctional signal transduction pathways and abnormal protein phosphorylation. Hence, it is not surprising to find that signal transduction therapeutics is a rapidly expanding field, potentially providing novel therapeutic strategies for a variety of dysfunctional conditions.

Acknowledgments

We would like to thank L. Mucke (Gladstone Institute of Neurological Disease, University of California, San Francisco, Calif., USA) for his kind gift of the B103 cell line.

This work was supported by grants to O.A.B.C.S. from the Fundação para a Ciência e Tecnologia of the Portuguese Ministry of Science and Higher Education (POCTI/NSE/33520/1999 and POCTI/BCI/34349/1999) and by the 5th Framework Program of the European Union (Project DIADEM, QLK3-CT-2001-02362). S.I.V. and S.R. were recipients of PhD fellowships from Fundação para a Ciência e Tecnologia (PRAXIS XXI/BD/16218/98) and from the Instituto de Investigação of the Universidade de Aveiro, respectively.

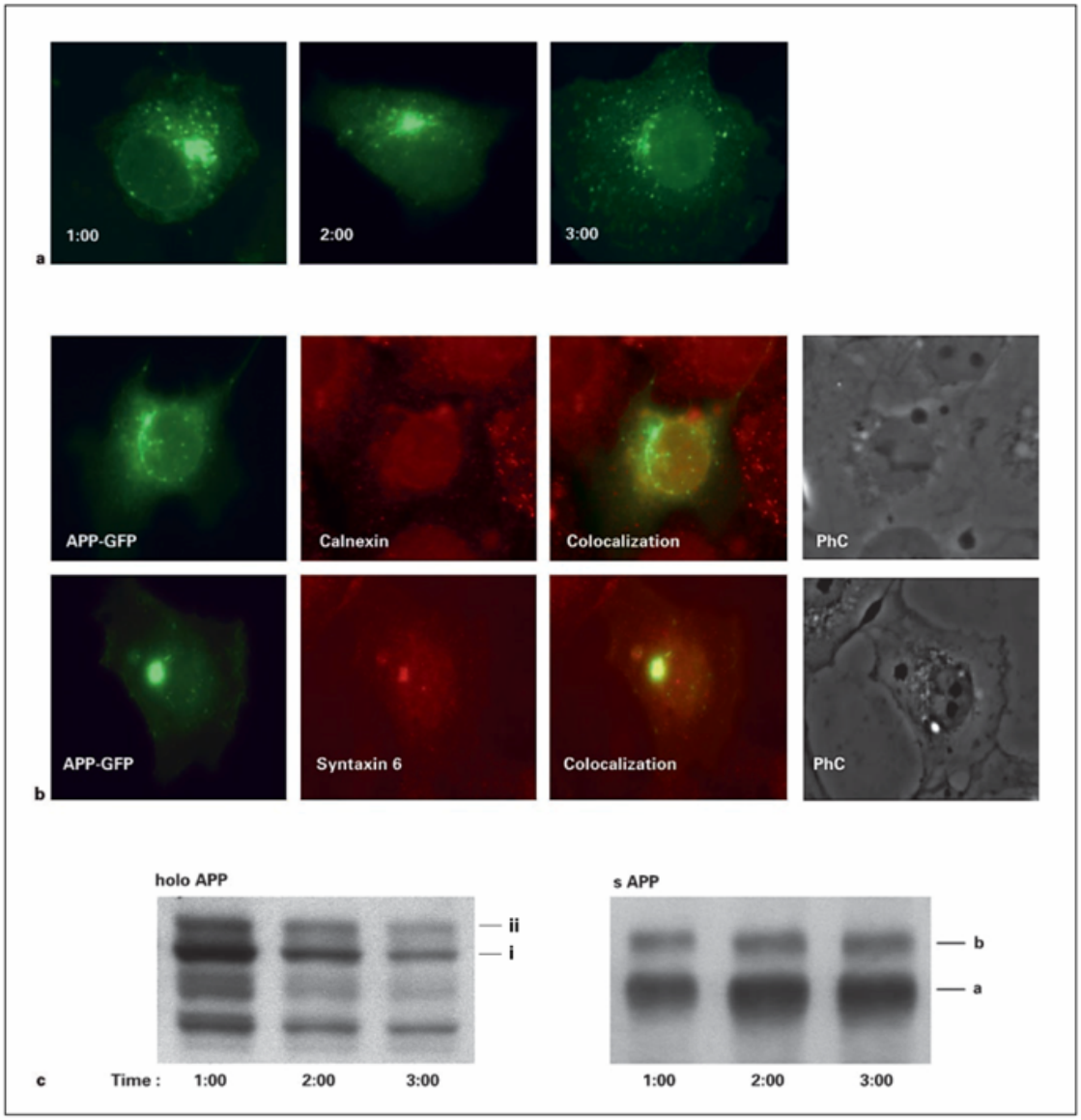

Fig. 5. Fluorescence microscopy analysis of wild-type APP-GFP trafficking in COS-7 cells. **a** Representative wild-type APP-GFP fluorescence distribution pattern detected after 1, 2 and 3 h in the presence of cycloheximide. **b** Colocalization analysis of APP-GFP fusion protein fluorescence and two subcellular compartment markers (calnexin for the ER and syntaxin 6 for the Golgi network) detected by immunocytochemistry with Texas Red-linked secondary antibodies. PhC = Phase contrast. **c** Immunoblot analysis with antibody 22C11 of the corresponding cell lysates and culture medium for holo-APP-GFP and sAPP, respectively. i and ii transfected APP-GFP in its immature and mature forms, respectively. Secreted sAPP accumulates in the medium: $sAPP_{695}$ mostly derived from transfected pAPP-GFP (a) and endogenous sAPP751/770 (b).

References

1 Hardy J, Selkoe DJ: The amyloid hypothesis of Alzheimer's disease: Progress and problems on the road to therapeutics. Science 2002;297: 353–356.

2 Lee VM-Y: Tauists and baptists united – well almost! Science 2001;293:1446–1447.

3 Maiorini AF, Gaunt MJ, Jacobsen TM, McKay AE, Waldman LD: Potential novel targets for Alzheimer pharmacotherapy. I. Secretases. J Clin Pharm Ther 2002;27:169–183.

4 Rockeinstein EM, McConlogue L, Tan H, Power M, Masliah E, Mucke L: Levels and alternative splicing of amyloid beta protein precursor (APP) transcripts in brains of APP transgenic mice and humans with Alzheimer's disease. J Biol Chem 1995;270:28257–28267.

5 Sandbrink R, Masters CL, Beyreuther K: APP gene family. Alternative splicing generates functionally related isoforms. Ann NY Acad Sci 1996;777:281–287.

6 Oltersdorf T, Ward PJ, Henriksson T, Beattie EC, Neve R, Lieberburg I, Fritz LC: The Alzheimer amyloid precursor protein. Identification of a stable intermediate in the biosynthetic/degradative pathway. J Biol Chem 1990; 265:4492–4497.

7 Griffith LS, Mathes M, Schmitz B: Beta-amyloid precursor protein is modified with O-linked N-acetylglucosamine. J Neurosci Res 1995;41:270–278.

8 Gouras GK: Current theories for the molecular and cellular pathogenesis of the Alzheimer's disease. Exp Rev Mol Med 2001;31:1–11.

9 Caporaso GL, Takei K, Gandy SE, Matteoli M, Mundigl O, Greengard P, De Camilli P: Morphologic and biochemical analysis of the intracellular trafficking of the Alzheimer beta/A4 amyloid precursor protein. J Neurosci 1994;14: 3122–3138.

10 McLaughlin M, Breen KC: Protein kinase C activation potentiates the rapid secretion of the amyloid precursor protein from rat cortical synaptosomes. J Neurochem 1999;72:273–281.

11 Stamer K, Vogel R, Thies E, Mandelkow E, Mandelkow EM: Tau blocks traffic of organelles, neurofilaments, and APP vesicles in neurons and enhances oxidative stress. J Cell Biol 2002;156:1051–1063.

12 Nitsch RM, Slack BE, Farber SA, Borghesani PR, Schulz JG, Kim C, Felder CC, Growdon JH, Wurtman RJ: Receptor-coupled amyloid precursor protein processing. Ann NY Acad Sci 1994;881:122–127.

13 Checler F: Processing of the β-amyloid precursor protein and its regulation in Alzheimer's disease. J Neurochem 1995;65:1431–1444.

14 Selkoe DJ, Yamazaki M, Citron M, Podlisny MB, Koo EH, Teplow DB, Haass C: The role of APP processing and trafficking pathways in the formation of amyloid β-protein. Ann NY Acad Sci 1996;777:57–64.

15 Cook DG, Forman MS, Sung JC, Leight S, Kolson DL, Iwatsubo T, Lee VM, Doms RW: Alzheimer's Abeta (1–42) is generated in the endoplasmic reticulum/intermediate compartment of NT2N cells. Nat Med 1997;3:1021–1023.

16 Greenfield JP, Tsai J, Gouras GK, Hai B, Thinakaran G, Checler F, Sisodia SS, Greengard P, Xu H: Endoplasmic reticulum and trans-Golgi network generate distinct populations of Alzheimer beta-amyloid peptides. Proc Natl Acad Sci USA 1999;96:742–747.

17 Pasternak SH, Callahan JW, Mahuran DJ: The role of the endosomal/lysosomal system in amyloid-beta production and the pathophysiology of Alzheimer's disease: Reexamining the spatial paradox from a lysosomal perspective. J Alzheimers Dis 2004;6:53–65.

18 Sandbrink R, Masters CL, Beyreuther K: APP gene family: Unique age-associated changes in splicing of Alzheimer's betaA4-amyloid protein precursor. Neurobiol Dis 1994;1:13–24.

19 Haass C, Koo EH, Capell A, Teplow DB, Selkoe DJ: Polarized sorting of beta-amyloid precursor protein and its proteolytic products in MDCK cells is regulated by two independent signals. J Cell Biol 1995;128:537–547.

20 Xia W, Zhang J, Ostaszewski BL, Kimberly WT, Seubert P, Koo EH, Shen J, Selkoe DJ: Presenilin 1 regulates the processing of beta-amyloid precursor protein C-terminal fragments and the generation of amyloid beta-protein in endoplasmic reticulum and Golgi. Biochemistry 1998;37:16465–16471.

21 Pimpl P, Denecke J: Protein-protein interactions in the secretory pathway, a growing demand for experimental approaches in vivo. Plant Mol Biol 2002;50:887–902.

22 Ando K, Iijima KI, Elliott JI, Kirino Y, Suzuki T: Phosphorylation-dependent regulation of the interaction of amyloid precursor protein with Fe65 affects the production of beta-amyloid. J Biol Chem 2001;276:40353–40361.

23 Gillespie SL, Golde TE, Younkin SG: Secretory processing of the Alzheimer amyloid β/A4 protein precursor is increased by protein phosphorylation. Biochem Biophys Res Commun 1992;187:1285–1290.

24 da Cruz e Silva EF, da Cruz e Silva OAB, Zaia CTBV, Greengard P: Inhibition of protein phosphatase 1 stimulates secretion of Alzheimer amyloid precursor protein. Mol Med 1995; 1:535–541.

25 da Cruz e Silva EF, Cruz e Silva OAB: Protein phosphorylation and APP metabolism. Neurochem Res 2003;28:1551–1559.

26 da Cruz e Silva OA, Iverfeldt K, Oltersdorf T, Sinha S, Lieberburg I, Ramabhadran TV, Suzuki T, Sisodia SS, Gandy S, Greengard P: Regulated cleavage of Alzheimer beta-amyloid precursor protein in the absence of the cytoplasmic tail. Neuroscience 1993;57:873–877.

27 Gandy SE, Caporaso GL, Buxbaum JD, da Cruz e Silva O, Iverfeldt K, Nordstedt C, Suzuki T, Czernik AJ, Nairn AC, Greengard P: Protein phosphorylation regulates utilization of processing pathways for Alzheimer beta-A4 amyloid precursor protein. Ann NY Acad Sci 1993;695:117–121.

28 Hung AY, Haass C, Nitsch RM, Qiu WQ, Citron M, Wurtman RJ, Growdon JH, Selkoe DJ: Activation of protein kinase C inhibits cellular production of the amyloid beta-protein. J Biol Chem 1993;268:22959–22962.

29 Jacobsen JS, Spruyt MA, Brown AM, Sahasrabudhe SR, Blume AJ, Vitek MP, Muenkel HA, Sonnenberg-Reines J: The release of Alzheimer's disease beta amyloid peptide is reduced by phorbol treatment. J Biol Chem 1994;269: 8376–8382.

30 da Cruz e Silva OAB, Fardilha M, Henriques AG, Rebelo S, Vieira S, da Cruz e Silva EF: Signal transduction therapeutics: Relevance for Alzheimer's disease. J Mol Neurosci 2004;23: 123–142.

31 Bibb JA, da Cruz e Silva EF: Identification of post-translational modification sites by site directed mutagenesis; in Hemmings HC Jr (ed): Regulatory Protein Modification. Neuromethods. Totowa, Humana Press, 1997, vol 30, pp 275–307.

32 Rebelo S, Henriques AG, da Cruz e Silva EF, da Cruz e Silva OAB: Effect of cell density on intracellular levels of the Alzheimer's amyloid precursor protein. J Neurosci Res 2004;76: 406–414.

33 Amador FC, Henriques AG, da Cruz e Silva OAB, da Cruz e Silva EF: Monitoring protein phosphatase 1 isoform levels as a marker for cellular stress. Neurotoxicol Teratol 2004;26: 387–395.

34 Schubert D, Behl C: The expression of amyloid β protein precursor protects nerve cells from β-amyloid and glutamate toxicity and alters their interaction with the extracellular matrix. Brain Res 1993;629:275–282.

35 Li HL, Roch JM, Sundsmo M, Otero D, Sisodia S, Thomas R, Saitoh T: Defective neurite extension is caused by a mutation in amyloid beta/A4 (A beta) protein precursor found in familial Alzheimer's disease. J Neurobiol 1997; 32:469–480.

36 Brion C, Miller SG, Moore HP: Regulated and constitutive secretion: Differential effects of protein synthesis arrest on transport of glycosaminoglycan chains to the two secretory pathways. J Biol Chem 1992;267:1477–1483.

37 Parat M-O, Fox P: Palmitoylation of caveolin-1 in endothelial cells is posttranslational but irreversible. J Biol Chem 2001;276:15776–15782.

38 Satoh T, Enokido Y, Kubo T, Yamada M, Hatanaka H: Oxygen toxicity induces apoptosis in neuronal cells. Cell Mol Neurobiol 1998; 18:649–666.

39 Lusska A, Wu L, Whitlock JP Jr: Superinduction of CYP1A1 transcription by cycloheximide. Role of the DNA binding site for the liganded Ah receptor. J Biol Chem 1992;267: 15146–15151.

40 Miller WL: Mitochondrial specificity of the early steps in steroidogenesis. J Steroid Biochem Mol Biol 1995;55:607–616.

MONITORING 'DE NOVO' APP SYNTHESIS BY TAKING ADVANTAGE OF THE REVERSIBLE EFFECT OF CYCLOHEXIMIDE

Sandra Rebelo[1], PhD, Sandra Isabel Vieira[1], PhD, Edgar F. da Cruz e Silva[2], PhD and Odete A. B. da Cruz e Silva[1], PhD

[1]Laboratório de Neurociências and [2]Laboratório de Transdução de Sinais, Centro de Biologia Celular, Universidade de Aveiro, Aveiro, Portugal

Corresponding Author:

Odete A. B. da Cruz e Silva

Laboratório de Neurociências,

Centro de Biologia Celular,

Secção Autónoma de Ciências da Saúde,

Universidade de Aveiro,

3810-193 Aveiro, Portugal

Tel: +351-234-370-778

Fax: +351-234-426-408

E-mail: odetecs@ua.pt

ABSTRACT

We previously described a dynamic model system to monitor a specific population of Alzheimer's Amyloid Precursor Protein (APP) involving the addition of cycloheximide (CHX) to cells in culture to block 'de novo' protein synthesis. Here we show that the addition of CHX is non-toxic and reversible. Removal of the drug allowed cells to reinitiate 'de novo' protein synthesis and permitted the monitoring of anterograde APP transport. In particular, we addressed targeting of APP via the secretory pathway. The consensus NPTY motif in APP, typically associated with endocytosis, was mutated to NPTF or NPTE to mimic a constitutively dephosphorylated or phosphorylated residue, respectively. Our data reveals that disrupting the NPTY domain of APP not only affects its endocytosis, as shown previously, but also its incorporation into vesicles budding from the TGN. Thus, CHX can be a useful tool to study both anterograde and retrograde 'in vivo' transport of APP and other proteins.

Keywords: APP-GFP, Cycloheximide, 'de novo' protein synthesis, monitoring, anterograde transport.

INTRODUCTION

Monitoring intracellular targeting and processing of the Alzheimer's Amyloid Precursor Protein (APP) is a challenging task, given the many pathways via which it is processed and the various stages at which protein cleavage can occur. Among its many functions, APP has been proposed to be a signal transduction molecule. This places it among a class of proteins which are cleaved to produce fragments that can mediate a process of regulated intramembrane proteolysis (RIP), with an important role in signaling cascades [1]. APP routing in the cell entails export from the TGN (Trans-Golgi network), via the secretory pathway, followed by insertion into the cell membrane. Subsequently, APP is endocytosed and can suffer several fates typical of this pathway. Once endocytosed, the toxic fragment Abeta can also de produced, an event of specific pathological interest. Both the anterograde and retrograde transport of APP are highly regulated events, with protein phosphorylation likely to play a significant modulatory role. For example, data from our laboratory (da Cruz e Silva, in preparation) and previous reports indicate that TGN budding is dependent on protein kinase C [2], as is the production of Abeta [3].

Although APP is itself a phosphoprotein, few events regarding APP processing have been shown to be governed by specific phosphorylations of APP itself. Thr^{668}, within the ^{667}VTPEER^{672} functional domain, has been shown to be important in determining binding of FE65 to APP in a phosphorylation state dependent manner [4]. Another important domain in the C-terminus of APP is ^{682}YENPTY^{687}, which comprises a typical internalization signal (NPTY) for membrane associated receptor proteins [5-7]. Both Tyr^{682} and Tyr^{687} are phosphorylated *in vivo*. APP is tyrosine phosphorylated in cells expressing a constitutively active form of the *Abl* protooncogene, a non-receptor tyrosine kinase similar to c-Src, which can form a stable complex with APP and FE65 [8]. Abl-dependent Tyr^{682} phosphorylation appears to involve the nerve growth factor receptor TrkA, to mediate APP membrane internalization and to result in reduced γ-secretase APP processing [6,7,9]. This phosphorylation may also mediate protein-protein

interactions [8,9]. Consequently, attention was drawn away from Tyr^{687}, although this residue was reported to be phosphorylated in brain samples from AD patients [10]. Further, this residue is important in mediating endocytosis and we have previously shown that the Y687E mutant, mimicking constitutive phosphorylation, produces significantly less Abeta [11,12].

In order to determine the role of Tyr^{687} phosphorylation on APP processing, a model system was developed taking advantage of cycloheximide (CHX) blocking of 'de novo' protein synthesis [13]. The protein was tagged with GFP and low levels of transfection permitted monitoring APP turnover as it disappeared from the cell. APP turnover is virtually complete 5 h after CHX addition. Hence we were able to address retrograde processing of APP. In order to analyze anterograde transport, we expanded the model by removing CHX from the cells in culture and following 'de novo' APP synthesis. We were able to determine that CHX, as used in this context, is not detrimental to the cell and that its effects are reversible. In essence, removal of CHX permits 'de novo' protein synthesis to resume and subsequently one is able to monitor intracellular protein targeting. The reversibility of this model is discussed, as is its application to unraveling APP trafficking, particularly its anterograde transport.

MATERIALS AND METHODS

Production of APP-GFP fusion constructs

The Tyr^{687} residue of APP_{695} was mutated by site directed mutagenesis to either glutamate or phenylalanine in order to mimic the phosphorylated and dephosphorylated state of the protein, respectively [13,14]. Both phosphorylation mimicking mutants and wild-type APP were fused with GFP by inserting into the pEGFP-N1 mammalian expression vector (Clontech), as previously described [11,12].

Maintenance and transfection of cell cultures

Monkey kidney COS-7 cells were grown in Dulbecco's Modified Eagle's Medium (DMEM), supplemented with 10% foetal bovine serum, 100 U/ml penicillin, 100 mg/ml streptomycin and 3.7 g/l $NaHCO_3$ at 37ºC and 5% CO_2, until 90% confluent [15]. Transient transfections were performed at 80%-90% cell confluency using LipofectAMINE 2000, a cationic lipid transporter (Invitrogen Life Technologies). After 8 hours (h), cells were divided into six-well plates with coverslips pre-treated with 100 µg/ml polyornithine (Sigma), and left to recover for 4 h.

Tracking 'de novo' synthesis of APP fusion constructs

Transfected cells were then incubated in serum-free DMEM supplemented with 50 µg/ml cycloheximide (Sigma) for five hours. Cycloheximide containing medium was then removed, cells were washed two times with PBS and then incubated at 37 ºC in DMEM supplemented with 10% foetal bovine serum for 1 h, 2 h, 3 h, 4 h and 5 h. At each time point the cells were washed three times with PBS and fixed in 4% paraformaldehyde. Following cell fixation and subsequent coverslip preparation, the subcellular localization of APP was directly observed by fluorescence microscopy using an Olympus IX-81 inverted epifluorescence microscope. Cells were analysed for the

presence or absence of fluorescence in specific subcellular organelles. Subcellular structures were confirmed using specific markers. Calnexin was used as an ER marker (the 2h30 time point is shown as an example).

RESULTS

Our previously described model allowed for the monitoring of phospohorylation-dependent APP trafficking and processing [13]. Briefly, first we mimic the phosphorylation and dephosphorylation of APP target residues, allowing the evaluation of the functional impact of phosphorylation of those residues. Secondly, the constructs were fused in-frame with a reporter gene (GFP) in a mammalian expression vector, and used to achieve low level transient transfections. Finally, the addition of cycloheximide was particularly useful since it dramatically reduces the background of APP-GFP molecules being continuously synthesized. In essence, 'de novo' synthesis of APP-GFP was blocked and previously synthesized molecules were detected and followed over a period of time (Fig. 1). After 5 hours of incubation with cycloheximide, APP-GFP turnover was complete and inhibited from further processing given the absence of 'de novo' protein synthesis. Thus, by using this approach we were able to determine the importance of Tyrosine 687 on APP-GFP turnover rate, intracellular trafficking, processing and particularly endocytosis and Abeta production [11,12]. Hence, the retrograde transport of APP was monitored. Removal of CHX, on the other hand, should allow the study of the anterograde transport of APP (Fig. 1).

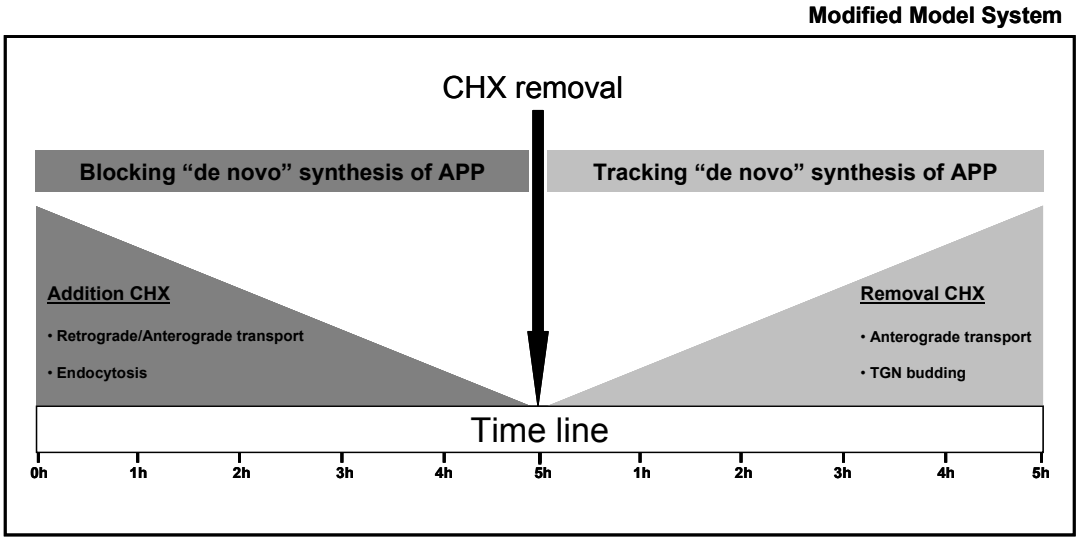

Figure 1. Modified model system. Schematic representation of the modified model system. The vertical arrow indicates the time point when cycloheximide (CHX) was removed.

"De novo" protein synthesis was blocked by adding 50 μg/ml CHX for 5 hours. After that period, the CHX was removed and fresh medium without CHX was added, and the cells were allowed to resume 'de novo' protein synthesis (Figs. 1 and 2). Thus, transiently transfected COS-7 cells were observed at 1 h, 2 h, 3 h, 4 h and 5h following CHX removal and analysed for the presence or absence of fluorescence in specific subcellular organelles. At time 0 h no fluorescence was observed. A representative example at each time point both for Wt-APP and the phosphorylation mimicking mutants (Y687E and Y687F) is presented in Figure 2.

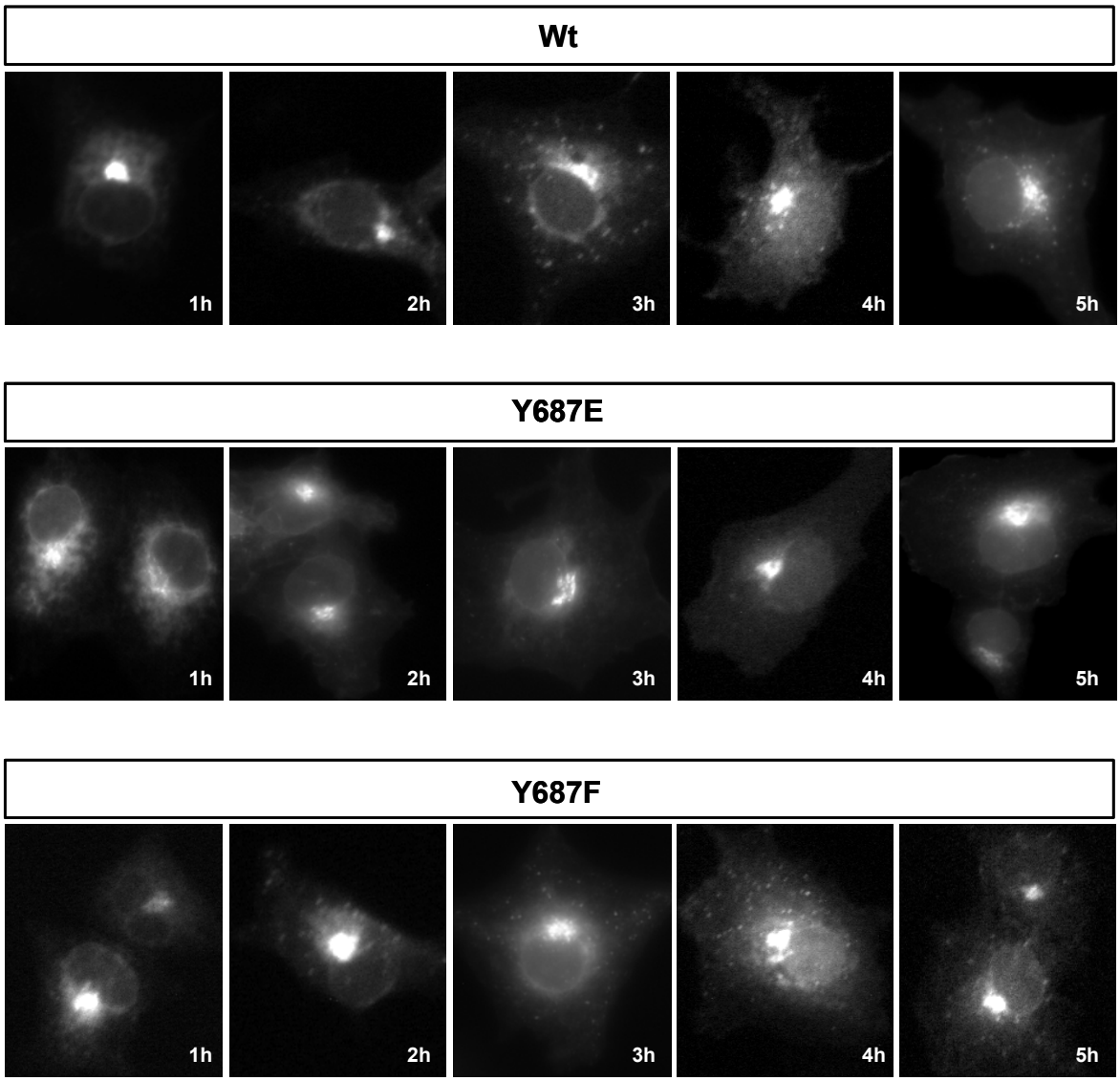

Figure 2. Wild-type and mutant (Y687E and Y687F) APP-GFP intracellular protein trafficking. Representative epifluorescence microphotographs of transiently transfected COS-7 cells at specific time points after CHX removal.

One hour after CHX removal we observed that APP-GFP is already being abundantly 'de novo' synthesized. Indeed, it is already detected in the ER and Golgi for wild-type, as well as for the two APP phosphomutants (Fig. 2, 1 h). At the 2h time point, it is evident that Wt-APP is already being incorporated into cytoplasmic vesicles and clearly reaches the plasma membrane by 3 h (Fig. 2). The nucleus is visible one hour later (Fig. 2, 4 h) and is clearer by the end of the experiment (Fig. 2, 5 h). The Y687E-APP mutant was also abundantly expressed after one hour of CHX removal. The protein, similar to Wt, could be detected in the ER and Golgi (Fig. 2, 1 h). However, some differences between the wild-APP and Y687E-APP mutant were already evident one hour later (2 h), since few cytoplasmic vesicles are visible with this mutant. Additionally, the plasma membrane is already detected in some cells (Fig. 2, 2 h). At the 3 h time point once again few cytoplasmic vesicles are present when compared with Wt-APP, and the plasma membrane seems to be more intensely marked for the phosphorylation mimicking mutant (Y687E-APP). During the last two time points the cytoplasmic vesicles as well as the nucleus are well visible (Fig. 2, 4 h and 5 h). Contrasting effects were obtained when monitoring 'de novo' protein synthesis of the dephosphorylation mimicking mutant (Y687F-APP). As with Wt, one hour after CHX removal, localization in ER and Golgi was clearly evident. Moreover, the Y687F-APP protein trafficking was very similar to Wt-APP at all time points. There was only a slight difference between them at the 2 h time point, since the Y687F-APP mutant was already visible in the plasma membrane of some cells. Hence, the two phosphorylation state mimicking mutants behaved differently and exhibited different distribution patterns.

Co-localization studies were validated with several markers, in particular calnexin which labels the endoplasmic reticulum. An example of co-localization with the Y687E-APP phosphorylation mimicking mutant is presented in Figure 3. As mentioned above, the Y687E-APP mutant does not produce clearly visible vesicles. In fact, it exhibits strong localization to the ER throughout the experiment. In conclusion, the reversible use of CHX permitted monitoring anterograde APP transport and unravelled the importance of residue Y687 in this process.

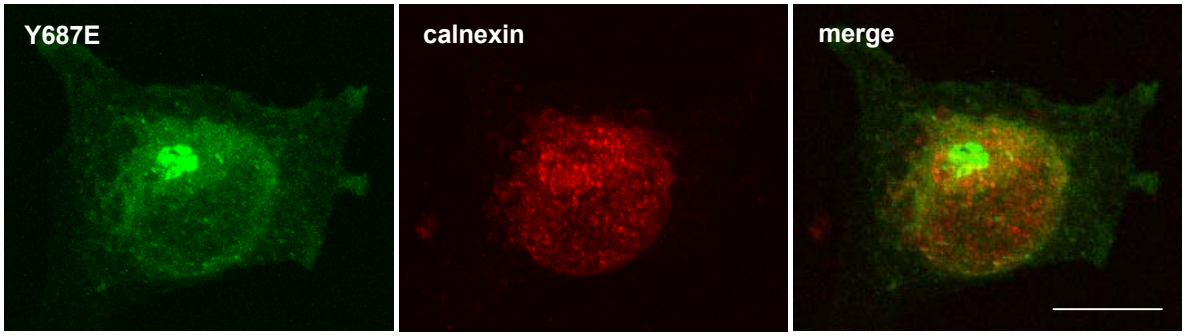

Figure 3. Y687E-APP-GFP co-localization with calnexin. COS-7 cells transfected with the phosphorylation mimicking mutant (Y687E-APP), were fixed and processed for immunocytochemical analysis using a specific antibody to detect endogenous calnexin (an endoplasmic reticulum marker). Bar, 10 μm.

DISCUSSION

Addressing a specific population of proteins is an important approach to study protein turnover. Methionine labeling is often used and certainly provides useful data. Here we present an alternative method which is non-radioactive, reversible and permits the study of anterograde and retrograde processing. In previous experiments [11,12] we used CHX, thus inhibiting 'de novo' protein synthesis and enabling protein turnover to be monitored, in particular endocytosis and subsequent targeting, such as to the TGN or the nucleus (Vieira, in preparation). By 5 hours, fluorescent APP protein is completely absent from the cell [13]. Thus, at this time point we removed the CHX, allowing 'de novo' synthesis of APP to reinitiate. The CHX inhibition of protein synthesis was reversible and cells were able to resume 'de novo' protein synthesis. The Y687E-APP mutant consistently failed to be incorporated into cytoplasmic vesicles under both conditions (in the presence and absence of CHX). Other aspects of transport of this mutant were also confirmed. Namely, the Y687E-APP mutant was still transported to the cell membrane, even in the absence of visible vesicles. Delivery of the Y687E-APP mutant protein to the cell membrane might be supported by the ER, consistent with previous findings by other authors [16].

Considering the data thus far obtained with the Tyr^{687} mutants, it is possible to propose a model of phosphorylation-dependent APP targeting in the cell (Fig. 4). Central to the development of this model was the observation that Y687E-APP and Y687F-APP exhibited contrasting behaviours, particularly with respect to TGN budding, as described above, and endocytosis [11,12]. In fact, Y687F-APP apparently incorporates more efficiently into vesicular structures than Wt-APP. The fact that the mutants behave so differently supports our hypothesis that phosphorylation of this key residue may in fact be a central regulatory event. In the model shown in Figure 4, we indicate subcellular structures abundant in both the dephosphorylation and phosphorylation mimicking mutants (black and white, respectively), and those where only the

dephosphorylation mimicking mutant was preferentially detected (black only). Hence, it would appear that APP needs to be dephosphorylated at Tyr^{687} in order to be incorporated into vesicular structures, both at the TGN and during endocytosis (Fig. 4). These are two critical sites for Abeta production [6,17-19] and this may explain why the dephosphorylation mimicking mutant produces less Abeta, as previously described [12]. APP export is likely to be mediated by multimeric complexes, the formation of which being probably regulated by phosphorylation. Such an example has already been described for FE65 binding to APP, which is modulated by phosphorylation of APP at Thr^{668} [4].

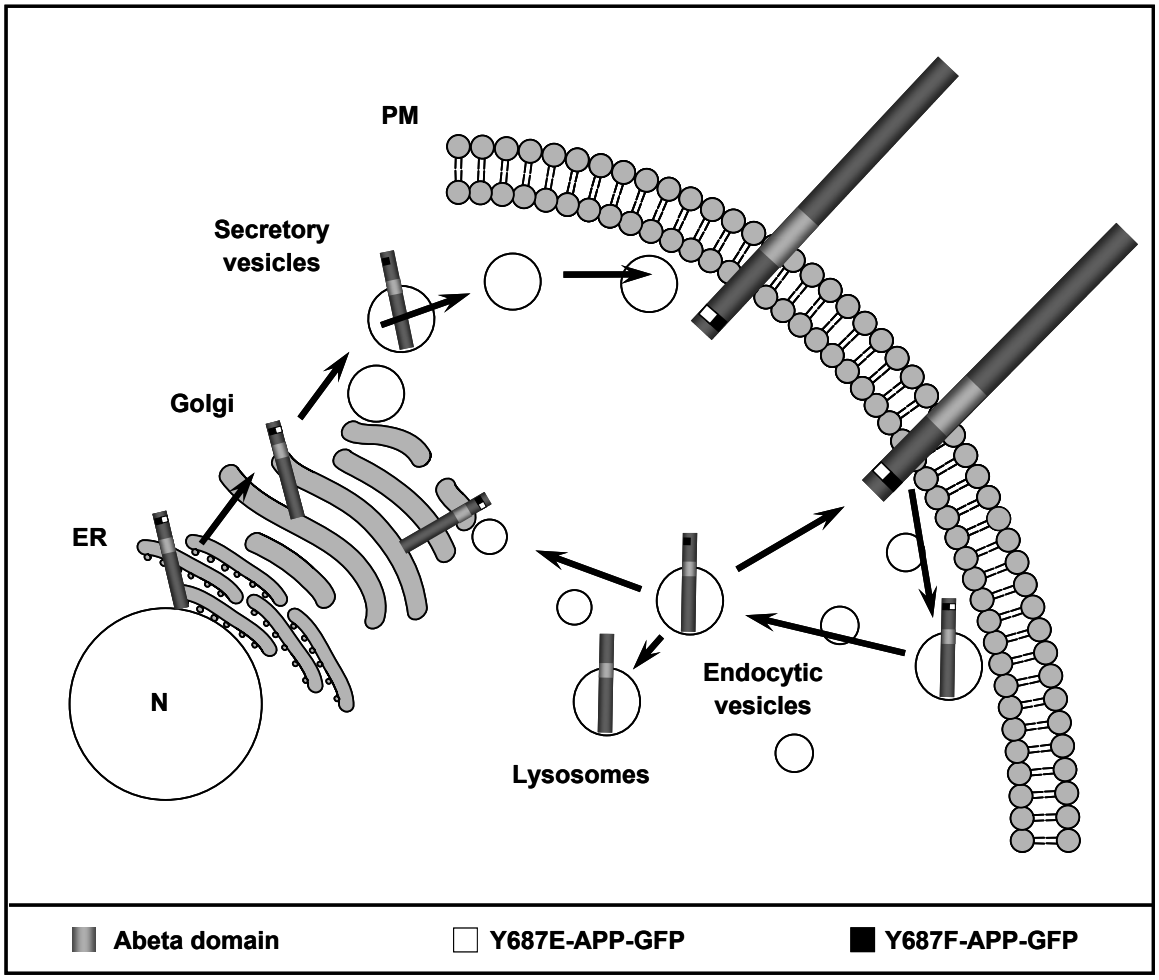

Figure 4. Tyrosine 687 phosphorylation/dephosphorylation-dependent APP subcellular targeting. N, nucleus; ER, endoplasmic reticulum.

One can conclude that the CHX based experimental model is useful to study both retrograde and anterograde processing, and that for APP the NPTY domain is important in both instances. The exposure to CHX appears to leave the cell machinery intact, such that the mutants behave in an identical manner both before and after removal of the drug. That is, Y687E-APP failed to be incorporated into vesicles, whereas Y687F-APP was incorporated more efficiently than wild-type APP. Another, advantage of this method, particularly in comparison to pulse chase methods, is that it allows direct real time *in vivo* monitoring of the GFP-tagged proteins. This is useful for Alzheimer's disease related studies addressing the use of signal transduction based therapeutics, where phosphorylation of a single site on a given protein can result in a cascade of events and affect other proteins directly or indirectly. By visualizing APP directly, and given all the other methodology already evolved, such as measuring Abeta levels, such effects on APP metabolism can be easily evaluated.

We had previously shown that disrupting the NPTY domain dramatically impaired endocytosis of APP and affected Abeta production [12]. APP turnover was monitored in the absence of 'de novo' protein synthesis by adding CHX to transfected cells in culture. The work presented here modified the previously described model system [13] by removing the CHX, thus permitting 'de novo' protein synthesis to resume. Consequently, all the cellular machinery should become available to permit 'normal' protein targeting. Notably, under these conditions the Y687E-APP mutant still fails to be incorporated into visible vesicular structures (Fig. 3). Overall, the method described for monitoring intracellular protein targeting has several advantages, and can be applied to the study of proteins other than APP.

ACKNOWLEDGMENTS

Supported by the EU V and VI Framework Programs (DIADEM and APOPIS), by the FCT (POCTI/NSE/40682/2001 and POCTI/SAU-OBS/57394/2004) of Portuguese Ministry of Science and Technology, and by Centro de Biologia Celular, University of Aveiro. SR was recipient of PhD Fellowship (SFRH/BD/17693/2004).

REFERENCES

1. Weihofen A, Martoglio B. Intramembrane-cleaving proteases: controlled liberation of proteins and bioactive peptides. Trends Cell Biol. 2003;13:71-78.

2. Xu H, Greengard P, Gandy S. Regulated formation of Golgi secretory vesicles containing Alzheimer beta-amyloid precursor protein. J Biol Chem. 1995;270:23243-23245.

3. Buxbaum JD, Koo EH, Greengard P. Protein phosphorylation inhibits production of Alzheimer amyloid beta/A4 peptide. Proc Natl Acad Sci U S A. 1993;90:9195-9198.

4. Ando K, Iijima KI, Elliott JI, Kirino Y, Suzuki T. Phosphorylation-dependent regulation of the interaction of amyloid precursor protein with Fe65 affects the production of beta-amyloid. J Biol Chem. 2001;276:40353-40361.

5. Chen WJ, Goldstein JL, Brown MS. NPXY, a sequence often found in cytoplasmic tails, is required for coated pit-mediated internalization of the low density lipoprotein receptor. J Biol Chem. 1990;265:3116-3123.

6. Koo EH, Squazzo SL. Evidence that production and release of amyloid beta-protein involves the endocytic pathway. J Biol Chem. 1994;269:17386-17389.

7. Lai A, Sisodia SS, Trowbridge IS. Characterization of sorting signals in the beta-amyloid precursor protein cytoplasmic domain. J Biol Chem. 1995;270:3565-3573.

8. Zambrano N, Bruni P, Minopoli G, Mosca R, Molino D, Russo C, et al. The beta-amyloid precursor protein APP is tyrosine-phosphorylated in cells expressing a constitutively active form of the Abl protoncogene. J Biol Chem. 2001;276:19787-19792.

9. Tarr PE, Roncarati R, Pelicci G, Pelicci PG, D'Adamio L. Tyrosine phosphorylation of the beta-amyloid precursor protein cytoplasmic tail promotes interaction with Shc. J Biol Chem. 2002;277:16798-16804.

10. Lee MS, Kao SC, Lemere CA, Xia W, Tseng HC, Zhou Y, et al. APP processing is regulated by cytoplasmic phosphorylation. J Cell Biol. 2003;163:83-95.

11. Rebelo S, Vieira SI, Esselmann H, Wiltfang J, da Cruz e Silva EF, da Cruz e Silva OA. Tyrosine 687 phosphorylated Alzheimer's amyloid precursor protein is retained intracellularly and exhibits a decreased turnover rate. Neurodegener Dis. 2007;4:78-87.

12. Rebelo S, Vieira SI, Esselmann H, Wiltfang J, da Cruz ESEF, da Cruz ESOA. Try687 dependent APP endocytosis and Abeta production. J Mol Neurosci. 2007;13.

13. da Cruz e Silva O, Vieira SI, Rebelo S, da Cruz e Silva EF. A model system to study intracellular trafficking and processing of the Alzheimer's amyloid precursor protein. Neurodegener Dis. 2004;1:196-204.

14. da Cruz e Silva OA, Iverfeldt K, Oltersdorf T, Sinha S, Lieberburg I, Ramabhadran TV, et al. Regulated cleavage of Alzheimer beta-amyloid precursor protein in the absence of the cytoplasmic tail. Neuroscience. 1993;57:873-877.

15. Rebelo S, Henriques AG, da Cruz e Silva EF, da Cruz e Silva OA. Effect of cell density on intracellular levels of the Alzheimer's amyloid precursor protein. J Neurosci Res. 2004;76:406-414.

16. Shin RW, Saido TC, Maeda M, Kitamoto T. Novel alpha-secretase cleavage of Alzheimer's amyloid beta precursor protein in the endoplasmic reticulum of COS7 cells. Neurosci Lett. 2005;376:14-19.

17. Selkoe DJ, Yamazaki T, Citron M, Podlisny MB, Koo EH, Teplow DB, et al. The role of APP processing and trafficking pathways in the formation of amyloid beta-protein. Ann N Y Acad Sci. 1996;777:57-64.

18. Greenfield JP, Tsai J, Gouras GK, Hai B, Thinakaran G, Checler F, et al. Endoplasmic reticulum and trans-Golgi network generate distinct populations of Alzheimer beta-amyloid peptides. Proc Natl Acad Sci U S A. 1999;96:742-747.

19. Perez RG, Soriano S, Hayes JD, Ostaszewski B, Xia W, Selkoe DJ, et al. Mutagenesis identifies new signals for beta-amyloid precursor protein endocytosis, turnover, and the generation of secreted fragments, including Abeta42. J Biol Chem. 1999;274:18851-18856.

CHAPTER III

CHAPTER III

TYROSINE 687 DEPENDENT ALZHEIMER'S AMYLOID PRECURSOR PROTEIN TRAFFICKING AND PROCESSING

Protein phosphorylation is a major regulatory mechanism, reversible in nature and controlling key events in molecular and cellular biology. It is perhaps not surprising that many pathologies exhibit altered protein phosphorylation profiles, among these Alzheimer's disease (AD). Moreover, APP is itself a phosphoprotein with eight putative phosphorylation sites on its C-terminal domain (Ser^{653}, Thr^{654}, Ser^{655}, Thr^{668}, Ser^{675}, Tyr^{682}, Thr^{686} and Tyr^{687}). Of these, tyrosine 687 (Y687) of the APP was shown to be phosphorylated in the brain of Alzheimer's disease patients by MALDI-TOF MS (Lee et al. 2003).

Additionally, this residue lies within a typical internalization signal (NPTY) for membrane associated receptor proteins, strongly suggesting a potential role for APP in signal transduction. Consequently, this chapter describes how phosphorylation of Y687 may be affecting APP in terms of its proteolytic cleavage and subcellular distribution. In the work described, Y687 was mutated to glutamate (Y687E-APP-GFP) to mimic a constitutively phosphorylated residue, or to phenylalanine (Y687F-APP-GFP) to mimic a constitutively dephosphorylated residue and the results are presented in the next two manuscripts (Rebelo et al. 2007a and Rebelo et al. 2007b). For detailed protocol information see the appendix.

Lee MS, Kao SC, Lemere CA, Xia W, Tseng HC, Zhou Y, Neve R, Ahlijanian MK, Tsai LH. 2003. APP processing is regulated by cytoplasmic phosphorylation. J Cell Biol 163(1):83-95.

Rebelo S, Vieira SI, Esselmann H, Wiltfang J, da Cruz E. Silva EF, da Cruz E. Silva OA. 2007a. Tyrosine 687 phosphorylated Alzheimer's amyloid precursor protein is retained intracellularly and exhibits a decreased turnover rate. Neurodegener Dis 4: 78-87.

Rebelo S, Vieira SI, Esselmann H, Wiltfang J, da Cruz E. Silva EF, da Cruz E. Silva OA 2007b. Try687 dependent APP endocytosis and Abeta production. J Mol Neurosci 32:1-8.

Neurodegenerative Diseases

Neurodegenerative Dis 2007;4:78–87
DOI: 10.1159/000101831

Tyrosine 687 Phosphorylated Alzheimer's Amyloid Precursor Protein Is Retained Intracellularly and Exhibits a Decreased Turnover Rate

Sandra Rebelo[a] Sandra Isabel Vieira[a] Hermann Esselmann[c] Jens Wiltfang[c]
Edgar F. da Cruz e Silva[b] Odete A.B. da Cruz e Silva[a]

[a]Laboratório de Neurociências and [b]Laboratório de Transdução de Sinais, Centro de Biologia Celular, Universidade de Aveiro, Aveiro, Portugal; [c]Molecular Neurobiology Laboratory, Department of Psychiatry and Psychotherapy, University of Erlangen-Nuremberg, Erlangen-Nuremberg, Germany

Key Words
Tyrosine 687 · Amyloid precursor protein phosphorylation · Subcellular amyloid precursor protein targeting · Amyloid precursor protein-GFP fusion · Abeta

Abstract
Tyrosine 687 (Y687) of the Alzheimer's amyloid precursor protein (APP) was shown to be phosphorylated in the brains of Alzheimer's disease patients. This residue lies within a typical endocytosis consensus motif commonly found in molecules with receptor functions, strongly suggesting a potential role for APP in signal transduction. Consequently, the work here described addressed how phosphorylation of Y687 may be affecting APP in terms of its proteolytic cleavage and subcellular distribution. Our data show that the APP mutant mimicking constitutive dephosphorylation of Y687 had a faster turnover rate, both in terms of maturation and metabolism, when compared to Wt-APP-GFP and even more so when compared to the mutant mimicking constitutive phosphorylation. Thus, the mutant mimicking constitutively phosphorylated Y687 had a much higher $t_{1/2}$ and was significantly retained both in the ER and TGN. Additionally, this mutant was not incorporated into visible vesicular structures, with a concomitant dramatic decrease in Aβ production. Our findings point to the direct phosphorylation of APP on Y687 as an important regulatory mechanism in terms of determining the subcellular localization of APP and modulating its processing via different proteolytic pathways.

Introduction

Protein phosphorylation is a major regulatory mechanism, reversible in nature and controlling key events in molecular and cellular biology. It is perhaps not surprising that many pathologies exhibit altered protein phosphorylation profiles, among these Alzheimer's disease (AD). With respect to the latter, tau hyperphosphorylation has been amply addressed [1, 2] and intensely studied as a relevant biomarker for the disease condition [3]. The Alzheimer's amyloid precursor protein (APP) however, being itself a phosphoprotein, has received comparatively less attention in this respect. APP has eight putative phosphorylation sites on its C-terminal domain. Of these, seven (Tyr^{653}, Ser^{655}, Thr^{668}, Ser^{675}, Tyr^{682}, Thr^{686} and Tyr^{687}) have been demonstrated to be phosphorylated in the brains of AD patients by MALDI-TOF MS [4].

APP processing has been widely studied and various processing pathways have been described [5, 6]. The non-amyloidogenic pathway, whereby APP can be cleaved by

KARGER
Fax +41 61 306 12 34
E-Mail karger@karger.ch
www.karger.com

1660–2854/07/0043–0078$23.50/0

Accessible online at:
www.karger.com/ndd

Odete A. B. da Cruz e Silva
Laboratório de Neurociências, Centro de Biologia Celular
Universidade de Aveiro
PT–3810-193 Aveiro (Portugal)
Tel. +351 234 370 778, Fax +351 234 426 408, E-Mail odetecs@bio.ua.pt

α-secretases (ADAM 10, ADAM 17 (TACE) and ADAM 9) at various subcellular locations, such as the late secretory compartment or at the cell surface, generates alpha cleaved sAPP (αsAPP), which can be secreted extracellularly [7]. In the amyloidogenic pathway APP can be processed by β-secretases (BACE1 and BACE2) to yield beta cleaved sAPP (βsAPP) [8, 9]. Further cleavages by the γ-secretase complex [10–13] can produce Aβ peptides and the AICD (APP intracellular domain), or shorter non-toxic peptides, also referred to as P3. APP processing can occur at several subcellular locations. For example, Aβ peptides are produced in the Golgi complex, especially in the trans-Golgi network (TGN), and in the endoplasmic reticulum (ER), albeit in lower levels, and also during the endocytic pathway. The correlation between the different pathways and the pathological condition has not been clearly elucidated, and important physiological functions may exist for Aβ. Thus, the production of the latter is not automatically or exclusively pathogenic in nature.

Different studies have also addressed the potential modulatory role of protein phosphorylation on APP processing [14–17]. Direct phosphorylation of APP on T668 was shown to be important in Aβ production [4] and the relevance of T668 phosphorylation in vivo has also been the subject of significant research [18, 19].

This dynamic reversible process may also be exerting its effect indirectly as was shown by the addition of phorbol esters, which stimulate PKC, or okadaic acid, which inhibits protein phosphatases 1 and 2A [20–23]. Upon addition of both compounds to cells in culture α-secretase cleavage was enhanced, and Aβ production decreased. The effect, however, was cell type specific and showed some variation. As mentioned above, little information is available regarding the putative role of the remaining phosphorylatable residues on APP and their physiological relevance remains unclear. Nonetheless, it is unlikely that they are irrelevant in the disease state, since APP can be found in its phosphorylated state in the brains of AD patients. Among them tyrosine 687 (Y687), which lies within a typical endocytosis signal (NPTY) of receptor molecules, provides a potential target for regulating APP metabolism [24]. In the study here described, Y687 was mutated to glutamate (Y687E-APP-GFP) to mimic a constitutively phosphorylated residue, or to phenylalanine (Y687F-APP-GFP) to mimic a constitutively dephosphorylated residue. We have also shown that the endocytosis of the Y687E-APP-GFP is highly compromised [Rebelo et al., in press]. Here we show that Y687E-APP-GFP is also retained in the TGN and the ER, which could all contribute to the reduced Aβ production observed. In contrast, Y687F-APP-GFP has a higher turnover rate, readily exiting from the TGN. In conclusion, we have shown that mimicking phosphorylation/dephosphorylation of Y687 has critical consequences for APP subcellular localization and proteolytic cleavage.

Methods

Antibodies

Primary anti-APP antibodies used in this study were monoclonal antibody 22C11 (Chemicon, USA), and monoclonal antibody 6E10 (Sigma, Portugal). Different Aβ peptide species were detected using the monoclonal antibody 1E8 (Schering AG, Germany). For co-localization studies, a monoclonal anti-syntaxin 6 antibody (BD Biosciences, USA) was used as a TGN marker and a polyclonal anti-calnexin antibody (Stressgen, USA) was used as an ER marker. Secondary antibodies used were Texas Red-conjugated anti-mouse and anti-rabbit IgG (Molecular Probes, USA) for immunocytochemistry, and anti-mouse IgG horseradish peroxidase-linked whole antibody (Amersham Pharmacia, Portugal), for enhanced chemiluminescence (ECL) detection.

APP695 Expression Vectors

As previously described [14, 25], APP695 cDNA mutants were prepared to mimic constitutive phosphorylation or dephosphorylation state of Tyr^{687}. The wild-type and the mutated APP cDNAs were further fused in frame with GFP using the pEGFP-N1 mammalian expression vector (Clontech, USA) to yield Y687E-APP-GFP, Y687F-APP-GFP, and Wt-APP-GFP. All constructs were verified by DNA sequencing.

Cell Culture and Transfections

Monkey kidney COS-7 cells were cultured as previously described [26, 27], and transiently transfected using a cationic lipid transporter (LipofectAMINE 2000, Invitrogen Life Technologies). Transfections were carried out with wild-type (Wt-APP-GFP) or either of the two Tyr^{687} mutant human APP cDNAs (Y687E-APP-GFP and Y687F-APP-GFP). Upon transfection cells were allowed to express these proteins for eight hours, and were subsequently divided into 6-well plates with (for subcellular localization studies) or without (for processing studies) coverslips pretreated with 100 μg/ml polyornithine, and left to recover for 4 h. Cells were then incubated in serum-free DMEM supplemented with a protein synthesis inhibitor, 50 μg/ml cycloheximide (Sigma, Portugal). At the specified times the cells were either fixed in 4% paraformaldehyde (for subcellular localization studies) or harvested with 1% SDS (for processing studies).

Analysis of holoAPP and Its Proteolytic Fragments

At the indicated times of incubation with cycloheximide, the cells and the conditioned media were harvested in 1% SDS. Samples were boiled and their total protein content determined by the BCA method (Pierce, USA). The samples were subjected to 6.5% SDS-PAGE in Tris-glycine buffer. Electrophoretic transfer was then performed onto nitrocellulose membranes and immunoblotting of the transferred proteins was performed by first blocking nonspecific binding sites with nonfat dry milk in 10 mM Tris-

HCl (pH 8.0)/150 mM NaCl. Incubation with the primary antibodies as indicated was carried out overnight. Immunoreactive bands were detected using an enhanced chemiluminescence detection system (Amersham Pharmacia Biotech, Portugal).

The analysis of Aβ peptides was carried out essentially as previously described [28, 29]. COS-7 cells were transfected with Wt or with the mutated APP constructs and incubated for 3 h as described above. After this period the conditioned media were collected without SDS and immediately frozen in liquid nitrogen. The conditioned media were further immunoprecipitated using 25 μl dynabeads (Dynal, Germany) coated with mAb 1E8 (Schering AG, Germany). Immunoprecipitates were separated on 12% Bicine/Tris gel containing 8 M urea. Different Aβ peptide species were revealed by immunoblotting using mAb 1E8. Synthetic Aβ peptides were run in parallel for the identification of the different Aβ peptide species. In the data set presented, we quantified the overall production of all Aβ fragments, but in other studies we address each of the Aβ species [Rebelo et al., in press].

Immunoblots or the corresponding autoradiograms were scanned and protein bands quantified using the manufacturer's Quantity One densitometry software. Data were expressed as mean ± SEM of determinations from at least three independent experiments. Statistical significance was conducted by one-way analysis of variance (ANOVA) with Tukey-Kramer test. Unless otherwise noted, a level of statistical significance is considered at $p < 0.05$.

Subcellular Localization of APP

After cell fixation and subsequent coverslip preparation, the subcellular localization of APP was easily observed by fluorescence microscopy using an Olympus IX-81 inverted epifluorescence microscope. Cell populations (120 cells/coverslip) were analyzed for the presence or absence of fluorescence in specific subcellular organelles: ER, Golgi complex, cytoplasmic vesicles, plasma membrane and nucleus. The subcellular structure was confirmed using organelle specific antibody markers (an example was selected for the 2:30 h time point).

For semiquantitative analysis of the APP-GFP intracellular trafficking, the presence of fluorescence in each subcellular compartment was scored for each APP species (Wt and both mutants). Sets of 40 cells were counted at least three times for statistical analysis and a typical example for each time point was also selected.

Results

Intracellular APP Expression and Phosphorylation-Dependent Turnover Rates

Before addressing the potential effects of mimicking Tyr687 phosphorylation on intracellular trafficking and APP processing, the transfection levels, turnover rates and maturation of transfected wild-type and mutant APP proteins were compared.

Transfected APP-GFP fusion proteins were immunoblotted with anti-APP (22C11) and anti-GFP (JL-8) antibodies. As expected (fig. 1a), antibody JL-8 recognized the APP-GFP fusion proteins (bands A and B) but did not recognize the endogenous APP isoforms (bands C). The rates of disappearance of bands A (mature APP-GFP) and B (immature APP-GFP) were monitored for each APP species (fig. 1b, c).

Table 1. Half-life of APP-GFP proteins

Protein	Immature APP-GFP, h	Mature APP-GFP, h
WT-APP-GFP	2.23 ± 0.13	2.46 ± 0.16
Y687E-APP-GFP	$2.58 \pm 0.04^{*,+++}$	$2.67 \pm 0.10^{+}$
Y687F-APP-GFP	$0.81 \pm 0.02^{***,+++}$	$1.63 \pm 0.35^{*,+}$

Data are expressed as mean ± SEM; When $p < 0.05$, ANOVA analysis was followed by posthoc Tukey-Kramer test; * Significantly different from the Wt-APP-GFP determinations; + significant differences between Y687E-APP-GFP and Y687F-APP-GFP determinations. */+ $p < 0.05$; ***/+++ $p < 0.001$.

Even though similar expression levels were obtained for the three constructs, results were normalized by setting initial transfection levels at 100% for each experimental data set. Figure 1 clearly demonstrates that both wild type and mutant APP-GFP proteins mature and disappear with time, in an analogous manner to what is seen for endogenous APP isoforms. For Wt-APP-GFP, the disappearance of the immature species, presumably mostly due to maturation, is significantly decreased by 3 h and almost depleted by 5 h (fig. 1a, b). In contrast, the turnover of immature Y687E-APP-GFP was slower. Whereas, approximately 75% of the Y687E-APP- GFP protein remained intact at the 2 h time point, the corresponding figure for Wt-APP-GFP was only around 50% (fig. 1b). At the 5 h time point similar amounts of both proteins remained in the cells. In comparison, immature Y687F-APP-GFP exhibited a faster rate of disappearance. The corresponding half-lives of the three immature proteins were 2.2, 2.6 and 0.8 h, for Wt-, Y687E- and Y687F-APP-GFP, respectively (table 1). Similarly, mature Wt-APP-GFP also disappears with time, presumably due to normal turnover and processing. Intracellular levels are significantly decreased by 3 h and virtually depleted by 5 h (fig. 1a, c).

Although the rate of disappearance of mature Y687E-APP-GFP is similar to wild type, again the corresponding Y687F-APP-GFP protein had a higher rate of disappearance. Thus, the corresponding half-lives for the turnover of the mature APP-GFP proteins were 2.5, 2.7 and 1.6 h for Wt-, Y687E- and Y687F-APP-GFP, respectively (table 1).

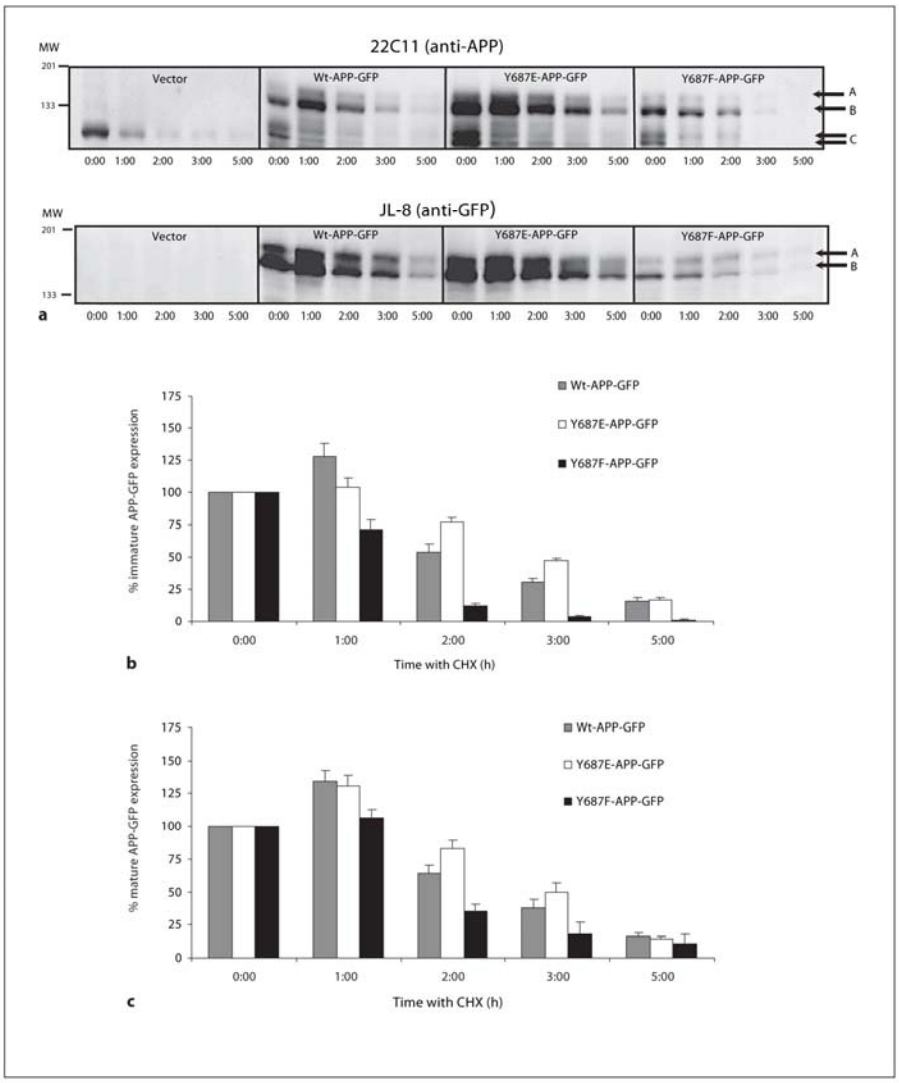

Fig. 1. Time course of APP expression in COS-7 cells transfected with vector (pEGFP-N1), Wild-type APP-GFP and mutated (Y687E and Y687F) APP-GFP, in the presence of cycloheximide. **a** Immunoblot of cell lysates with 22C11 antibody (anti-APP). APP isoforms: endogenous (C) and transfected (A and B), where A corresponds to the transfected mature APP_{695}-GFP and B to the transfected immature APP_{695}-GFP. Parallel blots were probed with an antibody to GFP (JL-8). **b** Quantification of the amounts of transfected immature APP_{695}-GFP expressed over time of incubation with cycloheximide. Data are presented as mean ± SEM from at least three independent experiments. **c** Quantification of amounts of transfected mature APP_{695}-GFP expressed over time of incubation with cycloheximide. Data are presented as mean ± SEM from at least three independent experiments.

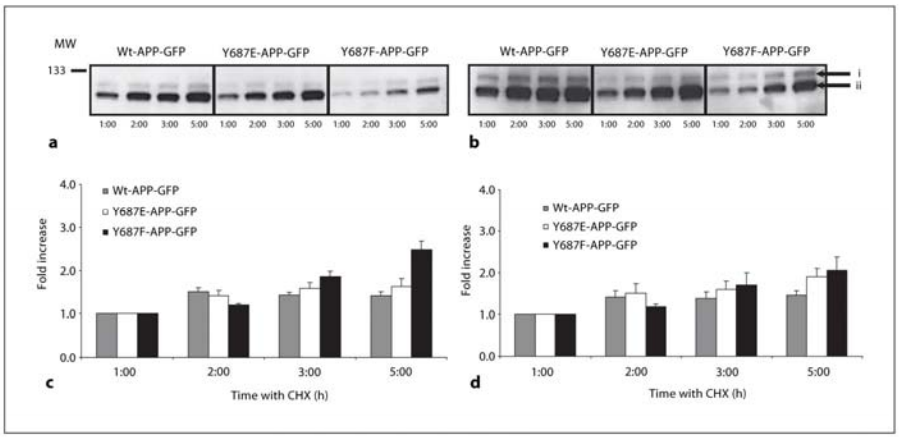

Fig. 2. Time course of sAPP production in COS-7 cells transfected with Wt-APP-GFP, Y687E-APP-GFP and Y687F-APP-GFP in the presence of cycloheximide. **a** Total sAPP secreted into the culture medium detected with the 22C11 antibody. **b** Alpha sAPP secreted into the culture medium detected with the 6E10 antibody. i = sAPP derived from isoforms 751/770; ii = sAPP derived from isoform 695. **c** Quantification of secreted total sAPP (fold increase) derived from the APP_{695} isoform. Data are presented as mean ± SEM from at least three independent experiments. **d** Quantification of secreted alpha sAPP (fold increase) derived from the APP 695 isoform. Data are presented as mean ± SEM of at least three independent experiments.

Table 2. sAPP production and Aβ secretion

Protein	Fold increase in total sAPP		Fold increase in alpha sAPP		Aβ secretion
	3 h	5 h	3 h	5 h	3 h
Wt-APP-GFP	1.42 ± 0.07	1.41 ± 0.10	1.37 ± 0.16	1.46 ± 0.10	1.00 ± 0.00
Y687E-APP-GFP	1.58 ± 0.14	$1.63 \pm 0.18^{++}$	1.59 ± 0.20	1.90 ± 0.20	$0.64 \pm 0.01^{**,+++}$
Y687F-APP-GFP	$1.90 \pm 0.12^{*}$	$2.50 \pm 0.18^{**,++}$	1.70 ± 0.29	2.10 ± 0.32	$1.18 \pm 0.01^{*,+++}$

Data are expressed as mean ± SEM; When $p < 0.05$, ANOVA analysis was followed by posthoc Tukey-Kramer test. * Significantly different from the Wt-APP-GFP determinations; $^{+}$ significant differences between Y687E-APP-GFP and Y687F-APP-GFP determinations. $^{*/+}$ $p < 0.05$; $^{**/++}$ $p < 0.01$; $^{***/+++}$ $p < 0.001$.

Phosphorylation-Dependent Proteolytic Cleavage of APP

The effect of phosphorylation on APP cleavage and the production of proteolytic fragments was also addressed (fig. 2). In terms of total sAPP production (fig. 2a, c) the Wt and phosphorylation-mimicking mutant (Y687E-APP-GFP) resulted in similar rates of secretion. The dephosphorylation-mimicking mutant, however, revealed a higher rate of total sAPP production. When only the production of alpha sAPP was monitored differences between each of the APP species were less marked (fig. 2b, d). Thus, rates of increase were calculated for both the 3 and 5 h time points. For the wild-type species total sAPP increased 1.41-fold at 5 h and alpha sAPP increased 1.46-fold by 5 h. The correlation between total and alpha sAPP production was quite different when the mutants were analyzed. At 5 h, the Y687E-APP-GFP mutant exhibited a 1.63-fold increase in total sAPP production, but alpha sAPP increased even more (1.90-fold), suggesting comparatively higher α-secretase cleavage. On the other hand, the Y687F-APP-GFP mutant was relatively favored for β-secretase cleavage at the same time point, being that the

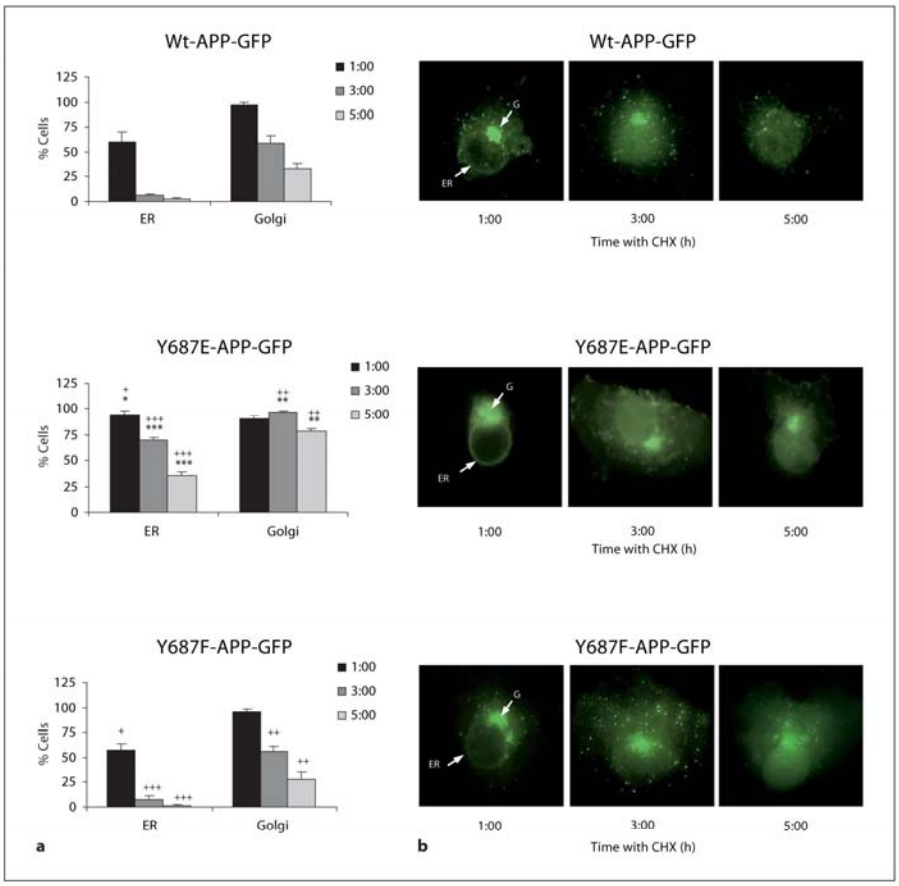

Fig. 3. APP-GFP intracellular trafficking. **a** Quantification of intracellular protein trafficking by monitoring APP-GFP fluorescence in specific cellular compartment with time of incubation with cycloheximide. Fluorescence was scored for each organelle for 20 transfected cells in triplicate for each of the Wt-APP-GFP and Y687-APP-GFP mutants. Fluorescence for each subcellular structure is represented as a percentage of the cells monitored. Data are expressed as mean ± SEM; when $p < 0.05$, ANOVA analysis was followed by posthoc Tukey-Kramer test. *Significantly different from Wt-APP-GFP determinations; $^{+}$ Significant differences between Y687E-APP-GFP and Y687F-APP-GFP determinations. $^{*/+}$ $p < 0.05$; $^{**/++}$ $p < 0.01$; $^{***/+++}$ $p < 0.001$. **b** Wild-type APP-GFP and mutant (Y687E and Y687F) APP-GFP intracellular protein trafficking, in transiently transfected COS-7 cells. Representative epifluorescence microphotographs of cells at specific time points. Specific time points are shown for each protein in the presence of CHX. ER-endoplasmic reticulum, G-golgi complex.

total increased 2.50-fold, but alpha sAPP increased less only 2.10-fold (table 2). Values for Aβ secretion support these observations (table 2). Aβ production was compared against Wt-APP-GFP at the 3 h time point. The mutant Y687F-APP-GFP, mimicking the constitutively dephosphorylated residue, produced more Aβ than Wt-APP-GFP, and in fact a fold increase double that observed for the mutant mimicking constitutive phosphorylation, Y687E-APP-GFP. Thus, it would appear that APP phosphorylation is also an important regulatory mechanism determining Aβ production.

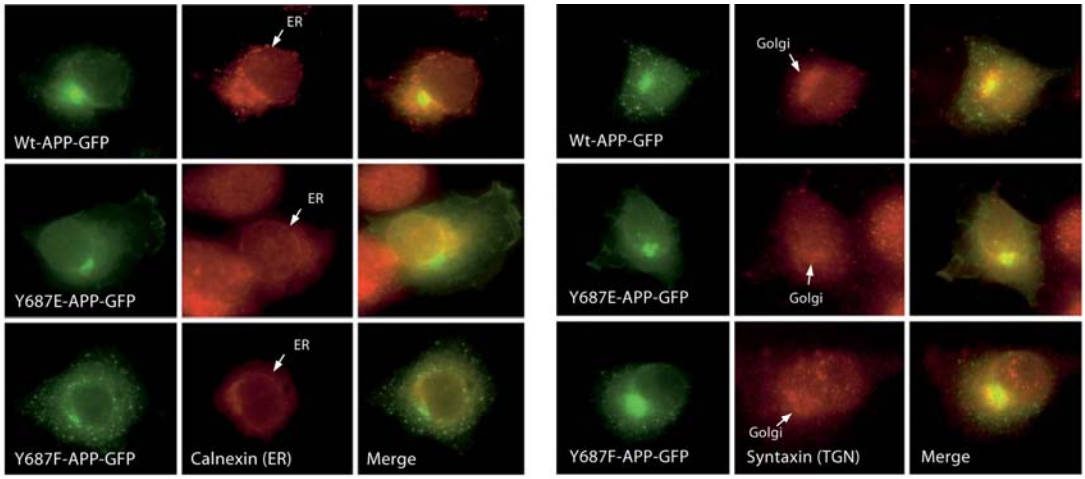

Fig. 4. Subcellular co-localizations using specific organelle markers. Co-localization at 2 h 30 min of incubation with cycloheximide for Wt-APP-GFP and Y687-APP-GFP mutants with calnexin (**a**) and syntaxin 6 (**b**), which recognize the endoplasmic reticulum (ER) and Golgi complex (TGN), respectively.

Phosphorylation-Dependent Intracellular Trafficking of APP

Semi-quantitative studies comparing intracellular trafficking were carried out whereby cells were scored as described for the presence of APP-GFP in specific cellular compartments (fig. 3a). Figure 3b compares typical time courses of subcellular localization for each of the APP species as observed by fluorescence microscopy. Co-localization studies with specific subcellular markers were performed at all time points in order to confirm the subcellular assignments made throughout this study, and such an example is shown in figure 4. It is important to note that the relative strength of the fluorescence was not scored, but only its presence or absence.

Wt-APP-GFP is seen to be abundantly expressed in the ER at the initial time point (fig. 3a), but the percentage of cells with a fluorescent ER drops dramatically over the 5 h from 60% to virtually 0%. An identical rapid drop in ER fluorescence can be detected for the Y687F-APP-GFP mutant. Similarly, for both the Wt-APP-GFP and the dephosphorylation-mimicking mutant, Golgi fluorescence drops progressively from 90% of cells initially, to approximately 30% after 5 h. In contrast, the subcellular distribution for the Y687E-APP-GFP fusion protein over time was considerably different (fig. 3). The latter experiences relative delays throughout its intracellular targeting. Thus, at the beginning of the experiment almost 100% of the cells analyzed showed intense ER, with the percentage of cells fluorescing dropping to approximately 40% after 5 h (fig. 3a). At this time point cells expressing the other two proteins exhibited an almost complete absence of ER fluorescence.

Difficulties in the export of the phosphorylated mimicking protein became even more accentuated, given that a sustainable large percentage of cells exhibit Golgi fluorescence (80–100%) at all time points. Thus, it would appear that Y687E-APP-GFP is retained both in the ER and the TGN, and has particular difficulties in being exported from the latter. Consistent with this failure to be exported from the Golgi, is the complete absence of visible vesicular structures for this mutant. As is evident in both figures 3 and 4, if one focus on the APP fluorescence alone, Wt-APP-GFP and Y687F-APP-GFP label many vesicular-like structures, and these are almost completely absent for the Y687E-APP-GFP mutant. The cell membrane is another structure which is clearly visible, reaching a maximum of 70% for Y687E-APP-GFP, 40% for Y687F-APP-GFP and 30% for Wt-APP-GFP (data not shown).

Subcellular co-localizations using specific organelle markers were performed simultaneously at all time points to confirm the correct identification of the fluorescent structures being scored for the Wt and mutant proteins. As we follow the proteins over time, clear co-localization was obtained with syntaxin 6, used as a TGN-specific marker, indicating that each of the three APP proteins was present in the TGN (fig. 4b). In contrast, however, the patterns of co-localization for Y687F-APP-GFP, Y687E-APP-GFP and Wt-APP-GFP with calnexin (typically stains the ER) were different at the same time point (fig. 4a). Wt-APP-GFP co-localized to the ER with a perinuclear distribution and only slightly around the TGN. Surprisingly, the intracellular ER network becomes more evident and consequently co-localization with calnexin becoming noticeably increased in cells expressing Y687E-APP-GFP (fig. 4, yellow/red). It would appear from these results that the 'phosphorylated' Y687E-APP-GFP protein exhibits increased co-localization to the ER, whereas for Wt-APP-GFP and the 'dephosphorylated' Y687F-APP-GFP protein this is reduced.

This increased co-localization reflects retention in ER, TGN and even in the plasma membrane, which is due to the failure of this mutant to be incorporated into vesicular-like structures.

Discussion

The use of the phosphorylation-mimicking mutants was strongly validated given that the overall effect of the phosphorylation- and dephosphorylation-mimicking states produced 'opposite' results, mirroring the true dynamics of reversible phosphorylation processes. For example, this is clearly evident from the $t_{1/2}$ of the APP mutants used: the dephosphorylation-mimicking mutant had a faster turnover rate compared to the phosphorylation-mimicking mutant. This was well correlated with the production of sAPP, given that the rate of sAPP production was higher for Y687F-APP-GFP, consistent with its shorter $t_{1/2}$. The overall lower basal levels for this mutant may also be explained if one considers that although levels of expression were similar, its processing was faster, and given that de novo protein synthesis was blocked, this species is depleted much faster.

APP phosphorylation also appears to be important in determining the metabolic pathway, resulting in the production of different proteolytic fragments. The results demonstrated that Y687F-APP-GFP had a relative preference for β-secretase cleavage, whereas Y687E-APP-GFP had a relative preference for α-secretase cleavage. In fact, this was confirmed by direct measurements of Aβ production [Rebelo et al., in press], or the quantification of total Aβ production (table 2). Indeed, the Y687E-APP-GFP mutant, mimicking constitutive phosphorylation at this residue, produced half of the fold increase in Aβ production, when compared to the Y687F-APP-GFP mutant (table 2).

As well as affecting proteolytic cleavage of APP, mimicking phosphorylation also appears to markedly determine its subcellular localization. The phosphorylation-mimicking mutant exhibited relatively considerable delays in the ER and TGN, whereas the dephosphorylated-mimicking mutant appears to behave in a manner similar to the Wt protein, or be exported marginally faster. Also common for Wt and Y687F-APP-GFP species is that all cells observed had clearly visible vesicular structures, in agreement with the notion that APP processing can occur via secretory and endocytic pathways. APP-GFP-labeled vesicles, however, were almost completely absent in cells expressing Y687E-APP-GFP. Hence, it is particularly interesting to compare the subcellular localization data with the production of the proteolytic fragments, in particular sAPP. On the one hand, subcellular localizations are dramatically affected by Y687 phosphorylation, with the phosphorylation-mimicking mutant being dramatically retained, and the dephosphorylation-mimicking mutant being readily targeted out of the TGN. In contrast, analysis of sAPP fragments did not reveal such dramatic differences. Taken together this suggests that APP processing can in fact occur at very distinct subcellular locations, and the 'preferred' or 'precise' site of action would appear from our data to be affected by protein phosphorylation.

This is in agreement with the various possible subcellular locations for APP processing described in the literature. For example, Y687E-APP-GFP is dramatically retained in the ER and TGN and does not suffer endocytosis, but is still proteolytically cleaved, although as we showed previously Aβ production is decreased. Other workers have demonstrated that both the ER and TGN can produce proteolytic fragments such as Aβ, albeit distinct subpopulations [30]. Whether subcellular targeting, as one might expect, involves APP-binding proteins, which are in turn regulated by protein phosphorylation, deserves further investigation.

The data here presented leads us to suggest that besides tau hyperphosphorylation, APP hyperphosphorylation may also be an AD-related event. It could be that the latter in particular reflects an endogenous neuropro-

tective mechanism. That is, in the presence of excess proteolytic fragments, namely Aβ, a feedback mechanism leads to APP phosphorylation and thus relative inhibition in producing further Aβ fragments. Hence, as an early response to stress (AD) APP could become phosphorylated in an attempt to reduce Aβ production. Clearly, under more adverse conditions and cellular apoptosis, APP processing would still result in the overproduction of Aβ, leading to the disease condition. In fact, it has been shown that ER stress can contribute to AD [31], associating ER-mediated apoptosis with Aβ neurotoxicity. Other workers have also demonstrated that if one perturbs ER calcium homeostasis this can also lead to stress [32]. Recently, Kudo et al. [33] showed that ER stress affects APP processing and does so by inducing the molecular chaperone BiP/GRP78. It is also noteworthy that Aβ has been found to bind to the cerebrospinal fluid ER chaperones ERp57 and calreticulin, which would bind the bulk of Aβ to the ER [34]. The authors go as far as to suggest that deficits in these chaperones may contribute to the disease condition.

The ER is in fact an extensive structure being continuous with the outer nuclear membrane and the plasma membrane [35, 36]. The ER besides associating with mitochondria also extends to growth cones, axon terminals and dendritic spines.

Further, it appears that calcium signaling in the ER is important not only for neuronal plasticity but may also be relevant in neurodegenerative disorders [37]. Our data show that APP is preferentially targeted to the ER when phosphorylated on Y687, yet it still arrives at the plasma membrane and is favored for α-secretase cleavage with a reduction in Aβ production. Shin et al. [38] have also shown that α-secretase cleavage can occur in the ER. Modulation of APP processing in favor of non-amyloidogenic processing has long been a target for therapeutic intervention [39]. Focusing on protein phosphorylation and in particular phosphorylation of APP itself narrows the field considerably. Further, if one considers the protein phosphatases themselves as potential therapeutic targets, these can indeed be quite precise. In fact as has been amply reported [40] phosphatase-binding proteins can be isoform-specific, binding protein-specific and even tissue-specific, thus enabling exquisite fine tuning in a signal transduction therapeutics approach.

Acknowledgements

Supported by the EU V and VI Framework Programs (DIADEM and APOPIS), by the FCT (POCTI/CBO/34349/2001, POCTI/NSE/40682/2001 and POCI/SAUOBS/57394/2004) of the Portuguese Ministry of Science and Technology, and by the CBC, Universidade de Aveiro. S.R. and S.I.V. were recipients of PhD Fellowships (SFRII/BD/17693/2004 and Praxis XXI/BD/16218/1998).

References

1 Grundke-Iqbal I, Iqbal K, Tung YC, Quinlan M, Wisniewski HM, Binder LI: Abnormal phosphorylation of the microtubule-associated protein tau (tau) in Alzheimer cytoskeletal pathology. Proc Natl Acad Sci USA 1986;83:4913–4917.

2 Alonso A, Zaidi T, Novak M, Grundke-Iqbal I, Iqbal K: Hyperphosphorylation induces self-assembly of tau into tangles of paired helical filaments/straight filaments. Proc Natl Acad Sci USA 2001;98:6923–6928.

3 Wiltfang J, Lewczuk P, Maler M, Bleich S, Smirnov A, Kornhuber J: Neurochemical early and differential diagnostics for Alzheimer's disease. MMW Fortschr Med 2004;146:38–40.

4 Lee MS, Kao SC, Lemere CA, Xia W, Tseng HC, Zhou Y, Neve R, Ahlijanian MK, Tsai LH: APP processing is regulated by cytoplasmic phosphorylation. J Cell Biol 2003;163:83–95.

5 Checler F: Processing of the beta-amyloid precursor protein and its regulation in Alzheimer's disease. J Neurochem 1995;65:1431–1444.

6 Selkoe DJ, Yamazaki T, Citron M, Podlisny MB, Koo EH, Teplow DB, Haass C: The role of APP processing and trafficking pathways in the formation of amyloid beta-protein. Ann NY Acad Sci 1996;777:57–64.

7 Lichtenthaler SF, Haass C: Amyloid at the cutting edge: activation of alphasecretase prevents amyloidogenesis in an Alzheimer disease mouse model. J Clin Invest 2004;113:1384–1387.

8 Bennett BD, Babu-Khan S, Loeloff R, Louis JC, Curran E, Citron M, Vassar R: Expression analysis of BACE2 in brain and peripheral tissues. J Biol Chem 2000;275:20647–20651.

9 Vassar R, Bennett BD, Babu-Khan S, Kahn S, Mendiaz EA, Denis P, Teplow DB, Ross S, Amarante P, Loeloff R, Luo Y, Fisher S, Fuller J, Edenson S, Lile J, Jarosinski MA, Biere AL, Curran E, Burgess T, Louis JC, Collins F, Treanor J, Rogers G, Citron M: Beta-secretase cleavage of Alzheimer's amyloid precursor protein by the transmembrane aspartic protease BACE. Science 1999;286:735–741.

10 Capell A, Beher D, Prokop S, Steiner H, Kaether C, Shearman MS, Haass C: Gamma-secretase complex assembly within the early secretory pathway. J Biol Chem 2005;280:6471–6478.

11 Sastre M, Steiner H, Fuchs K, Capell A, Multhaup G, Condron MM, Teplow DB, Haass C: Presenilin-dependent gamma-secretase processing of beta-amyloid precursor protein at a site corresponding to the S3 cleavage of Notch. EMBO Rep 2001;2:835–841.

12 Steiner H, Winkler E, Edbauer D, Prokop S, Basset G, Yamasaki A, Kostka M, Haass C: PEN-2 is an integral component of the gamma-secretase complex required for coordinated expression of presenilin and nicastrin. J Biol Chem 2002;277:39062–39065.

13 Lee SF, Shah S, Li H, Yu C, Han W, Yu G: Mammalian APH-1 interacts with presenilin and nicastrin and is required for intramembrane proteolysis of amyloid-beta precursor protein and Notch. J Biol Chem 2002; 277:45013–45019.

14 da Cruz e Silva OA, Iverfeldt K, Oltersdorf T, Sinha S, Lieberburg I, Ramabhadran TV, Suzuki T, Sisodia SS, Gandy S, Greengard P: Regulated cleavage of Alzheimer beta-amyloid precursor protein in the absence of the cytoplasmic tail. Neuroscience 1993;57:873–877.

15 da Cruz e Silva EF, da Cruz e Silva OA: Protein phosphorylation and APP metabolism. Neurochem Res 2003;28:1553–1561.

16 da Cruz e Silva EF, da Cruz e Silva OA, Zaia CT, Greengard P: Inhibition of protein phosphatase 1 stimulates secretion of Alzheimer amyloid precursor protein. Mol Med 1995;1: 535–541.

17 Hung AY, Haass C, Nitsch RM, Qiu WQ, Citron M, Wurtman RJ, Growdon JH, Selkoe DJ: Activation of protein kinase C inhibits cellular production of the amyloid beta-protein. J Biol Chem 1993;268:22959–22962.

18 Ando K, Oishi M, Takeda S, Iijima K, Isohara T, Nairn AC, Kirino Y, Greengard P, Suzuki T: Role of phosphorylation of Alzheimer's amyloid precursor protein during neuronal differentiation. J Neurosci 1999;19:4421–4427.

19 Suzuki T, Oishi M, Marshak DR, Czernik AJ, Nairn AC, Greengard P: Cell cycle-dependent regulation of the phosphorylation and metabolism of the Alzheimer amyloid precursor protein. EMBO J 1994;13:1114–1122.

20 Buxbaum JD, Gandy SE, Cicchetti P, Ehrlich ME, Czernik AJ, Fracasso RP, Ramabhadran TV, Unterbeck AJ, Greengard P: Processing of Alzheimer beta/A4 amyloid precursor protein: modulation by agents that regulate protein phosphorylation. Proc Natl Acad Sci USA 1990;87:6003–6006.

21 Buxbaum JD, Koo EH, Greengard P: Protein phosphorylation inhibits production of Alzheimer amyloid beta/A4 peptide. Proc Natl Acad Sci USA 1993;90:9195–9198.

22 Caporaso GL, Gandy SE, Buxbaum JD, Ramabhadran TV, Greengard P: Protein phosphorylation regulates secretion of Alzheimer beta/A4 amyloid precursor protein. Proc Natl Acad Sci USA 1992;89:3055–3059.

23 Gandy SE, Caporaso GL, Buxbaum JD, da Cruz Silva O, Iverfeldt K, Nordstedt C, Suzuki T, Czernik AJ, Nairn AC, Greengard P: Protein phosphorylation regulates relative utilization of processing pathways for Alzheimer beta/A4 amyloid precursor protein. Ann NY Acad Sci 1993;695:117–121.

24 Lai A, Sisodia SS, Trowbridge IS: Characterization of sorting signals in the beta-amyloid precursor protein cytoplasmic domain. J Biol Chem 1995;270:3565–3573.

25 da Cruz e Silva OAB, Vieira SI, Rebelo S, da Cruz e Silva EF: A model system to study intracellular trafficking and processing of the Alzheimer's Amyloid Precursor Protein. Neurodegenerative Dis 2004;1:196–204.

26 Rebelo S, Henriques AG, da Cruz e Silva EF, da Cruz e Silva OA: Effect of cell density on intracellular levels of the Alzheimer's amyloid precursor protein. J Neurosci Res 2004; 76:406–414.

27 Amador FC, Henriques AG, da Cruz e Silva OAB, da Cruz e Silva EF: Monitoring protein phosphatase 1 isoform levels as a marker for cellular stress. Neurotoxicol Teratol 2004; 26:387–395.

28 Wiltfang J, Esselmann H, Cupers P, Neumann M, Kretzschmar H, Beyermann M, Schleuder D, Jahn H, Ruther E, Kornhuber J, Annaert W, De Strooper B, Saftig P: Elevation of beta-amyloid peptide 2–42 in sporadic and familial Alzheimer's disease and its generation in PS1 knockout cells. J Biol Chem 2001;276:42645–42657.

29 Esselmann H, Maler JM, Kunz N, Otto M, Paul S, Lewczuk P, Rüther E, Kornhuber J, Wiltfang J: Lithium decreases secretion of A1–42 and C truncated species A 1–37/38/39/40 in chicken telencephalic cultures but specifically increases intracellular A 1–38. Neurodegenerative Dis 2004;1:236–241.

30 Greenfield JP, Tsai J, Gouras GK, Hai B, Thinakaran G, Checler F, Sisodia SS, Greengard P, Xu H: Endoplasmic reticulum and trans-Golgi network generate distinct populations of Alzheimer beta-amyloid peptides. Proc Natl Acad Sci USA 1999;96:742–747.

31 Nakagawa T, Zhu H, Morishima N, Li E, Xu J, Yankner BA, Yuan J: Caspase-12 mediates endoplasmic-reticulum-specific apoptosis and cytotoxicity by amyloid-beta. Nature 2000;403:98–103.

32 Mattson MP, Chan SL: Dysregulation of cellular calcium homeostasis in Alzheimer's disease: bad genes and bad habits. J Mol Neurosci 2001;17:205–224.

33 Kudo T, Okumura M, Imaizumi K, Araki W, Morihara T, Tanimukai H, Kamagata E, Tabuchi N, Kimura R, Kanayama D, Fukumori A, Tagami S, Okochi M, Kubo M, Tanii H, Tohyama M, Tabira T, Takeda M: Altered localization of amyloid precursor protein under endoplasmic reticulum stress. Biochem Biophys Res Commun 2006;344:525–530.

34 Erickson RR, Dunning LM, Olson DA, Cohen SJ, Davis AT, Wood WG, Kratzke RA, Holtzman JL: In cerebrospinal fluid ER chaperones ERp57 and calreticulin bind beta-amyloid. Biochem Biophys Res Commun 2005;332:50–57.

35 Rizzuto R, Pinton P, Carrington W, Fay FS, Fogarty KE, Lifshitz LM, Tuft RA, Pozzan T: Close contacts with the endoplasmic reticulum as determinants of mitochondrial Ca^{2+} responses. Science 1998;280:1763–1766.

36 Levine T, Loewen C: Inter-organelle membrane contact sites: through a glass, darkly. Curr Opin Cell Biol 2006;18:371–378.

37 Mattson MP, LaFerla FM, Chan SL, Leissring MA, Shepel PN, Geiger JD: Calcium signaling in the ER: its role in neuronal plasticity and neurodegenerative disorders. Trends Neurosci 2000;23:222–229.

38 Shin RW, Saido TC, Maeda M, Kitamoto T: Novel alpha-secretase cleavage of Alzheimer's amyloid beta precursor protein in the endoplasmic reticulum of COS7 cells. Neurosci Lett 2005;376:14–19.

39 Nitsch RM, Wurtman RJ, Growdon JH: Regulation of APP processing. Potential for the therapeutical reduction of brain amyloid burden. Ann NY Acad Sci 1996;777:175–182.

40 da Cruz e Silva OA, Fardilha M, Henriques AG, Rebelo S, Vieira S, da Cruz e Silva EF: Signal transduction therapeutics: relevance for Alzheimer's disease. J Mol Neurosci 2004;23:123–142.

J Mol Neurosci (2007) 32:1–8
DOI 10.1007/s12031-007-0001-z

Tyr^{687} Dependent APP Endocytosis and Abeta Production

Sandra Rebelo · Sandra Isabel Vieira · Hermann Esselmann · Jens Wiltfang · Edgar F. da Cruz e Silva · Odete A. B. da Cruz e Silva

Received: 26 October 2006 / Accepted: 27 November 2006 / Published online: 5 April 2007

Abstract The neurotoxic Abeta peptide is derived by proteolytic processing from the Alzheimer's amyloid precursor protein (APP), whose short cytoplasmic domain contains several phosphorylatable amino acids. The latter can be phosphorylated 'in vitro' and 'in vivo,' and in some cases phosphorylation appears to be associated with the disease condition. Using APP-GFP fusion proteins to monitor APP processing, the role of Tyr^{687} was addressed by mimicking its constitutive phosphorylation (Y687E) and dephosphorylation (Y687F). Contrasting effects on subcellular APP distribution were observed. Y687E-APP-GFP was targeted to the membrane but could not be detected in transferrin containing vesicular structures, and exhibited a concomitant and dramatic decrease in Abeta production. In contrast, Y687F-APP-GFP was endocytosed similarly to wild type APP, but was relatively favoured for beta-secretase cleavage. Overall, Tyr^{687} appears to be a critical residue determining APP targeting and processing via different pathways, including endocytosis and retrograde transport. Significantly, from a disease perspective, mimicking Tyr^{687} phosphorylation resulted in a hitherto undescribed inhibition of Abeta production. Our results provide novel insights into the role of direct APP phosphorylation on APP targeting, processing and Abeta production.

Keywords APP phosphorylation · Tyr^{687} · Endocytosis · Abeta · APP processing

S. Rebelo · S. I. Vieira · O. A. B. da Cruz e Silva (✉)
Laboratório de Neurociências, Centro de Biologia Celular,
Universidade de Aveiro,
3810-193 Aveiro, Portugal
e-mail: odetecs@bio.ua.pt

H. Esselmann · J. Wiltfang
Molecular Neurobiology Laboratory, Department of Psychiatry and Psychotherapy, University of Erlangen-Nuremberg,
Erlangen, Germany

E. F. da Cruz e Silva
Laboratório de Transdução de Sinais, Centro de Biologia Celular,
Universidade de Aveiro,
Aveiro, Portugal

Introduction

Alzheimer's disease (AD) is progressive and multifactorial. One of the major pathological hallmarks is the presence of amyloid plaques, rich in Abeta peptides. The latter range from 37–42 amino acids, and result from the sequential proteolytic cleavage of the Alzheimer's Amyloid Precursor Protein (APP). APP can be cleaved by α-secretases [ADAM 10, ADAM 17 (TACE) and ADAM 9] at various subcellular locations, generating alpha cleaved sAPP ($_{\alpha}$sAPP), but can also be processed by β-secretases (BACE1 and BACE2) to yield beta cleaved sAPP ($_{\beta}$sAPP). Further cleavage by the γ-secretase complex (presenilin-1 or 2, nicastrin, aph1 and pen2) (Esler et al. 2002; Lee et al. 2000; Li et al. 2000a, b; Steiner et al. 2002; Verdile et al. 2006) produces either p3 or Abeta and the AICD (APP Intra-Cellular Domain) fragment comprising 50 amino acids (Bennett et al. 2000; Vassar et al. 1999; Yan et al. 2001). Abeta production can occur in the Golgi complex, especially in the trans-Golgi network (TGN), and to a lesser extent in the endoplasmic reticulum (ER). Abeta can also be produced in the endocytic pathway (Koo and Squazzo 1994; Nixon et al. 2001; Perez et al. 1999).

Although the precise function of APP is unclear, it exhibits characteristics of a signal transduction molecule. In fact,

several proteins (e.g. FE65) interact with the cytoplasmic domain of APP (Borg et al. 1999; Bressler et al. 1996; da Cruz e Silva et al. 2004a; Kinoshita et al. 2002; McLoughlin and Miller 1999; Sabo et al. 2001), forming large multimolecular complexes. The adaptor proteins direct APP to specific molecular pathways. Such interactions can be regulated by protein phosphorylation, as described for FE65 binding (Ando et al. 2001), and APP itself can be phosphorylated 'in vitro' and 'in vivo' (Ando et al. 2001; Oishi et al. 1997; Tarr et al. 2002; Zambrano et al. 2001). Lee et al. (2003) demonstrated that seven of the eight potentially phosphorylatable residues in the intracellular domain of APP were phosphorylated in AD patients, namely Tyr^{653}, Ser^{655}, Thr^{668}, Ser^{675}, Tyr^{682}, Thr^{686} and Tyr^{687}. The latter lies within the ^{682}YENPTY^{687} domain, a typical internalization signal for membrane-associated receptor proteins (Chen et al. 1990; Koo and Squazzo 1994; Lai et al. 1995), which conforms to a consensus sequence for coated-pit mediated internalization (Chen et al. 1990). This domain is of significant biophysical importance, bearing a characteristic type I β-turn (Kroenke et al. 1997; Ramelot et al. 2000), and central to protein–protein interactions, as for example with X11 (Ramelot et al. 2000) and Dab 1 (Homayouni et al. 1999). Thus, in the work here described we used a dynamic model system (da Cruz e Silva et al. 2004b) to evaluate the effect of mimicking Tyr^{687} phosphorylation. The data presented indicates that APP subcellular localization and incorporation into vesicular structures is Tyr^{687} dependent. In particular, the Y687E mutant, mimicking Tyr^{687} phosphorylation, failed to incorporate into visible endocytic vesicular structures and exhibited greatly reduced Abeta production in the conditioned media.

Materials and Methods

APP_{695} Expression Vectors

APP_{695} cDNA mutants were prepared to mimic a phosphorylated or dephosphorylated Tyr^{687} residue (glutamate or phenylalanine, respectively), using site directed mutagenesis (da Cruz e Silva and da Cruz e Silva 2003; da Cruz e Silva et al. 2004b). APP phosphorylation mimicking mutants and Wt-APP_{695} cDNAs were subcloned into appropriate vectors and their nucleotide sequences confirmed. Both mutant and Wt-APP_{695}-GFP fusions were engineered by PCR, removing the APP_{695} stop codon using specifically designed primers. The fusion constructs were produced by inserting the resultant fragments in frame into the pEGFP-N1 mammalian expression vector (Clontech, USA). The nucleotide sequences of the inserts were fully verified by DNA sequencing.

Cell Culture and Endocytosis Assays

Monkey kidney COS-7 cells were grown at 37°C and 5% CO_2 in Dulbecco's Modified Eagle's Medium (DMEM), supplemented with 10% foetal bovine serum, 100 U/ml penicillin, 100 mg/ml streptomycin and 3.7 g/l $NaHCO_3$, until 90% confluent (Rebelo et al. 2004). Transient transfections were performed using a cationic lipid transporter (LipofectAMINE 2000, Invitrogen Life Technologies). After 8 h, cells were divided into six-well plates with (for endocytosis analysis) or without (for Abeta quantification) coverslips pre-treated with 100 μg/ml polyornithine (Sigma, Portugal), and left to recover for 4 h. Cells were then incubated in serum-free DMEM supplemented with a protein synthesis inhibitor, 50 μg/ml cycloheximide (Sigma, Portugal), and processed as described below.

Transferrin endocytosis assays were performed on the transiently transfected cells essentially as previously described (Benmerah et al. 1998). Following a 2 h 15 min incubation period under the conditions described above, cells were washed with antimycotic/antibiotic-free DMEM. The endocytosis experiment was initiated by incubating cells for 30 min at 37°C with antimycotic/antibiotic-free DMEM supplemented with cycloheximide and with 20 mM HEPES, in order to eliminate endogenous transferrin. The medium was replaced with fresh medium supplemented with 1 mg/ml BSA and 100 nM Texas Red-conjugated transferrin (Molecular Probes, USA), and the cells were incubated for a further 15 min at 37°C (Benmerah et al. 1998). Cells were then immediately cooled to 4°C, washed twice in ice-cold PBS and fixed as described below.

Alternatively, an antibody uptake assay was also used to monitor APP internalization. COS-7 cells were transiently transfected, prepared as described above and incubated for 2 h. Cells were then washed twice with ice-cold PBS and incubated for 20 min on ice in serum-free DMEM supplemented with the 22C11 antibody (Chemicon, USA). Cells were subsequently washed three times with ice-cold PBS and then incubated at 37°C in DMEM supplemented with 10% foetal bovine serum for 0, 10, and 20 min. At each time point the cells were washed twice with PBS, fixed in 4% paraformaldehyde and processed for immunocytochemistry. Texas Red-conjugated anti-mouse IgG (Molecular Probes, USA) was used as a secondary antibody.

Abeta Analysis

Cells transfected with Wt or each of the mutant APP constructs were incubated for 3 h as described above. Abeta peptides were detected and quantitated essentially as previously described (Esselmann et al. 2004; Wiltfang et al. 2001). Conditioned media were immunoprecipitated using 25 μl dynabeads (Dynal, Germany) coated with 1E8 mAb

(Schering AG, Berlin). Immunoprecipitates were separated on 12% Bicine/Tris gels containing 8 M urea. Different Abeta peptide species were revealed by immunoblotting using mAb 1E8. Synthetic Abeta peptides were run in parallel for the identification of the different Abeta peptide species.

Immunoblots or the corresponding autoradiograms were scanned in a Molecular Imager (Bio-Rad, Portugal) and protein bands quantified using the manufacturer's Quantity One densitometry software. Data were expressed as mean ± SEM of determinations from at least three independent experiments. Statistical significance was conducted by one-way analysis of variance (ANOVA) with Tukey-Kramer test. Unless otherwise noted, a level of statistical significance is considered $P < 0.05$.

Results

Endocytosis Assays

Intracellular protein tracking was achieved by engineering APP_{695}-GFP fusion constructs, and the saturation of intracellular pathways due to protein overexpression was avoided by using relatively low transfection levels and by blocking 'de novo' protein synthesis (da Cruz e Silva et al. 2004b). In essence, COS-7 cells were transfected with wild type (Wt-APP_{695}-GFP) or either of the two Tyr^{687} mutant human APP cDNAs (Y687E-APP_{695}-GFP and Y687F-APP_{695}-GFP). Endocytosis and processing of mutant and wild type proteins was monitored as described above. Both Wt-APP-GFP and Y687F-APP-GFP were efficiently endocytosed, as demonstrated for both constructs by the speckled vesicular-like green fluorescent structures observed (Fig. 1a). The co-localization of APP_{695}-GFP green fluorescence and transferrin-Texas red fluorescence observed for Wt-APP-GFP and the dephospho-mimicking Y687F-APP-GFP mutant (Fig. 1c) revealed that transferrin was co-localizing with APP, thus reinforcing that both of these APP species are readily internalized. Interestingly, Y687F-APP-GFP appeared to be endocytosed approximately 1.5 × more efficiently than Wt-APP-GFP, as estimated by counting the number of co-localizing yellow vesicles detected (data not shown). In sharp contrast, the phospho-mimicking Y687E-APP-GFP mutant could not be detected in vesicular-like structures. This is evident in Fig. 1a, when fluorescence due to Y687E-APP-GFP alone is analysed or when the number of co-localizing yellow/orange vesicles are scored (Fig. 1c). In fact, the number of yellow/orange vesicles was dramatically reduced in cells transfected with Y687E-APP-GFP, leading us to conclude that this mutant protein is not efficiently endocytosed via clathrin-coated pits.

In order to assess if the green fluorescence detected in cytoplasmic vesicles was due to the presence of intact or truncated APP species, the internalization of the three proteins was further monitored by tracking their *N*- and *C*-termini during endocytosis using the antibody uptake assay described. At time 0 all cells revealed 22C11-staining at the cell surface (red fluorescence), although with a stronger intensity for Y687E-APP-GFP (Fig. 2A). Observation of the cells after 10 min at 37°C indicated that both Wt-APP-GFP and the Y687F-APP-GFP mutant were efficiently endocytosed (Fig. 2B), and the red (22C11) and green (APP-GFP) fluorescence co-localized extensively. Analysis of the GFP fluorescence alone also revealed that the two APP species are readily internalized. Noticeably, at this time point, many of the endocytic vesicles observed for Y687F-APP-GFP

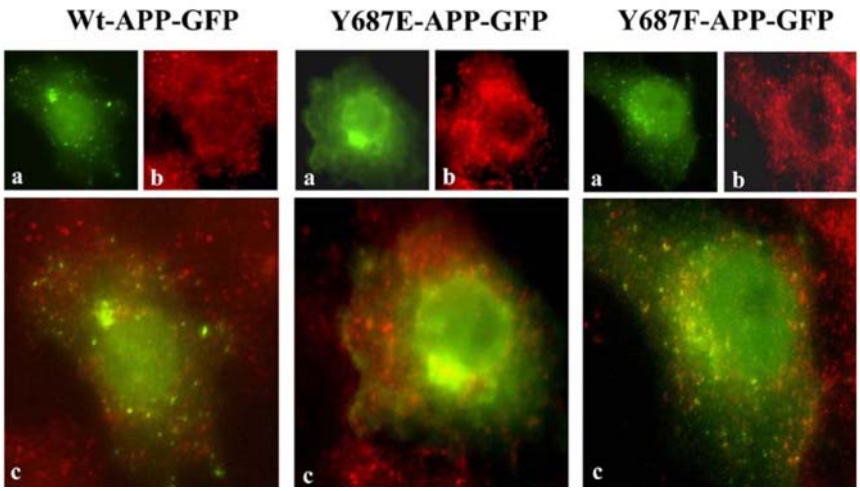

Fig. 1 Transferrin Assays. Internalization of Texas Red-conjugated transferrin was monitored in COS-7 cells transiently transfected with Wt-APP-GFP or either of the phospho-mimicking APP-GFP constructs. **a** APP-GFP fluorescence, **b** Transferrin-Texas red fluorescence, **c** Merged images of **a** and **b**

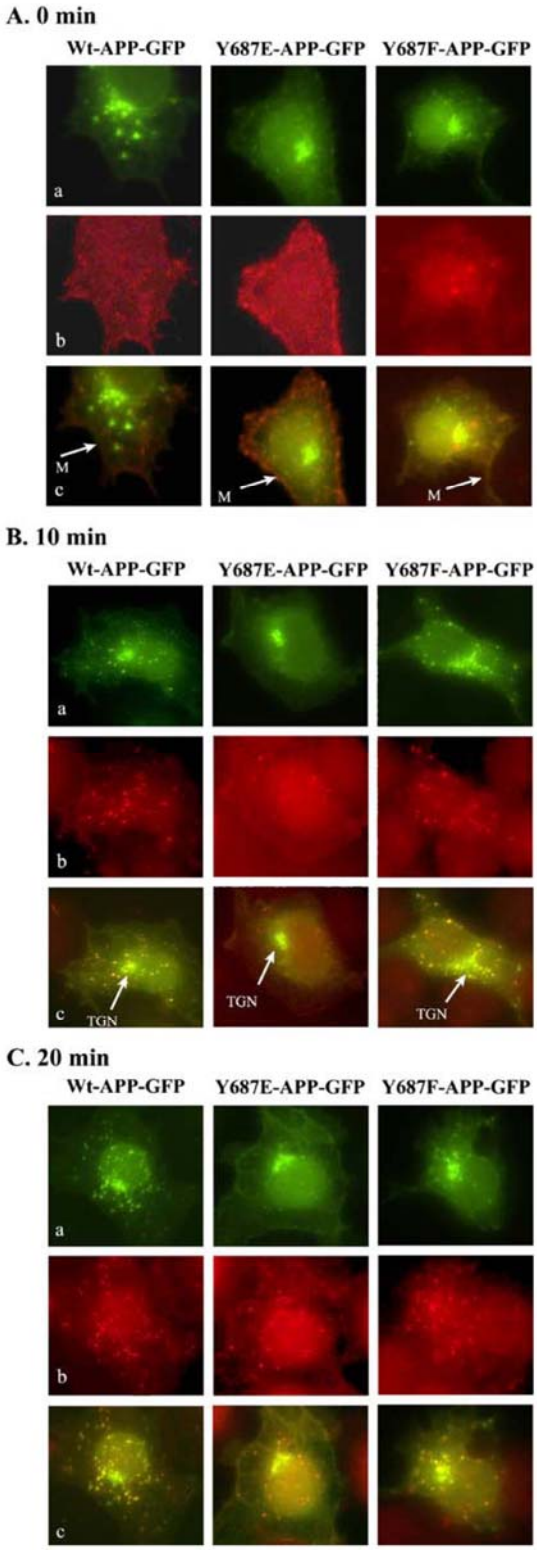

were already organized near the Golgi complex, consistent with Tyr^{687} dephosphorylated APP being endocytosed more efficiently/faster than Wt-APP-GFP. In contrast, the Y687E-APP-GFP mutant (mimicking phosphorylation) was not efficiently incorporated into vesicles and endocytosis of this mutant was not evident under our experimental conditions. Of note, the membrane staining remained intense, supporting poor endocytosis for this mutant (Fig. 2B). Unexpectedly, after 20 min at 37°C, Y687E-APP-GFP green fluorescence and the 22C11 staining were seen to co-localize in the vicinity of the TGN, suggesting that the phosphorylated protein may eventually also be internalized, albeit via a different route. On the other hand, and as for earlier time points, the Wt-APP-GFP and the Y687F-APP-GFP proteins continued to co-localize extensively in endocytic vesicles at 20 min. (Fig. 2C). Again, Y687F-APP-GFP appears to be more efficiently endocytosed and targeted for retrograde transport, as co-localization is clearly visible in the TGN. TGN co-localization for Wt-APP-GFP was much less marked. The Y687E-APP-GFP mutant, which as already mentioned is not visibly endocytosed, exhibits intense fluorescence at the cell membrane reinforcing that this mutant suffers impaired internalization (Fig. 2C). During the course of the experiment the vast majority of vesicles observed in cells expressing Y687E-APP-GFP stained red due to 22C11 binding to endogenously expressed APP, again supporting the hypothesis that this APP is not targeted to the vesicular structures normally visible.

Abeta Production

Abeta fragments secreted into the medium of cells transfected with the three constructs were quantitated as previously described (Esselmann et al. 2004; Wiltfang et al. 2001, 2002). This methodology allows for the separation, detection and quantitation of different Abeta species, including $Abeta_{1–37}$, $Abeta_{1–38}$, $Abeta_{1–39}$, $Abeta_{1–40}$, and $Abeta_{2–40}$. The results obtained with the three constructs are presented in Fig. 3. Y687F-APP-GFP and Wt-APP-GFP yielded a similar profile of Abeta production. Namely the Abeta species 1–37, 1–38, 1–39 and 1–40 were all clearly evident. A lower doublet (Fig. 3B) was also observed with the lower band co-migrating exactly with the $Abeta_{2–40}$ standard and the upper band was not defined. The Y687E-

◀**Fig. 2** Antibody Uptake Assays. The uptake of the 22C11 monoclonal antibody recognizing an epitope in the extracellular *N*-terminal domain of APP was monitored in COS-7 cells transiently transfected with Wt-APP-GFP or either of the phospho-mimicking APP-GFP constructs. Cells were monitored at 0 min (**A**), 10 min (**B**) and 20 min (**C**) after stimulation of antibody uptake. **a** APP-GFP fluorescence, **b** Transferrin-Texas red fluorescence, **c** Merged images of a and b. *M*—Plasma Membrane, *TGN*—Trans Golgi Network

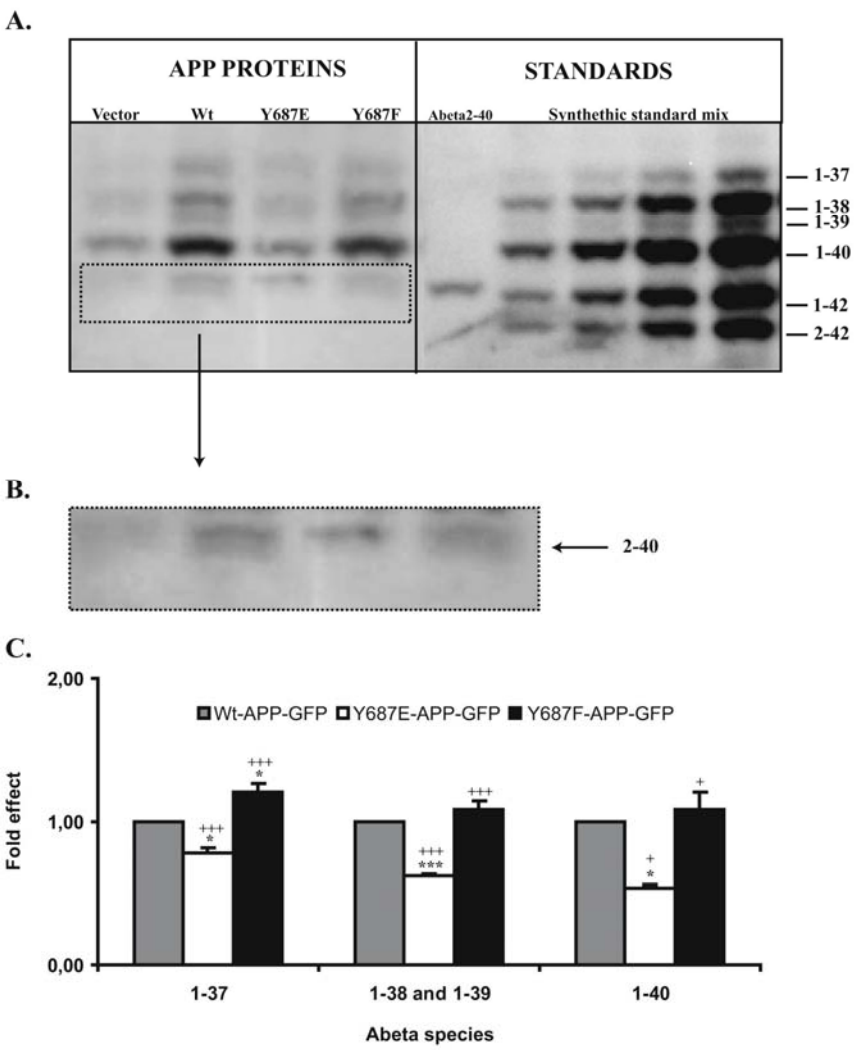

Fig. 3 Secretion of Abeta peptides. Conditioned media from cells transfected with one of the three constructs (Wt-APP-GFP, Y687E-APP-GFP and Y687F-APP-GFP) were collected and analyzed for Abeta production as described. Abeta production from endogenous APP was assessed from control cells transfected with the empty vector. Results were compared against a standard synthetic mix containing synthetic Abeta peptides of known size (**A**). The gel region corresponding to the $Abeta_{2-40}$ doublet was amplified (**B**). The intensities of the Abeta species observed (**C**) were quantified using a molecular imager with image analysis software (Quantity One)

APP-GFP protein, in contrast, produced significantly less of all Abeta species measured: $Abeta_{1-37}$ ($P < 0.05$), $Abeta_{1-38 \text{ and } 1-39}$ ($P < 0.001$) and $Abeta_{1-40}$ ($P < 0.05$), with $Abeta_{2-40}$ being almost completely absent (Fig. 3A–C).

Discussion

Protein phosphorylation as a regulatory mechanism in APP processing has been long been discussed (Gandy and Greengard 1994), however the precise molecular contributions have only recently began to be unravelled. In the work discussed here, low transfection levels and the use of cycloheximide to inhibit 'de novo' protein synthesis were vital to avoid overloading the normal APP processing pathways, thus allowing direct comparison of the intracellular localization of the Wt and Tyr^{687} phosphorylation site mutant APP-GFP proteins by epifluorescence. It is well established that APP has characteristics associated with cell surface receptors, can be re-internalized via clathrin-coated pits and be directed to the endosomal-lysosomal pathway. In our experimental system both Wt-APP-GFP and Y687F-APP-GFP were readily re-internalized via the endocytic pathway, with the 'dephosphorylated' mimicking protein being processed somewhat faster and more efficiently than the wild-type protein (Figs. 1, 2). In sharp contrast, the mutant mimicking phosphorylation on Tyr^{687}, Y687E-APP-GFP, was not incorporated into detectable vesicular structures (Figs. 1, 2), thus indicating that the membrane recycling of Y687E-APP-GFP is impaired. Nonetheless, the Y687E-APP-GFP protein was internalized, apparently via an alternative pathway which does not involve its incorpo-

ration into visible vesicles, as evidenced by the absence of the yellow/orange vesicular like structures, although yellow fluorescence could still be detected in the vicinity of the TGN (Fig. 2C). From our results, given the antagonic effects of mutating Try^{687} to Phenylalanine and Glutamate in comparison to the wild-type protein, it is reasonable to deduce that the phosphorylation state of Tyr^{687} results in the formation of different multimeric complexes which are differentially targeted. In fact, we have already initiated the analysis of the phosphorylation dependent APP interactome. An array of different APP binding proteins have been identified (unpublished data), depending on the residue of APP which is phosphorylated. This is not entirely unexpected if one considers for example that phosphorylation of APP at Thr^{668} affects its binding to FE65 (Nakaya and Suzuki 2006).

As a consequence of differential APP targeting, it appears that Tyr^{687} phosphorylated APP undergoes increased α-secretase processing, whereas its dephosphorylated counterpart appears to be relatively more favoured for β-secretase cleavage, as determined from sAPP production (data not shown). Direct measurement of Abeta secretion entirely supports this hypothesis (Fig. 3). Y687E-APP-GFP exhibited reduced Abeta production, with the almost complete absence of Abeta$_{2-40}$. Targeting and processing of APP via different pathways is important for Abeta production and the phosphorylation state of Tyr^{687} appears to be a critical determining factor. Hence, if one accepts that Y687E-APP-GFP mimics constitutive phosphorylation of Tyr^{687} and that Y687F-APP-GFP mimics its constitutive dephosphorylation, then it is reasonable to conclude that phosphoregulation of Tyr^{687} is an important regulatory mechanism not only for the incorporation of APP into endocytic vesicular structures and in regulating its transport from endosomes to the TGN, but this is also of consequence to APP proteolytic cleavages and Abeta production. Tyr^{687} phosphorylation has been described in samples from AD patients (Lee et al. 2003) where Abeta is found deposited in senile plaques. Hence, this appears contrary to what our results suggest, since Tyr^{687} phosphorylation produces less Abeta. However, one can envisage a protective endogenous mechanism at play, whereby Tyr^{687} phosphorylation reduces Abeta production, in a brain already producing excess of this toxic peptide. Notably, although Y687E-APP-GFP is not incorporated into visible vesicles, it is still processed, producing the other usual APP cleavage fragments. In fact, this partly explains why until now it has been difficult to detect differences in APP processing associated with direct phosphorylation of this intracellular domain. One is also forced to conclude that Y687E-APP is targeted and processed via an alternative pathway, potentially non-vesicular or otherwise involving vesicular structures/complexes below our detection limit. Of note, the simple measurement of APP proteolytic products provides no information as to the subcellular site of production and, indeed, they are likely to be produced at different subcellular locations. From our data it would appear that phospho-Tyr^{687} APP, although re-internalized to the ER and TGN, can still be cleaved by α-, β- and γ-secretases. This observation is consistent with the suggestion of Capell et al. (2005) that the γ-secretase complex could be completely assembled within the ER.

Our results showing that Abeta production can be modulated by direct APP phoshorylation may be of specific therapeutic relevance. It is interesting to note that the retrograde transport of BACE 1, responsible for the β-cleavage, is also regulated by the phosphorylation state of the protease (Wahle et al. 2005). Additionally, our conclusions favour the model that interaction of APP with its binding proteins may also be mediated by the phosphorylation state of APP itself (da Cruz e Silva et al. 2004a). Consequently, it may be possible to devise therapeutic strategies leading to decreased Abeta production, as observed here for Y687E-APP-GFP. Thus, signal transduction based diagnostics and therapeutics represent important future strategies of relevance to AD and other neurodegenerative diseases. The future identification of the kinases and phosphatases that act upon each of the APP phosphorylatable residues will likely prove useful in this respect.

Acknowledgements Supported by the EU V and VI Framework Programs (DIADEM and APOPIS), by the FCT (POCTI/CBO/34349/2001, POCTI/NSE/40682/2001 and POCTI/SAU-OBS/57394/2004) of the Portuguese Ministry of Science and Technology, and by CBC, Universidade de Aveiro. SR and SIV were recipients of PhD Fellowships (SFRH/BD/17693/2004 and Praxis XXI/BD/16218/1998).

JW was supported by grants from the German Federal Ministry of Education and Research (Competence Net Dementia, grant 01 GI 0420, Creutzfeldt-Jacob Disease Net, grant 01 GI 0301 and HBPP-NGFN2, grant 01 GR 0447).

References

Ando, K., Iijima, K. I., Elliot, J. I., Kirino, Y., & Suzuki, T. (2001). Phosphorylation-dependent regulation of the interaction of amyloid precursor protein with Fe65 affects the production of beta-amyloid. *Journal of Biological Chemistry, 276*, 40353–40361.

Benmerah, A., Lamaze, C., Begue, B., Schmid, S. L., Dautry-Varsat, A., & Cerf-Bensussan, N. (1998). AP-2/Eps15 interaction is required for receptor-mediated endocytosis. *Journal of Cell Biology, 140*, 1055–1062.

Bennett, B. D., Babu-Khan, S., Loeloff, R., Louis, J. C., Curran, E., Citron, M., et al. (2000). Expression analysis of BACE2 in brain and peripheral tissues. *Journal of Biological Chemistry, 275*, 20647–20651.

Borg, J. P., Lopez-Figueroa, M. O., de Taddeo-Borg, M., Kroon, D. E., Turner, R. S., Watson, S. J., et al. (1999). Molecular analysis of the X11-mLin-2/CASK complex in brain. *Journal of Neuroscience, 19*, 1307–1316.

Bressler, S. L., Gray, M. D., Sopher, B. L., Hu, Q., Hearn, M. G., Pham, D. G., et al. (1996). cDNA cloning and chromosome mapping of the human Fe65 gene: Interaction of the conserved cytoplasmic domains of the human beta-amyloid precursor protein and its homologues with the mouse Fe65 protein. *Human Molecular Genetics, 5*, 1589–1598.

Chen, W. J., Goldstein, J. L., & Brown, M. S. (1990). NPXY, a sequence often found in cytoplasmic tails, is required for coated pit-mediated internalization of the low-density lipoprotein receptor. *Journal of Biological Chemistry, 265*, 3116–3123.

Capell, A., Beher, D., Prokop, S., Steiner, H., Kaether, C., Shearman, M. S., et al. (2005). Gamma-secretase complex assembly within the early secretory pathway. *Journal of Biological Chemistry, 280*, 6471–6478.

da Cruz e Silva, E. F., & da Cruz e Silva, O. A. (2003). Protein phosphorylation and APP metabolism. *Neurochemical Research, 28*, 1553–1561.

da Cruz e Silva, O. A., Fardilha, M., Henriques, A. G., Rebelo, S., Vieira, S., & da Cruz e Silva, E. F. (2004a). Signal transduction therapeutics: Relevance for Alzheimer's disease. *Journal of Molecular Neuroscience, 23*, 123–142.

da Cruz e Silva, O. A., Vieira, S. I., Rebelo, S., & da Cruz e Silva, E. F. (2004b). A model system to study intracellular trafficking and processing of the Alzheimer's Amyloid Precursor Protein. *Neurodegenerative Diseases, 1*, 196–204.

Esler, W. P., Kimberly, W. T., Ostaszewski, B. L., Ye, W., Diehl, T. S., Selkoe, D. J., et al. (2002). Activity-dependent isolation of the presenilin-gamma-secretase complex reveals nicastrin and a gamma substrate. *Proceedings of the National Academy of Sciences of the United States of America, 99*, 2720–2725.

Esselmann, H., Maler, J. M., Kunz, N., Otto, M., Paul, S., Lewczuk, P., et al. (2004). Lithium decreases secretion of Aβ1-42 and C-truncated species Aβ1-37/38/39/40 in chicken telencephalic cultures but specifically increases intracellular Aβ1-38. *Neurodegenerative Diseases, 1*, 236–241.

Gandy, S., & Greengard, P. (1994). Regulated cleavage of the Alzheimer amyloid precursor protein: Molecular and cellular basis. *Biochimie, 76*, 300–303.

Homayouni, R., Rice, D. S., Sheldon, M., & Curran, T. (1999). Disabled-1 binds to the cytoplasmic domain of amyloid precursor-like protein 1. *Journal of Neuroscience, 19*, 7507–7515.

Kinoshita, A., Whelan, C. M., Berezovska, O., & Hyman, B. T. (2002). The gamma secretase-generated carboxyl-terminal domain of the amyloid precursor protein induces apoptosis via Tip60 in H4 cells. *Journal of Biological Chemistry, 277*, 28530–28536.

Koo, E. H., & Squazzo, S. L. (1994). Evidence that production and release of amyloid beta-protein involves the endocytic pathway. *Journal of Biological Chemistry, 269*, 17386–17389.

Kroenke, C. D., Ziemnicka-Kotula, D., Xu, J., Kotula, L., & Palmer, A. G. (1997). Solution conformations of a peptide containing the cytoplasmic domain sequence of the beta amyloid precursor protein. *Biochemistry, 36*, 8145–8152.

Lai, A., Sisodia, S. S., & Trowbridge, I. S. (1995). Characterization of sorting signals in the beta-amyloid precursor protein cytoplasmic domain. *Journal of Biological Chemistry, 270*, 3565–3573.

Lee, S. F., Shah, S., Li, H., Yu, C., Han, W., & Yu, G. (2000). Mammalian APH-1 interacts with presenilin and nicastrin and is required for intramembrane proteolysis of amyloid-beta precursor protein and Notch. *Journal of Biological Chemistry, 277*, 45013–45019.

Lee, M. S., Kao, S. C., Lemere, C. A., Xia, W., Tseng, H. C., Zhou, Y., et al. (2003). APP processing is regulated by cytoplasmic phosphorylation. *Journal of Cell Biology, 163*, 83–95.

Li, Y. M., Lai, M. T., Xu, M., Huang, Q., DiMuzio-Mower, J., Sardana, M. K., et al. (2000a). Presenilin 1 is linked with gamma-secretase activity in the detergent solubilized state. *Proceedings of the National Academy of Sciences of the United States of America, 97*, 6138–6143.

Li, Y. M., Xu, M., Lai, M. T., Huang, Q., Castro, J. L., DiMuzio-Mower, J., et al. (2000b). Photoactivated gamma-secretase inhibitors directed to the active site covalently label presenilin 1. *Nature, 405*, 689–694.

McLoughlin, D. M., & Miller, C. C. (1999). The intracellular cytoplasmic domain of the Alzheimer's disease amyloid precursor protein interacts with phosphotyrosine-binding domain proteins in the yeast two-hybrid system. *FEBS Letters, 397*, 197–200.

Nakaya, T., & Suzuki, T. (2006). Role of APP phosphorylation in FE65-dependent gene transactivation mediated by AICD. *Genes Cells, 11*, 633–645.

Nixon, R. A., Mathews, P. M., & Cataldo, A. M. (2001). The neuronal endosomal-lysosomal system in Alzheimer's disease. *Journal of Alzheimer's Disease, 3*, 97–107.

Oishi, M., Nairn, A. C., Czernik, A. J., Lim, G. S., Isohara, T., Gandy, et al. (1997). The cytoplasmic domain of Alzheimer's amyloid precursor protein is phosphorylated at Thr654, Ser655, and Thr668 in adult rat brain and cultured cells. *Molecular Medicine, 3*, 111–123.

Perez, R. G., Soriano, S., Hayes, J. D., Ostaszewski, B., Xia, W., Selkoe, D. J., et al. (1999). Mutagenesis identifies new signals for beta-amyloid precursor protein endocytosis, turnover, and the generation of secreted fragments, including Abeta42. *Journal of Biological Chemistry, 274*, 18851–18856.

Ramelot, T. A., Gentile, L. N., & Nicholson, L. K. (2000). Transient structure of the amyloid precursor protein cytoplasmic tail indicates preordering of structure for binding to cytosolic factors. *Biochemistry, 39*, 2714–2725.

Rebelo, S., Henriques, A. G., da Cruz E Silva, E. F., & da Cruz E Silva, A. O. B. (2004). Effect of cell density on intracellular levels of the Alzheimer's amyloid precursor protein. *Journal of Neuroscience Research, 76*, 406–414.

Sabo, S. L., Ikin, A. F., Buxbaum, J. D., & Greengard, P. (2001). The Alzheimer amyloid precursor protein (APP) and FE65, an APP-binding protein, regulate cell movement. *Journal of Cell Biology, 153*, 1403–1414.

Steiner, H., Winkler, E., Edbauer, D., Prokop, S., Basset, G., Yamasaki, A., et al. (2002). PEN-2 is an integral component of the gamma-secretase complex required for coordinated expression of presenilin and nicastrin. *Journal of Biological Chemistry, 277*, 39062–39065J.

Tarr, P. E., Contursi, C., Roncarati, R., Noviello, C., Ghersi, E., Scheinfeld, M. H., et al. (2002). Evidence for a role of the nerve growth factor receptor TrkA in tyrosine phosphorylation and processing of beta-APP. *Biochemical and Biophysical Research Communications, 295*, 324–329.

Vassar, R., Bennett, B. D., Babu-Khan, S., Kahn, S., Mendiaz, E. A., Denis, P., et al. (1999). Beta-secretase cleavage of Alzheimer's amyloid precursor protein by the transmembrane aspartic protease BACE. *Science, 286*, 735–741.

Verdile, G., Gandy, S. E., Martins, R. N. (2006). The Role of Presenilin and its Interacting Proteins in the Biogenesis of Alzheimer's Beta Amyloid. Neurochemical Research 2006 Aug 31, in press.

Wahle, T., Prager, K., Raffler, N., Haass, C., Famulok, M., & Walter, J. (2005). GGA proteins regulate retrograde transport of BACE1 from endosomes to the trans-Golgi network. *Molecular and Cellular Biochemistry, 29*, 453–461.

Wiltfang, J., Esselmann, H., Cupers, P., Neumann, M., Kretzschmar, H., Beyermann, M., et al. (2001). Elevation of beta-amyloid

peptide 2-42 in sporadic and familial Alzheimer's disease and its generation in PS1 knockout cells. *Journal of Biological Chemistry, 276*, 42645–42657.

Wiltfang, J., Esselmann, H., Bibl, M., Smirnov, A., Otto, M., Paul, S., et al. (2002). Highly conserved and disease-specific patterns of carboxyterminally truncated Abeta peptides 1-37/38/39 in addition to 1-40/42 in Alzheimer's disease and in patients with chronic neuroinflammation. *Journal of Neurochemistry, 81*, 481–496.

Yan, R., Munzner, J. B., Shuck, M. E., & Bienkowski, M. J. (2001). BACE2 functions as an alternative alpha-secretase in cells. *Journal of Biological Chemistry, 276*, 34019–34027.

Zambrano, N., Bruni, P., Minopoli, G., Mosca, R., Molino, D., Russo, C., et al. (2001). The beta-amyloid precursor protein APP is tyrosine-phosphorylated in cells expressing a constitutively active form of the Abl protoncogene. *Journal of Biological Chemistry, 276*, 19787–19792.

CHAPTER IV

CHAPTER IV

APP PROTEIN-PROTEIN INTERACTIONS MEDIATED BY THE NPTY DOMAIN

The results reported in Chapter III revealed antagonic effects of mutating Tyr^{687} to phenylalanine and glutamate, in comparison to the wild-type protein. It is resasonable to deduce that the phosphorylation state of Tyr^{687} may results in the formation of different multimeric complexes which are differently targeted. In fact, we have already initiated the analysis of the phosphorylation dependent APP interactome. An array of different APP binding proteins have been identified (unpublished data). RTN3-B is a novel APP interacting protein that was isolated when either the Wt-APP protein or the Y687F mutant protein was used as bait in a Yeast Two Hybrid screen. Further details are presented in the first paper of this section (Rebelo et al. 2008, in preparation).

Our conclusions so far, favour the model that interaction of APP with the binding proteins may also be mediated by the phosphorylation state of APP itself (da Cruz e silva et al. 2004). This is not a surprise if one considers for instance that the phosphorylation of APP at Thr^{668} affects its binding to FE65. Curiously, FE65 which binds at the ^{682}YENPTY^{687} domain of APP also depends on the phosphorylation state of Thr^{668} on the ^{667}VTPEER^{672} domain. When phosphorylated at Thr^{668}, AICD is no longer stabilized by FE65, and associates less with the latter. Indeed, the phosphorylation of APP at Thr^{668} had already been shown to affect the interaction between APP and FE65, probably because the phosphorylation of this residue induces structural changes from *trans*- to *cis*-conformations in the C-terminal domain of the protein (Ramelot and Nicholson 2001).

The hypothesis that subcellular targeting, as one might expect, involves APP binding proteins, which are in turn regulated by protein phosphorylation, deserves further investigation. This is addressed in the second paper of this section where we have shown that FE65 binds simultaneously to APP and PP1γ, both in neuronal and non-neuronal cell lines. The tri-complex was also detected in adult rat brain. Additionally, we demonstrated that FE65 is the bridging protein between APP and PP1γ (Rebelo et al. 2008, submitted).

da Cruz e Silva AO, Fardilha M, Henriques AG, Rebelo S, Vieira S, da Cruz e Silva EF.20004. Signal transduction therapeutics: relevance for Alzheimer's disease. J Mol Neurosci 23, 123-142.

Ramelot TA, Nicholson LK. 2001. Phosphorylation-induced structural changes in the amyloid precursor protein cytoplasmic tail detected by NMR. J Mol Biol 307(3):871-884.

Rebelo S, Domingues SCTS, Alves, R, da Cruz e Silva EF, da Cruz e Silva, OAB. 2008. Reticulon3–B, a novel APP binding protein that favours non-amyloidogenic processing (in preparation).

Rebelo S, Domingues SCTS, Vintém APB, Vieira SI, Fardilha M, Esteves LC, Wu W, da Cruz e Silva EF, da Cruz e Silva OAB. 2008. FE65 is the bridging protein between APP and PP1 in a trimeric complex. Mol and Cell Neurosci. (submitted).

in preparation

RETICULON 3-B, A NOVEL APP INTERACTING PROTEIN THAT FAVOURS NON-AMYLOIDOGENIC PROCESSING

Sandra Rebelo[a], Sara C. T. S. Domingues[a], Renato Alves[a], Edgar F. da Cruz e Silva[b], Odete A. B. da Cruz e Silva[a]

[a]Laboratório de Neurociências, Centro de Biologia Celular, Universidade de Aveiro, Aveiro, Portugal

[b]Laboratório de Transducção de Sinais, Centro de Biologia Celular, Universidade de Aveiro, Aveiro, Portugal

Corresponding author:

Odete A. B. da Cruz e Silva
Laboratório de Neurociências,
Centro de Biologia Celular,
Secção Autónoma de Ciências da Saúde,
Universidade de Aveiro,
3810-193 Aveiro, Portugal
Tel: +351-234-370-778
Fax: +351-234-426-408
E-mail: odetecs@ua.pt

ABSTRACT

Alzheimer's disease (AD) is the most common age-related dementia. The amyloid precursor protein (APP) has a central role in the development of the disease, although its precise function remains undefined. Unveiling the APP interactome will contribute to understanding its function, as well as contributing towards potential therapeutic targets for the treatment of AD. In Yeast Two-Hybrid screens using Wt-APP as well as a dephosphorylation-mimicking mutant (Y687F-APP), Reticulon 3 (RTN3-B) was identified from a human brain cDNA library. RTN3 is a protein associated with the endoplasmic reticulum (ER) and is involved in membrane trafficking. This protein had been associated with AD as a negative regulator of BACE-1 activity. Our results showed that RTN3-B and APP interact both *in vivo* and in a Y2H system and co-localize in human cells lines. We also show that overexpression of RTN3-B leads to increased secretion of sAPP along with a decrease in the levels of holo-APP. Given that RTN3-B can bind both BACE-1 and APP, a putative functional model is proposed.

Keywords: Alzheimer 's disease, Reticulon 3, Protein interactions, BACE-1, APP phosphorylation, Endoplasmic reticulum.

INTRODUCTION

Alzheimer's disease (AD) is the most common age-related dementia among elderly. World widely it affected aproxiamately 30 million persons in 2006 and is estimated to affect 100 million persons in 2050 (Brookmeyer et al. 2007). AD is characterized by two major histopathological hallmarks; intracellular neurofibrillary tangles and extracellular amyloid plaques. Neurofibrillary tangles contain hyperphosphorylated tau protein, while the amyloid plaques are mainly composed of Abeta aggregates. Strong evidence suggests that altered processing of the amyloid precursor protein (APP) is one of the early events in AD pathogenesis (Roner 2004). The amyloid hypothesis predicts that an alteration in the proteolytic processing of APP may lead to increased Abeta production, which then leads to its accumulation, a primary event in the pathogenesis of AD (Newman et al. 2007). Moreover, APP can be processed by various pathways, which can be amyloidogenic or non-amyloidogenic. In the non-amyloidogenic pathway, APP is cleaved by an α-secretase, within the Abeta sequence, producing the alpha secreted APP fragment ($sAPP_{\alpha}$) and alpha C-terminal fragment ($_{\alpha}CTF$) or C83. The latter is further cleaved by the γ-secretase complex and to produce the p3 fragment and the APP intracellular domain (AICD). In the amyloidogenic pathway, APP is cleaved by a β-secretase resulting in two fragments, beta secreted APP fragment ($sAPP_{\beta}$) and beta C-terminal fragment ($_{\beta}CTF$) or C99. The $_{\beta}CTF$ is further cleaved by the γ-secretase complex producing Abeta and the AICD (Kern et al. 2006).

ADAM10 and ADAM17 metalloproteinases are responsible for α-cleavage (Buxbaum et al. 1998; Koike et al. 1999; Lammich et al. 1999), whereas β-cleavage at the APP N-terminal was shown to be catalyzed by BACE-1 (Hussain et al. 1999; Vassar et al. 1999). This enzyme has been localized in the Golgi apparatus and endosomes (Vassar et al. 1999), which are the subcellular compartments where Abeta is produced (Roner 2004). The γ-secretase is a macromolecular complex that results from the interaction between the presenilins, nicastrin, APH-1 and PEN-2 (Esler et al. 2002; Francis et al. 2002; Lee et al. 2002). Protein phosphorylation has also been shown to play an important role in APP processing (da Cruz e Silva and da Cruz e Silva 2003). Indeed, intracellular signaling cascades have a central role in the regulation of APP cleavage (Gandy et al. 1993). Both protein kinase A (PKA) and protein kinase C (PKC) have been shown to phosphorylate proteins associated with the T*rans*-Golgi network. Phorbol esters, which are known to activate PKC, stimulate APP secretion while decreasing Abeta production (Buxbaum et al. 1993). Protein phosphatase 1 (PP1) may also play a role in the production of sAPP, as its inhibition stimulates

secretion of sAPP (da Cruz e Silva et al. 1995). Additionally, APP is itself a phosphoprotein, with potential phosphorylatable residues located on its cytoplasmic domain, namely Tyr^{653}, Ser^{655}, Thr^{668}, Ser^{675}, Tyr^{682}, Thr^{686} and Tyr^{687} (Lee et al. 2003b). Most of these phosphorylatable residues lie within important motifs within the AICD, such as the ^{653}YTSI^{656} basolateral sorting signal, the ^{667}VTPEER^{672} motif that regulates the α-helical structure of the cytoplasmic region and a typical internalization signal, ^{682}YENPTY^{687}. Several proteins have been identified as interacting with these AICD motifs. Among them the APP tail 1 (PAT1) may be involve in APP translocation towards the cell surface and requires Tyr^{653} located on the YTSI motif for binding (Zheng et al. 1998a). The GTP-binding protein G_0 binds to a larger domain containing the VTPEER motif (De Strooper and Annaert 2000). Particularly well studied are Fe65 and Mint 1, which bind to the YENPTY motif. The interaction of APP with these binding proteins appears to be regulated by protein phosphorylation, as has been described for FE65 binding. It was demonstrated that FE65 binding to the ^{682}YENPTY^{687} domain depends on the dephosphorylation of Thr^{668}. Many other proteins contribute directly or indirectly to APP processing. For example RTN3-B has been described as a negative modulator of BACE-1 activity (He et al. 2006; He et al. 2004; Wakana et al. 2005), to participate in the formation of dystrophic neuritis in AD (Hu et al. 2007) and was found to be down regulated in AD brains (Yokota et al. 2006).

Reticulons (RTNs) are a family of membrane-bound proteins with a highly conserved C-terminus, found in animals, plants and fungi (Oertle et al. 2003). Mammals have four genes, *rtn1* to *rtn4*, which lead to the expression of multiple isoforms that share a common 188 amino-acid domain in the C-terminal and is referred to as the Reticulon Homology Domain (RHD;Di Scala et al. 2005). Within the RHD, there are two stretches (28-36 amino acids) of hydrophobic residues separated by a 66-amino acid loop, and each is expected to embed RTNs in the membrane. The diverse N-terminal domain among RTNs allows each RTN member to possess a specific function. The *rtn3* gene transcripts (RTN3-A and RTN3-B) are primarily expressed in the brain (Di Scala et al. 2005; Oertle and Schwab 2003). RTN3-B is a splice variant bearing exons 1, 4, 5, 6, 7, 8 and 9, resulting in a protein with only 236 amino acids (Humans) and an expected molecular mass of 25 kDa. It is expressed in spinal cord, cortex and cerebellum (Di Scala et al. 2005). Moreover, RTN3-B is mainly localized to the ER and Golgi (He et al. 2004; He et al. 2007; Murayama et al. 2006; Wakana et al. 2005), but it is also found in the axons, dendrites and growth cones (Hu et al. 2007). The localization of RTN3-B in the neuritic region suggests its potential role in neuritic function (Hu et al. 2007). RTN3-B plays a role in membrane trafficking between the ER and Golgi and may be involved in the retrograde transport from ER-

Golgi intermediate compartment (ERGIC) to the ER, although it is not excluded that it may be implicated in the anterograde transport (Wakana et al. 2005).

In the work here described, we have demonstrated that APP and RTN3-B interact *in vivo*, and also that the RTN3-B expression level has a marked effect on APP processing, namely favouring the non-amyloidogenic pathway.

METHODS

Antibodies

The primary antibodies used were mouse monoclonal antibody 22C11 (Chemicon) to detect APP and sAPP, rabbit polyclonal anti-APP C-terminal antibody (Zymed) to detect CTFs, mouse monoclonal anti-Myc antibody (Cell Signaling) to detect Myc-RTN3-B and rabbit polyclonal anti-calnexin antibody (Stressgen) to detect endoplasmic reticulum (ER). Secondary antibodies used were anti-mouse IgG horseradish peroxidase-linked whole antibody (Amersham Pharmacia) and anti-rabbit IgG horseradish peroxidase-linked whole antibody (Amersham Pharmacia) for enhanced chemiluminescence (ECL) detection. Texas-Red-conjugated anti-mouse IgG (Molecular Probes), Fluorescein-conjugated anti-mouse IgG (Molecular Probes) and Alexa 350-conjugated anti-rabbit IgG (Molecular Probes) were used for co-localization studies.

Yeast Two-Hybrid screen

Yeast Two-Hybrid screens were carried out using either the wild type-APP or the phosphorylation/dephosphorylation mimicking mutants (Y687E- and Y687F-APP, respectively) as baits for a human brain cDNA library (Clontech) using a MATCHMAKER GAL4 Two-Hybrid System 2 (Clontech), as previously described (Fardilha et al. 2004). The positive clones obtained were sequenced and identified by sequence comparaison to the GeneBank database using the BLAST algorithm.

Plasmid construction

The coding region of the cDNA for RTN3-B (BC105981) was amplified by PCR using two primers which insert restriction sites for EcoRI before the initiation codon (RTN3-FW 5'-CTCGAATTCCCATGGCGGAGCCGTCGG-3') and Xho I after the stop codon (RTN3-RV 5'-GTTTCCTCGAGCTTATTCTGCCTTTTTTTTGGC-3'). The amplified product was inserted in pCMV-Myc Mammalian Expression Vector (Clontech) and pET-28c (+) (Novagen). A similar strategy was used to insert RTN3-B cDNA in pDsRed-Monomer-N1 vector (Clontech) using a different reverse primer (RTN3-Red 5'-CCATCCCGGGATTCTGCCTTTTTTTTGGCG-3') that removed the stop codon and added a restriction site for *Xma* I allowing it to be fused in frame with the N-terminal of the red fluorescent protein. The green fluorescent protein (GFP) constructs of wild-type APP, Y687E and Y687F phosphomutants have been previously described (da Cruz e Silva et al. 2004a). All constructs were verified by DNA sequencing.

Cell culture

HeLa cells were grown in minimal essential medium (MEM) supplemented with 10% fetal bovine serum (FBS), 100 U/ml penicillin and 100 mg/ml streptomycin at 37ºC in a controlled atmosphere with 5% CO_2/95% air. SH-SY5Y cells were grown in MEM supplemented with F-12 Nutrient Mixture (Gibco), 10% FBS, glutamine, 100 U/ml penicillin and 100 mg/ml streptomycin at 37ºC, 5% CO_2/95% air. Cells were normally grown in 100-mm plates at subconfluent conditions before transfection.

Rat cortical primary cultures were established from embryonic day 18 embryos. Briefly, after dissociation with 0.75 mg/ml trypsin, cells were plated on poly-D-lysine-coated dishes at a density of $1.0x10^5$ cells/cm^2 in B27-supplemented Neurobasal medium (GIBCO), a serum-free medium combination (Brewer et al. 1993). The medium was supplemented with glutamine (0.5 mM), gentamicin (60 μg/ml). Cultures were maintained in an atmosphere of 5% CO_2 at 37ºC for 10 days before being used for experimental procedures. Cell cultures (COS-7, HeLa and SH-SY5Y) and rat cortical primary cultures were transiently transfected using LipofectAMINE 2000 (Invitrogen Life Technologies) a cationic lipidic transporter, as described by the supplier. After 12-16 hours of transfection, cells were harvested (processing studies) as described below or divided into 6-well plates with coverslips pre-treated with 100 μg/ml polyornithine (Sigma), and left to recover for 4 hr (co-localization studies). After this period cells were fixed using 4% paraformaldehyde and used in immunocytochemical analysis.

Yeast co-transformation

The yeast strain AH109 was transformed using the lithium acetate method, with the following plasmids: (1) Wt-APP-pAS2-1+ RNT3-B-pACT2; (2) Y687E-APP-pAS2-1 + RNT3-B-pACT2; (3) Y687F-APP-pAS2-1 + RNT3-B-pACT2; (4) pAS2-1 + pACT2. Fresh yeast colonies expressing the interacting proteins being analyzed, were grown in 4 ml of SD TDO medium (-Trp, -Leu, -His). The negative control AH109 (pAS2-1 + pACT2) was grown on SD –Trp-Leu. The cultures were incubated overnight at 30ºC with shaking at 200 rpm. The optical density of the culture at 600nm was recorded. 1ml of the culture was centrifuged for 5 minutes at 14000 rpm, and the supernatant was removed for analysis. The assay was performed by combining 8μl of culture supernatant with 24μl of Assay Buffer (100mM PNP-α-Gal solution, 1X NaOAc [1:2 (v/v) ratio]). After incubation for 60 minutes at 30ºC the reaction was terminated with 960μl of 1X stop solution (0.1M NaCO3) and the optical density at 410nm was recorded. The α-galactosidase milliunits were calculated with the following formula, as described by the manufacturer (Yeast Protocols Handbook, Clontech) for the 1ml

assay format: [milliunits/(ml x cell)] = OD410 x 992 x 1000 / [OD600 x time (min) x 16.9 x 8].

Immunoprecipitation

Cell cultures (COS-7, HeLa and SH-SY5Y) or rat primary neurons were transiently transfected with 8 µg of Myc-RTN3-B cDNAs, cells were harvested and extracts were prepared in non-denaturating lysis buffer with a protease inhibitor cocktail. The cell extracts were immunoprecipitated using either the anti-Myc or 22C11 (or 6E10 in COS-7) antibodies overnight under agitation at 4ºC. Agarose beads were then added to each sample and the lysate-mixture samples were incubated for 2 hours at 4ºC with agitation. Agarose beads were then washed 4 times with washing buffer and finally resuspended in LB/SDS 1%. The samples were separated on SDS-PAGE followed by immunoblotting using either the 22C11 antibody (samples immunoprecipitated with anti-Myc antibody) or the anti-Myc antibody (samples immunoprecipitated with 22C11 antibody).

Immunocytochemical analysis

For Myc-RTN3-B co-localization with APP, HeLa and SH-SY5Y cells were permeabilized with methanol for 2 min and washed with phosphate buffer saline (PBS). Cells were first incubated with the anti-Myc primary antibody for 2h at room temperature, followed by Texas-red-conjugated anti-mouse secondary antibody. After washing with PBS, cells were incubated with the second primary antibody, anti-APP C-terminal antibody, for 4h at room temperature, followed by Fluorescein anti-rabbit secondary antibody. After thorough washing with PBS, preparations were mounted using Vectashield mounting media with DAPI (Vector) and visualized using an inverted motorized epifluorescence microscope (Olympus).

For Myc-RTN3-B co-localization with calnexin, SH-SY5Y cells were fixed, permeabilized with methanol for 2 min and washed with phosphate buffer saline (PBS). Cells were first incubated with the anti-Calnexin primary antibody for 2h at room temperature, followed by Alexa 350 conjugated anti-mouse secondary antibody. After thorough washing with PBS, preparations were mounted using Vectashield mounting media (Vector) and visualized using an inverted motorized epifluorescence microscope (Olympus).

RTN3-dependent APP processing studies

For processing studies, SH-SY5Y cells were transiently transfected with increasing amounts of Myc-RTN3-B (0-4 µg) and incubated for 13 hours. After that period the cell culture medium was replaced by fresh serum-free medium. After 3 hours, the conditioned medium was collected and the cell lysates were harvested into 1% SDS and processed for SDS-PAGE and immunoblotting as previously described (Rebelo et al. 2004). Myc-RTN3-B was detected with anti-Myc antibody, holo-APP and sAPP were detected with 22C11 antibody and CTFs were detected using an APP C-terminal antibody (Zymed), followed by incubation with horseradish peroxidase-linked secondary antibody and detection by enhanced chemiluminescence (Amersham). Quantitive analysis was carried out by densitometric analysis using Quantity One software (BioRad).

RESULTS

RTN3-B isoform characterization

Positive clones encoding the cDNA for RTN3-B were isolated from the Yeast Two-Hybrid (Y2H) screens with either the Wild type-APP (Wt-APP) or dephosphorylation mimicking mutant of APP (Y687F-APP). Full sequencing of these clones and *in silico* analysis allows its identification as RTN3-B isoform. This isoform was previously described by Di Scala et al. (2005): it comprises exons 1, 4, 5, 6, 7, 8 and 9 of the *rtn3* gene and encodes several interesting domains (Figure 1).

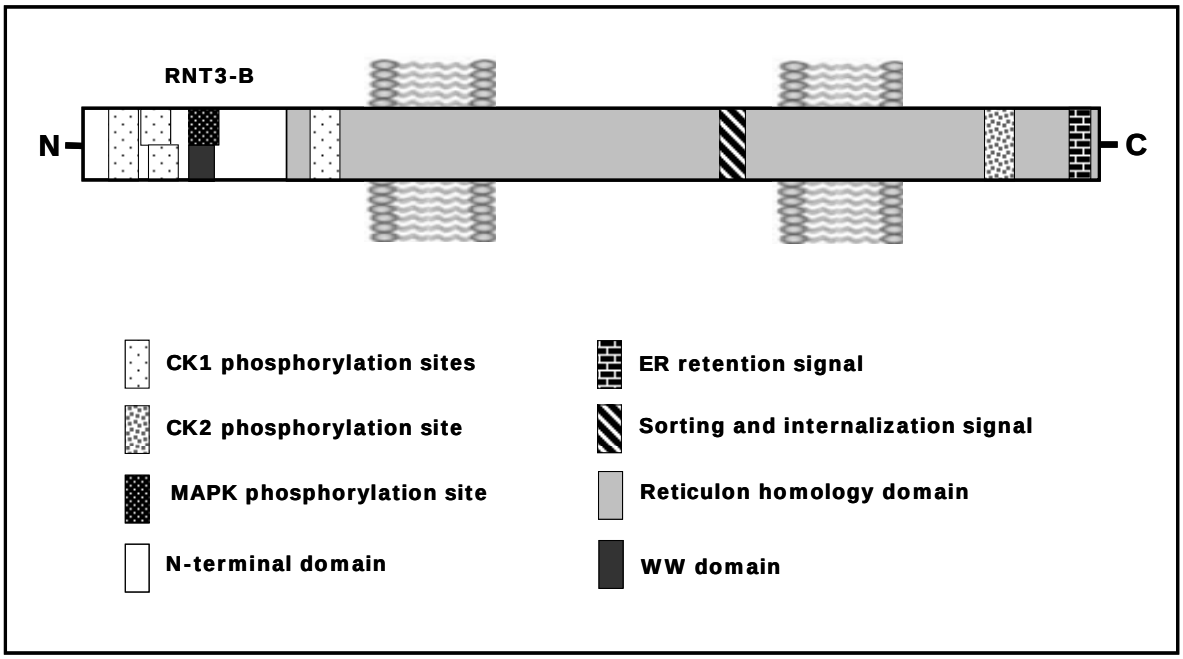

Figure 1. Shematic representation of RTN3-B isoform. Several phosphorylation sites and subcellular location signals are represented. The reticulon homology domain (RHD) is represented in solid grey and includes two transmembrane domains.

The reticulon homology domain (RHD) is a well conserved domain among the RTN family, while the N-terminus is specific for RTN3-B. The RHD domain encompasses two large transmembrane domains (Fig. 1). Thus, exons 4-9 encode the RHD domain and only exon 1 encodes the N-terminus domain. *In silico* analysis of the RTN3-B amino acid sequence, revealed the presence of several potentially interesting domains (Fig. 1). These include several phosphorylation sites for various kinases such us CK1, CK2 and MAPK. Moreover, the WW domain located at the N-terminus of the protein is important for phosphorylation-dependent interactions. An ER retention signal is usually found at the C-terminus of type I ER membrane proteins and

curiously it is also found at the C-terminus of RTN3-B (Fig. 1). The targeting of RTN3-B from Trans Golgi network (TGN) to endosomal-lysosomal compartments is mediated by the sorting and internalization signal, located between the two transmembrane domains.

RTN3-B interacts with APP

The newly described interaction between the RTN3-B and APP was confirmed *in vivo* using immunoprecipitation assays. COS-7, HeLa, SH-SY5Y and cortical neurons were transiently transfected with Myc-RTN3-B and subjected to immunoprecipitation using either the anti-Myc antibody or the 22C11 antibody. Additionally, COS-7 cell extracts were also IP with the 6E10 antibody (Fig. 2). The immunocomplexes were analysed by SDS-PAGE and immunoblotting. In COS-7 cells the presence of a strong band at 25 KDa (Fig. 2A, upper blot) indicates that Myc-RTN3-B binds to APP. Moreover, when we immunoprecipitate RTN3-B using a specific antibody that recognizes the Myc tag, the immunoblot (Fig. 2A, lower blot) revealed the presence of bands with the same weight as APP, confirming once again the interaction between those proteins.

Other cells lines were similarly analysed, namely HeLa and SH-SY5Y cells, and the results were very similar to the ones obtained with COS-7, indicating that the complex is also present in human cellular systems. Finally, when we tested primary rat cortical neurons we also observed complex formation between RTN3-B and APP. These immunoprecitation studies confirmed that the two proteins interact *in vivo*, because when we IP RTN3-B we detect the presence of several APP isoforms and when we IP APP we detect the RTN3-B isoform.

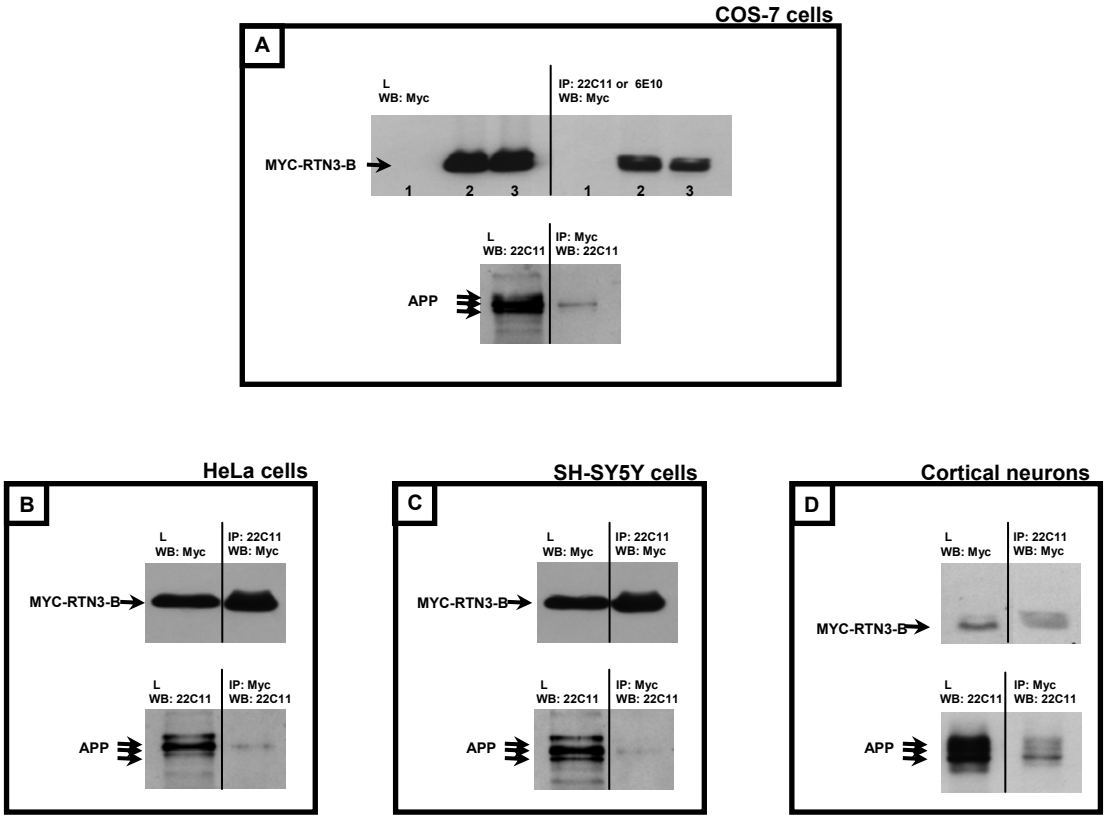

Figure 2. In vivo validation of the interaction between RNT3-B and APP. Panel A: Different cell lines and primary cultures were transfected with Myc-RTN3-B and tested for binding to APP. the cell lysate (L) is the control (left) of the IP with 22C11 and 6E10 (right). In the lower panel, the cell lysate (L) is the control (left) of the IP with anti-Myc antibody (right). 1. Non-transfected cells; 2. IP with 22C11; 3. IP with 6E10. **Panel B:** HeLa cells were IP using 22C11 (upper blots) or the anti-Myc antibody (lower blots). **Panel C:** SH-SY5Y cells were IP using 22C11 (upper blots) or anti-Myc antibody (lower blots). **Panel D:** Rat cortical neurons were IP using 22C11 (upper blotsl) or the anti-Myc antibody (lower blots)**.**

RTN3-B co-localizes with APP

In order to address the physiological role of this new interaction, we carried out co-localization studies using human cell lines. HeLa and SH-SY5Y cells were transiently transfected with Myc-RTN3-B and its distribution, as well as that of the endogenous APP, are shown (Fig. 3A). RTN3-B, as expected, is mainly located in the endoplasmic reticulum (ER) and endogenous APP and RTN3-B co-localize extensively within the cell as indicated by the yellow/orange colour (Fig. 3A, Merge). The ER localization was confirmed by transfecting HeLa cells were transiently transfected with both RTN3-B-Red and APP-GFP constructs, and incubating with an ER marker (anti-calnexin) (Fig. 3B). In both cases, using either the Myc or Red constructs, we observed very similar

subcellular distributions of RTN3-B consistent with ER distributions, as indicated by the white color observed (Fig. 3B, Merge). Both endogenous APP and Wt-APP-GFP co-localized with RTN3-B contructs.

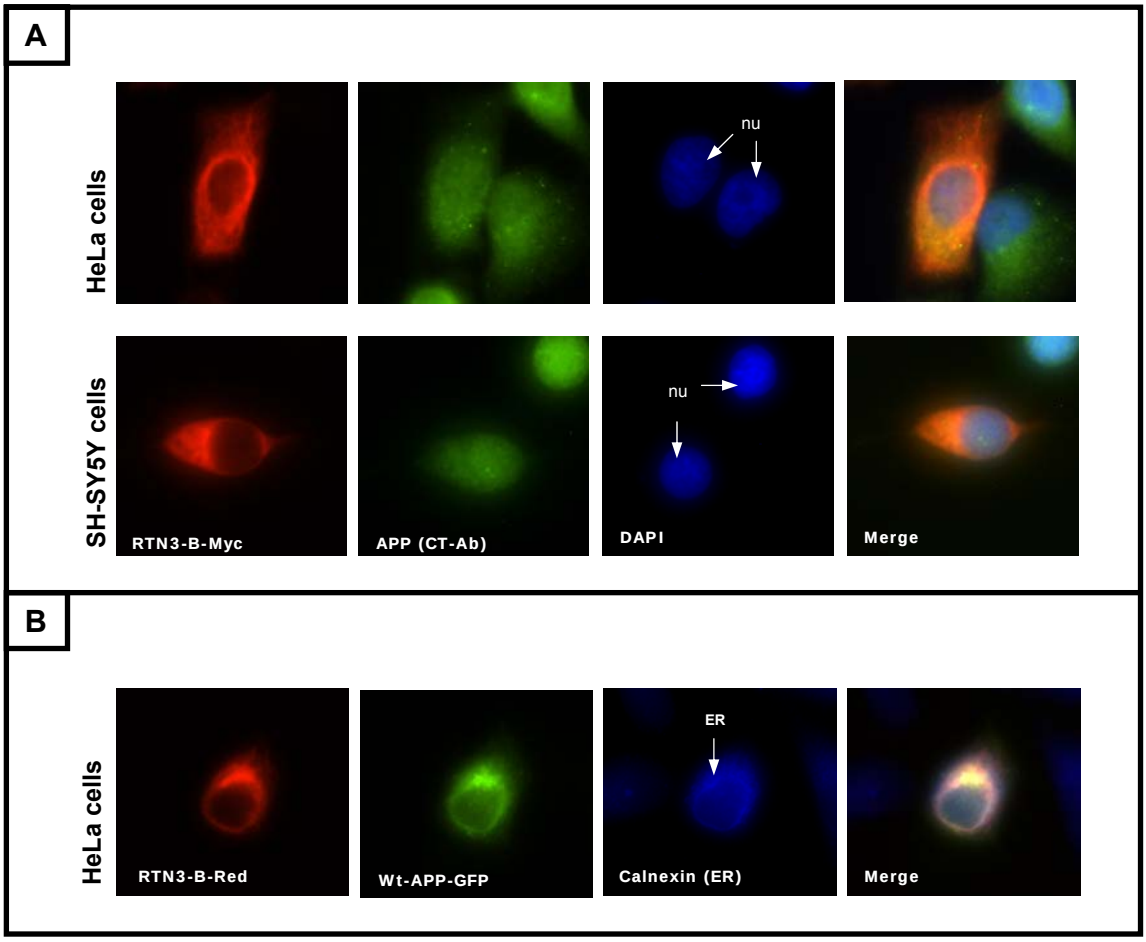

Figure 3. Co-localization of RTN3-B with APP. Panel A: co-localization of Myc-RTN3-B with endogenous APP in HeLa and SH-SY5Y cells, using DAPI to detect the nucleus (nu). The immunodetection of endogenous APP was carried out using a specific antibody that recognises the APP C-terminus (CT-Ab). **Panel B:** co-localization of RTN3-B-Red, Wt-APP-GFP and Calnexin [endoplasmic reticulum (ER) marker]**.**

RTN interacts with APP and APP phosphomutants in the Y2H system

The AH109 yeast strain was co-transformed with plasmids expressing RTN3-B and APP. Prior to α-galactosidase quantitative assays, Wt-APP and APP phosphomutants were assayed for positive interaction with RTN3-B in the Yeast Two-Hybrid system. The positive interactions were was shown by growth on SD/-Trp/-Leu/-His plates and by the blue color of the colonies, indicating expression of the *MEL1* reporter gene (Fig. 4A). For the α-galactosidase quantitative assays, the yeast cells were grown overnight in selective medium, after which cell-free supernatants were assayed for α-galactosidase activity (Fig. 4B).

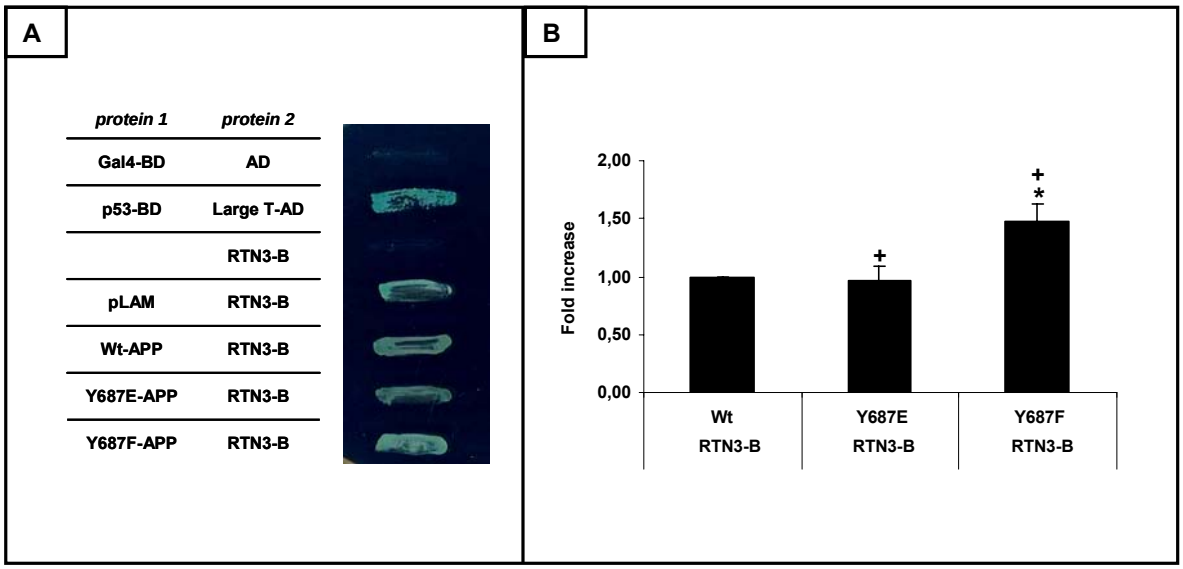

Figure 4. Yeast Two-Hybrid interaction of RTN3-B with Wt-APP, Y687E-APP and Y687F-APP. The yeast strain AH109 was co-transformed with the following plasmids: pACT2/pAS2-1; pACT2-RTN3-B/pAS2-1-Wt-APP; pACT2-RTN3-B/pAS2-1-Y687E-APP; pACT2-RTN3-B/pAS2-1-Y687F-APP. **Panel A:** yeast cells were grown on SD-Trp/-Leu/-His selective medium with X-α-Gal to test for the α-galactosidase expression. **Panel B:** yeast cells containing the various two-hybrid constructs were grown overnight in selective medium, after which cell-free supernatants were assayed for α-galactosidase activity. Data are expressed as mean ± SEM of triplicate determinations of three independent experiments. Statistical significance was conducted by one-way analysis of variance (ANOVA) with Tukey-Kramer test. Unless other wise noted, a level of statistical significance is considered $P<0.05$. Significant differences against the fold induction of α-galactosidase activity compared to the Wt-APP interaction are presented as * (P<0,05). + value statiscally different from each other (P<0,05).

In order to determine the relative strength of the interaction between RTN3-B and Wt-APP and Y687E- and Y687F-APP phosphomutants, a quantitative assay was carried out in other to measure the activity of α-galactosidase in yeast culture supernatants (Fig. 4B). The α-galactosidase activity was significantly higher with the dephosphorylation mimickingmutant, when compared with Wt-APP ($P<0,05$). In contrast, the yeast cultures expressing both Y687E+RTN3-B showed a level of α-galactosidase activity similar to Wt-APP (Fig. 4B). Hence, RTN3-B interacts with Wt-APP, as well as with both APP phosphomutants, in the Y2H system. However, the interaction is strongest with the dephosphorylation-mimicking mutant.

RTN3-B dependent APP processing

Thus, we confirmed the interaction between RTN3-B and APP both *in vivo* and *ex vivo* using several techniques. We also demonstrated that RTN3-B and APP share common subcellular localizations and hence we can hypothesize that together they are playing important cellular functions, with a possible role in subcellular processing. In order to address this, we transiently transfected SH-SY5Y cells with increasing amounts of Myc-RTN3-B and the corresponding immunoblot is presented in Fig. 5. It is clear that transfecting SH-SY5Y cells with increasing amounts of Myc-RTN3-B results in a corresponding increase in expression levels (Fig. 5A). We also analyzed the production of sAPP and CTFs, as well as holo APP levels. sAPP and CTFs are produced by α- or β-cleavage of APP, and CTFs are then γ-cleaved producing P3 or Abeta, respectively. Thus, altered levels in any of these products may be relevant for AD. It was observed that with increased amounts of Myc-RTN3-B being expressed there is an increasing in the amount of sAPP and CTFs being produced in SH-SY5Y cells (Fig. 5 C, D). In fact, sAPP levels 12-fold higher than control were obtained for the higher expression level of RTN3-B. Moreover, the same blot was probed with 6E10 (data not shown), showing and we verify that almost all sAPP production was alpha sAPP, and indicating that the non-amyloidogenic pathway was favoured. Additionally, this increase is accompanied by a decrease of the holo APP levels (Fig. 5B).

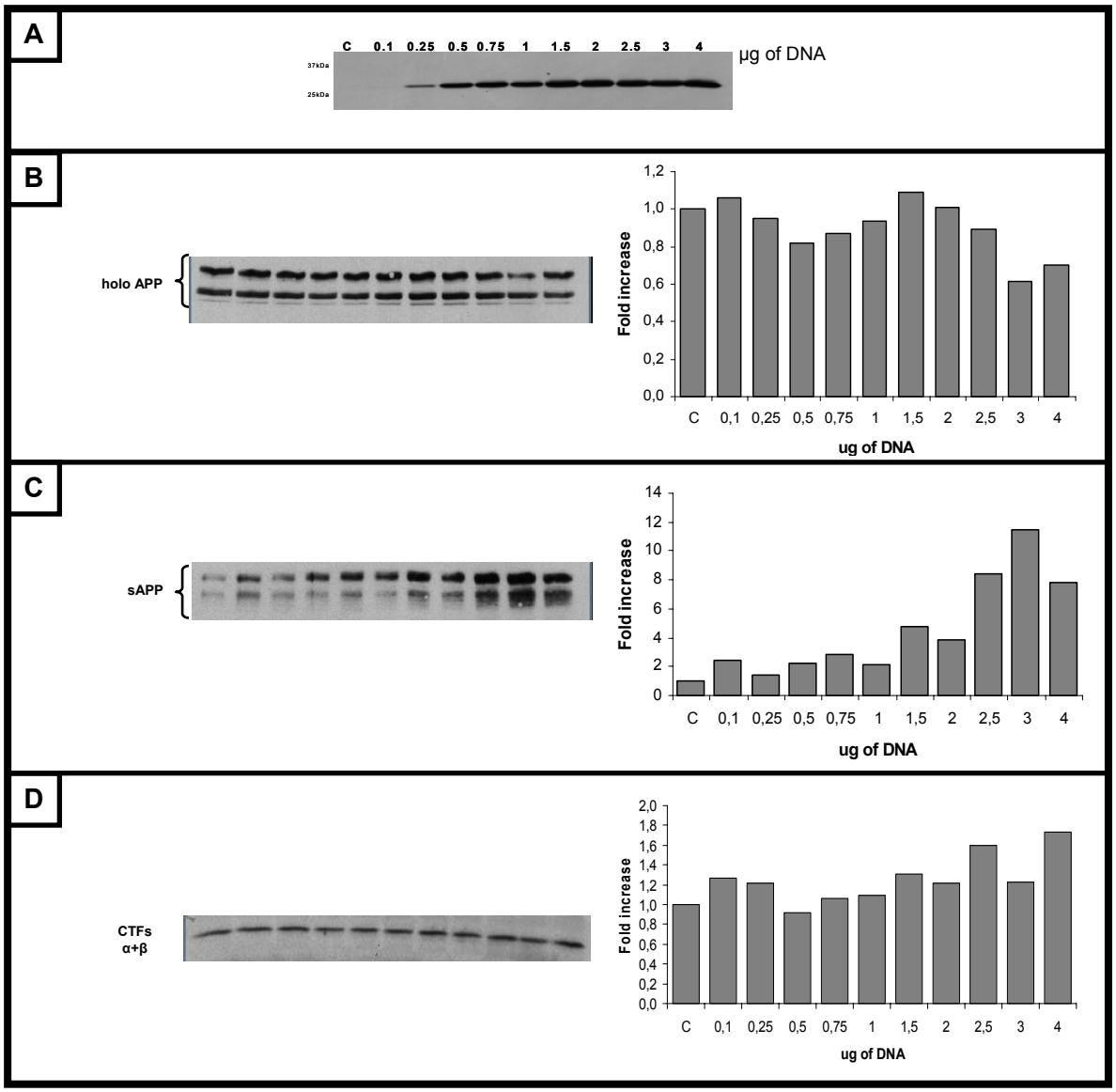

Figure 5. RTN3-B dependent APP processing in SH-SY5Y cells. Panel A: expression of Myc-RTN3-B in cells transfected with increasing amounts of Myc-RTN3-B. **Panel B:** immunoblot of APP in cell lysates detected with the 22C11 antibody and the respective quantitative data. **Panel C:** Immunoblot of sAPP production detected with the 22C11 antibody and the respective quantitative data. **Panel D:** immunoblot of total CTFs in cell lysates detected with anti-APP (C-terminal) antibody and the respective quantitative data. Quantitative data are shown as the fold increase relatively to the control (C - non-transfected cells).

DISCUSSION

In this study we show for the first time that RTN3-B binds to APP and, therefore, we propose that the two proteins are functionally related. The RTN3 role in AD has been so far attributed to its interaction with BACE-1, since RTN3 strongly inhibits BACE-1 activity (He et al. 2006; Murayama et al. 2006; Tang and Liou 2007). Recently, it has been described as contributing to the formation of dystrophic neurites in AD (Hu et al. 2007) and was found down regulated in AD brains (Yokota et al. 2006). In this respect altered APP processing may be a major contributing factor. RTN3-B is targeted from *Trans*-Golgi network (TGN) to endosomal-lysosomal compartments and this is mediated by the sorting and internalization signal. This domain is very important if we consider that several APP functions occur in the TGN and endocytic pathway, including amyloidogenic processing of APP. Our results strongly suggest that this novel RTN3-B: APP interaction is important in targeting the complex and influences APP processing. Co-localization of both proteins is consistent with this hypothesis. The relevance of this interaction in neuronal systems was evident given that the complex could also be immunoprecipitated from neuronal cultures. Given that the interaction between the two proteins was stronger for the Y687F protein, phosphorylation of APP may play an important regulatory role.

Having shown that RTN3-B and APP interact *in vivo*, we were able to investigate the physiological relevance of this new interaction, given that RTN3-B overexpression affected APP processing. The differences observed in sAPP production are consistent with the decrease in holo-APP levels, as well as with an increase in CTFs produced, when higher levels of RTN3-B are expressed (Fig. 6). This was demonstrated in SH-SY5Y cells, derived from a neuronal cell line, and therefore of specific relevance to this field of study. In essence, it appears that RTN3-B is involved in targeting APP to specific subcellular locations where proteolytic processing occurs. Our results clearly indicate that RTN3-B is directing APP to the non-amyloidogenic pathway. Curiously, BACE-1 cleavage was shown to be blocked by enriching the expression of RTN3-B (He et al. 2004). Recent data regarding RTN3 topology indicates that it forms a ω-shape structure with the N- and the C-termini of RTN3 facing the intracellular/cytosolic side (He et al. 2007). The determination of RTN3 topology would help to explain not only the interaction of RTN3 and BACE-1 but also the interaction of RTN3-B and APP. Because both C-terminal tails face the cytosolic side, the same topological orientation makes this binding compatible. So, if RTN3-B is increasing the processing of APP, and at the same time blocking BACE-1 cleavage, APP can only be

processed via the non-amyloidogenic pathway. Thus, our results are in agreement with previous RTN3 studies (He et al. 2004).

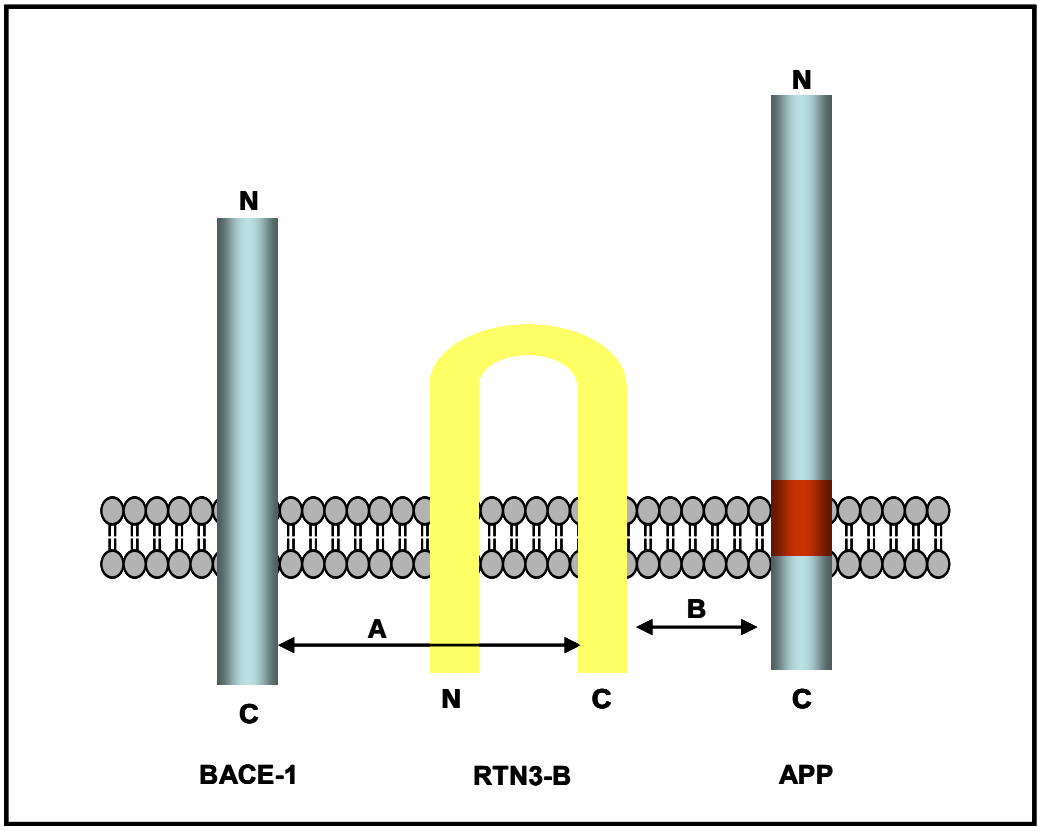

Figure 6. Schematic representation of RTN3-B/BACE-1 and RTN3-B/APP interactions. A. The conserved QID triplet within the C-terminal tail of RTNs is only critical sequence for the interaction between RTNs and BACE-1 (He et al. 2006). **B.** We hypothesize that RTN3-B interacts with APP through its C-terminus domain.

Therefore, RTN3-B represents a good candidate as a therapeutic target, given that it appears to regulate Abeta production without blocking APP processing, but rather favours non-amyloidogenic processing.

ACKNOWLEDGMENTS

Supported by the EU VI Framework Program (APOPIS), by the FCT (POCTI/NSE/40682/2001 and POCTI/SAU-OBS/57394/2004) of Portuguese Ministry of Science and Technology, by Centro de Biologia Celular, University of Aveiro and by AstraZeneca Foundation. We also thank the support from the Health Sciences and Biology Depatments. SR was recipient of PhD Fellowship (SFRH/BD/17693/2004).

REFERENCES

Brewer GJ, Torricelli JR, Evege EK, Price PJ. 1993. Optimized survival of hippocampal neurons in B27-supplemented Neurobasal, a new serum-free medium combination. J Neurosci Res 35(5):567-576.

Brookmeyer R, Johnson E, Ziegler-Graham K, Arrighi HM. 2007. Forecasting the global prevalence and burden of Alzheimer's Disease.

Buxbaum JD, Koo EH, Greengard P. 1993. Protein phosphorylation inhibits production of Alzheimer amyloid beta/A4 peptide. Proc Natl Acad Sci U S A 90(19):9195-9198.

Buxbaum JD, Liu KN, Luo Y, Slack JL, Stocking KL, Peschon JJ, Johnson RS, Castner BJ, Cerretti DP, Black RA. 1998. Evidence that tumor necrosis factor alpha converting enzyme is involved in regulated alpha-secretase cleavage of the Alzheimer amyloid protein precursor. J Biol Chem 273(43):27765-27767.

da Cruz e Silva EF, da Cruz e Silva OA. 2003. Protein phosphorylation and APP metabolism. Neurochem Res 28(10):1553-1561.

da Cruz e Silva EF, da Cruz e Silva OA, Zaia CT, Greengard P. 1995. Inhibition of protein phosphatase 1 stimulates secretion of Alzheimer amyloid precursor protein. Mol Med 1(5):535-541.

da Cruz e Silva O, Vieira SI, Rebelo S, da Cruz e Silva EF. 2004. A model system to study intracellular trafficking and processing of the Alzheimer's amyloid precursor protein. Neurodegener Dis 1(4-5):196-204.

De Strooper B, Annaert W. 2000. Proteolytic processing and cell biological functions of the amyloid precursor protein. J Cell Sci 113(11):1857-1870.

Di Scala F, Dupuis L, Gaiddon C, De Tapia M, Jokic N, Gonzalez de Aguilar JL, Raul JS, Ludes B, Loeffler JP. 2005. Tissue specificity and regulation of the N-terminal diversity of reticulon 3. Biochem J 385(Pt 1):125-134.

Esler WP, Kimberly WT, Ostaszewski BL, Ye W, Diehl TS, Selkoe DJ, Wolfe MS. 2002. Activity-dependent isolation of the presenilin- gamma -secretase complex reveals nicastrin and a gamma substrate. Proc Natl Acad Sci U S A 99(5):2720-2725.

Fardilha M, Wu W, Sa R, Fidalgo S, Sousa C, Mota C, da Cruz e Silva OA, da Cruz e Silva EF. 2004. Alternatively spliced protein variants as potential therapeutic targets for male infertility and contraception. Ann N Y Acad Sci 1030:468-478.

Francis R, McGrath G, Zhang J, Ruddy DA, Sym M, Apfeld J, Nicoll M, Maxwell M, Hai B, Ellis MC, Parks AL, Xu W, Li J, Gurney M, Myers RL, Himes CS, Hiebsch R, Ruble C, Nye JS, Curtis D. 2002. aph-1 and pen-2 are required for Notch pathway signaling, gamma-secretase cleavage of betaAPP, and presenilin protein accumulation. Dev Cell 3(1):85-97.

Gandy SE, Caporaso GL, Buxbaum JD, de Cruz Silva O, Iverfeldt K, Nordstedt C, Suzuki T, Czernik AJ, Nairn AC, Greengard P. 1993. Protein phosphorylation regulates relative utilization of processing pathways for Alzheimer beta/A4 amyloid precursor protein. Ann N Y Acad Sci 695:117-121.

He W, Hu X, Shi Q, Zhou X, Lu Y, Fisher C, Yan R. 2006. Mapping of Interaction Domains Mediating Binding between BACE1 and RTN/Nogo Proteins. J Mol Biol 363(3):625-634.

He W, Lu Y, Qahwash I, Hu XY, Chang A, Yan R. 2004. Reticulon family members modulate BACE1 activity and amyloid-beta peptide generation. Nat Med 10(9):959-965.

He W, Shi Q, Hu X, Yan R. 2007. The membrane topology of RTN3 and its effect on binding of RTN3 to BACE1. J Biol Chem 282(40):29144-29151.

Hu X, Shi Q, Zhou X, He W, Yi H, Yin X, Gearing M, Levey A, Yan R. 2007. Transgenic mice overexpressing reticulon 3 develop neuritic abnormalities. Embo J 26(11):2755-2767.

Hussain I, Powell D, Howlett DR, Tew DG, Meek TD, Chapman C, Gloger IS, Murphy KE, Southan CD, Ryan DM, Smith TS, Simmons DL, Walsh FS, Dingwall C, Christie G. 1999. Identification of a novel aspartic protease (Asp 2) as beta-secretase. Mol Cell Neurosci 14(6):419-427.

Kern A, Roempp B, Prager K, Walter J, Behl C. 2006. Down-regulation of Endogenous Amyloid Precursor Protein Processing due to Cellular Aging. J Biol Chem 281(5):2405-2413.

Koike H, Tomioka S, Sorimachi H, Saido TC, Maruyama K, Okuyama A, Fujisawa-Sehara A, Ohno S, Suzuki K, Ishiura S. 1999. Membrane-anchored metalloprotease MDC9 has an alpha-secretase activity responsible for processing the amyloid precursor protein. Biochem J 343 Pt 2:371-375.

Lammich S, Kojro E, Postina R, Gilbert S, Pfeiffer R, Jasionowski M, Haass C, Fahrenholz F. 1999. Constitutive and regulated alpha-secretase cleavage of Alzheimer's amyloid precursor protein by a disintegrin metalloprotease. Proc Natl Acad Sci U S A 96(7):3922-3927.

Lee MS, Kao SC, Lemere CA, Xia W, Tseng HC, Zhou Y, Neve R, Ahlijanian MK, Tsai LH. 2003. APP processing is regulated by cytoplasmic phosphorylation. J Cell Biol 163(1):83-95.

Lee SF, Shah S, Li H, Yu C, Han W, Yu G. 2002. Mammalian APH-1 interacts with presenilin and nicastrin and is required for intramembrane proteolysis of amyloid-beta precursor protein and Notch. J Biol Chem 277(47):45013-45019.

Murayama KS, Kametani F, Saito S, Kume H, Akiyama H, Araki W. 2006. Reticulons RTN3 and RTN4-B/C interact with BACE1 and inhibit its ability to produce amyloid beta-protein. Eur J Neurosci 24(5):1237-1244.

Newman M, Musgrave FI, Lardelli M. 2007. Alzheimer disease: Amyloidogenesis, the presenilins and animal models. Biochimica et Biophysica Acta (BBA) - Molecular Basis of Disease 1772(3):285-297.

Oertle T, Klinger M, Stuermer CA, Schwab ME. 2003. A reticular rhapsody: phylogenic evolution and nomenclature of the RTN/Nogo gene family. Faseb J 17(10):1238-1247.

Oertle T, Schwab ME. 2003. Nogo and its paRTNers. Trends Cell Biol 13(4):187-194.

Rebelo S, Henriques AG, da Cruz e Silva EF, da Cruz e Silva OA. 2004. Effect of cell density on intracellular levels of the Alzheimer's amyloid precursor protein. J Neurosci Res 76(3):406-414.

Roner S. 2004. New players in old amyloid precursor protein-processing pathways. International Journal of Developmental Neuroscience 22(7):467-474.

Tang BL, Liou YC. 2007. Novel modulators of amyloid-beta precursor protein processing. J Neurochem 100(2):314-323.

Vassar R, Bennett BD, Babu-Khan S, Kahn S, Mendiaz EA, Denis P, Teplow DB, Ross S, Amarante P, Loeloff R, Luo Y, Fisher S, Fuller J, Edenson S, Lile J, Jarosinski MA, Biere AL, Curran E, Burgess T, Louis JC, Collins F, Treanor J, Rogers G, Citron M. 1999. Beta-secretase cleavage of Alzheimer's amyloid precursor protein by the transmembrane aspartic protease BACE. Science 286(5440):735-741.

Wakana Y, Koyama S, Nakajima K, Hatsuzawa K, Nagahama M, Tani K, Hauri HP, Melancon P, Tagaya M. 2005. Reticulon 3 is involved in membrane trafficking between the endoplasmic reticulum and Golgi. Biochem Biophys Res Commun 334(4):1198-1205.

Yokota T, Mishra M, Akatsu H, Tani Y, Miyauchi T, Yamamoto T, Kosaka K, Nagai Y, Sawada T, Heese K. 2006. Brain site-specific gene expression analysis in Alzheimer's disease patients. Eur J Clin Invest 36(11):820-830.

Zheng P, Eastman J, Vande Pol S, Pimplikar SW. 1998. PAT1, a microtubule-interacting protein, recognizes the basolateral sorting signal of amyloid precursor protein. PNAS 95(25):14745-14750.

FE65 IS THE BRIDGING PROTEIN BETWEEN APP AND PP1 IN THE TRIMERIC COMPLEX

Sandra Rebelo[1], Sara C. T. S. Domingues[1], Ana Paula B. Vintém[2], Sandra Isabel Vieira[1], Margarida Fardilha[2], Sara L. C. Esteves[2], Wenjuan Wu[2], Edgar F. da Cruz e Silva[2] and Odete A. B. da Cruz e Silva[1]

[1]Laboratório de Neurociências and [2]Laboratório de Transdução de Sinais, Centro de Biologia Celular, Universidade de Aveiro, Aveiro, Portugal;

Corresponding Author:
Odete A. B. da Cruz e Silva
Laboratório de Neurociências,
Centro de Biologia Celular,
Secção Autónoma de Ciências da Saúde,
Universidade de Aveiro,
3810-193 Aveiro, Portugal
Tel: +351-234-370-778
Fax: +351-234-426-408
E-mail: odetecs@ua.pt

ABSTRACT

The Alzheimer's amyloid precursor protein (APP) binds several proteins conferring it specific functional significance. In this study we describe a novel tri-complex comprising APP, an APP binding protein (FE65) and a Ser/Thr protein phosphatase (PP1γ). We show that the trimeric complex (APP/FE65/PP1γ) occurs both in COS-7 cells and rat hippocampal and cortical primary neurons, as well as in adult rat hippocampus and cortex. The NPTY domain of APP is important for this interaction. FE65 was consequently shown to act as the bridging protein in the complex formed and thus we simultaneously describe another binding protein for PP1. This is singularly important given that PP1 binding proteins confer upon PP1 functional specificity and thus regulate its activity. Finally, identification of this complex supports the hypothesis that APP is involved in signal transduction pathways yet to be fully characterized.

Keywords: PP1 binding protein, APP Tri-complex, FE65

INTRODUCTION

Several neurodegenerative disorders are associated with altered signal transduction pathways. Alzheimer's disease (AD) is such an example, where abnormal protein kinase (Jin and Saitoh 1995) as well as protein phosphatase (Gong et al. 1993) activities have been reported in affected AD brains. Alterations include altered PKC activities and levels, decreased activity of protein phosphatases PP1 and PP2A, overexpression of calcineurin mRNA levels and hyperphosphorylation of the protein Tau and β-tubulin (Bennecib et al. 2000; Gong et al. 1993; Hata et al. 2001; Matsushima et al. 1996; Vijayan et al. 2001). A major consequence of altered signalling is the contribution to increased neuronal Abeta load (Nitsch et al. 1992; Selkoe 1993). Several studies have demonstrated that protein targeting to specific organelles, proteolytic processing and protein-protein interactions can be regulated by protein phosphorylation or by phosphorylation-dependent events (Rebelo et al. 2007a; Rebelo et al. 2007b). Protein phosphorylation is a dynamic and reversible process which involves protein kinases, phosphatases and multiple substrate proteins. It is consensual that protein phosphorylation plays a pivotal regulatory role in signal transduction cascades.

Even though many proteins contribute to the AD pathology, the central role of the Alzheimer's amyloid precursor protein (APP) is unquestionable. Several functions have been described for APP, including a role as a signal transduction mediator where APP phosphorylation may represent a key regulatory mechanism, modulating APP binding, traffic and processing. APP is a phosphoprotein *in vivo*, with several phosphorylation sites on its cytoplasmic domain, whose function is not clearly understood. The cytoplasmic phosphorylatable Ser/Thr and Tyr residues are located within three APP functional domains: ^{653}YTSI^{656}, ^{667}VTPEER^{672} and ^{682}YENPTY^{687}. These domains can be classified according to their attributed functions and are thought to be involved in regulating the rate of APP secretion, endocytosis, and Abeta production (Ando et al. 2001; Ando et al. 1999; da Cruz e Silva et al. 2004b; Iijima et al. 2000; Mueller et al. 2000; Roncarati et al. 2002; Sabo et al. 2001). Of note is the interplay which appears to occur between domains. For example, the binding of FE65 protein to APP at the ^{682}YENPTY^{687} domain also depends on the phosphorylation state of Thr^{668} on the ^{667}VTPEER^{672} domain. Thr^{668} has been extensively studied, and can be phosphorylated by several proline-directed kinases. When phosphorylated on Thr^{668}, the APP intracellular domain (AICD) is no longer stabilized by FE65, and associates less with the latter (Ando et al. 2001). Indeed, phosphorylation of Thr^{668} had already been shown to affect the interaction between APP and FE65, probably because the

phosphorylation of this residue induces structural changes from *trans*- to *cis*-conformations in the C-terminal domain of the protein (Ramelot and Nicholson 2001). Recently, it was reported that the Pin1 protein binds to the phosphorylated Thr^{668} and regulates AICD isomerization between the *cis*-and *trans*-conformations, affecting the processing of APP (Pastorino et al. 2006). In turn, the domain ^{682}YENPTY^{687} comprises not only a typical internalization signal for membrane-associated receptor proteins, but also two tyrosine residues; Tyr^{682} and Tyr^{687} that can be phosphorylated and regulate APP interactions with several PTB-containing adaptor proteins. However, the binding of PTB domains to the NPTY sequence can be independent of phosphorylation (Borg et al. 1996). Thus far, data strongly suggests an involvement of the ^{682}YENPTY^{687} domain, and Tyr^{682} and Tyr^{687} in particular, on APP traffic, processing and Abeta production.

The FE65 protein family contains several protein interacting domains, including two PTB domains and a WW region. Furthermore, the WW domain binds to MENA (mammalian enabled), which binds actin and thus links FE65 and APP to cytoskeletal dynamics and cellular motility (Ermekova et al. 1997). The PTB_1 domain of FE65 binds both the transcription factor complex CP2-LSF-LBP-1c, and the low density lipoprotein receptor-related protein (LRP). The PTB_2 domain of FE65 binds the APP C-terminus, providing a potential scaffold between APP and LRP (Kinoshita et al. 2001). The effect of FE65 expression on APP processing is unclear and may be dependent on both the cell type and the FE65 family member. FE65 can increase secretion of Abeta and sAPP from MDCK-695/FE65 cells (Sabo et al. 1999), and overexpression of FE65L1 leads to a decrease in cellular C83 and increased secretion of $Abeta_{1-40}$, resulting from increased processing through the γ-secretase pathway (Chang et al. 2003). FE65L1 has also been shown to enhance the maturation and secretion of APP (Duilio et al. 1998; Guenette et al. 1999). Contrastingly the FE65L2 family member has been demonstrated to increase secretion of Abeta in HEK 293 cells without affecting the production of other fragments of APP (Tanahashi and Tabira 2002).

Protein phosphorylation is an important regulatory mechanism and PP1 and PP2A together are responsible for over 90% of the total mammalian brain protein phosphoseryl/phosphothreonyl phosphatase activity. A decrease of about 20% in the activities of PP1 and PP2A has been reported in AD brains (Gong et al. 1994a; Gong et al. 1995; Gong et al. 1993; Gong et al. 1994c). Furthermore, PP1 was implicated in the regulation of APP processing through the use of specific inhibitors with different inhibitory potencies against PP1/PP2A (da Cruz e Silva et al. 1995; Henriques et al. 2007). Interestingly, PP1 is known to be involved in long-term potentiation (LTP) and

long-term depression (LTD), thereby influencing learning and memory (Genoux et al. 2002; Mulkey et al. 1994; Waddell 2003).

Previous data from our group indicates that Tyr687 appears to be a critical residue determining APP targeting and processing via different pathways, including endocytosis and retrograde transport (Rebelo et al. 2007a; Rebelo et al. 2007b). Moreover, given the antagonic effects on APP targeting and processing obtained by mutating Tyr687 to phenylalanine and glutamate in comparison to the wild-type protein, it is tempting to deduce that the phosphorylation state of Tyr687 may affect the formation of different multimeric complexes which are differentially targeted. The hypothesis that subcellular targeting, as one might expect, involves APP binding proteins, which are in turn regulated by protein phosphorylation, deserves further investigation.Here we show that FE65 binds simultaneously to APP and PP1γ, both in COS-7 cells, and hippocampal and cortical neurons. The trimeric complex was also detected in adult rat brain. Additionally, we demonstrated that FE65 is the bridging protein between APP and PP1γ.

EXPERIMENTAL METHODS

Antibodies

The primary antibodies used were monoclonal antibody 22C11 (Chemicon) to detect endogenous APP, the monoclonal JL-8 (BD Biosciences) that recognizes the transfected APP_{695}-GFP, a monoclonal antibody against FE65 (Upstate), a monoclonal antibody against Synaptophysin (Synaptic systems) and a monoclonal antibody (Zymed) to detect β-Tubulin. Rabbit polyclonal CBC3C recognizes PP1γ. Secondary antibodies used were anti-mouse and anti-rabbit horseradish peroxidase-linked whole antibody (GE Healthcare) for enhanced chemiluminescence (ECL/ECL plus) detection and Texas-Red-conjugated anti-mouse IgG (Molecular Probes) and Alexa 350-conjugated anti-rabbit IgG (Molecular Probes) for co-localization studies.

APP_{695} Expression Vectors

APP_{695}-GFP cDNA constructs (Wt and phosphorylation/dephosphorylation mimicking mutants: Y687E and Y687F, respectively) have been previously described (da Cruz e Silva et al. 2004a; da Cruz e Silva et al. 1993; Rebelo et al. 2007a; Rebelo et al. 2007b).

Yeast Tri-Hybrid Screen

The vector used to insert the BD-Bait (APP) and the inducible protein ($PP1\gamma_1$) cDNAs, was the Yeast Tri-hybrid (Y3H) vector. The bait cDNA coding for human APP_{695} was PCR amplified (forward primer 5'-CCGCGCACCATGGCGATGCTGCCCGGTTTGG-3'; reverse primer 5'-GTGGCCCCGGGCTAGTTCTGCATCTGCTCAAAG-3'). The bait cDNA was inserted into the Y3H vector using Nco*I*/*Sma*I restriction enzyme sites, in frame with the GAL4 DNA-BD. The cDNA coding for the inducible protein ($PP1\gamma_1$) was PCR amplified from pAS2-1-$PP1\gamma_1$ (Fardilha et al. 2004) with appropriate primers (forward primer 5'-ATTCGCGGCCGCGAGCCGGCG-3'; reverse primer 5'-GTTACGGATCCCGACTAGGCAGTG-3'), and inserted into the MCSII (*Not*I/*Bgl*II) of the Y3H vector.

The vector allows for the expression of two proteins: a DNA-binding domain fusion (in our screen the cDNA for APP was used) and an additional protein under the control of an inducible methionine promoter (in our screen the cDNA for PP1γ was used). This constructed plasmid was transformed into AH109 strain by the lithium acetate method (according to the manufacturer's instructions, Clontech). By mating the transformed AH109 (Mat a) strain with an activation domain (GAL4-AD) fusion (expressing the cDNAs from a human brain library) and reporter strain (Y187, Mat α) with an opposite

mating type from the GAL4-based two-hybrid system (Clontech), a tri-hybrid system was established for the identification of tri-complexes (Fardilha et al. 2004). Half of the diploid mixture was plated on SD/QDO/-Met (SD without Leu, Trp, Ade, His and Met), and the other half on SD/TDO/-Met (SD without Leu, Trp, His and Met). All plates were incubated at 30ºC until colonies appeared. The transformants were assayed for HIS3, ADE2 and MEL1 reporter genes. All positive clones were replated twice in SD/QDO medium containing X-α-Gal and incubated at 30ºC for 3-8 days. Yeast plasmid DNA was extracted from the positive clones using the breaking buffer method and the AD-library plasmids were rescued by transformation of *E. coli.* Library inserts were sequenced using the GAL4 AD primer (Clontech). A search for similar sequences in the GenBank database was performed using the BLAST algorithm.

Plasmid Construction

The human FE65 cDNA (Accession Nº BC010854) was PCR amplified (forward primer 5'-GGGGATCCCTTCATGGGGTATGGG-3'; reverse primer 5'-GCTGGGATCCCCATGTCTGTTCCATC-3') and inserted into the pACT2 (Clontech, Enzifarma) vector, using *BamHI* restriction endonuclease (New England Biolabs), in frame with the GAL4 activation domain. The APP intracellular domain (AICD) of human APP_{695} cDNA (Accession Nº NM_201414), corresponding to aminoacids 645-695, was PCR amplified (forward primer 5'-ATCACCATGGTGATGCTGAAGAAG-3'; reverse primer 5'-GTGGCCCCGGGCTAGTTCTGCATCTGCTCAAAG-3') and was inserted into the pAS2-1 using vector *Nco*I/*Sma*I restriction sites, in frame with the GAL4 DNA-BD. Similar constructs were prepared with AICD cDNAs carrying the mutations Y687E and Y687F.

Quantitative α-Galactosidase activity assay

Yeast strain AH109 was transformed using the lithium acetate method, with the following plasmids: (1) pACT2-FE65/pAS2-1-Wt-AICD; (2) pACT2-FE65/pAS2-1-Y687E-AICD; (3) pACT2-FE65/pAS2-1-Y687F-AICD; (4) pACT2/pAS2-1. Fresh yeast colonies expressing the pairs of interacting proteins being analyzed were grown in 4 ml of SD TDO (-Trp, -Leu, -His). The negative control AH109 (pAS2-1 + pACT2) was grown on SD –Trp-Leu. The cultures were incubated overnight at 30ºC with shaking at 200 rpm. The optical density of the culture at 600nm was recorded. The culture (1 ml) was centrifuged for 5 minutes at 14000 rpm, and the supernatant was removed for analysis. The assay was performed by combining 8µl of culture supernatant with 24µl of Assay Buffer (100mM PNP-α-Gal solution, 1X NaOAc [1:2 (v/v) ratio]). After incubation for 60 minutes at 30ºC the reaction was terminated with 960µl of 1X stop solution (0.1M $NaCO_3$) and the optical density at 410nm was recorded. The α-

galactosidase activity (milliunits) were calculated with the following formula, as described by the manufacturer (Yeast Protocols Handbook, Clontech) for the 1ml assay format: [milliunits/(ml x cell)] = OD_{410} x 992 x 1000 / [OD_{600} x time (min) x 16.9 x 8].

Cell Culture

COS-7 cells were grown in Dulbecco's modified Eagle's medium (DMEM) supplemented with 10% fetal bovine serum, 100 U/ml penicillin, 100 mg/ml streptomycin and 3.7 g/l $NaHCO_3$ (Complete DMEM) and maintained as previously described (Rebelo et al. 2004) at an atmosphere of 5% CO_2 at 37ºC.

Transient transfections of either COS-7 or primary rat cortical and hippocampal neurons were performed using LipofectAMINE 2000 (a cationic lipid transporter; Invitrogen Life technologies). After 12-16 hours of transfection, cells were harvested as described below or divided into 6-well plates with coverslips pre-treated with 100 μg/ml polyornithine (Sigma), and left to recover for 4 hours (colocalization studies). After this period cells were fixed using 4% paraformaldehyde and processeded for immunocytochemical analysis.

Rat cortical and hippocampal primary cultures were established from embryonic day 18 embryos. Briefly, after dissociation with 0.75 mg/ml trypsin for hippocampus and 0.45 mg/ml trypsin for cortex, cells were plated on poly-D-lysine-coated dishes at a density of $1.0x10^5$ cells/cm^2 in B27-supplemented Neurobasal medium (GIBCO), a serum-free medium combination (Brewer et al. 1993). The medium was supplemented with glutamine (0.5 mM), gentamicin (60 μg/ml) and glutamate (only for hippocampal neurons; 25 μM). Cultures were maintained in an atmosphere of 5% CO_2 at 37ºC for 10 days before being used for experimental procedures.

Immunocytochemical analysis

After fixing, COS-7 cells were permeabilized with methanol for 2 min and washed with phosphate buffer saline (PBS). Cells were first incubated with the anti-FE65 primary antibody for 3 hours at room temperature, followed by Texas-red-conjugated anti-mouse secondary antibody. After washing with PBS, cells were subsequently incubated with a second primary antibody [anti-PP1γ (CBC3C)] for 3 hours at room temperature, followed by Alexa 350-conjugated anti-rabbit secondary antibody. After thorough washing with PBS, preparations were mounted using Vectashield mounting media (Vector) and visualized using a LSM510-Meta confocal microscope (Zeiss).

Immunoprecipation analysis

Cells transfected with 8 µg of Wt or either phosphorylation mimicking mutant (Y687E and Y687F) cDNAs were harvested, and cell extracts were prepared in non-denaturant lysis buffer with a protease inhibitor cocktail. The cell extracts were immunoprecipited with either the anti-FE65, CBC3C or 22C11 antibodies overnight with agitation at 4ºC. Agarose beads were then added to each sample and the lysate-mixture samples were incubated for 2 hours at 4ºC with agitation. The agarose beads were washed 4 times and finally resuspended into LB/SDS 1%. The samples were further analyzed by SDS-PAGE and immunoblotted using the antibodies indicated.

SDS-PAGE and Immunobloting

Samples were separated on 10% SDS-PAGE and electrophoretically transferred onto nitrocellulose, followed by immunological detection with the indicated antibodies. Membranes were saturated in 5% non-fat dry milk in TBS-T for 4 hours and incubated overnight with monoclonal antibody 22C11, recognizing the APP N-terminus, the anti-GFP JL-8 antibody, to detect the APP-GFP fusion product. Detection was carried out using horseradish peroxidase-conjugated anti-mouse IgGs as secondary antibody and proteins visualized by enhanced chemiluminescence (GE Healthcare).

Blot Overlay Analysis

FE65 and APP_{695} proteins were generated by in vitro transcription (IVT) from pET-FE65 and pET-APP_{695} expression vectors, respectively using the TnT-coupled transcription/translation kit (Promega), according to the manufacture's instructions. The radioactive detection of proteins was carried by taking advantage of the incorporated [^{35}S]-methionine. For the overlay assays, two samples of 250 ug of purified recombinant PP1γ protein were separated on a 12% SDS-PAGE. The proteins were transferred to nitrocellulose membranes and one was overlaid for 1h30 with the [^{35}S]-APP-IVT (as a control), while the second sample was overlaid with FE65-IVT. After washing to remove excess binding protein, the latter was then overlaid with the [^{35}S]-APP-IVT. Blots were washed thoroughly and then exposed to X-ray film, the resulting signal was quantified.

Quantification and Statistic Analysis

Immunoreactive bands were quantified by densitometric analysis and QuantityOne software (Biorad, Portugal). Data are expressed as mean ± SEM of triplicate determinations, from at least three independent experiments. Statistical significance was determined by one way analysis of variance (ANOVA), followed by Tukey-Kramer

post-hoc test. Unless otherwise noted, a level of statistical significance is considered $P<0.05$.

RESULTS

A new trimeric complex (APP/PP1γ/FE65) was identified using the Yeast Tri-Hybrid system

Our present knowledge of signalling cascades and multimeric complexes formed, as well as the previously described role of PP1 in APP processing, led us to perform a Yeast Tri-Hybrid screen of a human brain library as previously described (Fardilha et al. 2004). The system allows for the simultaneous expression of two proteins: the bait cDNA fused to a Gal4-DNA binding domain (BD-Bait) and an additional protein under the control of an inducible methionine promoter (Inducible protein). In this screen, the bait fused to Gal4-DNA BD was APP_{695} cDNA and the inducible protein was PP1γ. A total of $7x10^7$ library clones were screened and 563 positives were obtained (Table 1). So far, all clones analyzed encoded FE65, demonstrating the existence of a new tri-complex APP/PP1γ/FE65.

Table 1. Yeast Tri-hybrid Screen.

BD-Bait	Inducible protein	Positive clones	Screened clones
APP	PP1γ	563	$7x10^7$

Moreover, using *in silico* analysis of the FE65 sequence we verified the presence of an additional interesting domain, besides the three previously mentioned (WW domain, PTB1 domain and PTB2 domain). Particularly, the presence of a consensus PP1 binding motif (RVGW) was revealed, confirming the interaction between FE65 and PP1.

Expression profile of the proteins in the trimeric complex

Given the importance of APP in neuronal systems, the expression pattern of the proteins involved in this trimeric complex described above was analyzed in neuronal cultures using specific antibodies (Fig. 1). Synaptophysin and β-tubulin were used as controls. The expression of the three proteins increased with time in culture (Fig. 1 A-C). However, while PP1γ expression levels increase up to 6 DIV and remained constant thereafter, the levels of expression of APP and FE65 appeared to increase over the entire period of the experiment, reaching a maximum level of expression at 14 DIV.

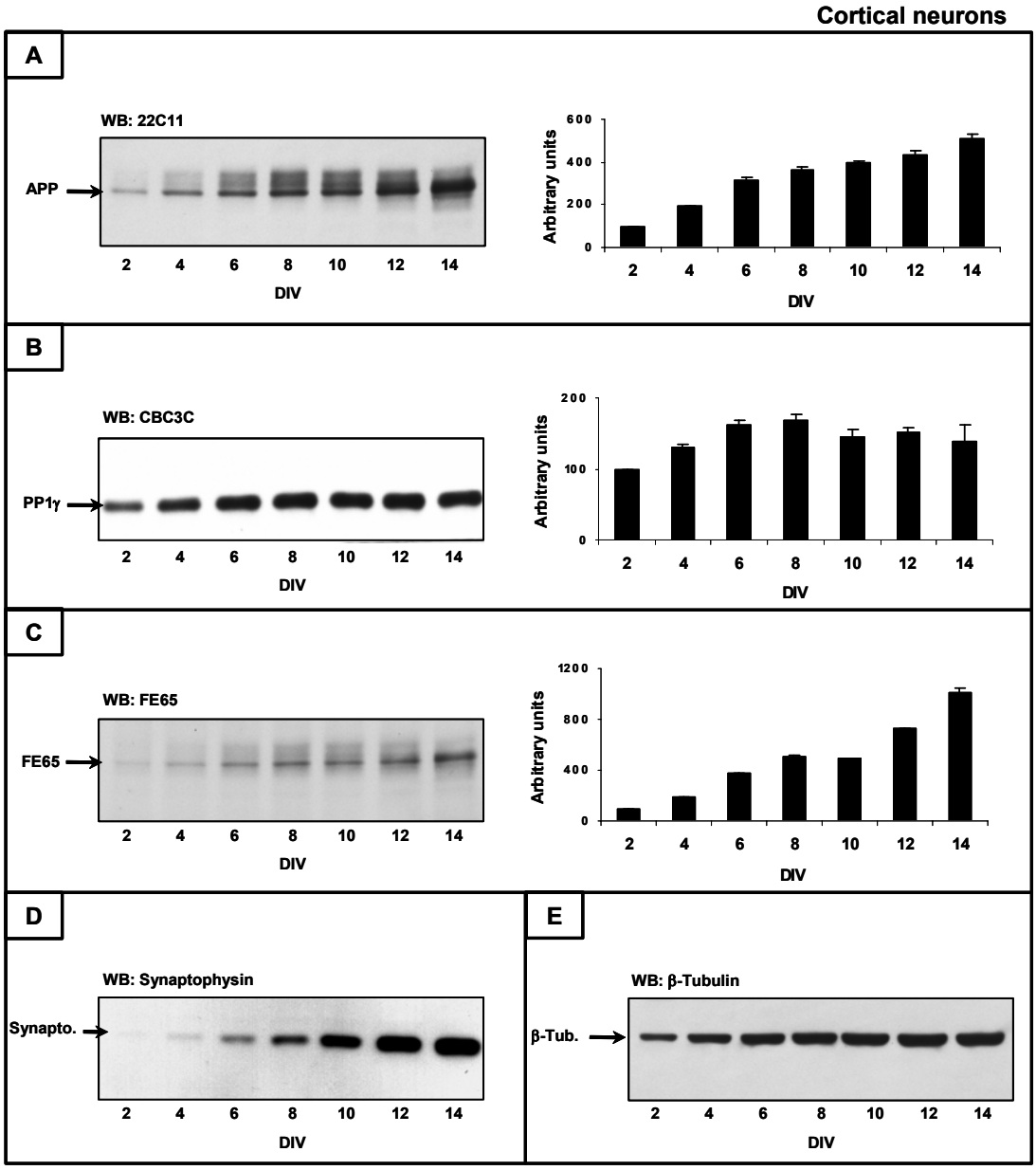

Figure 1. FE65, APP and PP1γ expression profile in primary rat cortical neurons. The expression pattern of the three proteins was determined using specific antibodies for each protein: 22C11 was used to detect the APP expression pattern **(A)**; CBC3C to detect the PP1γ **(B)**; and anti-FE65 to detect the FE65 **(C).** The quantitative data for A, B and C are presented on the right. As controls the expression patterns of synaptophysin **(D)** and β-tubulin **(E)** were also analyzed.

FE65 interaction with APP is phosphorylation dependent

Previous work showed that FE65 binds APP in the ^{682}YENPTY^{687} domain, and it is dependent on the phosphorylation state of Thr^{668}. Here we addressed if the phosphorylation state of the Tyr^{687} could also play a role in this interaction. Yeast strain (AH109) was co-transformed with the following pairs of plasmids: pACT2-FE65/pAS2-1-Wt-AICD; pACT2-FE65/pAS2-1-Y687E-AICD; pACT2-FE65/pAS2-1-Y687F; and the control pACT2/pAS2-1. Prior to α-galactosidase quantitative assays, Wt AICD and AICD phosphorylation mimicking mutants (Y687E and Y687F) were assayed for interaction with FE65 in the Yeast Two-Hybrid system. FE65 was shown to interact with Wt AICD, as described before, and also with both phosphorylation mutants. Positive interactions were shown by growth on SD/-Trp/-Leu/-His plates and by the blue colour of the colonies, indicating expression of the *MEL1* reporter gene (data not shown). In order to assess the relative strength of the interaction of FE65 with Wt-AICD, and with the Y687E and Y687F phosphomutants, a quantitative assay measuring the activity of α-galactosidase was carried out in yeast culture supernatants. The α-galactosidase activity of the Y687F-AICD-FE65 co-transformants showed a 1.36-fold induction, in relation to the wild-type (Fig. 2).

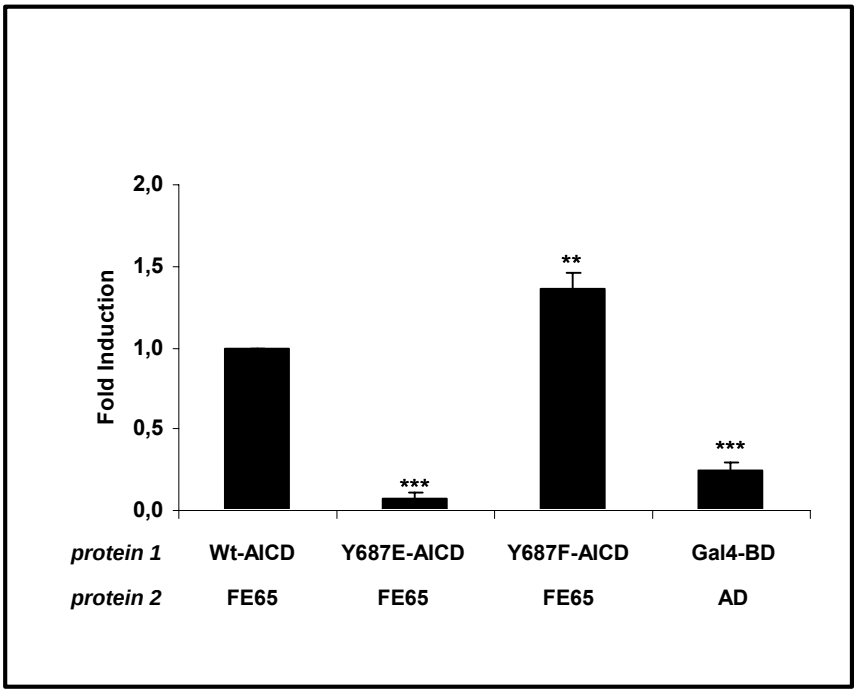

Figure 2. Yeast Two-hybrid interaction of FE65 with Wt AICD, Y687E AICD and Y687F AICD. The yeast AH109 strain was co-transformed with the following plasmids: pACT2-FE65/pAS2-1-Wt-AICD; pACT2-FE65/pAS2-1-Y687E-AICD; pACT2-FE65/pAS2-1-Y687F; and the control pACT2/pAS2-1. The yeast cells were grown overnight in selective

medium, after which cell-free supernatants were assayed for α-galactosidase activity. Data are expressed as mean ± SEM of triplicate determinations of three independent experiments. Statistical significance was assessed by one-way analysis of variance (ANOVA) with Tukey-Kramer test. Unless otherwise noted, a level of statistical significance is considered $P<0.05$. Significant differences of the fold induction of α-galactosidase activity compared to the Wt AICD+FE65 interaction are presented as (**), for p<0,01 and (***), for P<0,001.

Consequently, the interactions were further validated by co-immunoprecipitation. COS-7 cells were transfected with either the wild-type APP or the two Tyr^{687} phosphorylation mimicking mutants (Y687E and Y687F). Homogenates were prepared as described above, endogenous FE65 was immunoprecipitated and FE65 binding proteins were detected by immunoblot analysis. As expected, FE65 immunoprecipitated wild-type APP_{695}-GFP protein, but it also immunoprecipitated the phosphorylation mimicking mutant (Y687E and Y687F; Fig. 3A). However, compared to Wt and Y687E, FE65 immunoprecipitated more efficiently the dephosphorylation mimicking mutant (Y687F). which is in agreement with the previously obtained data (Fig. 2). Consequently, we tested if FE65 could also co-immunoprecipitate PP1γ. Figure 3B shows unequivocally that the FE65 immunoprecipitate also contained the PP1γ isoform. This seems to correlate with the preferential APP binding, given that the APP Y687F mutant immunoprecipitated more FE65 and more PP1γ, compared to the Wt and the Y687E mutant. (Fig. 3).

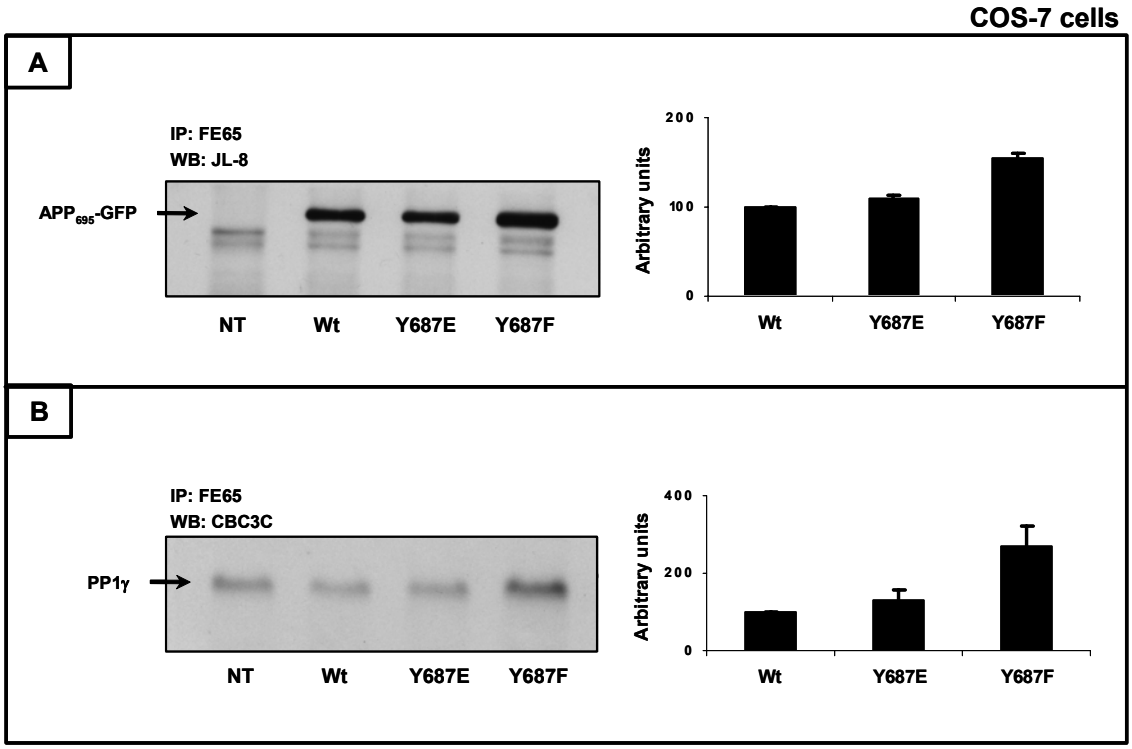

Figure 3. Tricomplex detection in COS-7 cells. COS-7 cells not transfected (NT) or transfected with either the Wt or the phosphorylation mimicking mutants (Y687E and Y687F) were homogenized and immunoprecipitated with anti-FE65. FE65 binding proteins were detected by immunoblot analysis using either the anti-GFP JL-8 antibody (A) or the anti-PP1γ CBC3C antibody (B). The respective quantitative data are also presented.

Immunocytochemistry studies further confirmed the association between APP, FE65 and PP1γ, in COS-7 cells transfected with either the Wt or the two phospho-state mimicking mutants (Fig. 4). PP1γ and FE65 were found distributed throughout the cytoplasm, diffuse and in vesicular structures. Extensive colocalization of the two (violet colour) was evident. APP exhibited a somewhat different distribution, being found mainly in the ER, Golgi and vesicular structures, as previously described. However, strong co-localization of the three proteins was evident in ER, Golgi and vesicular structures, as indicated by the white colour (Fig. 4; merge).

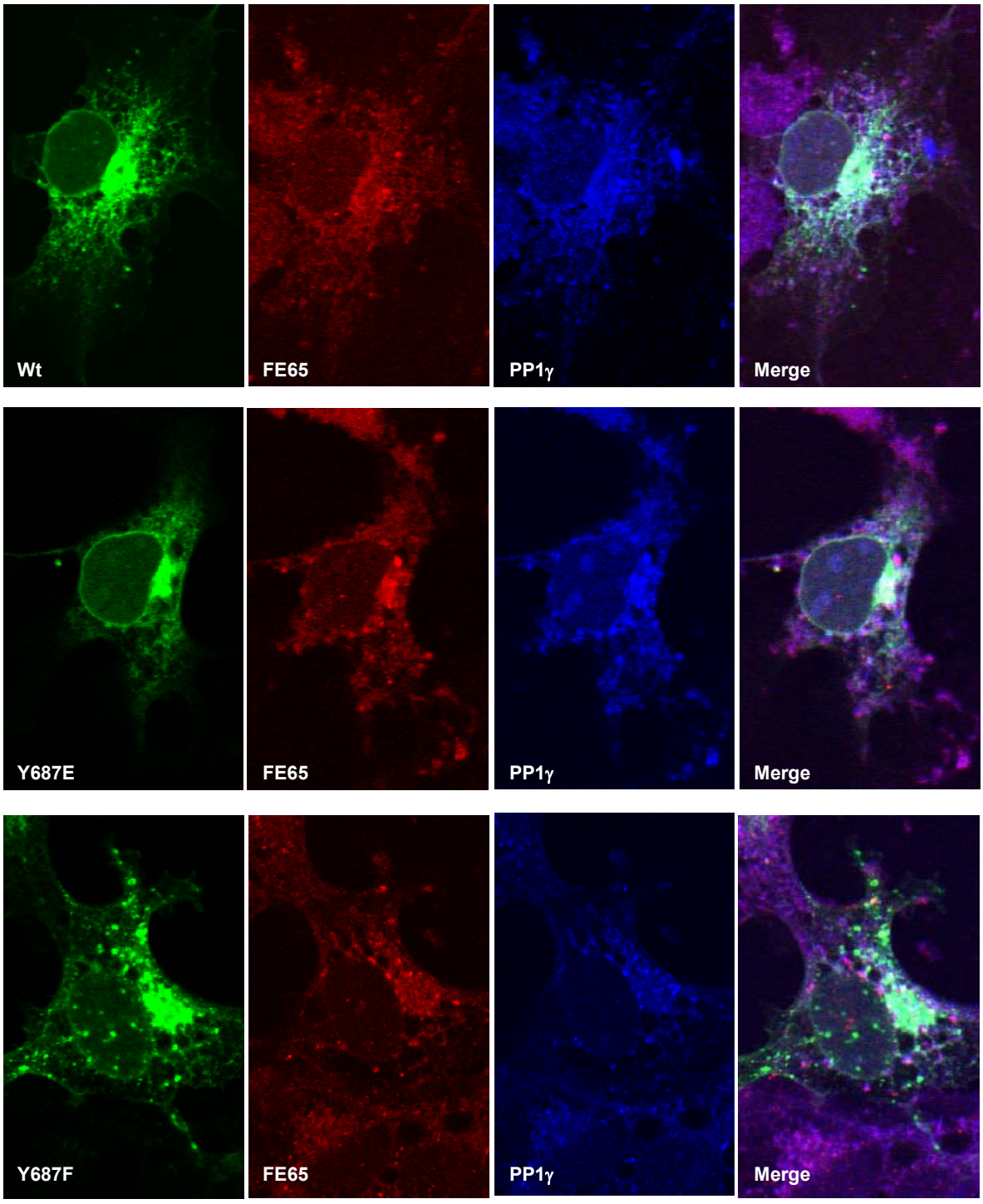

Figure 4. APP, FE65 and PP1 subcellular distribution. Following COS-7 cells transfection with either the Wt or the phosphorylation mimicking mutants (Y687E and Y687F) of APP, cells were fixed and processed for immunocytochemical analysis using specific antibodies to detect endogenous FE65 and PP1γ.

Validation of the trimeric complex in neuronal cultures

To test whether the putative tri-complex (APP, FE65, PP1γ) is also present in neurons, rat cortical and hippocampal cultures were established and maintained for 10 days, after which they were transfected with either the Wt or the two APP phosphomutants. The interactions between FE65-PP1γ and FE65-APP, both in cortical and hippocampal neurons (Fig. 5) were also evident. Moreover, in cortical neurons (Fig. 5, panel I) Wt-APP, as well as the phosphorylation (Y687E) and dephosphorylation (Y687F) mimicking mutants, interact with FE65 and this binding is more intense with the Y687F mutant. The binding of PP1γ to FE65 was also detected. As with COS-7 cells, FE65 co-immunoprecipitates more Y687F, which also produces a stronger band for PP1γ. These results suggest that in neurons the two proteins bind to FE65. An identical set of experiments was carried out, but instead of using cortical neurons, hippocampal neurons were used and the results are presented in Fig. 5, Panel II. Results are identical for both types of neuronal cultures.

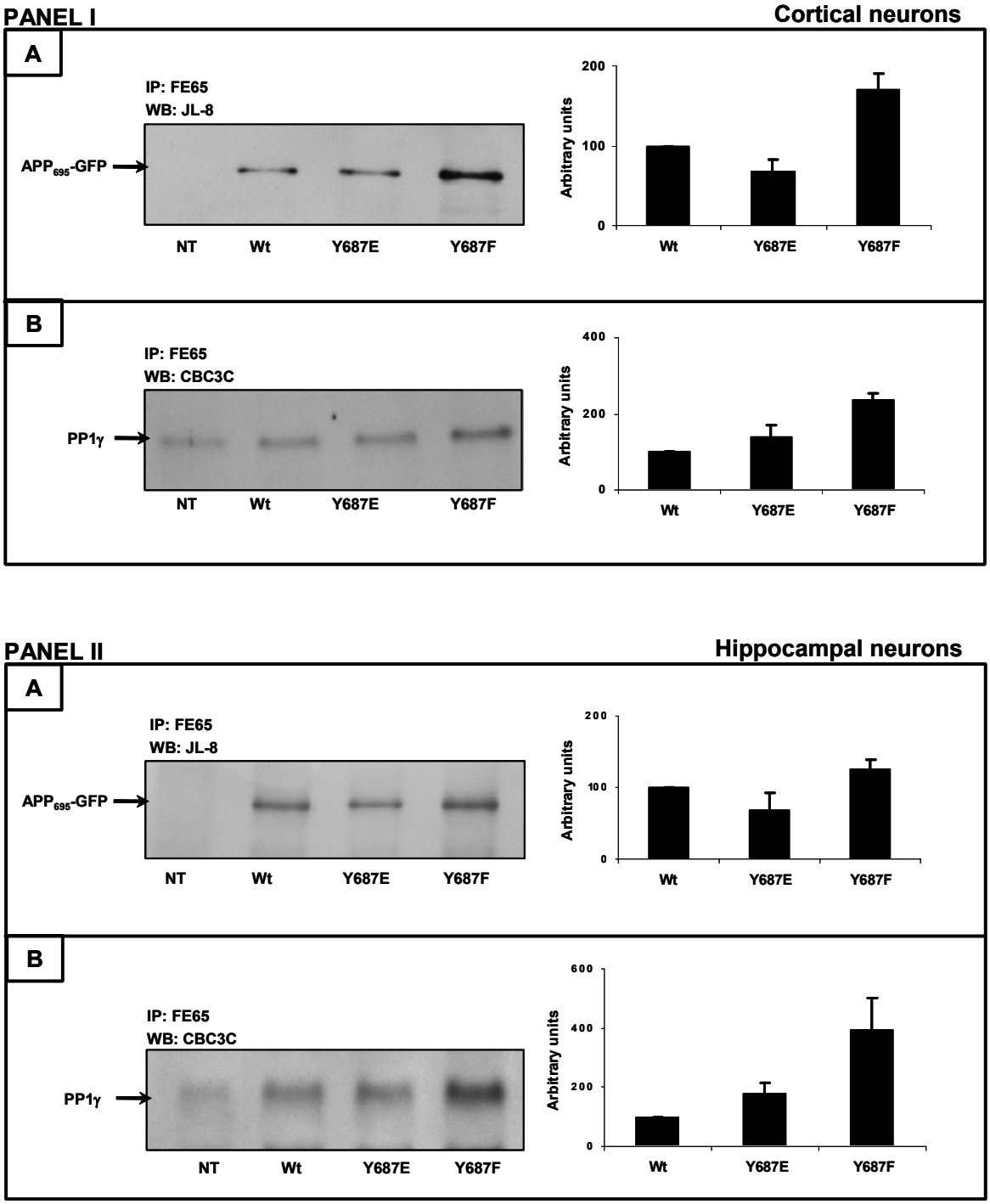

Figure 5. Trimeric complex validation in neurons. Cortical (Panel I) and hippocampal (Panel II) neurons were transfected with either the Wt or the phosphorylation mimicking mutants (Y687E and Y687F). Homogenates were prepared and endogenous FE65 was immunoprecipitated. FE65 binding proteins were detected by immunoblot analysis using either the anti-GFP JL-8 antibody (**A**) or the anti-PP1γ CBC3C antibody (**B**). The respective quantitative data are also presented.

The tri-complex is present *in vivo* in adult rat brain

Adult rat hippocampus and cortex were isolated and immediately lysed using a buffer supplemented with a cocktail of protease inhibitors. Following complete homogenization, immnoprecipitations (IPs) were carried out with specific antibodies and results are presented in Figure 6. Homogenates were immunoprecipitated with each of the three antibodies and each immnoprecipitate was tested for the other two putative binding proteins. Similar results were obtained for adult rat hippocampus and cortex, as presented in Figure 6 panel I and II, respectively. Hence, for hippocampus, when we IP with FE65 (Fig. 6; panel I A) we can detect the other two proteins: PP1γ and APP, suggesting that the three proteins form a tri-complex. Additionally, we detected both FE65 and APP when we IP with PP1γ (CBC3C antibody) and when we IP with APP (22C11 antibody) we can detect FE65 and PP1γ (Fig. 6, Panel I). Similar results were obtained using adult rat cortex revealing a similar relationship between these three endogenous proteins (Figure 6, Panel II).

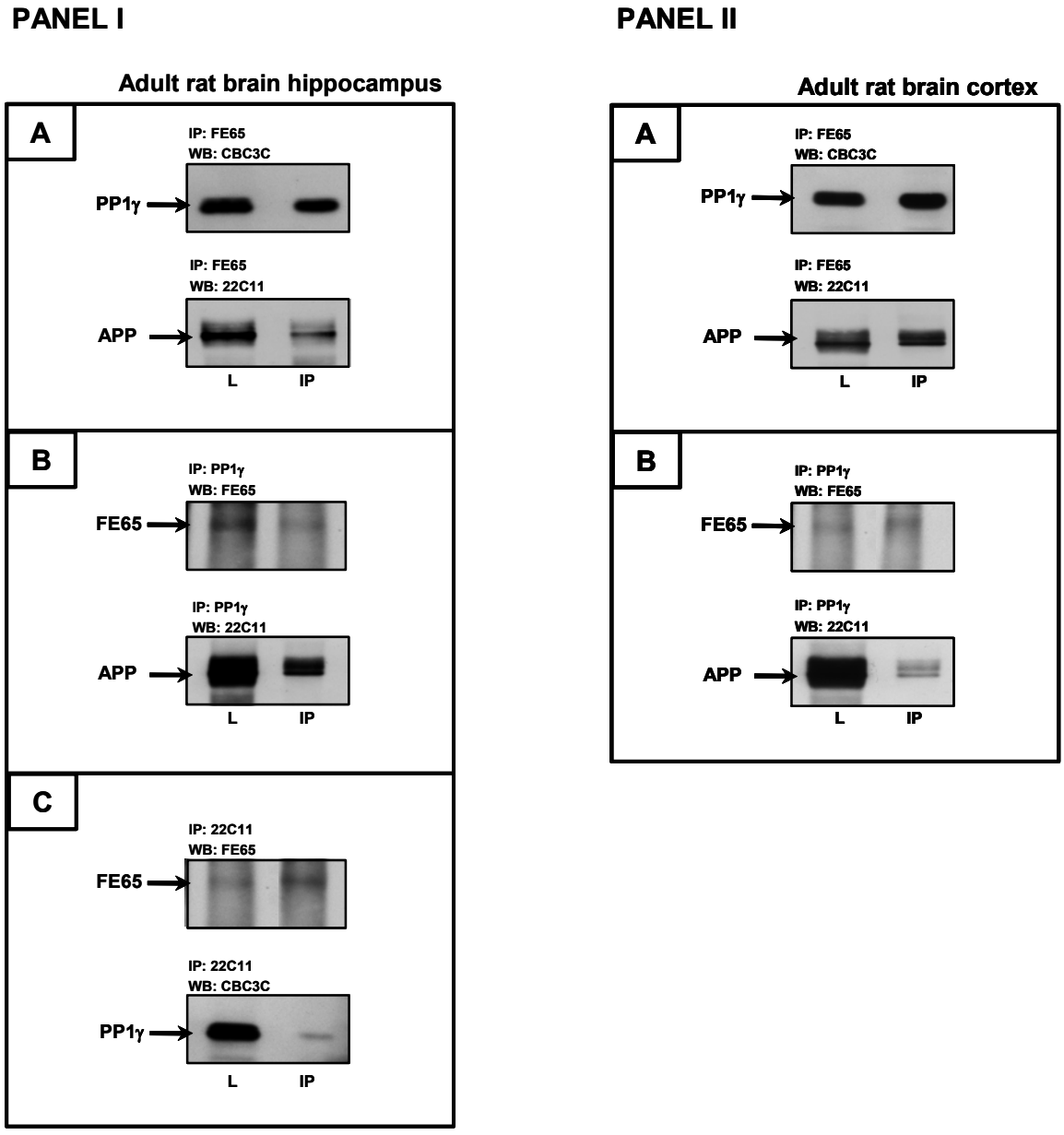

Figure 6.Tri-complex presence in adult rat brain. Adult rat hippocampus (Panel I) and cortex (Panel II) were isolated and immediately lysed. After complete homogenization, immnoprecipitations (IPs) were carried out using specific antibodies. **Panel I A.** Immunoprecipitation using the FE65 antibody (FE65). **B.** Immunoprecipitation using the PP1γ antibody (CBC3C). **C.** Immunoprecipitation using the APP antibody (22C11). **Panel II A.** Immunoprecipitation using the FE65 antibody (FE65). **B.** Immunoprecipitation using the PP1γ antibody (CBC3C). In each case Westen Blot (WB) analysis was carried out to detect specific proteins in the putative tri-complex; for PP1g (CBC3C antibody), for APP (22C11 antibody) and for FE65 (FE65 antibody).

FE65 is the bridge protein between APP and PP1γ

The results obtained so far demonstrated that both APP and PP1γ bind to FE65 in COS-7 cells, in cortical and hippocampal neurons, as well as in adult rat brain (cortex and hippocampus). Taken together these results suggest that FE65 is probably the bridging protein. In order to prove unequivocally that FE65 is the bridging protein between APP and PP1γ an *in vitro* assay was used. Briefly, two samples of purified recombinant PP1γ protein were separated by 12% SDS-PAGE. The resulting blot was divided in two, one half was overlaid with the [^{35}S]-APP-IVT (Figure 7A) while a second one was overlaid with FE65-IVT (Figure 7B). After washing to remove excess binding protein, the latter was subsequently overlaid using the [^{35}S]-APP-IVT. The results are presented in the Figure 7A and B. Figure 7A clearly shows that the APP does not bind to PP1γ directly. Alternatively, when we first overlay the membrane with FE65-IVT (Fig. 7B) and then with [^{35}S]-APP-IVT, we verify that APP does bind to the complex. A clear band is evident (Fig. 7B) indicating the presence of complex anchoring onto the PP1γ originally loaded and transferred onto the blot. From these results we can conclude that FE65 is the bridging protein between APP and PP1γ, suggesting that *in vivo* FE65 brings together these two proteins, allowing them to interact in signaling pathways.

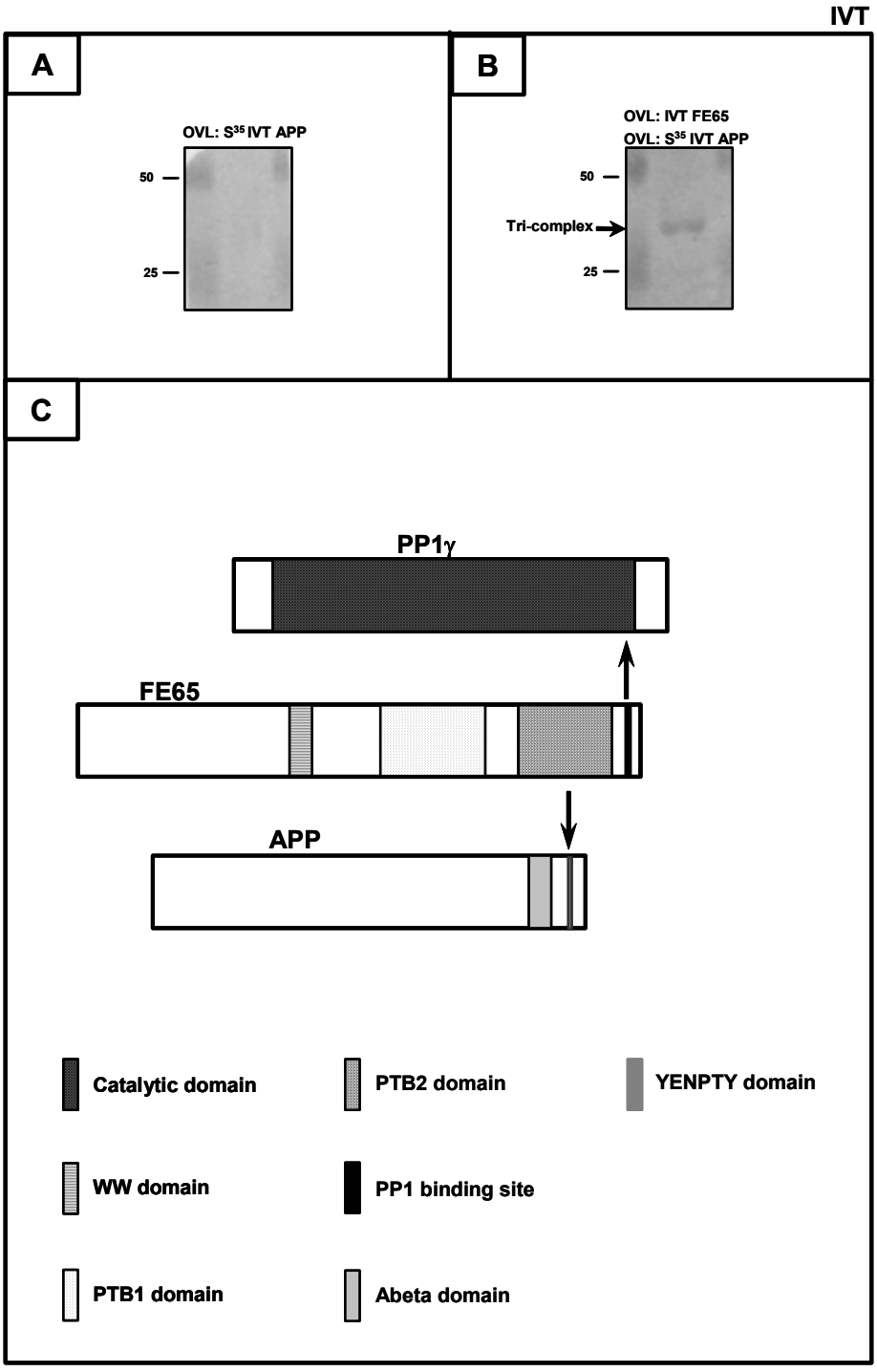

Figure 7. FE65 is the bridging protein between APP and PP1γ. Two samples of purified recombinant PP1γ protein (**A** and **B**) were separated by SDS-PAGE and the resulting blot was overlaid with other proteins. **A.** The blot was overlaid using the [^{35}S]-APP-IVT. **B.** The blot was overlaid with FE65-IVT, washed to remove excess binding protein, and then overlaid using the [^{35}S]-APP-IVT. **C.** Schematic representation of the novel tri-complex formed by APP/FE65/PP1γ. The arrows indicates the regions through which the FE65 binds specifically to APP and PP1γ.

DISCUSSION

In this study we show for the first time a clear relationship between protein phosphatase PP1γ, APP and FE65. We propose that the three are functionally related given that they interact simultaneously. The new tricomplex was first identified using the Yeast Tri-hibrid system (Table 1). Furthermore, using *in silico* analysis we recognized a consensus PP1 binding motif in the FE65 sequence and therefore this interaction was further validated using other *in vivo* methodologies.

As already reported by others, FE65 binds to APP. In this study, we went on to analyze the effect of Tyr^{687} phosphorylation on this interaction. We demonstrated that both phosphorylation mimicking mutants (Y687E and Y687F) interact with FE65, but that the interaction is strongest with the dephosphorylated mimicking Y687F mutant (Fig. 2), indicating that when Tyr^{687} is dephosphorylated it recruits more FE65.

Immunoprecipitations were essential for *in vivo* validation of the tricomplex (APP/FE65/PP1γ). Having shown that FE65 preferentially immunoprecipitated Y687F, we went on to show that PP1γ also preferentially immunoprecipitated with Y687F, thus presenting a consistent correlation for the putative complex. Differential interaction with the phosphorylation mimicking mutants was not surprising, given that differences of subcellular targeting, namely endocytosis, of these mutants have been previously described. From the data it appears that the mutant that is more efficiently endocytosed (Y687F) and produces more Abeta (Rebelo et al. 2007b), also binds more efficiently to FE65. The interaction is consistent and in agreement with previously published data (Sabo et al., 1999).

Immunoprecitations of adult rat brain demonstrated that the tri-complex is also present in brain (Figure 6). This data is of importance and of relevance in terms of AD therapeutics. FE65 is the bridging protein between the APP and PP1γ, meaning that FE65 is responsible for mediating their interaction. PP1 and PP2A together account for over 90% of the total mammalian brain protein phosphoseryl/phosphothreonyl phosphatase activity and any alteration in the activity of these two phosphatases may significantly affect the phosphorylation state of tau or of other phosphorylated proteins. A decrease of about 20% in the activities of PP1 and PP2A has been reported in AD brains (Gong et al. 1994a; Gong et al. 1995; Gong et al. 1993; Gong et al. 1994c). *In vitro* studies demonstrated that hyperphosphorylated tau from AD brain (ADP-tau) can be dephosphorylated by PP1, PP2A and PP2B, but not by PP2C (Gong et al. 1994a; Gong et al. 1994b; Gong et al. 1994c). Moreover, Lee et al. (2003b) demonstrated that 7 of the 8 potentially phosphorylatable residues in the intracellular domain of APP were phosphorylated in AD patients, namely Tyr^{653}, Ser^{655}, Thr^{668},

Ser^{675,} Tyr^{682}, Thr^{686} and Tyr^{687}. A very attractive hypothesis is that FE65 is promoting the interaction between APP and PP1γ, and that PP1γ, in turn, is responsible for the dephosphorylation of APP at one or more of the previously mentioned residues or another protein relevant for APP processing. The exact mechanism needs to be further addressed.

Several studies suggest a role for the AICD/FE65 complex as a transcriptional activator. Moreover, other reports also identified PP1γ as nuclear protein with an important role in the transcriptional machinery (Bennett 2005; Moorhead et al. 2007). Given the trimeric complex (APP/FE65/PP1γ) identified and co-localization of the three proteins we may have a potential regulatory mechanism for transcription activation.

Our experiments proved unequivocally that FE65 is the bridging protein between APP and PP1γ. Taken together, all the results are consistent with this hypothesis. Therefore, FE65 is included in the group of proteins known as "scaffold" or "bridge" proteins. These proteins are molecular intermediaries that help cell signaling proteins to interact and are also responsible for the recruitment of some effectors in the pathway. Furthermore, the idea of APP as a signal transduction molecule becomes stronger and gains more support. Thus, signal transduction based diagnostics and therapeutics represent important future strategies of relevance to AD and other neurodegenerative diseases. The future identification of the kinases and phosphatases that act upon each of the APP phosphorylatable residues will likely prove useful in this respect. One powerful candidate is PP1γ.

ACKNOWLEDGMENTS

Supported by the EU VI Framework Program (APOPIS), by the FCT (POCTI/NSE/40682/2001 and POCTI/SAU-OBS/57394/2004) of Portuguese Ministry of Science and Technology, and by Centro de Biologia Celular, University of Aveiro. SR was recipient of PhD Fellowship (SFRH/BD/17693/2004).

REFERENCES

Ando, K., Iijima, K.I., Elliott, J.I., Kirino, Y., Suzuki, T., 2001. Phosphorylation-dependent regulation of the interaction of amyloid precursor protein with Fe65 affects the production of beta-amyloid. J Biol Chem 276, 40353-40361.

Ando, K., Oishi, M., Takeda, S., Iijima, K., Isohara, T., Nairn, A.C., Kirino, Y., Greengard, P., Suzuki, T., 1999. Role of phosphorylation of Alzheimer's amyloid precursor protein during neuronal differentiation. J Neurosci 19, 4421-4427.

Bennecib, M., Gong, C.X., Grundke-Iqbal, I., Iqbal, K., 2000. Role of protein phosphatase-2A and -1 in the regulation of GSK-3, cdk5 and cdc2 and the phosphorylation of tau in rat forebrain. FEBS Lett 485, 87-93.

Bennett, D., 2005. Transcriptional control by chromosome-associated protein phosphatase-1. Biochem Soc Trans 33, 1444-1446.

Borg, J.P., Ooi, J., Levy, E., Margolis, B., 1996. The phosphotyrosine interaction domains of X11 and FE65 bind to distinct sites on the YENPTY motif of amyloid precursor protein. Mol Cell Biol 16, 6229-6241.

Brewer, G.J., Torricelli, J.R., Evege, E.K., Price, P.J., 1993. Optimized survival of hippocampal neurons in B27-supplemented Neurobasal, a new serum-free medium combination. J Neurosci Res 35, 567-576.

Chang, L., Bakhos, L., Wang, Z., Venton, D.L., Klein, W.L., 2003. Femtomole immunodetection of synthetic and endogenous amyloid-beta oligomers and its application to Alzheimer's disease drug candidate screening. J Mol Neurosci 20, 305-313.

da Cruz e Silva, E.F., da Cruz e Silva, O.A., Zaia, C.T., Greengard, P., 1995. Inhibition of protein phosphatase 1 stimulates secretion of Alzheimer amyloid precursor protein. Mol Med 1, 535-541.

da Cruz e Silva, O., Vieira, S.I., Rebelo, S., da Cruz e Silva, E.F., 2004a. A model system to study intracellular trafficking and processing of the Alzheimer's amyloid precursor protein. Neurodegener Dis 1, 196-204.

da Cruz e Silva, O.A., Fardilha, M., Henriques, A.G., Rebelo, S., Vieira, S., da Cruz e Silva, E.F., 2004b. Signal transduction therapeutics: relevance for Alzheimer's disease. J Mol Neurosci 23, 123-142.

da Cruz e Silva, O.A., Iverfeldt, K., Oltersdorf, T., Sinha, S., Lieberburg, I., Ramabhadran, T.V., Suzuki, T., Sisodia, S.S., Gandy, S., Greengard, P., 1993. Regulated cleavage of Alzheimer beta-amyloid precursor protein in the absence of the cytoplasmic tail. Neuroscience 57, 873-877.

Duilio, A., Faraonio, R., Minopoli, G., Zambrano, N., Russo, T., 1998. Fe65L2: a new member of the Fe65 protein family interacting with the intracellular domain of the Alzheimer's beta-amyloid precursor protein. Biochem J 330 (Pt 1), 513-519.

Ermekova, K.S., Zambrano, N., Linn, H., Minopoli, G., Gertler, F., Russo, T., Sudol, M., 1997. The WW domain of neural protein FE65 interacts with proline-rich motifs in Mena, the mammalian homolog of Drosophila enabled. J Biol Chem 272, 32869-32877.

Fardilha, M., Wu, W., Sa, R., Fidalgo, S., Sousa, C., Mota, C., da Cruz e Silva, O.A., da Cruz e Silva, E.F., 2004. Alternatively spliced protein variants as potential therapeutic targets for male infertility and contraception. Ann N Y Acad Sci 1030, 468-478.

Genoux, D., Haditsch, U., Knobloch, M., Michalon, A., Storm, D., Mansuy, I.M., 2002. Protein phosphatase 1 is a molecular constraint on learning and memory. Nature 418, 970-975.

Gong, C.X., Grundke-Iqbal, I., Damuni, Z., Iqbal, K., 1994a. Dephosphorylation of microtubule-associated protein tau by protein phosphatase-1 and -2C and its implication in Alzheimer disease. FEBS Lett 341, 94-98.

Gong, C.X., Grundke-Iqbal, I., Iqbal, K., 1994b. Dephosphorylation of Alzheimer's disease abnormally phosphorylated tau by protein phosphatase-2A. Neuroscience 61, 765-772.
Gong, C.X., Shaikh, S., Wang, J.Z., Zaidi, T., Grundke-Iqbal, I., Iqbal, K., 1995. Phosphatase activity toward abnormally phosphorylated tau: decrease in Alzheimer disease brain. J Neurochem 65, 732-738.
Gong, C.X., Singh, T.J., Grundke-Iqbal, I., Iqbal, K., 1993. Phosphoprotein phosphatase activities in Alzheimer disease brain. J Neurochem 61, 921-927.
Gong, C.X., Singh, T.J., Grundke-Iqbal, I., Iqbal, K., 1994c. Alzheimer's disease abnormally phosphorylated tau is dephosphorylated by protein phosphatase-2B (calcineurin). J Neurochem 62, 803-806.
Guenette, S.Y., Chen, J., Ferland, A., Haass, C., Capell, A., Tanzi, R.E., 1999. hFE65L influences amyloid precursor protein maturation and secretion. J Neurochem 73, 985-993.
Hata, R., Masumura, M., Akatsu, H., Li, F., Fujita, H., Nagai, Y., Yamamoto, T., Okada, H., Kosaka, K., Sakanaka, M., Sawada, T., 2001. Up-regulation of calcineurin Abeta mRNA in the Alzheimer's disease brain: assessment by cDNA microarray. Biochem Biophys Res Commun 284, 310-316.
Henriques, A.G., Vieira, S.I., Rebelo, S., Domingues, S.C., da Cruz e Silva, E.F., da Cruz e Silva, O.A., 2007. Isoform specific amyloid-beta protein precursor metabolism. J Alzheimers Dis 11, 85-95.
Iijima, K., Ando, K., Takeda, S., Satoh, Y., Seki, T., Itohara, S., Greengard, P., Kirino, Y., Nairn, A.C., Suzuki, T., 2000. Neuron-specific phosphorylation of Alzheimer's beta-amyloid precursor protein by cyclin-dependent kinase 5. J Neurochem 75, 1085-1091.
Jin, L.W., Saitoh, T., 1995. Changes in protein kinases in brain aging and Alzheimer's disease. Implications for drug therapy. Drugs Aging 6, 136-149.
Kinoshita, A., Whelan, C.M., Smith, C.J., Mikhailenko, I., Rebeck, G.W., Strickland, D.K., Hyman, B.T., 2001. Demonstration by fluorescence resonance energy transfer of two sites of interaction between the low-density lipoprotein receptor-related protein and the amyloid precursor protein: role of the intracellular adapter protein Fe65. J Neurosci 21, 8354-8361.
Lee, M.S., Kao, S.C., Lemere, C.A., Xia, W., Tseng, H.C., Zhou, Y., Neve, R., Ahlijanian, M.K., Tsai, L.H., 2003. APP processing is regulated by cytoplasmic phosphorylation. J Cell Biol 163, 83-95.
Matsushima, H., Shimohama, S., Chachin, M., Taniguchi, T., Kimura, J., 1996. Ca2+-dependent and Ca2+-independent protein kinase C changes in the brain of patients with Alzheimer's disease. J Neurochem 67, 317-323.
Moorhead, G.B., Trinkle-Mulcahy, L., Ulke-Lemee, A., 2007. Emerging roles of nuclear protein phosphatases. Nat Rev Mol Cell Biol 8, 234-244.
Mueller, H.T., Borg, J.P., Margolis, B., Turner, R.S., 2000. Modulation of amyloid precursor protein metabolism by X11alpha /Mint-1. A deletion analysis of protein-protein interaction domains. J Biol Chem 275, 39302-39306.
Mulkey, R.M., Endo, S., Shenolikar, S., Malenka, R.C., 1994. Involvement of a calcineurin/inhibitor-1 phosphatase cascade in hippocampal long-term depression. Nature 369, 486-488.
Nitsch, R.M., Slack, B.E., Wurtman, R.J., Growdon, J.H., 1992. Release of Alzheimer amyloid precursor derivatives stimulated by activation of muscarinic acetylcholine receptors. Science 258, 304-307.
Pastorino, L., Sun, A., Lu, P.J., Zhou, X.Z., Balastik, M., Finn, G., Wulf, G., Lim, J., Li, S.H., Li, X., Xia, W., Nicholson, L.K., Lu, K.P., 2006. The prolyl isomerase Pin1 regulates amyloid precursor protein processing and amyloid-beta production. Nature 440, 528-534.
Ramelot, T.A., Nicholson, L.K., 2001. Phosphorylation-induced structural changes in the amyloid precursor protein cytoplasmic tail detected by NMR. J Mol Biol 307, 871-884.

Rebelo, S., Henriques, A.G., da Cruz e Silva, E.F., da Cruz e Silva, O.A., 2004. Effect of cell density on intracellular levels of the Alzheimer's amyloid precursor protein. J Neurosci Res 76, 406-414.

Rebelo, S., Vieira, S.I., Esselmann, H., Wiltfang, J., da Cruz e Silva, E.F., da Cruz e Silva, O.A., 2007a. Tyrosine 687 phosphorylated Alzheimer's amyloid precursor protein is retained intracellularly and exhibits a decreased turnover rate. Neurodegener Dis 4, 78-87.

Rebelo, S., Vieira, S.I., Esselmann, H., Wiltfang, J., da Cruz, E.S.E.F., da Cruz, E.S.O.A., 2007b. Try687 dependent APP endocytosis and Abeta production. J Mol Neurosci 13.

Roncarati, R., Sestan, N., Scheinfeld, M.H., Berechid, B.E., Lopez, P.A., Meucci, O., McGlade, J.C., Rakic, P., D'Adamio, L., 2002. The gamma-secretase-generated intracellular domain of beta-amyloid precursor protein binds Numb and inhibits Notch signaling. Proc Natl Acad Sci U S A 99, 7102-7107.

Sabo, S.L., Ikin, A.F., Buxbaum, J.D., Greengard, P., 2001. The Alzheimer amyloid precursor protein (APP) and FE65, an APP-binding protein, regulate cell movement. J Cell Biol 153, 1403-1414.

Sabo, S.L., Lanier, L.M., Ikin, A.F., Khorkova, O., Sahasrabudhe, S., Greengard, P., Buxbaum, J.D., 1999. Regulation of beta-amyloid secretion by FE65, an amyloid protein precursor-binding protein. J Biol Chem 274, 7952-7957.

Selkoe, D.J., 1993. Physiological production of the beta-amyloid protein and the mechanism of Alzheimer's disease. Trends Neurosci 16, 403-409.

Tanahashi, H., Tabira, T., 2002. Characterization of an amyloid precursor protein-binding protein Fe65L2 and its novel isoforms lacking phosphotyrosine-interaction domains. Biochem J 367, 687-695.

Vijayan, S., El-Akkad, E., Grundke-Iqbal, I., Iqbal, K., 2001. A pool of beta-tubulin is hyperphosphorylated at serine residues in Alzheimer disease brain. FEBS Lett 509, 375-381.

Waddell, S., 2003. Protein phosphatase 1 and memory: practice makes PP1 imperfect? Trends Neurosci 26, 117-119.

CHAPTER V

CHAPTER V

DISCUSSION

5. 1 OVERVIEW

AD is multifactorial in its etiology and the complex cause-consequence mechanisms are still not completely understood. In the last few years, the cellular mechanisms by which APP is regulated have started to be unravelled. Related research has characterized APP binding proteins, identified some of the domains involved in these interactions, as well as their physiological relevance. APP is a transmembranar protein processed via the secretory and endocytic pathways (see Chapter I) and, as part of population is cleaved during its subcellular translocation, regulation of APP trafficking is thus of paramount importance. APP proteolytic cleavages may be regulated by temporal APP substrate/enzyme co-distribution, and by substrate and enzyme activation. A possible scenario would involve APP substrate targeting to specific subcellular microdomains in order to perform a specific cellular function, as for example activation of gene expression, being cleaved or not during the process. Several factors have been described to regulate APP trafficking and proteolysis, among them protein phosphorylation. Moreover, APP phosphorylation and APP protein-protein interactions are found to be intimately related (Ando et al. 2001; Scheinfeld et al. 2002; Taru et al. 2004), with APP phosphorylation now emerging as a regulatory mechanism of APP binding to other proteins. Interestingly AD patients exhibit not only impairment of cellular phosphorylation equilibria (Fisher et al. 1996) but also alterations of the APP phosphorylation state (Lee et al. 2003b). Additionally, Abeta phosphorylated on serine residue 26 was reported in AD brains and this phosphorylation was putatively implicated in Abeta toxicity (Milton 2005). Nonetheless, little is known regarding the role of APP phosphoresidues, namely the Tyr^{687} located in the NPTY domain.

5.2 THE NPTY DOMAIN

The asparagiNe-Proline-any-tYrosine (N-P-X-Y) motif in the cytoplasmic domain of type I transmembrane proteins was identified as an evolutionary conserved sorting signal that targets proteins for clathrin pit localization and transport via clathrin-coated vesicles from the cell surface to endosomes (Chen et al. 1990). Likewise, the clathrin coat complex transports type-I transmembrane proteins from the TGN to endosomes. Moreover, this highly conserved domain (NPTY) was identified in the APP cytoplasmic domain, allowing for specific predictions regarding its sorting itinerary. Additionally, the sorting D-X-X-L-L dileucine motif, present in the cytoplasmic tail of BACE, is a separate type of sorting signal involved with clathrin-coat transport between the TGN and endosome (He et al. 2005; Wahle et al. 2005). More recently, cell biology studies identified and characterized a novel coat complex, the retromer, involved primarily in retrograde transport from the endosome (Bonifacino and Rojas 2006; Seaman 2004) to the TGN. The retromer was further implicated in APP and BACE sorting (He et al. 2005; Small et al. 2005).

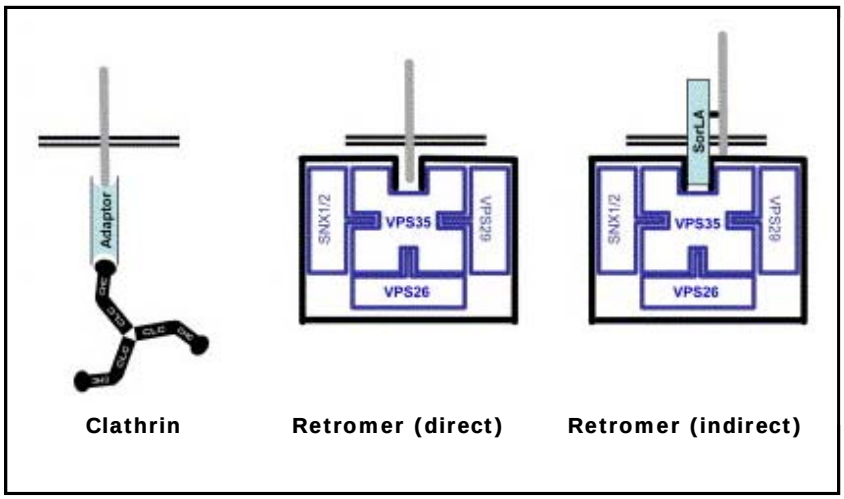

Figure 1. Coat complexes in Alzheimer's disease. The clathrin coat (left). The clathrin coat complex transports type-I transmembrane proteins to the endosome from the TGN or from the cell surface. The adaptor proteins impose cargo and itinerary specificity. The NPTY motif found in APP binds a wide-range of adaptor proteins engaged in clathrin-mediated transport from the cell surface to the endosome. **The retromer (centre and right)**. The retromer coat complex transports type-I transmembrane proteins from the endosome to the TGN. VPS35 is the core of the retromer and binds directly to the to-be-transported type-I transmembrane protein cargo (grey bar). VPS26, VPS29, and sortin nexins (SNX) 1 and 2 assemble onto VPS35 to generate the complete functional retromer complex. Recent findings suggest that the retromer sorts APP and BACE, by direct binding either to the retromer or by

indirect binding to the transmembranar adptor protein sorLA (blue) (taken from Small and Gandy 2006).

Based on the sorting motifs described above for both APP and BACE, it is plausible to deduce that the clathrin coat complex transports these proteins (Bonifacino and Traub 2003). Each clathrin molecule is composed of three clathrin light chains (CLC) and three heavy chains (CHC) (Hirst and Robinson 1998). Clathrin does not bind directly to its cargo, but rather, the globular tail of each CHC binds to "adaptor" proteins which, in turn, bind to the transmembrane cargo proteins to be sorted (Hirst and Robinson 1998; Morris et al. 1999). The adaptor proteins determine cargo and itinerary specificity. Clathrin coats are involved in two main sorting routes, the endocytic pathway connecting the cell surface to the endosome, and the pathway connecting the TGN to the endosome (Traub 2005).

As mentioned above, the cytoplasmic tail of APP contains the NPTY amino acid motif, a motif which governs the targeting of cargo to clathrin-coated vesicles (Chen et al. 1990). Motifs such as this are important for generating predictions about sorting events. However, direct experimental proof of these predictions is required before these sorting itineraries are established. Indeed, mutagenesis studies have been used to assess and confirm that each amino acid within the NPXY motif plays some role in transport of APP from the cell surface to endosomes. A number of families of adaptor proteins have been found to mediate the binding of the NPTY motif to clathrin coats. Hence, a number of clathrin adaptor proteins have been described to bind APP through the NPTY motif and therefore serve as regulators of APP endocytosis.

5.3 DEVELOPMENT OF MODEL SYSTEMS TO STUDY APP TRAFFICKING AND PROCESSING

In order to determine the functional impact of phosphorylation at specific amino acids we mutated target residues. Thus, mimicking constitutive phosphorylation and dephosphorylation and allowing for the *in vivo* and *in vitro* evaluation of the functional impact of phosphorylating specific amino acids, without the potential interference of cellular phosphatase and/or kinase activities that may act upon those sites (Bibb and da Cruz e Silva 1997).

The model system established consisted of the combined usage of site-directed mutagenesis, with an in-frame fusion to a reporter gene (GFP) in a mammalian expression vector. It was also important to ensure low levels of expression, and

inhibiting 'de novo' protein synthesis, thus allowing the monitoring of an APP protein pool in a time-dependent manner using either epifluorescence microscopy or/and immunoblotting analysis. A significantly novel aspect to the method described is provided by the fact that we can mimic a constitutively phosphorylated and contrast it to a dephosphorylated residue and so analyse its impact on APP trafficking and processing. The inhibition of expression upon by addition of cycloheximide dramatically reduced the background of fluorescence typically obtained when proteins are continuously synthesized. Hence, we were able to follow the disappearance/turnover of a specific protein population. This drug has been previously used to study the importance of other posttranslational protein modifications (Parat and Fox 2001).

The use of this methodology represents an attractive model to study APP metabolism, including not only the tracking of its subcellular localization and targeting but also rates of processing and degradation. The usefulness of our model system was entirely validated by the results obtained where the APP wild type and the different mutants of the same residue were processed differently with time (Fig. 6, Pag. 110). The results also indicated that the phosphorylation state of specific amino acids in the APP intracellular domain are of extreme importance for targeting APP to specific subcellular locations, deciding its processing and metabolic fate. The model system developed not only represents a powerful tool in the study of intracellular protein trafficking, but also provides a useful method for studying the role that some specific amino acid residues and/or specific posttranslational modifications may have in a protein's intracellular fate.

In order to determine the consequence of APP Tyr^{687} site specific phosphorylation, located with the NPTY domain, in the dynamic process of APP targeting and processing, the methology described above was employed. The results obtained are discussed in the previous chapters and are now object of an integrative analysis.

5.4 TYROSINE 687 DEPENDENT APP SUBCELLULAR TRAFFICKING

ER exit. As a secretory protein, APP is synthesized in the ER, where it suffers its first maturation process, and is translocated to the *cis*-Golgi. The ER to Golgi translocation of the Y687E mutant is delayed (Fig. 3, Pag. 138), since at the beginning of the experiment 100% of cells analysed showed intense ER fluorescence and this dropped to 40% of cells by the end of the experiment, while with the other two APP-GFP species (Wt and Y687F) it dropped to virtually 0%. Moreover, the rate of disappearance of its immature form was slower (Fig. 1, Fig.3 and Table 1, Pag. 135, 136 and 138), with Y687E-APP having a half-life of 2.58 ± 0.04 h, while the Wt- and Y687F-APP have half-lives of 2.23 ± 0.13 and 0,81 ± 0.02, respectively (Table 1, Pag. 135). The mature APP-GFP also disappears with time, presumably due to normal turnover and processing. Y687F-APP has a faster maturation rate as compared to Wt- and Y687E-APP. The last two possess identical maturation rates (Fig. 1 and Table 1, Pag. 135 and 136). Hence, it is that seems that when APP is phosphorylated at Tyr^{687} it experiences delays exiting the ER and this is consistent with the observed decreased rate of disappearance for the immature species. However, once mature Y687-APP has normal rate of turnover and processing.

Golgi/TGN exit. Difficulties in being exported are evident for the Y687E-APP mutant, since a large percentages of cells exhibit Golgi fluorescence (80-100%) at all experimental time points (Fig.3, Pag. 138). These results indicate that this mutant is not only retained in the ER but also in the Golgi. Consistent with this failure to be exported from Golgi is the almost complete absence of visible vesicular structures for this mutant. Thus, we can hypothesize that this mutant is not so efficiently packeged into post-TGN vesicles. On the other hand, the Y687F-APP mutant behaves similarly to Wt-APP and exhibited an apparently normal TGN/Golgi exit dynamics.

Cell surface endocytosis. The differences observed in increased GFP fluorescence and increased APP retention for the Y687E-APP mutant at the plasma membrane, suggested that Y687E-APP was less efficiently endocytosed (Fig. 1, Pag. 145). The APP-GFP/transferrin co-localization assay (Fig. 1, Pag. 145) also indicated that Y687E-APP could not be incorporated into endocytic vesicles. Further support was obtained from the antibody uptake assays, either from microscopy analysis of the differential cell surface APP (Fig. 2, Pag. 146), or from directly scoring the number of surface internalized APP-GFP vesicles (Fig. 2, Pag. 146). In sharp contrast, the Wt- and

Y687F-APP co-localization with transferrin allowed us to conclude that these two species are readily endocytosed. In summary, this significant novel finding shows that the Y687 phosphorylation state is critical for APP endocytosis, and is consistent with the ^{682}YENPTY^{687} domain being a consensus signal for internalization. In fact, in 1990, it was pointed out that the cytoplasmic domain of APP contained a tetrapeptide sequence, NPTY, which is a consensus sequence required for rapid endocytosis of the low density lipoprotein receptor (LDLP, Chen et al. 1990). This observation raised the possibility that APP might participate in receptor-mediated endocytosis and that membrane trafficking of APP might influence the generation of Abeta.

In conclusion, Y687 dephosphorylation seems to promote APP cell surface internalization by increasing APP endocytosis. Moreover, when Y687 is phosphorylated it is not efficiently targeted for endocytosis. Another possibility is that the rates of cell surface APP recycling (back to plasma membrane) may also be increased for this mutant. Hence, tyrosine 687 is a critical residue for APP targeting to the endocytic pathway.

Plasma membrane-TGN retrograde transport. Once at the plasma membrane, APP can be internalized (endocytic pathway), recycled back to the plasma membrane. The cell membrane is a structure which is clearly visible during almost all experimental time points with Y687E-APP, reaching a maximum of 70% for the Y687E-APP, 40% for the Y687F-APP and 30% for the Wt-APP. The antibody uptake assay allows us to monitor once again the internalization of APP (Fig. 2, Pag. 146). At time point 0, all cells revealed 22C11-staining at the cell surface (red fluorescence). Moreover, during the time of the experiment (30 min) we determined that the Y687E-APP mutant was not efficiently endocytosed, a no co-localization was observed between red and green vesicles (APP-GFP and endogenous APP). However, both the Y687F- and Wt-APP were well endocyosed and it seems that Y687F is more efficiently targeted to TGN than the Wt protein. Indeed, retrograde transport of endocytosed APP to the TGN was found to be enhanced for Y687F. Dephosphorylation of APP at the cytoplasmic Y687 residue appears to function as a signal for endocytosis, as well as a targeting signal for APP retrieval to the trans-Golgi network.

From the analysis of the APP-GFP trafficking and catabolism results, we conclude that the APP NPTY domain must be involved in the targeting of APP at several sorting stations, and that Y687 phosphorylation regulates the protein sorting and/or the kinetics at each specific stage. At the TGN and cell surface, Y687 dephosphorylation seems to lead to higher transport efficiencies, as for example, a preference for Y687F-APP to be vesicle-incorporated. Upon internalization, different

scenarios are possible, depending where APP sorting towards the TGN occurs. If it occurs at the early/sorting endosomes, the Y687 phosphorylation state would be decisive for membrane recycling, APP late endosomes delivery, for TGN recycling and possibly even in the targeting to lysosomes.

5.5 TYROSINE 687 DEPENDENT APP PROTEOLYTIC PROCESSING

The different subcellular targeting of the APP-GFP phosphomutants in COS-7 cells had important effects on the rate of APP-GFP cleavage by α- and β-secretases. Indeed, given the data available it seems reasonable to deduce that APP proteolytic cleavages may not to be directly dependent on the APP Y687-phosphorylation state, but being that the latter influences APP subcellular targeting, it may have consequences on APP availability for subsequent cleavages. That is, the phosphomutants are differentially targeted subcellularly and this affects APP cleavage events which occur in specific organelles.

α-secretase processing. In terms of total sAPP production, Wt- and Y687E-APP yielded similar rates of secretion (Fig. 2 and Table 2, Pag. 137). The Y687F-APP mutant, however, revealed a faster rate of total sAPP production. Interestingly, when alpha sAPP secretion was monitored it became evident that the Y687E mutant was favoured for α-secretase cleavage because at the 5h time point it exhibits a 1.63-fold increase in total sAPP production, while alpha sAPP increased even more (1.90-fold). The opposite was observed for the Y687F-APP mutant, which was relatively favoured for β-secretase cleavage at the same time point, with a total sAPP increase of 2.50-fold, but alpha sAPP increased only 2.10 fold (Fig. 2 and Table 2, Pag. 137). The Abeta production values are in agreement with these results and will be discussed below.

β-secretase processing. Studies from Klafki el at. (1996) and Wiltfang et al. (1997) were able to demonstrate the electrophoretic baseline separation of Abeta peptides, differing in length by only one single amino acid, could be achieved using an urea-based multiphasic bicine/sulphate SDS-PAGE system (Wiltfang et al. 2001). A quintet of Ct-truncated Abeta peptides ($Abeta_{1-37}$, $Abeta_{1-38}$, $Abeta_{1-39}$, in addition to $Abeta_{1-40}$ and $Abeta_{1-42}$) are normally observed. We applied this technique in collaboration with Prof. Jens Wiltfang, and were able to further characterize APP Y687-phosphorylation state-dependent processing and correlate with Abeta production. Different Abeta

species produced were quantified. The Y687F-APP mutant and Wt-APP yielded a similar profile of Abeta production, namely $Abeta_{1-37}$, $Abeta_{1-38}$, $Abeta_{1-39}$ and $Abeta_{1-40}$. However, Y687E-APP produced significantly lower levels of all Abeta species analysed. Another truncated Abeta specie present was $Abeta_{2-40}$, which was almost absent in the phosphotylation-mimicking mutant. Thus, it would appear that APP phosphorylation is also an important regulatory mechanism determining Abeta production. The processing data are in agreement with the previously discussed subcellular targeting results, because the two reported main subcellular locations of Abeta production, namely the TGN and endosomes, are subcellular organelles enriched in β-secretase and γ-secretase. Although both Y687 mutants were found at the TGN, only Y687F-APP is targeted to the endosomes. However, Y687E-APP has a higher time of residence at the Golgi, and this seems insufficient for cleavage by the β-secretase, in fact it seems to favour α-secretase cleavage. In addition, some competition between the Y687 phosphorylation-dependent sorting/α-secretase and β-secretase cleavage may exist.

One hypothesis may be the preference of phospho Y687 APP to be target to the plasma membrane where it will be α-secretase cleaved, while dephospho Y687 APP would have an efficient vesicle incorporation (increased endocytosis) and targeting to TGN and so could be more available for β-secretase and γ-secretase cleavage. Thus, APP phosphorylation on Y687 could indirectly affect Abeta production.

5.6 SCHEMATIC REPRESENTATION OF Y687 PHOSPHORYLATION-DEPENDENT APP SUBCELLULAR TARGETIG AND PROCESSING

A schematic summary of the results obtained for the cellular fate of Y687 phosphomutants in COS-7 cells is presented in Figure 1. These schemes show the main subcellular compartments of residence for both the Y687E-APP and Y687F-APP mutants, and the observed alterations in terms of their cellular sorting and targeting.

A. Y687E-APP-GFP

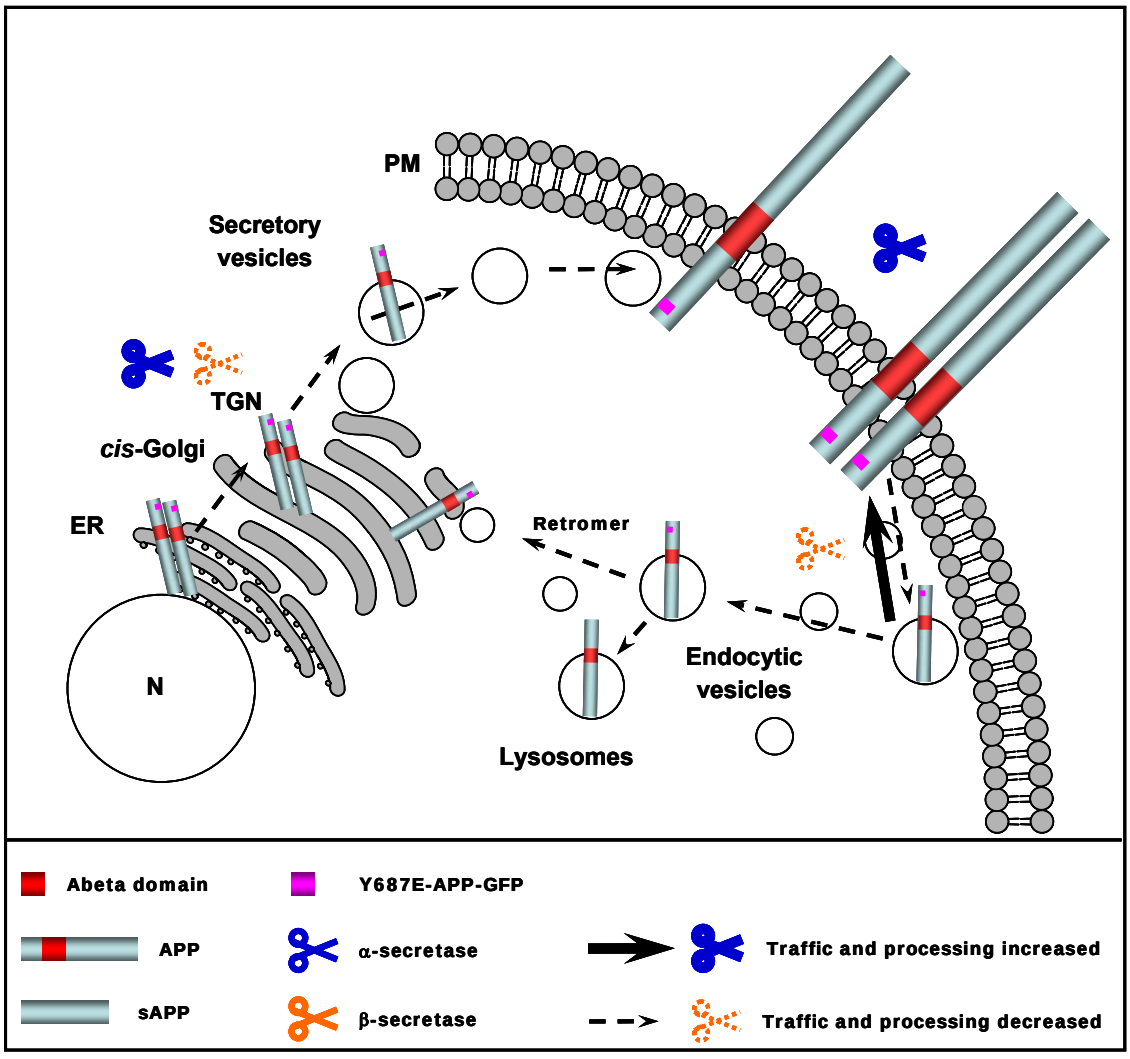

B. Y687F-APP-GFP

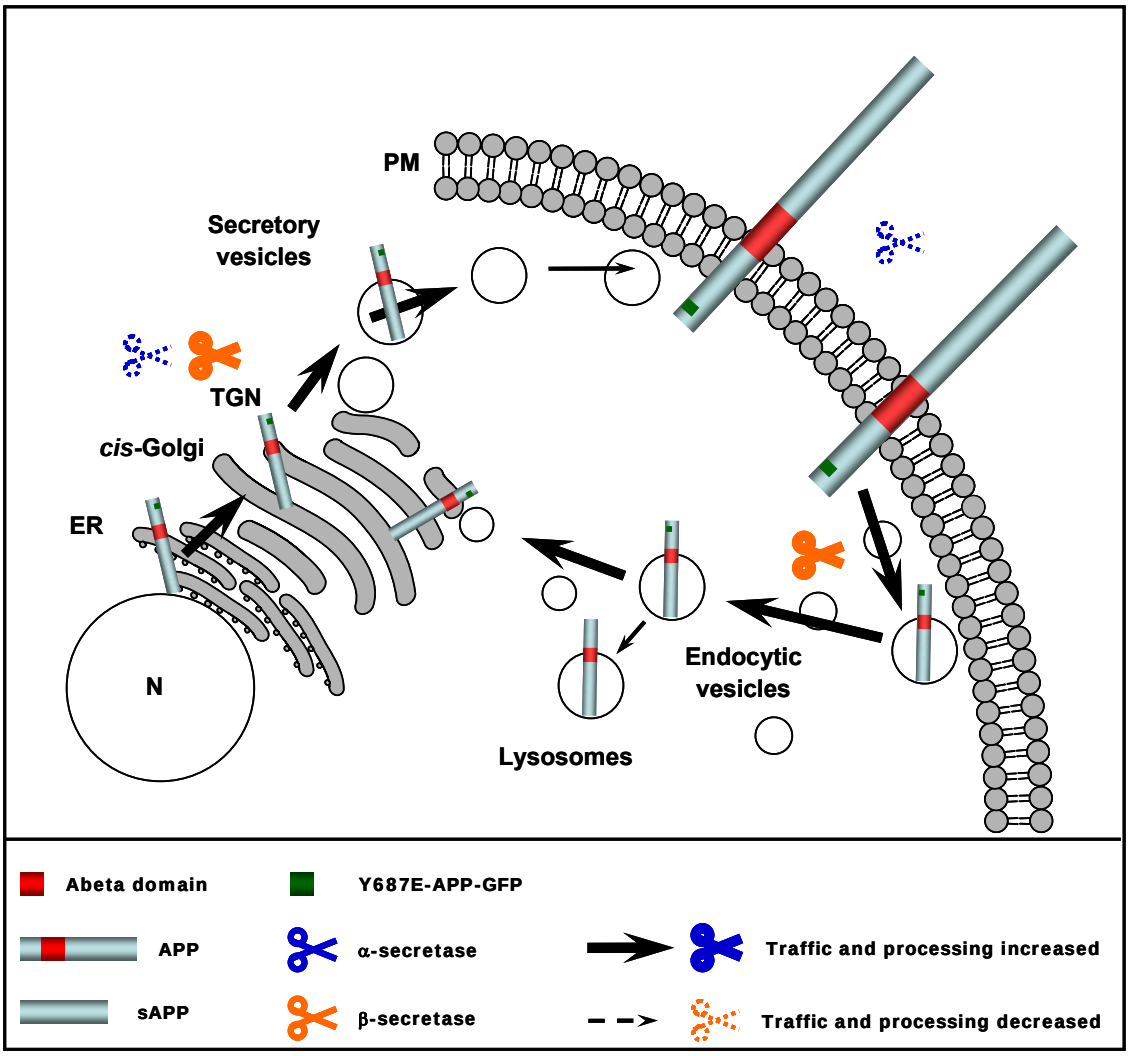

Figure 2. Schematic representation of Y687 phosphorylation state-dependent APP cellular traffic and proteolytic processing. Summary of APP Y687 phosphomutants (A: Y687E; B: Y687F) subcellular traffic and processing. **ER**, endoplasmic reticulum; **TGN**, trans-Golgi network; **PM**, plasma membrane; **N**, Nucleus; Note: endosomes are not a single organelle, but rather comprise multiple subtypes including early endosomes, sorting endosomes, recycling endosomes, late endosomes and multivesicular bodies. Nevertheless, for clarity, we used the term endosome to encompass all subtypes.

Taken together, all results support that Y687 phosphorylation is a cellular mechanism which favours APP to be preferentially cleaved through the α-secretase pathway and to generate its derived physiological active fragments: αsAPP and AICD. This is accomplished by targeting it to the subcellular compartments where α-secretase cleaves APP, namely the TGN and the plasma membrane. Another interesting aspect that is in agreement with this idea of preferential cleavage, isthat this mutant resides at the plasma membrane accompanied and does nor suffer endocytic targeting. One possible explanation is that the Y687 phosphorylation enables faster protein recycling to the plasma membrane where it can be further cleaved by α-secretase.

In sharp contrast, Y687 dephosphorylation is important for APP endocytosis and also appears to be a target signal for APP retrieval to the TGN (retromer). We believe that the increase of this mutant in the endocytic pathway is responsible for its increased Abeta production.

Our results showing that Abeta production can be modulated by direct APP phosphorylation may be of specific therapeutic relevance. It is interesting to note that the retrograde transport of BACE-1, responsible for β-secretase activity, is also regulated by the phosphorylation state of the protease (Wahle et al. 2005). In addition, our conclusions favour a model where interaction of APP with its binding proteins may also be mediated by the phosphorylation state of APP itself (da Cruz e Silva et al. 2004b).

5.7 APP PROTEIN-PROTEIN INTERACTIONS MEDIATED BY Y687 PHOSPHORYLATION/DEPHOSPHORYLATION

Phosphorylation of APP at its C-terminus is believed to regulate binding of APP to other cellular proteins that participate and mediate APP cellular processing and function. Ando et al (2001) showed that the phosphorylation state of Thr^{668} regulates APP interactions at the ^{682}YENPTY^{687} motif. XL11 and mDab1 bind APP regardless of the phosphorylation state of APP Thr^{668}, while FE65 interaction with the APP recognition motif is weaker upon Thr^{668} phosphorylation. In addition, phosphorylation at this residue is associated with a preference for APP to be cleaved in the β-secretase pathway (Lee et al. 2003a; Muresan and Muresan 2005a). Nonetheless, it is still a matter of controversy if Thr^{668} phosphorylation results in higher or decreased AICD nuclear targeting and transactivation (Kimberly et al. 2005; Muresan and Muresan 2004; Zheng et al. 2003).

The targeting of APP to the α-secretase pathway by APP direct phosphorylation prior to our findings had not been observed. The underlying Tyr^{687} phosphorylation/dephosphorylation regulatory mechanisms most probably include controlling APP binding to specific proteins. For example, Tyr^{687} phosphorylation may induce alterations in the APP affinity for specific APP interacting proteins with a role such as coat proteins resulting in enhanced APP targeting to post-TGN and endocytic vesicles. For example, S498 phosphorylation enhances BACE-1 binding, through the S498-containing sorting motif, to the adaptor protein GGA (Shiba et al. 2004). This protein is involved in TGN anterograde transport and GGA-BACE-1 binding was later shown to be responsible for the phosphorylation-dependent BACE-1 retrograde transport (Wahle et al. 2005). A similar mechanism, involving a serine residue immediately upstream a sorting motif, occurs for the cation independent MRP protein (Kato et al. 2002). In a similar manner APP Tyr^{687} phosphorylation may t accelerate specific vesicle traffic steps such as APP cargo packaging, vesicle release, or vesicle targeting. The proteins that interact with these domains/sequences are the best candidates to be the putative APP binding proteins, interacting with APP in a Tyr^{687} phosphorylation-dependent manner. The known proteins to fall into this group are so far: **ARH** (Noviello et al. 2003), **Numb** (Berdnik et al. 2002; Roncarati et al. 2002), **disabled family member (Dab) 1** and **2** (Homayouni et al. 1999; Yun et al. 2003), **c-Jun N-terminal kinase interaction (Jip1b)** protein (Inomata et al. 2003; Matsuda et al. 2001; Scheinfeld et al. 2002; Taru et al. 2002), **SHC** (Russo et al. 2002; Russo et al. 2001; Tarr et al. 2002; Zambrano et al. 2001), **Grb2** (Venezia et

al. 2004; Zhou et al. 2004), **c-Abl** (Russo et al. 2001; Tarr et al. 2002; Zambrano et al. 2001), members of **X11 family**, namely **X11α** (Borg et al. 1996; McLoughlin et al. 1999; Tomita et al. 1999) and members of **FE65 family** (including **FE65**, **FE65L1** and **FE65L2)** (Borg et al. 1996; Bressler et al. 1996; Duilio et al. 1998; Fiore et al. 1995; Guenette et al. 1996; Tanahashi and Tabira 1999b; Zambrano et al. 1997).

Figure 3 summarizes putative Y687 phosphorylation-dependent bindings of the APP C-terminus to proteins with which it may form signalling complexes physiologically relevant in APP cellular fate and processing.

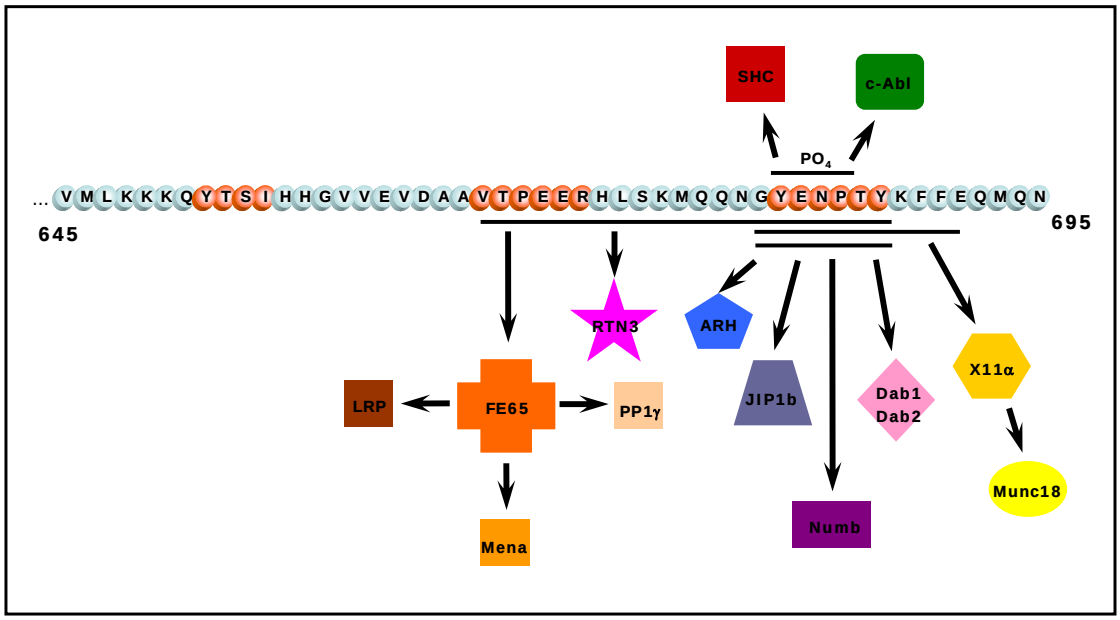

Figure 3. Proteins that interact with the cytoplasmic tail of APP. The X11 family, FE65 family, JIP family, Dab1 and 2 and ARH all contain PTB domains that interact with the YENPTY domain in the intracellular C-terminus of APP. FE65 may also require Thr^{668} for binding. The crystal structure of the X11α PTB domain bound to a YENPTY with additional residues essential for stabilization. SHC and Abl may be recruited to the YENPTY domain when the first tyrosine residue is phosphorylated.

FE65

Members of the FE65 family contain several protein interacting domains, including two PTB domains and a WW region. The interaction between APP and FE65 involves binding of the YENPTY domain and non-phosphorylated Thr^{668} in APP. Furthermore, the WW domain binds to MENA (mammalian enabled), which binds actin and thus links FE65 and APP to cytoskeletal dynamics and cellular motility . The PTB1

domain of FE65 binds both the transcription factor complex CP2-LSF-LBP-1c, and the low density lipoprotein receptor-related protein (LRP). The PTB2 domain of FE65 binds the APP C-terminus, providing a potential scaffold between APP and LRP (Kinoshita et al. 2001). Additionally, *in silico* analysis of the FE65 sequence reveals the presence of a well conserved Ser/Thr protein phophatases type 1 (PP1) binding motif (RVGW), suggesting that hypothetically FE65 binds to PP1. *In vivo* studies confirmed this interaction. Thus, the hypothesis that subcellular targeting, involves APP binding proteins, which are in turn regulated by protein phosphorylation, becomes stronger and deserves further investigation.

In this work we demonstrate that both phosphorylation state mimicking mutants (Y687E and Y687F) interact with FE65, but that the interaction is strongest with the dephosphorylation mimicking mutant (Fig. 3 and 5, Pag. 191 and 194). Hence the idea of a tri-complex was forthcoming and became stronger with the fact that PP1γ is preferentially immunoprecipitated with the Y687F mutant. Differential interaction between the phosphorylation mimicking mutants was not unexpected given the previously discussed differences on subcellular targeting, namely endocytosis, as described for these mutants. Interestingly, the Y687F mutant that is readily endocytosed and produces more Abeta, also binds more efficiently to FE65 that is in agreement with previously described data (Sabo et al. 1999). The Yeast Two-Hybrid data also support the immunoprecipitation data indicating that FE65 binds significantly more to the Y687F mutant. The occurrence *in vivo* of the tri-complexformat suggests that the three proteins are interacting. Moreover, we demonstrate that FE65 binds simultaneously to APP and PP1γ both in neuronal and non-neuronal cell lines. It seems that FE65 is the bridging protein between APP and PP1γ meaning that FE65 is responsible for mediating this interaction.

In vitro studies demonstrated that hyperphosphorylated tau in AD brains (ADP-tau) can be dephosphorylated by PP1, PP2A and PP2B, but not by PP2C (Gong et al. 1994a; Gong et al. 1994b; Gong et al. 1994c). PP1 and PP2A together account for over 90% of the total mammalian brain protein phosphoseryl/phosphothreonyl phosphatase activity and any alteration in the activity of these two phosphatases may significantly affect the phosphorylation state of tau or of other phosphorylated proteins. A decrease of about 20% in the activities of PP1 and PP2A has been reported in AD brains (Gong et al. 1994a; Gong et al. 1995; Gong et al. 1993; Gong et al. 1994c). Moreover, Lee et al (2003b) demonstrated that 7 of the 8 potentially phosphorylatable residues in the intracellular domain of APP were phosphorylated in AD patients, namely Tyr^{653}, Ser^{655}, Thr^{668}, $Ser^{675,}$ Tyr^{682}, Thr^{686} and Tyr^{687}.

One very attractive model is that FE65 is promoting the interaction between the APP and PP1γ, and that PP1γ in turn is responsible for the dephosphorylation of APP at one of the previously mentioned residue or another protein relevant in APP processing. However, the exact mechanism needs further investigation. Using overlay experiments, we proved unequivocally that FE65 is thebridge protein between FE65 and PP1γ, given that in the absence of FE65, APP and PP1γ were no longer able to interact. Taken together, the results are consistent with this hypothesis. Therefore, FE65 is included in the group of proteins known as "scaffold" or "bridge" proteins. These proteins are molecular intermediaries that help cell signaling proteins to interact and are also responsible for the recruitment of some effectors in the pathway. Furthermore, the idea of APP as a signal transduction molecule becomes stronger and gains additional support. Thus, signal transduction based diagnostics and therapeutics (discussed later) represent important future strategies of relevance to AD and other neurodegenerative diseases. The future identification of the kinases and phosphatases that act upon each of the APP phosphorylatable residues will likely prove useful in this respect.

RTN3

Prior to the work here presented, RTN3 had been linked to AD given that it interacts with BACE-1 and inhibits its activity (He et al. 2006; Tang and Liou 2007) (Murayama et al. 2006). Recently, RTN3 it has been described as contributing to the formation of dystrophic neurites in AD (Hu et al. 2007) and was found down regulated in AD brains (Yokota et al. 2006). We described a novel interaction between RTN3-B and APP, and therefore propose that these two proteins are functionally related. Evidence of the potential functional roles of RTN3-B have emerged from *in silico* analysis. Besides the reticulon homology domain (RHD) located at C-terminal tail which encompasses two large transmembrane domains, it contains a WW domain located at the N-terminus of the protein, important to mediate phosphorylation-dependent interactions (Fig. 1, Pag. 164). Moreover, it contains several phosphorylation sites for various kinases, including CK1, CK2 and MAPK, suggesting that this protein can be regulated by protein phosphorylation. The targeting of RTN3-B from the *trans*-Golgi network (TGN) to the endosomal-lysosomal compartments is mediated by protein sorting and the internalization signal. This domain is of extreme importance if we consider that APP processing can occur during its residence in the TGN and in the endocytic pathway, including amyloidogenic processing. Our results strongly suggest that there is a role involving a direct interaction between RTN3-B and

APP and the former may be responsible for altered APP targeting and processing. Co-immunoprecipitations and co-localization studies confirmed this interaction.

Recent data concerning the RTN3 topology indicates that it forms a ω-shape structure with the N- and the C-terminal of RTN3 facing the intracellular/cytosolic side (He et al. 2007). The determination of RTN3 topology helps to explain not only the interaction of RTN3 and BACE-1 but also the interaction of RTN3-B and APP, because both C-terminal tails face the cytosolic side, the same topological orientation makes this binding compatible. These results confirm that the interaction proposed above is topologically possible.

The APP:RTN3-B interaction also caused increases in αsAPP and CTFs (Fig. 5, Fig. 170). These results suggest that RTN3-B seems to be involved in targeting APP to specific subcellular locations where its α-secretase proteolytic processing occurs, and directing it to the non-amyloidogenic pathway. This finding is particularly important in terms of AD therapy, because RTN3-B seems be a good target for therapeutic intervention, sincein its presence we are able to diminish the Abeta production.

5.8 AD PATHOPHYSIOLOGY AND THERAPY

Alzheimer's disease is the most common form of dementia in the industrialized countries. If more effective therapies are not developed that either prevent AD or block progression of the disease in its very early stages, the economic and socital coats of treating AD patients will be devastating.

There is now consensus that protein misfolding, aggregation, amyloid formation, or some combination of these events triggers many types of neurodegenerative diseases, including AD. Genetic studies of mutations that cause early onset AD provide tremendous support for the notion that preventing Abeta aggregation will prevent AD. All genetic alterations linked to AD alter Abeta in a way that increases it propensity to aggregate (Golde et al. 2000; Hardy and Selkoe 2002; Younkin 1998). Similarly, genetic evidence from frontal temporal dementia showing that mutations in tau lead to abnormal tau accumulation in NFT and possible other smaller aggregates suggest that the abnormal accumulation of tau is also linked to neurodegeneration. Thus, Abeta and tau are prime targets for disease therapeutics. Preventing the abnormal misfolding, aggregation and accumulation of Abeta, tau or both, should result in a disease modifying AD therapy. AD could be prevented or more effectively treated by: **(1)** decreasing Abeta and tau production; **(2)** preventing aggregation or misfolding of these proteins; **(3)** neutralizing or removing the toxic aggregate or misfolded forms of these proteins or **(4)** combination of these modalities. Despite the huge investment in research and development, only a few anti-Abeta therapies are being clinically evaluated and there are even fewer human trials targeting tau (Golde 2003, 2005)

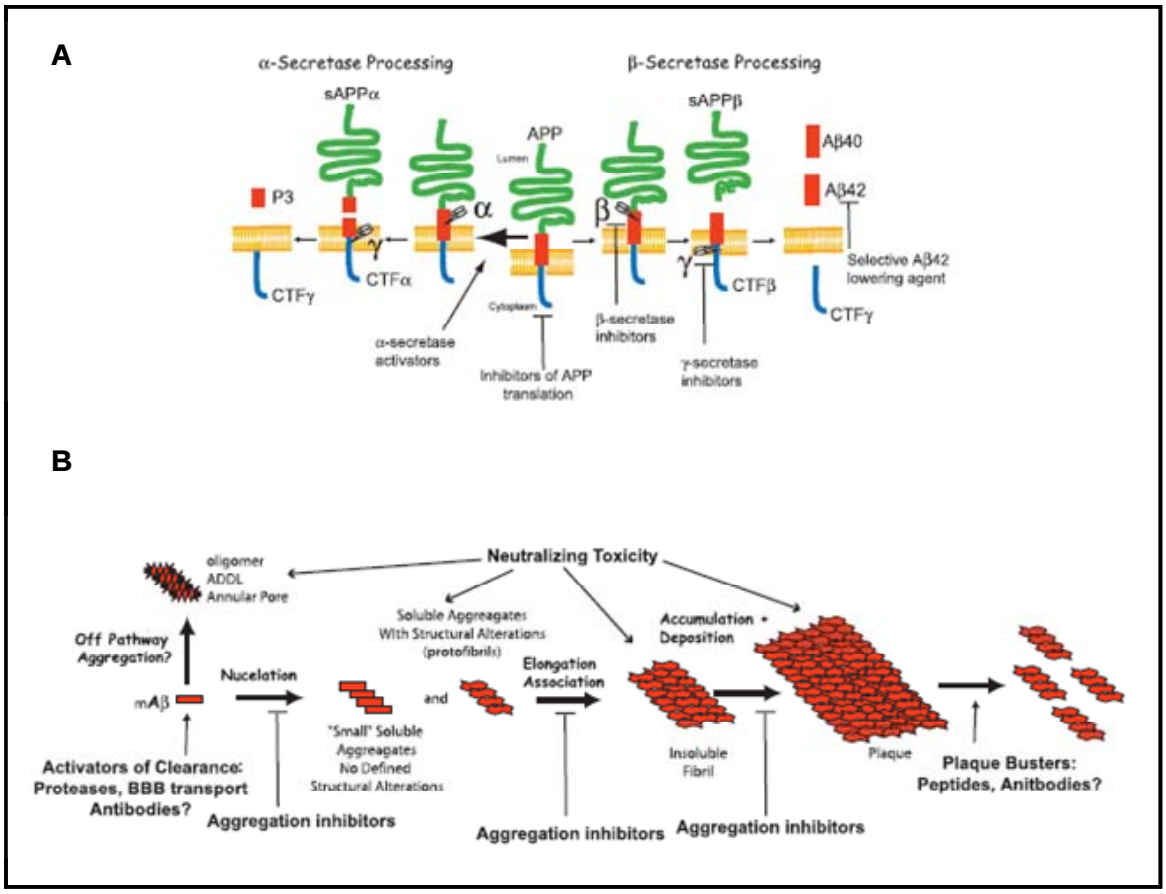

Figure 4. Abeta based therapeutic targets. A. Targets based on altering production of APP. In the α-secretase pathway, the Abeta sequence is cleaved in two and so is called non-amyloidogenic and therefore protective. Thus, increasing α-secretase cleavage is a possible therapeutic option. Multiple ways to interfere in amyloidogenic pathway (β-secretase processing of APP) have been identified and are summarized in this figure. Promising therapeutic targets include the aspartyl protease β-secretase, γ-secretase inhibitors that target presenilin and modulators that selectively alter $Abeta_{1-42}$ production. **B. Targets based on altering Abeta clearance or aggregation**. Abeta aggregation is thought to be a concentration dependent seeded polymerization reaction that proceeds through a nucleation event. As Abeta aggregates, it undergoes a structural conversion to a highly ordered β-sheet conformation that is characteristic of an amyloid deposit. At the moment is it not clear whether oligomeric species that have been identified are 'on' or 'off' pathway intermediates in the amyloid deposition process. Generic strategies for perturbing this pathway are shown and include aggregation inhibitors, antibody based therapies and methods to activate clearance of monomeric Abeta or Abeta aggregates (taken from Golde 2006).

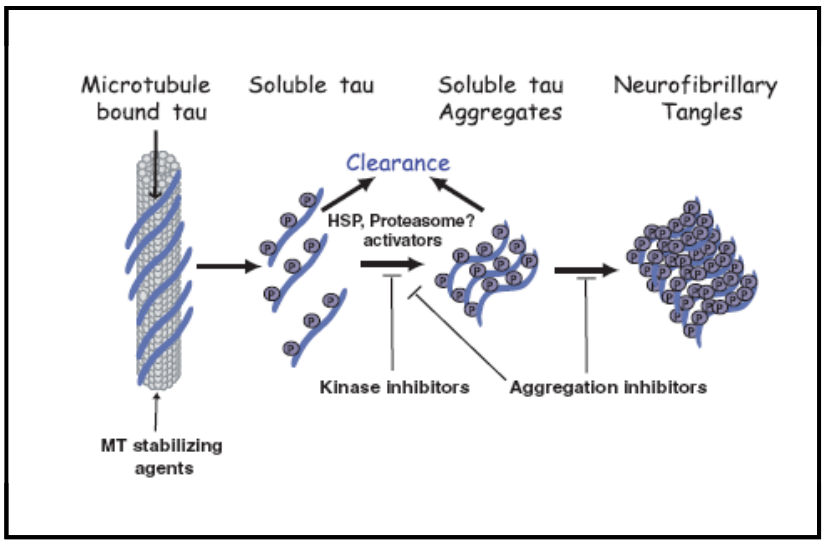

Figure 5. Tau based therapeutic targets. Tau binding to microtubules (MT) stabilizes the microtubule. Phosphorylated tau does not bind the microtubules as well, leading to the hypothesis that phosphorylation regulates tau binding to MT. Some soluble normally phosphorylated tau is present in the cell, but hyperphosphorylated tau accumulates in NFTs. It is thought that abnormal soluble aggregates of abnormally folded tau contribute to degenerative disease processes, though such small soluble tau assemblies have not been identified. In any case, soluble misfolded tau is thought to contribute to the disease process. Although tangles are often not thought of asd amyloid they are in fact amyloid structures within the cell. General strategies for altering tau accumulation are identified. These include microtubule stabilizing agents, kinase inhibitors, aggregation inhibitors and methods to enhance clearance of either soluble tau or tau aggregates via chaperones (e. g. HSPs, CHIP) or proteases (e. g. the proteasome) (taken from Golde 2006).

5.8.1 CURRENT THERAPY FOR AD

Currently approved drugs for the treatment of AD target the metabolic deficits observed in the disease, associated with reduced brain function and include two classes of drugs: the acetyl cholinesterase inhibitors (AchEI) (tacrine, donepizil, rivastigmine, galantamine) and the *N*-methyl-D-aspartate (NMDA) receptor antagonist memantine. These drugs appear to provide short-term benefits to patients based on enhancement of remaining cognitive functions. However, they do not provide a significant delay of disease progression Because of the limited efficacy of these drugs, the main focus of medical management of AD patients is therefore monitoring of progress of their disease and providing an appropriate level of supportative care

5.8.2 EXPERIMENTAL THERAPY FOR AD

As research into the onset and progression of AD has progressed over the last decade, an expanding range of potential mechanisms of intervention has emerged with the goal of developing disease-modifying therapies that will slow, if not reverse, the progression of disease. Experimental therapies based on modulation of APP/Abeta pathways can be broadly described as being based on three types of approaches: preventing the production of Abeta, preventing the formation of toxic forms of Abeta, preventing the toxic effects of Abeta. Representative experimental therapeutics targeting Abeta for the treatment of AD, which have reached clinical trials are described in Table 1. Antiamyloid strategies fall into three basic categories: immunotherapy agents, antiaggregants, and secretase modulators.

Immunotherapy agents. The most advanced of these approaches is that of immunotherapy based on vaccination with Abeta. The potential importance of immunotherapy approaches to AD was first demonstrated by Salomon et al. (1997) using antibodies raised against $Abeta_{28}$ which bound to and disaggregated premade Abeta fibrils. Antibodies were also shown to block the toxic effects of fibrillar Abeta on cells. Subsequent and somewhat speculative experiments with active vaccination with Abeta produced rather extraordinary positive results in transgenic mice (Janus et al. 2000; Morgan et al. 2000; Schenk et al. 1999). Following this observation, these effects were obtained using passive vaccination, the direct administration of antibodies raised against Abeta (DeMattos et al. 2001). Even brief administration of anti-Abeta antibodies was found to produce a cognitive benefit in the absence of a significant effect on amyloid burden (Dodart et al. 2002). Because of robust effects in animal

models, this approach has entered clinical trials and has provided evidence of efficacy in a small number of patients. While the first vaccine appeared to be safe and could elicit an immune response in a majority of subjects, with repeated injections (Bayer et al. 2005)(, this first trial was put on hold because of significant side effect of meningoencephalitis in a small subset of patients (Mathews and Nixon 2003; Orgogozo et al. 2003) which raised concerns with immunotherapy approaches (McGeer and McGeer 2003).

Table 1. Experimental therapeutics targeting Abeta for the treatment of AD in clinical development.

MECHANISM OF ACTION	COMPANY, PRODUCT, (STAGE OF DEVELOPMENT)
Abeta aggregation inhibitor	Neurochem, Alzhemed™ (tramiprosate; Phase III)
γ-secretase modulators	Myriad Genetics, Flurizan (tarenflurbil; Phase III) Eisai, E2012 (Phase I)
γ-secretase inhibitors	Lilly, LY450139 (Phase I) Wyeth, GSI-953 (Phase I)
Passive immunization against Abeta	Wyeth/Elan. Bapineuzumab (AAB-001; Phase III) Lilly, humanised m266 (LY206430; Phase I) Wyeth/Elan, AAB-002 (Phase 0) Pfizer/Rinat RN1219 (Phase I)
Active immunization against Abeta	Novartis/Cytos, anti-Abeta fragment (Phase I) Wyeth/Elan, ACC-001 (Phase I)
Abeta-ROS-directed metal chelator	Prana, PBT1 (cliquinol, Phase IIa, discontinued) PBT2 (Phase IIa)

Antiaggregants. Similarly advanced is the effort to develop an antagonist of Abeta aggregation. Numerous reports have been published describing a range of compounds that inhibit the transition of monomeric Abeta to toxic oligomers and/or polymers. Neurochem is developing a compound mimicking the glycosaminoglycans that inhibits Abeta aggregation. Their compound for AD, 3-aminopropane-1-sulfonate also named Alzhemed™, is now in Phase III clinical trials (Aisen, 2005). At least two other aggregation inhibitors are known to have entered clinical trials, the peptidic compound Apan™ of Praecis Pharmaceuticals (Findeis, 2002), and *scyllo*-inositol at Transition Therapeutics (McLaurin et al. 2000).

Secretase modulators. Despite difficulties encountered in the development of drug-like selective β-secretase inhibitors, it is almost certain, given the investment by pharmaceutical companies and others in this area, that brain penetrant, orally bioavailable, selective β-secretase inhibitors will be developed in the next few years. It remains to be determined whether long-term treatment with β-secretase inhibitors will be tolerated.

Potent inhibitors that target the multicomponent γ-secretase enzyme, have been developed and even entered into Phase I human clinical trials (Golde and Eckman, 2003; Siemers et al. 2005). These inhibitors appear to target presenilin 1 or 2, which are apparent catalytic components of the γ-secretase complex. However, the continued development of these inhibitors as AD therapeutics is controversial due to target-based toxicities attributable to effects on other γ-secretase substrates such as Notch (De Strooper et al. 1999; Saxena et al. 2001). Targeting γ-secretase cleavage with non-steroidal anti-inflammatory compounds (NSAIDs) and their derivatives is being used. These types of compounds modulate γ-secretase by shifting cleavage from $Abeta_{1-42}$ to shorter Abeta peptides and do not result in substrate accumulation or functional impairment of other g-secretase substrates (Weggen et al. 2001). A selective $Abeta_{1-42}$ lowering agent, R-Flurbiprofen (Flurizan) is currently being evaluated in a Phase II human trial. Notably, one year randomized, placebo-controlled, double-blind Phase 2 study of R-flurbiprofen (MPC-7869, Myriad Pharmaceuticals, Inc.), in 2007 subjects with mild to moderate AD subjects receiving the highest dose of MPC-7869, a statistically significant benefit was observed in activities of daily living and global function with positive trends in cognition (Black et al. 2006).

Muscarinic agonist, hormone replacement and statins have all been tested as possible AD therapies in clinical trials (Nitsch 1996; Sparks et al. 2005). Whether such agents could work in AD by altering α-secretase activity is not clear. They clearly have multiple pharmacologic targets. Indeed, a recent study in AD mouse model that

develops both amyloid deposition and neurobibrillary pathology using the M1 agonist AF267B suggest that inhibitors of this type increase α-secretase cleavage of APP and may also decrease GSK3β activity and thus reduce tau pathology (Caccano et al.2006).

Another approach that has reached human clinic trials is that of modulating the aparent ability of Abeta to promote the generation of toxic reactive oxygen species (ROS). Certain metal chelators have been shown to reduce the toxicity associated with Abeta. An initial trial with clioquinol provided evidence of efficacy (Ritchie et al. 2003) and a second generation compound, PBT2, is now in the clinic trials (http://www.pranabio.com/research/clinical_trials.asp).

5.9 Y687 PHOSPHORYLATION IN AD PATHOPHYSIOLOGY AND THERAPY

APP abnormal cleavage may arise from various sources including altered APP trafficking. For example, a major FAD gene (Barinaga 1995) encodes a protein homologous to the *C. elegans* Spe4, a protein that plays a role in membrane sorting (L'Hernault and Arduengo 1992), raising the possibility that missorting of APP may contribute to some forms of AD. The high Abeta levels observed in AD patients may lead to altered protein traffic, and many authors now defend impaired APP-dependent secretory traffic as a possible mechanism of AD pathogenesis. Hence, it would be desirable to transiently set a cellular system in which APP could still perform its nuclear signalling but where Abeta levels would not be significantly enhanced and APP traffic would not be inhibited. Our results suggest that APP Y687 phosphorylation is suitable for all these purposes, and further work will be carried out to clarify its the role in neuronal cells.

Nowadays, combination therapy is believed to be the future therapeutic strategy for AD that gives maximum results. Not all studies favour the superior efficacy of combination therapy, but some studies show some evidence for synergistic combination effects of symptomatic therapy, including delay or prevention of disease progression (Schmidt et al. 1997). Results discussed above highlight the possible benefits of a combined strategy of targeting APP to the α-secretase processing, even in a background of high β-secretase processing. Considering this APP processing pathway, several drugs with brain protective beneficial effects and that lower Abeta production, such as NSAIDs, statins and flavonoids, were recently found to channel APP to non-amyloidogenic processing (review in Tang 2005). Anti-AChE drugs increasing acetylcholine brain levels also lead to an up-regulation in the αsAPP

processing through M1 receptors. The benefit of neurotrophic factors in dementia has been highlighted (Levy et al. 2005), and αsAPP is one such factor. Besides having synaptogenic properties, this APP fragment counteracts Abeta toxicity and glutamate-induced excitotoxicity and dendrite outgrowth inhibition, through modulation of cGMP and intracellular calcium levels (reviewed in Mattson and Chan 2003). Y687 phosphorylation seems to 'activate' the APP molecule to be targeted to subcellular sites of α-secretase processing. In speculative terms, favouring the cerebral production of the neuroprotective αsAPP through Y687 phosphorylation looks appealing, as it could also potentially maintain Abeta levels low. The development of therapeutic drugs targeting APP Tyr^{687} phosphorylation could also involve protein phosphatases and selective targets of these proteins may be accomplished by identifying protein phosphatase interacting which can be tissue-specific and provide ideal target proteins for therapeutics. (da Cruz e Silva and da Cruz e Silva 2003; da Cruz e Silva et al. 2004b).

5.10 REFERENCES

Ando K, Iijima KI, Elliott JI, Kirino Y, Suzuki T. 2001. Phosphorylation-dependent regulation of the interaction of amyloid precursor protein with Fe65 affects the production of beta-amyloid. J Biol Chem 276(43):40353-40361.

Barinaga M. 1995. New Alzheimer's gene found. Science 268:1845-1846. .

Bayer AJ, Bullock R, Jones RW, Wilkinson D, Paterson KR, Jenkins L, Millais SB, Donoghue S. 2005. Evaluation of the safety and immunogenicity of synthetic Abeta42 (AN1792) in patients with AD. Neurology 64(1):94-101.

Berdnik D, Torok T, Gonzalez-Gaitan M, Knoblich JA. 2002. The endocytic protein alpha-Adaptin is required for numb-mediated asymmetric cell division in Drosophila. Dev Cell 3(2):221-231.

Bibb J, da Cruz e Silva E. 1997. Identification of posttranslational modification sites by site-directed mutagenesis. Jr. HH, editor. Totowa: NJ Humana Press. 275–307 p.

Black S, Wilcock G, Hawworth J, Hendrix S, Zavitz K, Christensen D-H, Bass S, Laughlin M, Swabb E. 2006. efficacy and safety of MPC-7869 (R.-flurbiprofen), a selective Abeta42 loering agent in mild Alzheimer's disease: results of 12-month phase 2 trial and 1-year follow on study. Neurology 66:A347.

Bonifacino JS, Rojas R. 2006. Retrograde transport from endosomes to the trans-Golgi network. Nat Rev Mol Cell Biol 7(8):568-579.

Bonifacino JS, Traub LM. 2003. Signals for sorting of transmembrane proteins to endosomes and lysosomes. Annu Rev Biochem 72:395-447.

Borg JP, Ooi J, Levy E, Margolis B. 1996. The phosphotyrosine interaction domains of X11 and FE65 bind to distinct sites on the YENPTY motif of amyloid precursor protein. Mol Cell Biol 16(11):6229-6241.

Bressler SL, Gray MD, Sopher BL, Hu Q, Hearn MG, Pham DG, Dinulos MB, Fukuchi K, Sisodia SS, Miller MA, Disteche CM, Martin GM. 1996. cDNA cloning and chromosome mapping of the human Fe65 gene: interaction of the conserved cytoplasmic domains of the human beta-amyloid precursor protein and its homologues with the mouse Fe65 protein. Hum Mol Genet 5(10):1589-1598.

Chen WJ, Goldstein JL, Brown MS. 1990. NPXY, a sequence often found in cytoplasmic tails, is required for coated pit-mediated internalization of the low density lipoprotein receptor. J Biol Chem 265(6):3116-3123.

da Cruz e Silva EF, da Cruz e Silva OA. 2003. Protein phosphorylation and APP metabolism. Neurochem Res 28(10):1553-1561.

da Cruz e Silva OA, Fardilha M, Henriques AG, Rebelo S, Vieira S, da Cruz e Silva EF. 2004. Signal transduction therapeutics: relevance for Alzheimer's disease. J Mol Neurosci 23(1-2):123-142.

De Strooper B, Annaert W, Cupers P, Saftig P, Craessaerts K, Mumm JS, Schroeter EH, Schrijvers V, Wolfe MS, Ray WJ, Goate A, Kopan R. 1999. A presenilin-1-dependent gamma-secretase-like protease mediates release of Notch intracellular domain. Nature 398(6727):518-522.

DeMattos RB, Bales KR, Cummins DJ, Dodart JC, Paul SM, Holtzman DM. 2001. Peripheral anti-A beta antibody alters CNS and plasma A beta clearance and decreases brain A beta burden in a mouse model of Alzheimer's disease. Proc Natl Acad Sci U S A 98(15):8850-8855.

Dodart JC, Bales KR, Gannon KS, Greene SJ, DeMattos RB, Mathis C, DeLong CA, Wu S, Wu X, Holtzman DM, Paul SM. 2002. Immunization reverses memory deficits without reducing brain Abeta burden in Alzheimer's disease model. Nat Neurosci 5(5):452-457.

Duilio A, Faraonio R, Minopoli G, Zambrano N, Russo T. 1998. Fe65L2: a new member of the Fe65 protein family interacting with the intracellular domain of the Alzheimer's beta-amyloid precursor protein. Biochem J 330 (Pt 1):513-519.

Fiore F, Zambrano N, Minopoli G, Donini V, Duilio A, Russo T. 1995. The regions of the Fe65 protein homologous to the phosphotyrosine interaction/phosphotyrosine

binding domain of Shc bind the intracellular domain of the Alzheimer's amyloid precursor protein. J Biol Chem 270(52):30853-30856.

Fisher A, Heldman E, Gurwitz D, Haring R, Karton Y, Meshulam H, Pittel Z, Marciano D, Brandeis R, Sadot E, Barg Y, Pinkas-Kramarski R, Vogel Z, Ginzburg I, Treves TA, Verchovsky R, Klimowsky S, Korczyn AD. 1996. M1 agonists for the treatment of Alzheimer's disease. Novel properties and clinical update. Ann N Y Acad Sci 777:189-196.

Golde TE. 2006. Disease modifying therapy for AD? J Neurochem 99(3):689-707.

Golde TE, Eckman CB, Younkin SG. 2000. Biochemical detection of Abeta isoforms: implications for pathogenesis, diagnosis, and treatment of Alzheimer's disease. Biochim Biophys Acta 1502(1):172-187.

Gong CX, Grundke-Iqbal I, Damuni Z, Iqbal K. 1994a. Dephosphorylation of microtubule-associated protein tau by protein phosphatase-1 and -2C and its implication in Alzheimer disease. FEBS Lett 341(1):94-98.

Gong CX, Grundke-Iqbal I, Iqbal K. 1994b. Dephosphorylation of Alzheimer's disease abnormally phosphorylated tau by protein phosphatase-2A. Neuroscience 61(4):765-772.

Gong CX, Shaikh S, Wang JZ, Zaidi T, Grundke-Iqbal I, Iqbal K. 1995. Phosphatase activity toward abnormally phosphorylated tau: decrease in Alzheimer disease brain. J Neurochem 65(2):732-738.

Gong CX, Singh TJ, Grundke-Iqbal I, Iqbal K. 1993. Phosphoprotein phosphatase activities in Alzheimer disease brain. J Neurochem 61(3):921-927.

Gong CX, Singh TJ, Grundke-Iqbal I, Iqbal K. 1994c. Alzheimer's disease abnormally phosphorylated tau is dephosphorylated by protein phosphatase-2B (calcineurin). J Neurochem 62(2):803-806.

Guenette SY, Chen J, Jondro PD, Tanzi RE. 1996. Association of a novel human FE65-like protein with the cytoplasmic domain of the beta-amyloid precursor protein. Proc Natl Acad Sci U S A 93(20):10832-10837.

Hardy J, Selkoe DJ. 2002. The amyloid hypothesis of Alzheimer's disease: progress and problems on the road to therapeutics. Science 297(5580):353-356.

He W, Hu X, Shi Q, Zhou X, Lu Y, Fisher C, Yan R. 2006. Mapping of interaction domains mediating binding between BACE1 and RTN/Nogo proteins. J Mol Biol 363(3):625-634.

He W, Shi Q, Hu X, Yan R. 2007. The membrane topology of RTN3 and its effect on binding of RTN3 to BACE1. J Biol Chem 282(40):29144-29151.

He X, Li F, Chang WP, Tang J. 2005. GGA proteins mediate the recycling pathway of memapsin 2 (BACE). J Biol Chem 280(12):11696-11703.

Hirst J, Robinson MS. 1998. Clathrin and adaptors. Biochim Biophys Acta 1404(1-2):173-193.

Homayouni R, Rice DS, Sheldon M, Curran T. 1999. Disabled-1 binds to the cytoplasmic domain of amyloid precursor-like protein 1. J Neurosci 19(17):7507-7515.

Hu X, Shi Q, Zhou X, He W, Yi H, Yin X, Gearing M, Levey A, Yan R. 2007. Transgenic mice overexpressing reticulon 3 develop neuritic abnormalities. Embo J 26(11):2755-2767.

Inomata H, Nakamura Y, Hayakawa A, Takata H, Suzuki T, Miyazawa K, Kitamura N. 2003. A scaffold protein JIP-1b enhances amyloid precursor protein phosphorylation by JNK and its association with kinesin light chain 1. J Biol Chem 278(25):22946-22955.

Janus C, Pearson J, McLaurin J, Mathews PM, Jiang Y, Schmidt SD, Chishti MA, Horne P, Heslin D, French J, Mount HT, Nixon RA, Mercken M, Bergeron C, Fraser PE, St George-Hyslop P, Westaway D. 2000. A beta peptide immunization reduces behavioural impairment and plaques in a model of Alzheimer's disease. Nature 408(6815):979-982.

Kato Y, Misra S, Puertollano R, Hurley JH, Bonifacino JS. 2002. Phosphoregulation of sorting signal-VHS domain interactions by a direct electrostatic mechanism. Nat Struct Biol 9:532-536.
Kimberly WT, Zheng JB, Town T, Flavell RA, Selkoe DJ. 2005. Physiological regulation of the beta-amyloid precursor protein signaling domain by c-Jun N-terminal kinase JNK3 during neuronal differentiation. J Neurosci 25(23):5533-5543.
Kinoshita A, Whelan CM, Smith CJ, Mikhailenko I, Rebeck GW, Strickland DK, Hyman BT. 2001. Demonstration by fluorescence resonance energy transfer of two sites of interaction between the low-density lipoprotein receptor-related protein and the amyloid precursor protein: role of the intracellular adapter protein Fe65. J Neurosci 21(21):8354-8361.
Klafki HW, Wiltfang J, Staufenbiel M. 1996. Electrophoretic separation of betaA4 peptides (1-40) and (1-42). Anal Biochem 237(1):24-29.
L'Hernault SW, Arduengo PM. 1992. Mutation of a putative sperm membrane protein in Caenorhabditis elegans prevents sperm differentiation but not its associated meiotic divisions. . J Cell Biol 119:55-68.
Lee EB, Skovronsky DM, Abtahian F, Doms RW, Lee VM. 2003a. Secretion and intracellular generation of truncated Abeta in beta-site amyloid-beta precursor protein-cleaving enzyme expressing human neurons. J Biol Chem 278(7):4458-4466.
Lee MS, Kao SC, Lemere CA, Xia W, Tseng HC, Zhou Y, Neve R, Ahlijanian MK, Tsai LH. 2003b. APP processing is regulated by cytoplasmic phosphorylation. J Cell Biol 163(1):83-95.
Levy YS, Gilgun-Sherki Y, Melamed E, Offen D. 2005. Therapeutic potential of neurotrophic factors in neurodegenerative diseases. BioDrugs 19(2):97-127.
Mathews PM, Nixon RA. 2003. Setback for an Alzheimer's disease vaccine: lessons learned. Neurology 61(1):7-8.
Matsuda S, Yasukawa T, Homma Y, Ito Y, Niikura T, Hiraki T, Hirai S, Ohno S, Kita Y, Kawasumi M, Kouyama K, Yamamoto T, Kyriakis JM, Nishimoto I. 2001. c-Jun N-terminal kinase (JNK)-interacting protein-1b/islet-brain-1 scaffolds Alzheimer's amyloid precursor protein with JNK. J Neurosci 21(17):6597-6607.
Mattson MP, Chan SL. 2003. Neuronal and glial calcium signaling in Alzheimer's disease. Cell Calcium 34(4-5):385-397.
McGeer PL, McGeer E. 2003. Is there a future for vaccination as a treatment for Alzheimer's disease? Neurobiol Aging 24(3):391-395.
McLoughlin DM, Irving NG, Brownlees J, Brion JP, Leroy K, Miller CC. 1999. Mint2/X11-like colocalizes with the Alzheimer's disease amyloid precursor protein and is associated with neuritic plaques in Alzheimer's disease. Eur J Neurosci 11(6):1988-1994.
Milton NG. 2005. Phosphorylated amyloid-beta: the toxic intermediate in alzheimer's disease neurodegeneration. Subcell Biochem 38:381-402.
Morgan D, Diamond DM, Gottschall PE, Ugen KE, Dickey C, Hardy J, Duff K, Jantzen P, DiCarlo G, Wilcock D, Connor K, Hatcher J, Hope C, Gordon M, Arendash GW. 2000. A beta peptide vaccination prevents memory loss in an animal model of Alzheimer's disease. Nature 408(6815):982-985.
Morris NJ, Ross SA, Neveu JM, Lane WS, Lienhard GE. 1999. Cloning and characterization of a 22 kDa protein from rat adipocytes: a new member of the reticulon family. Biochim Biophys Acta 1450(1):68-76.
Murayama KS, Kametani F, Saito S, Kume H, Akiyama H, Araki W. 2006. Reticulons RTN3 and RTN4-B/C interact with BACE1 and inhibit its ability to produce amyloid beta-protein. Eur J Neurosci 24(5):1237-1244.
Muresan Z, Muresan V. 2004. A phosphorylated, carboxy-terminal fragment of beta-amyloid precursor protein localizes to the splicing factor compartment. Hum Mol Genet 13(5):475-488.

Muresan Z, Muresan V. 2005. c-Jun NH2-terminal kinase-interacting protein-3 facilitates phosphorylation and controls localization of amyloid-beta precursor protein. J Neurosci 25(15):3741-3751.

Nitsch RM. 1996. From acetylcholine to amyloid: neurotransmitters and the pathology of Alzheimer's disease. Neurodegeneration 5(4):477-482.

Noviello C, Vito P, Lopez P, Abdallah M, D'Adamio L. 2003. Autosomal recessive hypercholesterolemia protein interacts with and regulates the cell surface level of Alzheimer's amyloid beta precursor protein. J Biol Chem 278(34):31843-31847.

Orgogozo JM, Gilman S, Dartigues JF, Laurent B, Puel M, Kirby LC, Jouanny P, Dubois B, Eisner L, Flitman S, Michel BF, Boada M, Frank A, Hock C. 2003. Subacute meningoencephalitis in a subset of patients with AD after Abeta42 immunization. Neurology 61(1):46-54.

Parat M-O, Fox P. 2001. Palmitoylation of caveoli-1 in endothelial cells is pottranslational but irreversible. J Biol Chem 276:15776-15782.

Ritchie CW, Bush AI, Mackinnon A, Macfarlane S, Mastwyk M, MacGregor L, Kiers L, Cherny R, Li QX, Tammer A, Carrington D, Mavros C, Volitakis I, Xilinas M, Ames D, Davis S, Beyreuther K, Tanzi RE, Masters CL. 2003. Metal-protein attenuation with iodochlorhydroxyquin (clioquinol) targeting Abeta amyloid deposition and toxicity in Alzheimer disease: a pilot phase 2 clinical trial. Arch Neurol 60(12):1685-1691.

Roncarati R, Sestan N, Scheinfeld MH, Berechid BE, Lopez PA, Meucci O, McGlade JC, Rakic P, D'Adamio L. 2002. The gamma-secretase-generated intracellular domain of beta-amyloid precursor protein binds Numb and inhibits Notch signaling. Proc Natl Acad Sci U S A 99(10):7102-7107.

Russo C, Dolcini V, Salis S, Venezia V, Zambrano N, Russo T, Schettini G. 2002. Signal transduction through tyrosine-phosphorylated C-terminal fragments of amyloid precursor protein via an enhanced interaction with Shc/Grb2 adaptor proteins in reactive astrocytes of Alzheimer's disease brain. J Biol Chem 277(38):35282-35288.

Russo C, Salis S, Dolcini V, Venezia V, Song XH, Teller JK, Schettini G. 2001. Amino-terminal modification and tyrosine phosphorylation of [corrected] carboxy-terminal fragments of the amyloid precursor protein in Alzheimer's disease and Down's syndrome brain. Neurobiol Dis 8(1):173-180.

Sabo SL, Lanier LM, Ikin AF, Khorkova O, Sahasrabudhe S, Greengard P, Buxbaum JD. 1999. Regulation of beta-amyloid secretion by FE65, an amyloid protein precursor-binding protein. J Biol Chem 274(12):7952-7957.

Saxena MT, Schroeter EH, Mumm JS, Kopan R. 2001. Murine notch homologs (N1-4) undergo presenilin-dependent proteolysis. J Biol Chem 276(43):40268-40273.

Scheinfeld MH, Roncarati R, Vito P, Lopez PA, Abdallah M, D'Adamio L. 2002. Jun NH2-terminal kinase (JNK) interacting protein 1 (JIP1) binds the cytoplasmic domain of the Alzheimer's beta-amyloid precursor protein (APP). J Biol Chem 277(5):3767-3775.

Schenk D, Barbour R, Dunn W, Gordon G, Grajeda H, Guido T, Hu K, Huang J, Johnson-Wood K, Khan K, Kholodenko D, Lee M, Liao Z, Lieberburg I, Motter R, Mutter L, Soriano F, Shopp G, Vasquez N, Vandevert C, Walker S, Wogulis M, Yednock T, Games D, Seubert P. 1999. Immunization with amyloid-beta attenuates Alzheimer-disease-like pathology in the PDAPP mouse. Nature 400(6740):173-177.

Schmidt M, Schmidtke G, Kloetzel PM. 1997. Structure and structure formation of the 20S proteasome. . Mol Biol Rep 24:103-112.

Seaman MN. 2004. Cargo-selective endosomal sorting for retrieval to the Golgi requires retromer. J Cell Biol 165(1):111-122.

Shiba T, Kametaka S, Kawasaki M, Shibata M, Waguri S, Uchiyama Y, Wakatsuki S. 2004. Insights into the phosphoregulation of beta-secretase sorting signal by the VHS domain of GGA1. Traffic 5(6):437-448.

Small SA, Gandy S. 2006. Sorting through the cell biology of Alzheimer's disease: intracellular pathways to pathogenesis. Neuron 52(1):15-31.
Small SA, Kent K, Pierce A, Leung C, Kang MS, Okada H, Honig L, Vonsattel JP, Kim TW. 2005. Model-guided microarray implicates the retromer complex in Alzheimer's disease. Ann Neurol 58(6):909-919.
Solomon B, Koppel R, Frankel D, Hanan-Aharon E. 1997. Disaggregation of Alzheimer beta-amyloid by site-directed mAb. Proc Natl Acad Sci U S A 94(8):4109-4112.
Sparks DL, Sabbagh MN, Connor DJ, Lopez J, Launer LJ, Petanceska S, Browne P, Wassar D, Johnson-Traver S, Lochhead J, Ziolkowski C. 2005. Atorvastatin therapy lowers circulating cholesterol but not free radical activity in advance of identifiable clinical benefit in the treatment of mild-to-moderate AD. Curr Alzheimer Res 2(3):343-353.
Tanahashi H, Tabira T. 1999. Molecular cloning of human Fe65L2 and its interaction with the Alzheimer's beta-amyloid precursor protein. Neurosci Lett 261(3):143-146.
Tang BL. 2005. Alzheimer's disease: channeling APP to non-amyloidogenic processing. Biochem Biophys Res Commun 331(2):375-378.
Tang BL, Liou YC. 2007. Novel modulators of amyloid-beta precursor protein processing. J Neurochem 100(2):314-323.
Tarr PE, Roncarati R, Pelicci G, Pelicci PG, D'Adamio L. 2002. Tyrosine phosphorylation of the beta-amyloid precursor protein cytoplasmic tail promotes interaction with Shc. J Biol Chem 277(19):16798-16804.
Taru H, Iijima K, Hase M, Kirino Y, Yagi Y, Suzuki T. 2002. Interaction of Alzheimer's beta -amyloid precursor family proteins with scaffold proteins of the JNK signaling cascade. J Biol Chem 277(22):20070-20078.
Taru H, Yoshikawa K, Suzuki T. 2004. Suppression of the caspase cleavage of beta-amyloid precursor protein by its cytoplasmic phosphorylation. FEBS Lett 567(2-3):248-252.
Tomita S, Ozaki T, Taru H, Oguchi S, Takeda S, Yagi Y, Sakiyama S, Kirino Y, Suzuki T. 1999. Interaction of a neuron-specific protein containing PDZ domains with Alzheimer's amyloid precursor protein. J Biol Chem 274(4):2243-2254.
Traub LM. 2005. Common principles in clathrin-mediated sorting at the Golgi and the plasma membrane. Biochim Biophys Acta 1744(3):415-437.
Venezia V, Russo C, Repetto E, Salis S, Dolcini V, Genova F, Nizzari M, Mueller U, Schettini G. 2004. Apoptotic cell death influences the signaling activity of the amyloid precursor protein through ShcA and Grb2 adaptor proteins in neuroblastoma SH-SY5Y cells. J Neurochem 90(6):1359-1370.
Wahle T, Prager K, Raffler N, Haass C, Famulok M, Walter J. 2005. GGA proteins regulate retrograde transport of BACE1 from endosomes to the trans-Golgi network. Mol Cell Neurosci 29(3):453-461.
Weggen S, Eriksen JL, Das P, Sagi SA, Wang R, Pietrzik CU, Findlay KA, Smith TE, Murphy MP, Bulter T, Kang DE, Marquez-Sterling N, Golde TE, Koo EH. 2001. A subset of NSAIDs lower amyloidogenic Abeta42 independently of cyclooxygenase activity. Nature 414(6860):212-216.
Wiltfang J, Esselmann H, Maler JM, Bleich S, Huther G, Kornhuber J. 2001. Molecular biology of Alzheimer's dementia and its clinical relevance to early diagnosis and new therapeutic strategies. Gerontology 47(2):65-71.
Wiltfang J, Smirnov A, Schnierstein B, Kelemen G, Matthies U, Klafki HW, Staufenbiel M, Huther G, Ruther E, Kornhuber J. 1997. Improved electrophoretic separation and immunoblotting of beta-amyloid (A beta) peptides 1-40, 1-42, and 1-43. Electrophoresis 18(3-4):527-532.
Yokota T, Mishra M, Akatsu H, Tani Y, Miyauchi T, Yamamoto T, Kosaka K, Nagai Y, Sawada T, Heese K. 2006. Brain site-specific gene expression analysis in Alzheimer's disease patients. Eur J Clin Invest 36(11):820-830.
Younkin SG. 1998. The role of A beta 42 in Alzheimer's disease. J Physiol Paris 92(3-4):289-292.

Yun M, Keshvara L, Park CG, Zhang YM, Dickerson JB, Zheng J, Rock CO, Curran T, Park HW. 2003. Crystal structures of the Dab homology domains of mouse disabled 1 and 2. J Biol Chem 278(38):36572-36581.

Zambrano N, Bruni P, Minopoli G, Mosca R, Molino D, Russo C, Schettini G, Sudol M, Russo T. 2001. The beta-amyloid precursor protein APP is tyrosine-phosphorylated in cells expressing a constitutively active form of the Abl protoncogene. J Biol Chem 276(23):19787-19792.

Zambrano N, Buxbaum JD, Minopoli G, Fiore F, De Candia P, De Renzis S, Faraonio R, Sabo S, Cheetham J, Sudol M, Russo T. 1997. Interaction of the phosphotyrosine interaction/phosphotyrosine binding-related domains of Fe65 with wild-type and mutant Alzheimer's beta-amyloid precursor proteins. J Biol Chem 272(10):6399-6405.

Zheng B, Kimberly WT, Selkoe DJ. Temporal Regulation of the endogenous APP intracellular domain (AICD) in primary neurons. ; 2003. SFN.

Zhou D, Noviello C, D'Ambrosio C, Scaloni A, D'Adamio L. 2004. Growth factor receptor-bound protein 2 interaction with the tyrosine-phosphorylated tail of amyloid beta precursor protein is mediated by its Src homology 2 domain. J Biol Chem 279(24):25374-25380.

APPENDIX

APPENDIX I

REAGENTS AND SOLUTIONS

1. DNA Manipulation

Solutions for bacterial cultures, transformation and DNA extraction

- **SOB** (Fluka) 25.5 g/L

- **SOC**

- SOB	49 ml
- 1 M Glucose stock solution	1 ml

- **Competent cells solutions**

Solution I (1 L)**:**

- $MnCl_2.4H_2O$	9.9 g
- $CaCl_2.2H_2O$	1.5 g
- Glycerol	150 g
- KHAc	30 ml (1 M)

Adjust pH to 5.8 with HAc, filter through a 0.2 μm filter and store at 4ºC.

Solution II (1 L)**:**

- MOPS (0.5 M, pH 6.8)	20 ml
- RbCl	1.2 g
- $CaCl_2.2H_2O$	11 g
- Glycerol	150 g

Filter through a 0.2 μm filter and store at 4 ºC.

- **LB (Luria-Broth) medium** (Sigma) 20 g/L

- **LB agar plates**

For a final volume of 1 L, add 12 g of agar to 950 ml of LB medium. Mix until the solutes have dissolved. Adjust the volume of the solution to 1 litre with LB medium and sterilize by autoclaving. When at cooled splite the medium into plates (~ 20 ml/ 100 mm plate).

- **100 mg/ml Antibiotics stock solutions (Ampicilin or Kanamycin)**

Dissolve 1 g of the antibiotic in 10 ml of deionized H_2O. Mix until the solutes have dissolved, filter through a 0.2 μm filter, aliquot and store at -20 ºC.

■ **DNA extraction ('mini and maxi preps')**

Solution I ('resuspension'):

- Glucose	50 mM
- Tris.Cl (pH 8.0)	25 mM
- EDTA (pH 8.0)	10 mM

Solution II ('alkaline lysis'):

- NaOH	0.2 N
- SDS	1 %

Solution III ('neutralization'):

- 5 M Potassium acetate	3 M
- Glacial acetic acid	2 M

■ **50X TAE solution** (1 L)

- Tris base	242 g
- Glacial acetic acid	57.1 ml
- EDTA (pH 8.0)	100 ml

■ **TE buffer, pH 7.5**

- Tris-HCl (pH 7.5)	10 mM
- EDTA (pH 8.0)	1 mM

■ **RNase stock solution** 10 mg/ml

■ **10 mM dNTPs solution** (100 µl)

- dATP	10 µl
- dTTP	10 µl
- dCTP	10 µl
- dGTP	10 µl
- H_2O	60 µl

aliquot and keep at -20 ºC.

2. Cell Culture and Rat primary neuronal cultures

Cells seeding, maintenance and experiments

■ **DMEM medium (COS-7 cells)**

For a final volume of 1 L, dissolve one pack of DMEM powder (with L-glutamine and 4500 mg glucose/L, Sigma Aldrich) in deionised H_2O and add:

- $NaHCO_3$ (Sigma-Aldrich) 3.7 g

adjust to pH 7.4. Sterilize by filtering through a 0.2 μm filter and store at 4 ºC.

■ **Complete DMEM (COS-7 cells)**

For a final volume of 1 L, when preparing DMEM medium adjust to pH 7.4 and before sterilizing add:

- Fetal Bovine Serum (FBS) (Gibco BRL, Invitrogen) 100 ml (10% v/v)

Notes: FBS is heat-inactivated for 30 min at 56 ºC. For cells maintenance, prior to pH adjustment add 100 U/ml penicillin and 100 mg/ml streptomycin [10 ml Streptomycin/ Penicilin/ Amphotericin solution (Gibco BRL, Invitrogen)].

DMEM Components:	**(g/L)**
L-Arginine•HCl	0.084
L-Cystine•2HCl	0.0626
L-Glutamine	0.584
Glycine	0.03
L-Histidine•HCl• H2O	0.042
L-Isoleucine	0.105
L-Leucine	0.105
L-Lysine•HCl	0.146
L-Methionine	0.03
L-Phenylalanine	0.066
L-Serine	0.042
L-Threonine	0.095
L-Tryptophan	0.016
L-Tyrosine 2Na•2H2O	0.10379
L-Valine	0.094
Choline Chloride	0.004
Folic Acid	0.004
myo-Inositol	0.0072
Niacinamide	0.004
D-Pantothenic Acid hemicalcium	0.004
Pyridoxal•HCl	0.004
Riboflavin	0.0004
Thiamine•HCl	0.004
Calcium Chloride [Anhydrous]	0.2
Ferric Nitrate•9H2O	0.0001
Magnesium Sulfate [Anhydrous]	0.09767
Potassium Chloride	0.4
Sodium Chloride	6.4

Sodium Phosphate Monobasic [Anhydrous]	0.109
Glucose	4.5
Phenol Red•Na	0.0159

■ **PBS (1x)**

For a final volume of 500 ml, dissolve one pack of BupH Modified Dulbecco's Phosphate Buffered Saline Pack (Pierce) in deionised H_2O. Final composition:

- Sodium Phosphate	8 mM
- Potassium Phosphate	2 mM
- NaCl	140 mM
- KCl	10 mM

Sterilize by filtering through a 0.2 μm filter and store at 4 ºC.

■ **Complete Neurobasal medium (Cortex primary cultures)**

This serum-free medium (Neurobasal; Gibco, BRL) is supplemented with:

- B27 supplement (Gibco, BRL)	2%
- L-glutamine (Gibco, BRL)	0.5 mM
- Gentamicine (Gibco, BRL)	60 μg/ml
- Phenol Red (Sigma Aldrich, Portugal)	0.001%

Adjust to pH 7.4. Sterilize by filtering through a 0.2 μm filter and store at 4 ºC.

■ **Complete Neurobasal medium (Hippocampus primary cultures)**

This serum-free medium (Neurobasal; Gibco, BRL) is supplemented with:

- B27 supplement (Gibco, BRL)	2%
- L-glutamine (Gibco, BRL)	0.5 mM
- L-glutamate (Gibco, BRL)	0.5 mM
- Gentamicine (Gibco, BRL)	60 μg/ml
- Phenol Red (Sigma Aldrich, Portugal)	0.001%

Adjust to pH 7.4. Sterilize by filtering through a 0.2 μm filter and store at 4 ºC.

■ **Hank's balanced salt solution (primary neuronal cultures)**

This salt solution is prepared with deionised H_2O. Final composition:

- NaCl	137 mM
- KCl	5.36 mM
- KH_2PO_4	0.44 mM
- $Na_2HPO_42H_2O$	0.34 mM
- $NaHCO_3$	4.16 mM
- Glucose	5 mM
- Sodium pyruvate	1 mM
- HEPES	10 mM

Adjust to pH 7.4. Sterilize by filtering through a 0.2 μm filter and store at 4 ºC.

3. Cells fixation and Imunocytochemistry:

- **1 mg/ml Poly-L-ornithine solution (10x) (COS-7 cells)**

  To a final volume of 100 ml, dissolve in deionised H_2O 100 mg of poly-L-ornithine (Sigma-Aldrich, Portugal).

- **10 mg/ml Poly-D-lysine stock (100x) (rat primary neuronal cultures)**

  To a final volume of 10 ml, dissolve in deionised H_2O 100 mg of poly- D-lysine (Sigma-Aldrich).

- **Borate buffer (at primary neuronal cultures)**

  To a final volume of 1 L, dissolve in deionised H_2O 9.28 g of boric acid (Sigma-Aldrich). Adjust to pH 8.2, sterilize by filtering through a 0.2 μm filter, and store at 4 ºC.

- **Poly-D-lysine solution (neuronal cells)**

  To a final volume of 100 ml, dilute 1 ml of the 10 mg/ml poly-D-lysine stock solution in borate buffer.

- **4% Paraformaldehyde Fixative solution**

  For a final volume of 100 ml, add 4 g of paraformaldehyde to 25 ml deionised H_2O. Dissolve by heating the mixture at 58 ºC while stirring. Add 1-2 drops of 1 M NaOH to clarify the solution and filter (0.2 μm). Add 50 ml of 2X PBS and adjust the volume to 100 ml with deionised H_2O.

4. Proteins Manipulation

SDS-PAGE

■ **LGB (Lower gel buffer) (4x)** (1 L)

- Tris	181.65 g
- SDS	4 g

Shake until the solutes have dissolved. Adjust the pH to 8.9 with HCl and adjust the volume to 1 L with deionised H_2O.

■ **UGB (Upper gel buffer) (5x)**

Per litre, to 900 ml of deionised H_2O add 75.7 g of Tris base. Shake until the solute has dissolved. Adjust the pH to 6.8 with HCl and adjust the volume to 1 L with deionised H_2O.

■ **30 % Acrylamide / 0.8 % Bisacrylamide solution**

Per 100 ml, to 70 ml of deionised H_2O add:

- Acrylamide	29.2 g
- Bisacrylamide	0.8 g

Shake until the solutes have dissolved. Adjust the volume to 100 ml with deionised H_2O. Filter through a 0.2 μm filter and store at 4 ºC.

■ **10 % APS (ammonium persulfate)**

In 10 ml of deionised H_2O dissolve 1 g of APS. Note: prepare fresh before use.

■ **10 % SDS (sodium dodecilsulfate)**

In 10 ml of deionised H_2O dissolve 1 g of SDS.

■ **Loading (sample) buffer (4x)** (10 ml)

- 1M Tris solution (pH 6.8)	2.5 ml (250 mM)
- SDS	0.8 g (8%)
- Glicerol	4 ml (40%)
- β-Mercaptoetanol	2 ml (2%)
- Bromofenol blue	1 mg (0.01%)

Adjust the volume to 10 ml with deionised H_2O. Store in darkness at RT.

■ **1 M Tris (pH 6.8) solution**

For a final volume of 250 ml, dissolve 30.3 g of Tris base in 150 ml of deionised H_2O, adjust pH to 6.8, and adjust final volume to 250 ml.

■ **Running buffer (10x)** (1 L)

- Tris	30.3 g (250 mM)
- Glycine	144.2 g (2.5 M)
- SDS	10 g (1%)

Dissolve in deionised H_2O, adjust pH to 8.3, and adjust volume to 1 liter.

(1.5 mm gels)

■ **Resolving (lower) gel solution** (60 ml)	**7.5 %**	**12 %**	**6.5 %**
- H_2O	29.25 ml	20.7 ml	31.25ml
- 30% Acryl/0.8% Bisacryl solution	15.0 ml	24.0 ml	13.0 ml
- LGB (4x)	15.0 ml	15.0 ml	15.0 ml
- 10% APS	300 µl	300 µl	300 µl
- TEMED	30 µl	30 µl	30 µl

■ **Stacking (upper) gel solution** (20 ml)	**3.5 %**
- H_2O	13.2 ml
- 30% Acryl/0.8% Bisacryl solution	2.4 ml
- UGB (5x)	4.0 ml
- 10% SDS	200 µl
- 10% APS	200 µl
- TEMED	20 µl

Immunoblotting solutions

■ **Electrotransfer buffer (1x)**

Per litre, to 700 ml of deionised H_2O add:

- Tris	3.03 g (25 mM)
- Glycine	14.41 g (192 mM)

Mix until solutes dissolution. Adjust the pH to 8.3 with HCl and adjust the volume to 800 ml with deionised H_2O. Just prior to use add 200 ml of methanol (20%).

■ **TBS (Tris Buffered Saline) (10x)**

Per litre, to 700 ml of deionised H_2O add

- Tris	12.11 g (10 mM)
- NaCl	87.66 g (150 mM)

Adjust the pH to 8.0 with HCl and adjust the volume to 1 L with deionised H_2O.

■ **TBS-T (Tris Buffered Saline + Tween) (10x)**

For a final volume of 1 L, to 700 ml of deionised H_2O add

- Tris	12.11 g (10 mM)
- NaCl	87.66 g (150 mM)
- Tween 20	5 ml (0.05%)

Adjust the pH to 8.0 with HCl and adjust the volume to 1 L with deionised H_2O.

■ **Blocking solution** (100 ml)

- TBS-T stock solution (10x)	10 ml
- non-fat milk (dry powder)	5 g

Dissolve in deionised H_2O and adjust volume to 100 ml.

■ **Antibody solution** (25 ml)

- TBS-T stock solution (10x)	2.5 ml
- non-fat milk (dry powder)	0.75 g

Dissolve in deionised H_2O and adjust volume to 25 ml. Add antibody, mix gently without vortex, and store at -20 ºC.

■ **Alkaline Phosphatase (AP) Reaction Solution** (1 L)

- Tris-HCl (pH 9.5)	12.11 g (100 mM)
- NaCl	5.85 g (100 mM)
- $MgCl_2$	1.02 g (5 mM)

Dissolve Tris base in deionised H_2O and adjust solution to pH 9.5 with HCl. Dissolve the other solutes and adjust volume to 1 L.

■ **AP Stop Solution** (1 L)

- Tris-HCl (pH 9.5)	2.42 g (20 mM)
- EDTA	1.86 g (5 mM)

Dissolve Tris in deionised H_2O and adjust with HCl to pH 9.5. Add EDTA after and adjust volume to 1000 ml.

■ **Membranes Stripping Solution** (500 ml)

- Tris-HCl (pH 6.7)	3.76 g (62.5 mM)
- SDS	10 g (2%)
- β-mercaptoethanol	3.5 ml (100 mM)

Dissolve Tris and SDS in deionised H_2O and adjust with HCl to pH 6.7. Add the mercaptoethanol and adjust volume to 500 ml.

APPENDIX II

METHODS AND KITS

1. DNA Manipulation

PCR (polymerase chain reaction) for mutant and wt APP cDNAs amplification

PCR was performed using Pfu DNA polymerase (Promega), and the amplification reactions were set up according to the manufacturer instructions. The standard amplification reactions were performed in 0.2 ml microtubes as follows (Table AII.1)

Table AII.1. Reagents mixtures used in APP isoform 695 cDNAs PCR amplification. Total volume: 50 μl

Tube	Template 0.1 ng	Template 1.0 ng	Negative Control 1 (w/primers, w/o template)	Negative Control 2 (w/o primers, w/ template)
10x Pfu buffer	5 μl	5 μl	5 μl	5 μl
dNTPs (10 mM)	1.5 μl	1.5 μl	1.5 μl	1.5 μl
Primer NAPN	1.5 μl (10 pmol)	1.5 μl (10 pmol)	1.5 μl (10 pmol)	-
Primer S1	1.5 μl (10 pmol)	1.5 μl (10 pmol)	1.5 μl (10 pmol)	-
APP cDNA (template)	1 μl	10 μl	-	1 μl Wt APP cDNA
Pfu polymerase	1 μl	1 μl	1 μl	1 μl
H_2O	38.5 μl	29.5 μl	39.5 μl	41.5 μl

■ **PCR amplification program**

1 min	94 ºC	1x	(Denaturation)
30 sec	94 ºC		
30 sec	67 ºC	5x	(Denaturation, Annealing, Polymerization)
1 min	72 ºC		
30 sec	94 ºC	25x	(Denaturation, Polymerization)
3 min	72 ºC		
7 min	72 ºC	1x	(Polymerization; "Extension" step)

The annealing temperature depends on the primers melting temperatures (Tm) and it should usually be =(Tm – 8) ºC. For some reactions it was necessary to undergo further amplification cycles: more 20 cycles (30 sec 94 ºC, 3 min 72 ºC) followed by another extension step of 1x 7 min 72 ºC. Amplification was confirmed by resolving a PCR reaction aliquot (10 μl) in a 1.2% agarose gel electrophoresis.

PCR cDNA products digestion with restriction enzymes

The amplified APP cDNA fragments were sequentially digested with the restriction endonucleases *Nru* I and *Age* I to allow further insertion into the EGFP-N1 plasmid. APP cDNAs were inserted between the *Sma* I and *Age* I sites of the pEGFP-N1 vector, upstream of the enhanced green fluorescent protein (EGFP) cassette and in the correct open reading frame. For a typical DNA digestion, the following components were added to the following concentrations:

100 μg/ml cDNA
1X reaction buffer (specific for each restriction enzyme)
1U restriction enzyme /μg cDNA

The mixture was incubated at the appropriate temperature for a few hours (or overnight if convenient). When sequential digestions with different enzymes were carried out the DNA was purified between the two reactions (see below). Table AII.2 presents the restriction enzymes and specific mixtures used in the APP-GFP translational fusions production and previous confirmation before sequencing. Prior to sequencing, the plasmid DNA extracted from transformants and the EGFP-N1 vector (for control), were sequentially digested with *Xba* I, *EcoR* I, and *Pst* I.

Table AII.2. Mixtures used in APP_{695} and EGFP vector cDNAs digestion with restriction enxymes. Restriction enzymes: *Nru* I and *Age* I (NEB); *Sma* I, *Xba* I and *EcoR* I(Fermentas).

Objective:	**APP subcloning into the EGFP vector**				**Confirmation of APP-GFP fusion**		
Restriction Enzyme / Mixture Components	***Nru* I** (APP cDNAs, PCR products)	***Age* I** (APP cDNAs, PCR products)	***Sma* I** (N1 vector)	***Age* I** (N1 vector)	***Xba* I** (putative APP-GFP clones)	***EcoR* I** (putative APP-GFP clones, after *Xba* I confirmation)	***Pst* I** (putative APP-GFP clones, after *Xba* I confirmation)
Buffer 10x	10 μl	5 μl	10 μl	10 μl	1 μl	1 μl	1 μl
Enzyme	2 μl	1 μl	3.5 μl	3.5 μl	1 μl	1 μl	1 μl
DNA	40 μl of PCR product	Pellet of purified cDNA pre-cuted with *Nru*I	20 μl (± 12 μg) of gel extracted N1	Pellet of purified cDNA pre-cuted with *Sma*I	3 μl of the clone miniprep	3 μl of the clone miniprep	3 μl of the clone miniprep
H_2O	48 μl	44 μl	66.5 μl	86.5 μl	5 μl	5 μl	5 μl
Final Volume	100 μl	50 μl	100 μl	100 μl	10 μl	10 μl	10 μl
Temperature	37 ºC	25 ºC	30 ºC	25 ºC	37 ºC	37 ºC	37 ºC
Reaction Time	4 h	Overnight	4 h	Overnight	2 h	4 h	4 h

DNA purification

■ Method 1: QIAquick PCR Purification Kit Protocol (QIAgen # 28706)

This kit was used to purify DNA fragments from PCR and other enzymatic reactions. It allowed purification from primers, nucleotides, DNA polymerases and salts by using QIAquick spin columns in a microfuge tube. The manufacturer's protocol was used as follows: 5 volumes of buffer PB were added to 1 volume of the reaction to be purified, and mixed. The QIAquick spin column was placed in a provided 2 ml collection tube and the sample was applied to the column and centrifuged for 1 min at 14,000 rpm to allow for DNA binding. The first flow-through was discarded and the column washed with 0.75 ml of buffer PE and centrifuged for 1 min at 14,000 rpm. The second flow-through was discarded, the column placed back in the same tube and centrifuged again to remove traces of washing buffer. The column was finally placed in a clean microtube, 50 μl of H_2O were added and let to stand for 1 min. To elute the DNA, the column was centrifuged for 1 min at 14,000 rpm.

■ Method 2: DNA precipitation with ethanol

This method was used to concentrate nucleic acids as well as to purify them (e.g. for cell culture transfection). Approximately 1/10 volume of 3 M sodium acetate (pH 5.2) was added to the DNA solution to adjust the salt concentration, followed by 2 volumes of ice-cold ethanol. The solution was mixed thoroughly and stored at –20 ºC for 30 min to allow the DNA precipitate to form. DNA was recovered by centrifugation at 4 ºC for 15 min at 14,000 rpm. The supernatant was carefully removed without disturbing the pellet. The microtube was half filled with ice-cold 70% ethanol and re-centrifuged using the same conditions as above for 5 min. The supernatant was again removed and the pellet allowed to dry before being resuspended in sterile water.

Electrophoretic analysis of DNA

An electrophoresis apparatus was prepared and the electrophoresis tank was filled with enough 1X TAE to cover the agarose gel. The appropriate amount of agarose (to a final percentage of 0.8 – 1.2%) was transferred to an Erlenmeyer with 50 ml 1X TAE, and this slurry was heated until agarose dissolution and allowed to cool to 60 ºC before adding ethidium bromide to a final concentration of 0.5 μg/ml. The agarose solution was poured into the tray and a comb was positioned on it. After

the gel was completely set, the comb was carefully removed and the gel mounted in the tank. DNA samples were mixed with the 6X DNA loading buffer (DNA LB) (0.25% bromophenol blue/30% glycerol in water) and the mixture was loaded into the slots of the submerged gel. Marker DNA (λ-Hind III fragments or Invitrogen 1 Kb ladder) of known size was also loaded into the gel. The lid of the gel tank was closed and the electrical leads were attached so that the DNA migrated towards the anode. The gel was run at 100 V, and finally examined by UV light and photographed, or analysed on a Molecular Imager (Biorad).

DNA Gel Extraction kit (QIAgen)

For the EGFP-N1 cDNA extraction, 0.8% gels were set as described above with some differences. 10 μl of non-cutted and 90 μl of *Sma* I/*Age* I cutted EGFP-N1 vector cDNA were loaded and resolved. The DNA standard and 10 μl lanes were UV exposed and the migration distance of the digested cDNA band registered. The 90 μl band was finally extracted from the gel (without being exposed to UV light) with a clean spatula. The destination microtube was weighted, before and after receiving the extracted band, to calculate the cDNA weight. EGFP-N1 cDNA was further purified by using the QIAquick Gel Extraction Kit protocol. Briefly, 3 volumes of Buffer QG were added to 1 volume of gel (100 mg ~100 μl). This mixture was incubated at 50 ºC for 10 min (or until the gel slice was completely dissolved), while inverting the microtube every when. After the gel slice complete dissolution, pH was confirmed to be ≤ 7.5, and 1 gel volume of isopropanol was added to the sample and mixed. This sample was applied to a QIAquick spin column, previously placed in a 2 ml collection tube, and the tube centrifuged at 10,000 x *g* or 1 min. The flow-through was discarded, 0.5 ml of Buffer QG were applied to the column and a further 1 min centrifugation was performed. 0.75 ml of Buffer PE were used to wash the column by two sequential centrifugations at 10,000 x *g*, and the flow-through discarded. The column was placed in a clean 1.5 ml tube and the DNA eluted with 50 μl of deionised H_20 after 1 min standing in the column and a last 1 min centrifugation.

Ligation of cohesive termini and blunt ended DNA

Digested fragments (*Sma* I/*Age* I EGFP-N1 plasmid and the Nru I/*Age* I APP-GFP cDNA fragment to be inserted) were separated by gel electrophoresis and purified. 0.1 μg of vector DNA were transferred to a microtube with an equimolar amount (or more) of insert DNA. Ligations were performed using the bacteriophage T4 DNA ligase (Promega), in a total volume mixture of 20 μl, and were carried out for 4 h at room temperature or overnight at 16 ºC. Additional control reactions were also set up (Table AII.3).

Table AII.3 – APP/GFP bacteriophage T4 DNA Ligations.

	Ligations		**Ligations Controls**		
Tube	**1** (2 μl of *Nru* I/*Age* I PCR product)	**2** (6 μl of *Nru* I/*Age* I PCR product)	**Control 1** (w/o cDNA)	**Control 2** (non-cutted EGFP vector)	**Control 3** (cutted EGFP vector)
10x T4 ligase buffer	2 μl	2 μl	2 μl	2 μl	2 μl
EGFP vector cDNA	3.5 μl (100 ng)	3.5 μl (100 ng)	-	1 μl (1 ng)	3.5 μl (100 ng)
APP PCR products	2.5 μl (± 20 ng)	6.0 μl (± 50 ng)	-	-	-
T4 DNA ligase	1.0 μl	1.0 μl	1.0 μl	1.0 μl	1.0 μl
H_2O	13.5 μl	11 μl	17 μl	16 μl	14.5 μl

Bacteria Transformation

■ Preparation of competent cells

A single colony of *E. coli* XL1-Blue was incubated overnight in 10 ml SOB medium at 37 ºC. 1 ml of this overnight culture was used to incubate 50 ml SOB until OD_{550}= 0.3. This culture was incubated on ice for 15 min and centrifuged at 4,000 rpm (4 ºC) for 5 min. The supernatant was discarded and 15 ml of Solution I were added. After allowing standing on ice for 15 min, cells were centrifuged at 4,000 rpm (5 min, 4 ºC) and 3 ml of Solution II were added to the pellet. Cells were immediately divided in 0.1 ml aliquots and stored at -80 ºC.

■ Bacteria transformation with plasmid DNA

Competent cells (50 μl) were thawed on ice and 2 or 5 μl of each ligation product (0.1 - 50 ng of DNA) were added to the cells with gentle swirling. The microtubes were incubated on ice for 20 min and heat shocked at 42 ºC for 60 sec. Further incubation on ice for 2 min was performed, and 0.9 ml of SOC medium was added. The tubes were incubated at 37 ºC for 1 hour with shaking at 225 rpm. 1/10 and 9/10 of this cells solution were plated on the appropriate antibiotic (100 μg/ml kanamycin) agar medium plates (pre-heated) and incubated at 37 ºC for ~16 h until colonies appeared. Control transformations were also performed in parallel, which always included a negative control transformation without DNA and a positive control transformation with 0.1 ng of the control plasmid.

Amplification and isolation of plasmid DNA from bacteria

■ Alkaline lysis mini-prep

This method was used to screen the bacterial plates for transformant colonies. A single positive (transformant) bacterial colony was transferred to a tube containing 5 ml of LB plus antibiotic medium and incubated overnight at 37 ºC with vigorous shaking. After overnight culture growth, 1 ml of the 5 ml culture was centrifuged at 14,000 rpm and 4 ºC for 1 min. The medium was removed by aspiration and the bacterial pellet ressuspended in 100 μl of ice-cold solution I ('ressuspension' solution) by vigorous vortexing. Afterwards, 200 μl of Solution II was added ('alkaline lysis'), and the content of the tube mixed by inverting it several times. The microtube was placed on ice, 150 μl of ice-cold solution III ('neutralization' solution) was added and the tube gently vortexed. After standing on ice for 5 min,

a 10 min centrifuge at 14,000 x *g* and 4 ºC was performed, and the supernatant transferred to a clean microtube. The DNA was precipitated with 2 volumes of ethanol at RT and this mixture was allowed to stand for 10 min at RT. After this period, the microtube was centrifuged at 14,000 x *g* and 4 ºC for 5 min. The supernatant was completely removed and the pellet washed with 70% ethanol and allowed to air-dry for 10 min. Purified DNA was dissolved in 20 μl H_2O containing DNAse-free pancreatic RNAse (20 μg/ml) and stored at -20 ºC.

■ **Mega-prep (Promega)**

The Promega kit Wizard™ Plus Megapreps DNA purification System # A7300 was used in this procedure. One litre of a single-transformant cell culture was pelleted by centrifugation at 1,500 x *g* for 20 min at RT. The cell pellet was resuspended in 30 ml of cell resuspension solution [50 mM Tris-HCl (pH 7.5)/10 mM EDTA/100 μg/ml RNAase A] by manually disrupting the pellet with a pipette. Afterwards, 30 ml of cell lyses solution (0.2 M NaOH/ 1% SDS) were added to the cells and the solution mixed gently by tube inversion until it became clear and viscous. 30 ml of neutralization solution [1.32 M potassium acetate (pH 4.8)] were added and the tube immediately mixed by inversion. After centrifugation at 14,000 x *g* for 15 min at RT the clear supernatant was transferred by filtering it through gauze swabs into a new tube, and the supernatant volume was measured. At this stage 0.5 volumes of RT isopropanol were added and the solution mixed by inversion. This solution was centrifuged at 14,000 x *g* for 15 min at RT, the supernatant discarded and the pellet resuspended in 4 ml of TE buffer. 20 ml of Wizard ™ Megapreps DNA purification Resin were added to the DNA and mixed by swirl. A Wizard ™ Megacolumn was inserted into the vacuum manifold port and the DNA/resin mix was transferred onto the Megacolumn. Vacuum was applied to pull the mix into the Megacolumn. Two washes with 25 ml of column wash solution (80 mM potassium acetate/8.3 mM Tris-HCl/40 μM EDTA/55% ethanol) were performed and the resin was rinsed with 10 ml of 80% ethanol. The Megacolumn was inserted into a 50 ml screw cap tube and centrifuged at 2,500 rpm for 5 min using a swinging bucket rotor centrifuge. The Megacolumn was removed from the tube and placed in a clean tube, and 3 ml of pre-heated water (70 ºC) were added to the column. After 1 min standing, the DNA was eluted by centrifugation at 2,500 rpm for 5 min. The DNA was stored at –20 ºC, and a 400 μl DNA aliquot was purified by ethanol (and kept sterile) and its concentration and 260/280 nm purity ratio calculated by densitometry measurements at the indicated wavelengths.

APP-GFP DNA sequencing

All the DNA samples to be sequenced followed the same protocol. In a microtube the following components were added: 1 ng dsDNA (column purified)

4 μl of Ready Reaction Mix*
15 pmol primer (1.5 μl of 10 pmol/μl)
H_2O to a final volume of 20 μl

* Ready Reaction Mix is composed of: dye terminators, deoxynucleoside triphosphates, AmpliTaq DNA polymerase, FS, rTth pyrophosphatase, magnesium chloride and buffer (Applied Biosystems).

This reaction mixture was vortexed and spun down for a few seconds. PCR was then performed using the following conditions:

96 ºC 30 sec
42 ºC 15 sec } 25 cycles
60 ºC 4 min

Afterwards, samples were purified by ethanol precipitation (as described above). Briefly, 2.0 μl of 3 M sodium acetate (pH 5.2) and 50 μl of 95% ethanol were added to the reaction microtube. The microtube was vortexed and incubated at RT for 15 min to precipitate the extension products. The microtube was then centrifuged at 14,000 rpm for 20 min at RT. After discarding the supernatant, 250 μl of 70% ethanol were added, the microtube was briefly vortexed and re-centrifuged for 5 min at 14,000 rpm at RT. The supernatant was again discarded and the pellet dried. After this procedure the samples were loaded in the ABIPRISM (Applied Biosystems) Automated DNA Sequencer.

2. Cell culture and Rat primary cultures

COS-7 cell culture maintenance

COS-7 cells were grown in complete DMEM medium (DMEM medium supplemented with 10% FBS) to which 100 U/ml penicillin and 100 mg/ml streptomycin (Gibco BRL, Invitrogen) were added. Cells were plated in 100 mm diameter plates or 6-well plates (35 mm diameter), and grown in a humidified incubator at 37 ºC and 5% CO_2. Cells were subcultured whenever ~95% confluence was reached.

Rat cortical/hippocampal primary cultures

Rat cortical neurons were isolated from cortex of Wistar Hannover 18 days rat embryos whose mother was killed by rapid cervical dislocation. After cortex dissection, tissues were treated for 10 min at 37 ºC with a 0.45 mg/ml trypsin/0.18 mg/ml deoxyribonuclease solution in Ca^{2+}- and Mg^{2+}-free HBSS (Gibco, BRL), supplemented with BSA (Merck, VWR International). Cells were washed with HBSS supplemented with 10% FBS to stop trypsinization, centrifuged at 1,000 rpm for 3 min, and further washed and centrifuged with HBSS for serum withdraw. Cells pellet was ressuspended in complete Neurobasal medium, which is supplemented with 2% B27. Viability and cellular concentration were assessed by using the Trypan Blue excluding dye [0.4% Trypan Blue solution (Sigma)], and cells with (dead) or without (living) intracellular blue staining were counted in a hemocytometer chamber. Cellular viability was calculated and normally higher than 95%. These neuronal cells were plated at 9.0 x 10^4 cells/cm^2 on 100 μg/ml poly-D-lysine pre-coated glass coverslips that were placed in six-well plates. Cells were maintained in 2 ml of complete Neurobasal medium in a humidified incubator at 37 ºC and 5% CO_2. Three and seven days after plating, 500 μl of cultured medium was replaced with 750 μl of gentamicine-free complete Neurobasal medium.

Rat cortex isolation

Young (1-2 month old) adult male rats were sacrificed by cervical dislocation and decapitation. Cerebral cortex was rapidly dissected on ice-cold 0.32 M sucrose/10 mM HEPES (pH 7.4) solution and weighted. Boiling SDS was added to a final 1% SDS solution (at ≅ 10% w/v solution), samples were homogenised with a Potter-Elvehjem type homogenizer and further boiled for 10 min.

Cells cDNA Transfection with Lipofectamine 2000

Lipofectamine 2000 (Invitrogen) is a cationic liposome formulation that functions by complexing with nucleic acid molecules, allowing them to overcome the electrostatic repulsion of the cell membrane and to be taken by the cell. The method of DNA delivery in culture cell lines and primary neurons is well described in Dalby et al. (2004), from where the following protocols were based:

■ **COS-7 cell line** (Table AII.4)

Cells were grown in complete DMEM until 85 - 95% confluence and at the transfection day the culture medium was replaced for complete medium (antibiotic/antymicotic-free). The appropriate amount of DNA for each plate/well was diluted in DMEM (serum- and antibiotic/antymicotic-free). The Lipofectamine 2000 reagent was diluted at the appropriated amount in the same medium, and the tubes were left to rest for 5 min. The DNA solution was added to the Lipofectamine solution drop by drop, and the solution was mixed by gentle bubbling with the pipette. In order to form the DNA-lipid complexes, the tube was left to rest at for 25 - 30 min RT, after what the complexes solution was directly added onto the cells medium, drop by drop and with gentle rocking of the plate. The cells were further incubated at 37 ºC/5% CO_2 for the indicated transfection time prior to cell collection or fixation.

Table AII.4 – COS-7 cells transfection reagents

Culture Plates	Medium w/ serum	DNA (µg)	Lipofectamine 2000 (µl)	Medium w/o serum
100 mm	15 ml	8	50	1500 µl
60 mm plate	5.0 ml	4	15	500 µl
35 mm 6-	2.0 ml	2	10	250 µl

■ **Primary Neuronal cultures**

Replace the culture medium in each 35 mm well for 0.8 ml of fresh gentamicine-free complete Neurobasal medium. Per each 35 mm well to transfect, 8 μl of Lipofectamine 2000 were diluted in 100 μl of DMEM, and the microtube was left to rest at RT for 5 min. 2 μg of APP-GFP cDNA were also diluted in 100 μl of DMEM, and this solution was added drop by drop to the Lipofectamine solution. The final solution was mixed by gentle bubbling with the pipette, and left to rest for 25 - 30 min at RT in order to form the DNA-lipid complexes. This 200 μl DMEM complexes solution was directly added onto the cells medium, drop by drop and with gentle rocking of the plate. Neuronal cells were further incubated at 37 ºC and 5% CO_2 for 5 h, after what medium was substituted by fresh complete neurobasal medium and left for 24 h prior to cell collection or fixation.

Culture cells Fixation and Immunocytochemistry

COS-7 and neuronal primary cells were grown in 1M HCl pre-treated glass coverslips pre-coated with 100 μg/ml poly-L-ornithine or poly-D-lysine, respectively. After the experimental procedures, cells were washed three times with 1 ml of the serum-free DMEM, after which 1 ml of a 1:1 DMEM/4% paraformaldehyde fixative solution was gently added and allowed to stand for 1-2 min. Subsequently, 1 ml of fixative solution was gently added for 25 minutes. Finally, cells were washed 3 times with PBS for 10 min, being ready for immunocytochemistry procedures or to be directly mounted with 1 drop of anti-fading reagent (Fluoroguard, BioRad) on glass microscope slides for epifluorescence microscopy analysis. For immunocytochemistry procedures, a permeabilization step with methanol was taken (2 min at RT) and cells were immediately washed four times with PBS. Afterward, cells were incubated with primary antibody diluted in 3% BSA in PBS for 2-4 h at RT. The primary antibody was removed by washing the coverslips 3 times with PBS and a secondary antibody (also diluted in 3% BSA in PBS) was added for 2 h at RT. After washing three times with PBS the coverslips were mounted with one drop of the antifading reagent on a glass slide.

3. Proteins Manipulation

Protein Assay kit (BCA, Pierce)

Samples total protein measurements were performed with Pierce's BCA protein assay kit, following the manufacturer's instructions. The method combines the reduction of Cu^{2+} to Cu^{+} by protein in an alkaline medium (the biuret reaction) with a sensitive colorimetric detection of the Cu^{+} cation using a reagent containing bicinchoninic acid (BCA). The purple-coloured reaction product of this assay is formed by the chelation of two molecules of BCA with one Cu^{+} ion. This water-soluble complex exhibits a strong absorbance at 562 nm that is linear with increasing protein concentration over a working range of 20 μg/ml to 2000 μg/ml.

■ **Working Reagent (W.R.)**

The W.R. was prepared by mixing X ml of BCA reagent A with Y ml of BCA reagent B in the proportion of 50:1.

■ **Samples preparation**

A microtube per sample was prepared to be assayed with 25 μl of each sample plus 25 μl of the solution in which the sample was collected (1% SDS).

■ **Standard curve**

Microtubes with standard protein concentrations were prepared as described below (Table AII.5).

Table AII.5 – Standards used in the BCA protein assay method. BSA, Bovine serum albumin solution (2 mg/ml).

Standard	BSA (μl)	10% SDS	H_2O (μl)	Protein mass	W.R. (ml)
P_0	-	5	45	0	1
P_1	1	5	44	2	1
P_2	2	5	43	4	1
P_3	5	5	40	10	1
P_4	10	5	35	20	1
P_5	20	5	25	40	1
P_6	40	5	5	80	1

■ **Incubation and absorbance measurement**

1 ml of W.R. was rapidly added to each microtube (standards and samples) and the microtubes were incubated at 37 ºC exactly for 30 min. Tubes cool to RT and immediately measure their absorbance at 562 nm.

■ **Samples concentration**

A standard curve is prepared by plotting BSA standard absorbance vs. BSA concentration, and used to determine the total protein concentration of each sample.

SDS-PAGE (for Western blotting)

SDS polyacrylamide gel electrophoresis (SDS-PAGE) separations were carried out using well established methods (Laemmli, 1970), where proteins are separated by their molecular weight and negative net charge due to SDS-amino acid binding. The gels percentage and size chosen depend on the molecular weight of the proteins to be separated in the gel. Gels were prepared by mixing several components (Appendix I). The resolving gel solution was immediately and carefully pipetted down the spacer into the gel sandwich, leaving free space for the stacking gel. Water was carefully added to cover the top of the gel and the gel was allowed to polymerize for 1 h. Stacking gel solution was prepared according to Appendix I. The water was poured out and the stacking gel was added to the gel sandwich; a comb was inserted and the gel allowed to polymerize for 1 h. In parallel, samples were prepared by adding to the protein sample solution ¼ volume of 4X LB (Loading Buffer). Samples microtubes were boiled and spinned down, the combs removed and the gels wells filled with Tris-Glycine running buffer. The samples were carefully loaded into the wells, and electrophoretically separated using a 90 mA electric current. Molecular weight markers (Kaleidoscope Prestained Standards or Prestained SDS-PAGE Standards – Broad Range, Bio Rad) were also loaded and resolved side-by-side with the samples.

Proteins Electrotransfer

Through the Western Blotting technique, proteins that were electrophoretically separated by SDS-PAGE can be transferred to membranes (nitrocellulose membranes, for instance), while keeping their positions. 3MM blotter papers and a nitrocellulose membrane were used to build up the transfer sandwich. The gel was removed from the electrophoresis device and the stacking gel discarded. A transfer

sandwich was assembled under transfer buffer, in the following order: sponge, 3MM blotter paper, gel, nitrocellulose membrane, 3MM paper, sponge. The cassette was placed in the transfer device, previously filled with transfer buffer, oriented so that the negatively charged proteins migrate towards the anode. Electrotransfer was allowed to proceed for 18 h at 200 mA, after what the membrane was allowed to dry on a clean paper.

Immunoblot analysis

After proteins electrotransfer, the nitrocellulose membranes could be used immediately, and membranes were initially soaped in 1X TBS for 10 min. Blocking of possible non-specific binding sites of the primary antibody was performed by immersing the membrane in 5% (w/v) non-fat dry milk in 1X TBST solution for 1 - 4 h. Further incubation with primary antibody was carried out for the specified times, ranging from 2 h to overnight incubation at 4 ºC with agitation. After three washes with 1X TBS-T, of 10 min each, the membrane was further incubated with the appropriate secondary antibody for 2 h with agitation. All primary and secondary antibodies used were diluted in 1X TBS-T/non-fat dry milk (3% w/v) at the dilutions specified in Chapters II, IV and V (Table II.1, IV.1 and V.1). Membranes were additional washed three times with 1X TBST, before being submitted to one of the following detection methods:

- **Colorimetric detection (NBT/BCIP, Pierce)**

  Each 15 cm membrane was developed by adding to it a solution of 66 µl NBT and 33 µl BCIP in 10 ml Alkaline Phosphatase reaction buffer. When a coloured signal was achieved, the developing reaction was stopped by adding 20 ml of AP stop solution. Membrane was washed twice with deionised water and air dried at RT.

- **Enhanced chemiluminescence detection (ECL and ECL+ Kits, Amersham Pharmacia)**

  ECL™ Western blotting from Amersham Pharmacia Biotech is a light emitting non-radioactive method for detection of immobilised specific antigens, conjugated directly or indirectly with horseradish peroxidase-labelled antibodies (Fig. A.II.1).

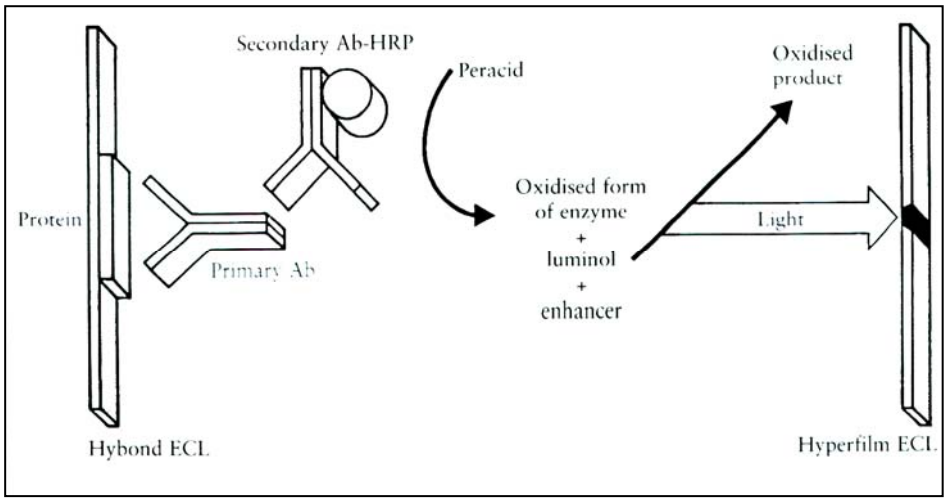

Figure A.II.1. The ECL analysis system detects the presence of an antibody labelled with horseradish peroxidase by catalysing the oxidation of luminol, leading to the emission of light, which can be detected by an autoradiography film (From the manufacturer datasheet).

The membrane was incubated for 1 min at RT with the ECL detection solution or for 5 min with the ECL+ detection solution. These solutions were prepared fresh following the manufacturer's instructions. ECL/ECL+ detection solution in excess was drained by touching the edge of the membrane against tissue paper and the membrane was gently wrapped in cling-film, eliminating all the air bubbles. In a dark room, an autoradiography film (XAR-5 film, Kodak, Sigma Aldich) was placed on the top of the membrane, inside a film cassette. The cassette was closed and the blot exposed for an appropriate period of time. The film was then removed and developed in a developing solution (Kodak, Sigma Aldrich), washed in water, and fixed in a fixing solution (Kodak, Sigma Aldrich).

APPENDIX III

SEQUENCES AND TECHINICAL DATA

APP_{695} sequences (GenBank Acession NM_201414)

■ cDNA sequence

1 **atg**ctgcccg gtttggcact gctcctgctg gccgcctgga cggctcgggc gctggaggta cccactgatg
71 gtaatgctgg cctgctggct gaaccccaga ttgccatgtt ctgtggcaga ctgaacatgc acatgaatgt
141 ccagaatggg aagtgggatt cagatccatc agggaccaaa acctgcattg ataccaagga aggcatcctg
211 cagtattgcc aagaagtcta ccctgaactg cagatcacca atgtggtaga agccaaccaa ccagtgacca
281 tccagaactg gtgcaagcgg ggccgcaagc agtgcaagac ccatccccac tttgtgattc cctaccgctg
351 cttagttggt gagtttgtaa gtgatgccct tctcgttcct gacaagtgca aattcttaca ccaggagagg
421 atggatgttt gcgaaactca tcttcactgg cacaccgtcg ccaaagagac atgcagtgag aagagtacca
491 acttgcatga ctacggcatg ttgctgccct gcggaattga caagttccga ggggtagagt ttgtgtgttg
561 cccactggct gaagaaagtg acaatgtgga ttctgctgat gcggaggagg atgactcgga tgtctggtgg
631 ggcggagcag acacagacta tgcagatggg agtgaagaca aagtagtaga agtagcagaggaggaagaag
701 tggctgaggt ggaagaagaa gaagccgatg atgacgagga cgatgaggat ggtgatgagg tagaggaaga
771 ggctgaggaa ccctacgaag aagccacaga gagaaccacc agcattgcca ccaccaccac caccaccaca
841 gagtctgtgg aagaggtggt tcgagaggtg tgctctgaac aagccgagac ggggccgtgc cgagcaatga
911 tctcccgctg gtactttgat gtgactgaag ggaagtgtgc cccattcttt tacggcggat gtggcggcaa
981 ccggaacaac tttgacacag aagagtactg catggccgtg tgtggcagcg ccatgtccca aagtttactc
1051 aagactaccc aggaacctct tgcccgagat cctgttaaac ttcctacaac agcagccagt acccctgatg
1121 ccgttgacaa gtatctcgag acacctgggg atgagaatga acatgcccat ttccagaaag ccaaagagag
1191 gcttgaggcc aagcaccgag agagaatgtc ccaggtcatg agagaatggg aagaggcaga acgtcaagca
1261 aagaacttgc ctaaagctga taagaaggca gttatccagc atttccagga gaaagtggaa tctttggaac
1331 aggaagcagc caacgagaga cagcagctgg tggagacaca catggccaga gtggaagcca tgctcaatga
1401 ccgccgccgc ctggccctgg agaactacat caccgctctg caggctgttc ctcctcggcc tcgtcacgtg
1471 ttcaatatgc taaagaagta tgtccgcgca gaacagaagg acagacagca caccctaaag catttcgagc
1541 atgtgcgcat ggtggatccc aagaaagccg ctcagatccg gtcccaggtt atgacacacc tccgtgtgat
1611 ttatgagcgc atgaatcagt ctctctccct gctctacaac gtgcctgcag tggccgagga gattcaggat
1681 gaagttgatg agctgcttca gaaagagcaa aactattcag atgacgtctt ggccaacatg attagtgaac
1751 caaggatcag ttacggaaac gatgctctca tgccatcttt gaccgaaacg aaaaccaccg tggagctcct
1821 tcccgtgaat ggagagttca gcctggacga tctccagccg tggcattctt ttggggctga ctctgtgcca
1891 gccaacacag aaaacgaagt tgagcctgtt gatgcccgcc ctgctgccga ccgaggactg accactcgac
1961 caggttctgg gttgacaaat atcaagacgg aggagatctc tgaagtgaag atggatgcag aattccgaca
2031 tgactcagga tatgaagttc atcatcaaaa attggtgttc tttgcagaag atgtgggttc aaacaaaggt
2101 gcaatcattg gactcatggt gggcggtgtt gtcatagcga cagtgatcgt catcaccttg gtgatgctga
2171 agaagaaaca gtacacatcc attcatcatg gtgtggtgga ggttgacgcc gctgtcaccc cagaggagcg
2241 ccacctgtcc aagatgcagc agaacggcta cgaaaatcca acctacaagt tctttgagca gatgcagaac
2311 **tag**

■ **Amino acid sequence**

L P G L A L L L L A A W T A R A L E V P T D G N A G L L A E P Q I A M F C G R L N M H
M N V Q N G K W D S D P S G T K T C I D T K E G I L Q Y C Q E V Y P E L Q I T N V V
E A N Q P V T I Q N W C K R G R K Q C K T H P H F V I P Y R C L V G E F V S D A L L V
P D K C K F L H Q E R M D V C E T H L H W H T V A K E T C S E K S T N L H D Y G M L
L P C G I D K F R G V E F V C C P L A E E S D N V D S A D A E E D D S D V W W G G A
D T D Y A D G S E D K V V E V A E E E E V A E V E E E E A D D D E D D E D G D E V E
E E A E E P Y E E A T E R T T S A I T T T T T T T T E S V E E V V R V P T T A A S T PD AV
D K Y L E T P G D E N E H A H F Q K A K E R L E A K H R E R M S Q V M R E W E E A E
R Q A K N L P K A D K K A V I Q H F Q E K V E S L E Q E A A N E R Q Q L V E T H M A
R V E A M L N D R R R L A L E N Y I T A L Q A V P P R P R H V F N M L K K Y V R A E Q
K D R Q H T L K H F E H V R M V D P K K A A Q I R S Q V M T H L R V I Y E R M N Q S
L S L L Y N V P A V A E E I Q D E V D E L L Q K E Q N Y S D D V L A N M I S E P R I S
Y G N D A L M P S L T E T K T T V E L L P V N G E F S L D D L Q P W H S F G A D S V P
A N T E N E V E P V D A R P A A D R G L T T R P G S G L T N I K T E E I S E V K M *D A*
E F R H D S G Y E V H H Q K L V F F A E D V G S N K G A I I G L M V G G V V I A T V I
V I T L V M L K K K Q Y T S I H H G V V E V D A A V T P E E R H L S K M Q Q N G **^{682}Y**
E N P T Y^{687} K F F E Q M Q N

Legend:
Italic – Abeta sequence
Bold – Cytoplasmic sequence

Oligonucleotides

■ **Primers used for APP-GFP constructs engineering**

NAPN (N-terminal APP primer with *NruI* consensus sequence). Length: 32 nts; Melting Temperature: 102 ºC.

5' – CTT AAG CTT CGC GAT GCT GCC CGG TTT GGC AC – 3'

S1 (C-terminal APP primer without STOP codon and with *AgeI* consensus sequence). Length: 38 nts; Melting Temperature: 114 ºC.

5' – ATG GTA CCG GTG GGT TCT GCA TCT GCT CAA AGA ACT TG – 3'

■ **Primers used for APP-GFP constructs sequencing**

NAPN (above).

APP 500 (at the beginning of APP exon 5, nucleotide 478 - APP_{695} numbering). Length: 24 nts; Melting Temperature: 70 ºC.

5' – GAG AAG AGT ACC AAC TTG CAT GAC – 3'

APP 1100 (at the beginning of APP exon 9, nucleotide 866 - APP_{695} numbering). Length: 14 nts; Melting Temperature: 42 ºC.

5' – TCC TAC AAC AGC AG – 3'

APP 1500 (at the end of APP exon 11, nucleotide 1204 - APP_{695} numbering). Length: 14 nts; Melting Temperature: 44 ºC.

5' – ATC ACC GCT CTG CA – 3'

APP 1800 (at the beginning of APP exon 14, nucleotide 1507 - APP_{695} numbering). Length: 16 nts; Melting Temperature: 46 ºC.

5' – GCC AAC ATG ATT AGT G – 3'

APP 2000 (at the end of APP exon 16, nucleotide 1806 - APP_{695} numbering). Length: 22 nts; Melting Temperature: 60 ºC.

5' – TGA CTC AGG ATA TGA AGT TCA T – 3'

pEGFP-N1 Plasmid

- pEGFP-N1 (Clontech, BD Biosciences; GenBank Accession #U55762)

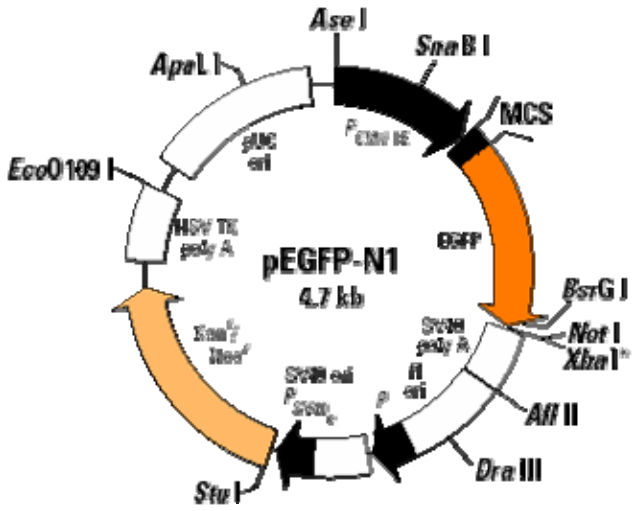

MCS:

Restriction Map and Multiple Cloning Site of pEGFP-N1. (Unique restriction sites are in color or bold.) The *Not* I site follows the EGFP stop codon. The *Xba* I site (*) is methylated in the DNA provided by CLONTECH. If you wish to digest the vector with this enzyme, you will need to transform the vector into a *dam*- host and make fresh DNA.

http://www.bdbiosciences.com/clontech/techinfo/vectors/vectorsE/pEGFP-N1.shtml - top#top**Description:** pEGFP-N1 encodes a red-shifted variant of wild-type GFP (1-3) which has been optimized for brighter fluorescence and higher expression in mammalian cells. (Excitation maximum = 488 nm; emission maximum = 507 nm.) The MCS in pEGFP-N1 is between the immediate early promoter of CMV ($P_{CMV\ IE}$) and the EGFP coding sequences. Genes cloned into the MCS will be expressed as fusions to the N-terminus of EGFP if they are in the same reading frame as EGFP and there are no intervening stop codons. SV40 polyadenylation signals downstream of the EGFP gene direct proper processing of the 3' end of the EGFP mRNA. A bacterial promoter upstream of this cassette (P_{amp}) expresses kanamycin resistance in *E. coli*. The pEGFP-N1 backbone also provides a pUC19 origin of replication for propagation in *E. coli* and an f1 origin for single-stranded DNA production.

http://www.bdbiosciences.com/clontech/techinfo/vectors/vectorsE/pEGFP-N1.shtml - top#top**Use:** Fusions to the N-terminus of EGFP retain the fluorescent properties of the native protein allowing the localization of the fusion protein *in vivo*. The target gene should be cloned into pEGFP-N1 so that it is in frame with the EGFP coding sequences, with no intervening in-frame stop codons. The inserted gene should include the initiating ATG codon. The recombinant EGFP vector can be transfected into mammalian cells using any standard transfection method. If required, stable transformants can be selected using G418 (7). pEGFP-N1 can also be used simply to express EGFP in a cell line of interest (e.g., as a transfection marker).

■ **Bacteria strain (plasmid DNA amplification)**

E. coli XL1- blue:
recA endA1 gyrA96 thi-1 hsdR17 supE44 relA1 lac[F' proAB lacZ∆M15 Tn10(Tetr)]

Protein Markers of Subcellular Compartments

■ **Monoclonal Antibody anti-Syntaxin 6** (BD Transduction Laboratories)

Syntaxin 6 is a 255 amino acid member of the Syntaxin family. It contains a C-terminal transmembrane domain and is located at the Golgi apparatus.

■ **Policlonal Antibody Anti-Calnexin (**StressGen Biotechnologies**)**

Calnexin is a ~90 KDa unglycosylated molecular chaperone and a resident ER transmembrane protein.

Fluorophores Excitation and Emission Spectra

■ **EGFP-N1 (pEGFP encoded)** (Clontech, BD Biosciences). Excitation and Emission Spectra for BD Living Colors™ Fluorescent Proteins*:*

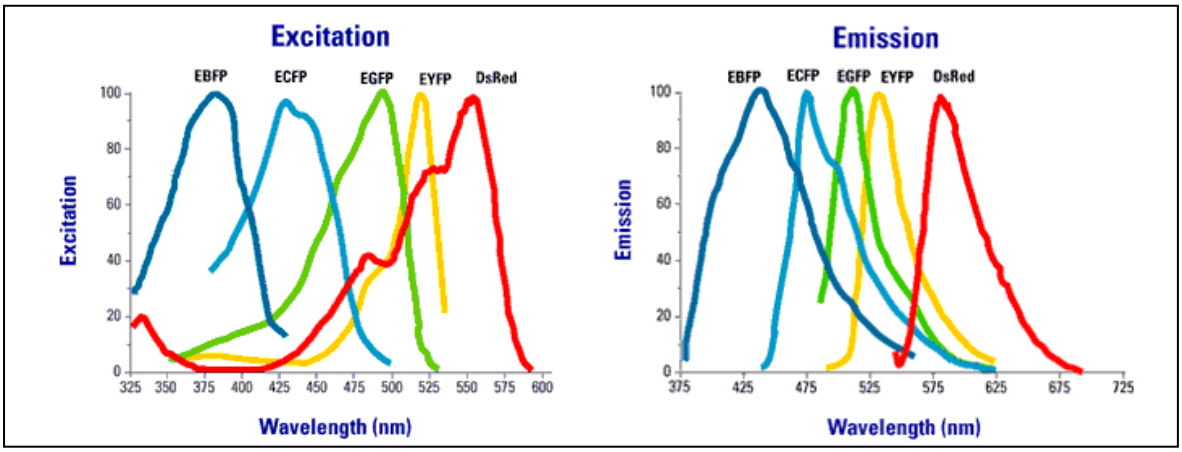

■ **Secondary Fluorescent Antibodies:**

A. Fluorescein goat anti–mouse IgG antibody/pH 8.0 (Molecular Probes) (fluorescence absorption and emission spectra in pH 8.0 buffer)

B. Texas Red-X goat anti–mouse IgG antibody/pH 7.2 (Molecular Probes) (fluorescence excitation and emission spectra in pH 7.2 buffer)

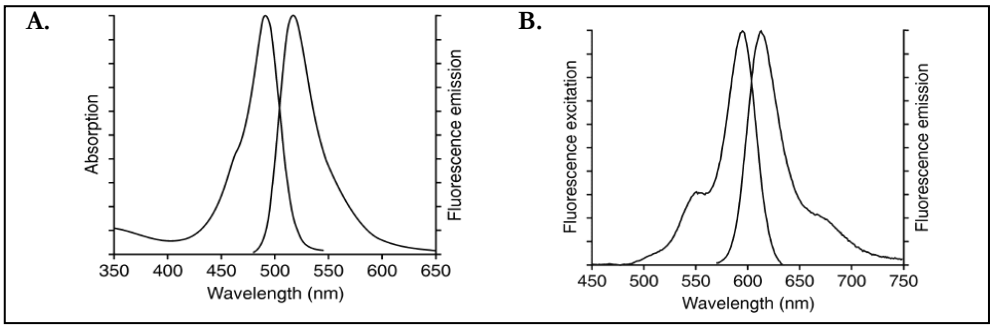

Protein Markers Epifluorescence filter cubes (Chroma)**:**

Set ID: 41020
Fluorophore: EGFP. Narrow-band GFP for eliminating auto-fluorescence

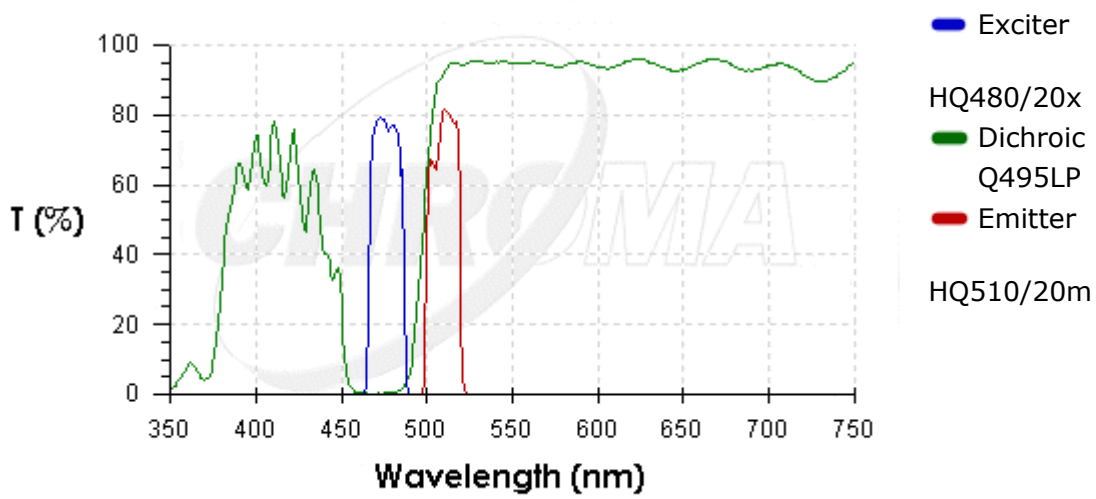

Set ID: 41004
Fluors: Texas Red. Other: Alexa 568™ Alexa 594™ Bodipy TR Calcium Crimson™ Cy3.5™ DsRed Rhodamine Mitotracker Red 580 Mitottracker Red Mitottracker Red 580 Rhodamine Red Tetramethylrhodamine Texas Red™ X-Rhodamine

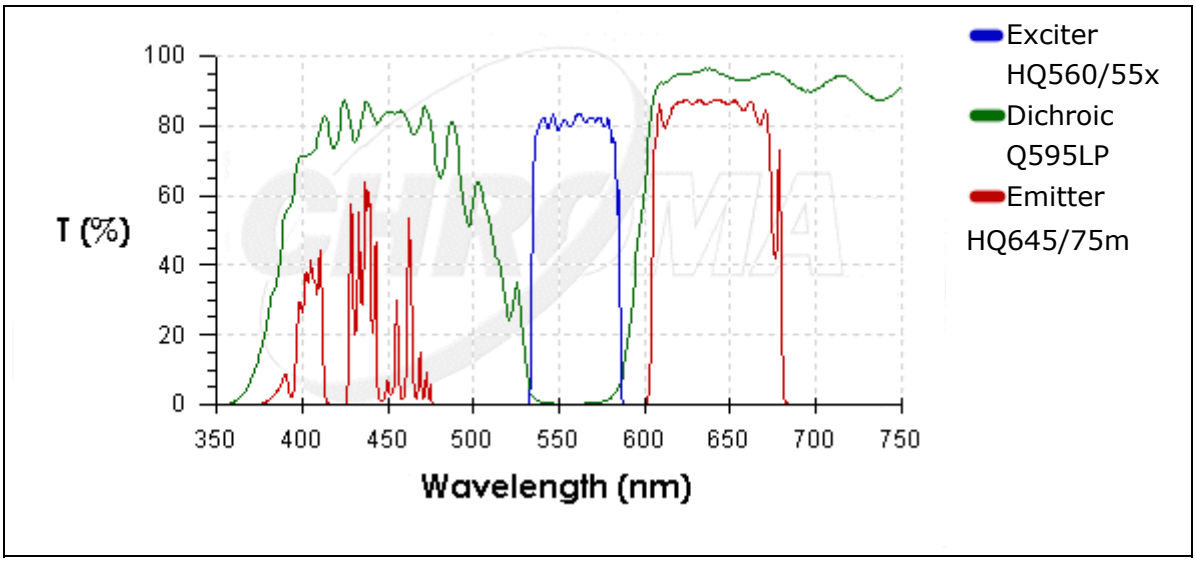
T (%)
100
80
60
40
20
0
350
400
450
500
550
600
650
700
750
Wavelength (nm)
Exciter
HQ560/55x
Dichroic
Q595LP
Emitter
HQ645/75m